Photocatalytic degradation of atrazine

Allen, David Peter

Award date:
1995

Awarding institution:
University of Bath

Photocatalytic Degradation of Atrazine

submitted by David Peter Allen

for the degree of PhD
of the University of Bath
1995

ProQuest LLC
789 East Eisenhower Parkway
P.O. Box 1346
Ann Arbor, MI 48106-1346

Acknowledgements

I would like to thank the EPSRC and Wessex Water for their support throughout this project.

I would like to thank Richard Rathbone for his supervision and David Craft at Wessex Water for my industrial training.

Thanks to all my friends in Bath:

all in 2.12 - Sanjay, Boris, Andy, Gordana, Shauna, Sam and persons now abroad - Christophe and Luisa.

those who kept my letter writing skills finely honed: Karen (Aus) and Dave and Karen +3 (US).

Special thanks to Meloney Bartlett and Gordana Spirovska for help, friendship and support.

and all those at Allen Towers - Mum, Dad and Richard.

and now a poem...

... only kidding!!

List of Figures

Summary

The photocatalytic degradation of the s-triazine herbicide, atrazine, has been studied with the aim of using this technique to purify potable (drinking) water supplies.

Degradations have been carried out in a small volume (500ml) batch annular reactor at relatively high atrazine concentrations (mg/L). This has allowed the evaluation of a number of catalyst types (predominately titanium dioxide TiO_2 based) and provided data on the reaction intermediates formed in the photocatalytic process.

Analysis was carried out using HPLC for quantitative determination and GC-MS for qualitative determination of reaction intermediates. Solid Phase Extraction (SPE) was used for the concentration of low levels of compounds before analysis.

A number of catalyst types have been evaluated in the batch scale for potential use in the pilot scale reactor, including tabletted TiO_2 and various supported catalysts produced via sol-gel methods.

The effect of these different catalyst types along with parameters such as atrazine concentration, catalyst loading, and the presence of inorganic ions on atrazine degradation rates and intermediate concentrations were studied.

Results were then obtained in an annular flow-through pilot scale reactor where powdered TiO_2 and larger catalyst particles were evaluated for the degradation of atrazine at concentrations commonly found in water supplies (ng/L).

The effect of catalyst loading and oxygen sparging rate has been investigated and the problems of catalyst attrition are discussed.

Degradation of atrazine and concentrations of the main intermediates were analysed with a simple kinetic model.

A number of conclusions and recommendations have been made as to the applicability of photocatalysis to practical water treatment processes and to atrazine removal in particular.

1 Introduction

There is widespread interest today in methods for degrading or mineralising pollutants which occur in our environment as air, water, or solid residues. Some of the current methods available for the removal of organic contaminants from water include granular activated carbon (GAC), air stripping, and advanced oxidation processes (AOPs). The major drawbacks of GAC removal and air stripping are that these are non-destructive technologies, the pollutant being transferred from one phase to another. In the case of GAC the spent adsorbent itself may have to be handled as a hazardous waste.

There are a number of technologies which can be combined under the banner of advanced oxidation processes. These techniques often employ a combination of two or more processes which generate highly reactive radical species which can then mineralise organic compounds to non-toxic carbon dioxide and water. The advanced oxidation processes which have been studied for the treatment of organic pollutants in water can be classified as homogeneous, such as UV-ozone [1] and UV-hydrogen peroxide [2]; and those which employ heterogeneous reactions using photoreactive metal semiconductors such as titanium dioxide (TiO_2) [3,4]. In all these techniques the UV light provides a source of oxidising species either via the breakdown of the combined chemical (in the case of ozone and peroxide methods) or via the process known as photocatalysis. Interest in photocatalysis in particular has increased in the past few years and research has developed to the point where the 1st international conference on photocatalysis was recently held [5].

Photocatalysis is the process whereby the illumination of a solid causes a reaction to take place, the solid not being consumed or changed by the reaction, as

defined in simple catalysis. These photocatalysts (or photosensitisers) are invariably semiconductor based. A good example of a common photocatalytic process, which in this case is unwanted, is the degradation of paint exposed to sunlight. Here the organic polymer, used as a binder, reacts with the pigment, TiO_2, which is acting as a semiconductor photocatalyst when illuminated by sunlight.

In general the reaction taking place in the photocatalytic process can be summarised as follows:

$$\text{organic pollutant} + O_2 \xrightarrow[\text{ultra-bandgap light}]{\text{semiconductor}} CO_2 + H_2O + \text{mineral acids} \qquad (1.1)$$

In recent years there has been a rise in interest in the uses of advanced oxidation techniques, and photocatalysis in general, for the degradation of organic pollutants since it provides a potential route which mineralises the pollutant completely to CO_2 without need for further treatment. In the case of GAC adsorption, which is commonly used in the water industry to remove organics, the carbon, once exhausted, has to be regenerated, the pollutant problem having been transferred from one matrix to another but not eliminated.

Another advantage of photocatalysis is the potential for the use of solar illumination [6,7,8] as an energy source making the economics of photocatalysis more favourable in countries less climatically-challenged as the UK.

The aim of this project was to try to extend the knowledge gained about photocatalytic degradation of pollutants and to look at the problems involved in

developing a system (reactor / catalyst / and associated equipment) which could be used by a water supply company.

It was decided that the project would concentrate on the degradation and possible mineralisation of the s-triazine herbicide atrazine.

Atrazine is a pre- and post-emergent herbicide widely used for the control of broadleaf and grassy weeds in corn and other crops [9]. Until recently it was also used in the UK by local councils and British Rail to control weeds in urban areas. Because of it's prolonged and widespread use and it's ecological persistence, traces of atrazine and other triazine herbicides, such as simizine and propazine, have been found in groundwater. In 1980 the EEC issued a directive to it's member states concerning the quality of waters for human consumption setting the maximum permissible concentrations for individual s-triazine herbicides at 0.1 ppb and 0.5 ppb for the total concentration of herbicides / pesticides [10]. Levels exceeding this limit have been found in many countries in Europe as well as in the US. In the UK most water companies meet the EEC limits but some, particularly those who serve rural communities, have levels in some water sources close to the 0.1 ppb limit. An additional concern is that if the level of the water table undergoes any major change, as can happen in periods of drought or high rainfall, concentrations of persistent pollutants such as atrazine may show an increase in drinking water supplies. The setting of the EEC limits as well as general public concern about levels of pollutants in drinking water have led the water supply companies to look for possible technologies for reducing or removing these compounds. It is also possible that the EEC limit will become legally enforced, in some form, in the near future. This is the background against which the research efforts in photocatalysis are played.

2 Semiconductor Photocatalysis

There has been a wide range of research carried out in the area of semiconductor photocatalysis particularly over the past 10 years. During this time the use of photocatalytic techniques for the solution of environmental problems has been suggested. The underlying fundamental principles are based on semiconductor theory although this work has been expanded in an attempt to explain the primary reactions which occur, leading to the oxidation of organic chemicals. There are many studies on the degradation of individual or classes of organic compounds along with the effects of reaction variables on reaction rates. There has also been considerable effort in looking at the practical application of photocatalytic technology, in particular reactor design and catalyst development.

2.1 Photocatalysis Fundamentals

2.1.1 Semiconductors

Unlike the electrons in metals, where the energy bands overlap, the electrons in a semiconductor are divided discrete bands corresponding to their energy levels. There are two main classes of semiconductor:

Intrinsic semiconductors have two energy levels, the difference between them being known as the semiconductor band gap. The lower energy level is known as the valence band, containing electrons participating in the valence bonds of the crystal. The upper energy level, known as the conduction band, is empty unless electrons are promoted by heat or radiation from their valence positions [11,12]. Electrons which have been promoted are able to migrate with the application of an electric field i.e.

conduction, and the corresponding "hole" left by the migrating electron is available to conduct electrical energy in the opposite direction.

These intrinsic semiconductors are in general not important in catalysis since the amount of energy required for electron promotion and the corresponding hole production is too high. It will be seen that the production of electron-hole pairs plays a primary role in photocatalytic reactions.

More important for uses as catalysts are the n-type and p-type semiconductors shown in figure 2.1.

Titanium dioxide (TiO_2) or titania, the semiconductor most widely used for photocatalysis, is an example of an n-type, the structure being nonstoichiometric containing an excess of Ti^+ ions. The small cation is easily accommodated into interstitial positions in the crystal generating energy levels close to the conduction band. This means that the amount of energy (thermal or radiation) required for electron promotion is greatly reduced.

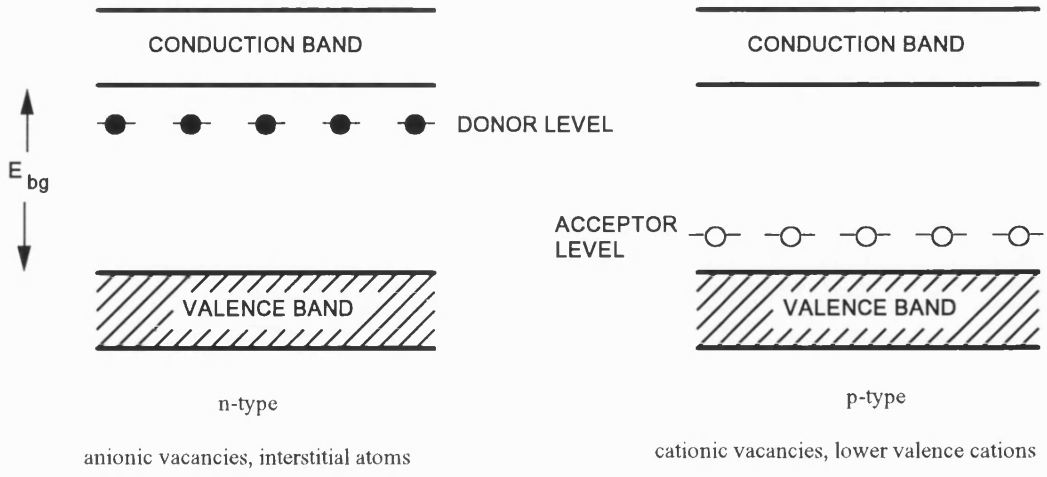

Figure 2.1: *n-type and p-type Semiconductors*

2.1.2 Photocatalysis

In order to be activated, the photocatalyst needs to absorb a photon of energy larger than the bandgap, E_{bg}. This causes an electron, e^-, to be promoted from the valence band into the conduction band with the creation of a corresponding hole, h^+. The photocatalytic process will then continue with the reaction of the generated hole and electron with adsorbed hydroxyl ions and oxygen respectively, as shown in figure 2.2.

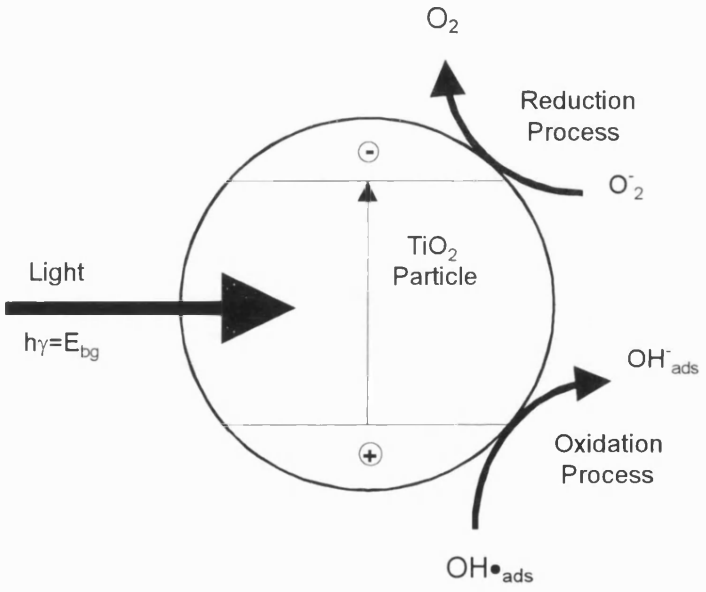

Figure 2.2: *Schematic of Semiconductor Charge Transfer Induced by Band Gap Excitation*

In the absence of a suitable electron-donating redox couple, photogenerated holes will either, build up at the surface reacting with the solvent or electrolyte, be trapped by a surface state which could cause the corrosion of the semiconductor surface, or recombine with a photogenerated conduction band electron .

The reacting scheme which is proposed for a photocatalytic process [13] in aqueous solution is presented in figure 2.3.

The primary reaction is the illumination of the TiO_2 particle by near-UV light (wavelengths < 380nm) generating the electron-hole pairs (eqn 2.2).The recombination reaction is rapid (eqn 2.3) and one important aspect of the photocatalytic process in general is the electron trapping reaction (eqn 2.9) where pre-adsorbed or photoadsorbed molecular oxygen gives the superoxide radical anion. It has been reported that no photocatalytic degradation occurs in the absence of either oxygen or water [13].

$$TiO_2 + h\nu\ (E_{bg}) \longrightarrow e^- + h^+ \quad (2.2)$$

$$e^- + h^+ \longrightarrow TiO_2 + \text{heat and/or } h\nu \quad (2.3)$$

$$(Ti^{IV}\text{-}O^{2-}\text{-}Ti^{IV}) + h^+_{VB} \longrightarrow (Ti^{IV}\text{-}O^{\cdot-}\text{-}Ti^{IV}) \quad (2.4)$$

$$(\text{-}Ti^{IV}\text{-}) + e^-_{CB} \longrightarrow (\text{-}Ti^{III}\text{-}) \quad (2.5)$$

$$h^+_{VB} + Red_{2,ads} \longrightarrow Ox_{2,ads} \quad (2.6)$$

$$e^-_{CB} + Ox_{1,ads} \longrightarrow Red_{1,ads} \quad (2.7)$$

$$(Ti^{IV}\text{-}O^{2-}\text{-}Ti^{IV})\text{-}OH^- + h^+_{VB} \longleftrightarrow (Ti^{IV}\text{-}O^{2-}\text{-}Ti^{IV})\text{-}OH\cdot \quad (2.8a)$$

$$(Ti^{IV}\text{-}O^{2-}\text{-}Ti^{IV})\text{-}OH_2 + h^+_{VB} \longleftrightarrow (Ti^{IV}\text{-}O^{2-}\text{-}Ti^{IV})\text{-}OH\cdot + H^+ \quad (2.8b)$$

$$O_{2(ads)} + e^- \longrightarrow O_2^{-}\cdot_{(ads)} \quad (2.9)$$

$$H_2O_2 + O_2^{-}\cdot \longrightarrow OH\cdot + OH^- + O_2 \quad (2.10)$$

$$H_2O_2 + h\nu \longrightarrow 2\ OH\cdot \quad (2.11)$$

Figure 2.3: *Proposed Photocatalytic Reaction Scheme*

The electrons and holes which migrate rapidly to the particle surface (a few picoseconds for e^- and a few nanoseconds for h^+) are bound by intrinsic sub-surface energy traps $\{Ti^{IV} - O^{2-} - Ti^{IV}\}$ for the holes and surface traps $\{- Ti^{IV}-\}$for electrons (equn. 2.4 and 2.5) . There are a number of further methods by which the electrons and holes can be trapped, namely via surface states (for instant by doping the oxide with metal ions), and extrinsic traps with interfacial electron transfer with surface adsorbed electron donors and acceptors (equn 2.6 and 2.7). In a hydrated and hydroxylated TiO_2 surface, hole trapping by interfacial electron transfer proceeds to give surface bound OH• radicals (equn 2.8a and 2.8b). The reverse reaction, electron-hole recombination which is a rapid reaction requires that both electron donors and acceptors have to be adsorbed at the surface for reaction to take place.

These reactions highlight the importance of adsorption/desorption in photocatalysis. This is dependent on the pH of the medium, the point of zero charge for the catalyst (pzc for anatase 6.0-6.4) which in turn is affected by the particle environment (i.e. the nature of ions present in solution, ionic strength etc.). In general, in low pH environments (acidic conditions) the surface will be positively charged and adsorption of anionic and polar substrates should be enhanced. In high pH environments (alkaline conditions) the surface will be negatively charged and the adsorption of cationic species will be favoured.

Trapped electrons and holes may also recombine. To prevent this e^- can be scavenged by pre- and photo- adsorbed oxygen to give the superoxide radical anion $O_2^{-\bullet}$ (ads). This may be further reduced to the peroxide dianion, O_2^{2-} (ads). Surface peroxo species can form either by hydroxyl radical-hole pairing or by sequential two-hole capture by the same OH group or by dismutation of $O_2^{-\bullet}$.

2.1.3 Photocatalytic Oxidising Species

The major oxidising species formed in the photocatalytic process, OH• radicals in particular, but also h^+, are known to react rapidly with organic solutes. In aromatic compounds, hydroxylation of the aromatic moiety occurs followed by ring opening due to successive oxidation/addition steps. The resulting intermediate compounds formed, often aldehydes and carboxylic acids, are then further decarboxylated, finally producing CO_2.

There have been many studies to determine which is the primary oxidising mechanism in photocatalytic systems. The main questions are whether the mechanism is via free or surface adsorbed oxidising radicals or by direct hole oxidation.

The first of these pathways assumes that the photogenerated holes react with surface bound water and/or catalyst surface OH^- groups yielding OH• radicals. These radicals which are highly oxidising species then react with the substrate (in most cases of interest organic compounds). The alternative pathway involves the direct hole oxidation of the substrate, a view supported by a study which failed to detect any OH intermediates following flash-photolysis of a range of substrates [14], including potassium iodide, 2,4,5 trichlorophenol, tris(1,10-phenanthroline) iron (II) perchlorate, *N, N, N', N'* -tetramethyl-*p*-phenylenediamine, and thianthrene.

Evidence found for OH• as the primary oxidising species include:

(i) electron spin resonance (ESR) studies which have detected OH• species in illuminated solutions of TiO_2 [15] although there is some evidence that other radical species can give similar results;

(ii) reactions carried out in organic solvents show only partial oxidation suggesting that the presence of water or hydroxyl groups is essential [16]; In redox-inert solvents mineralisation does not occur, only some partial oxidation involving photo-oxygenation. Reactions in acetonitrile and dichloromethane have been found to proceed via direct h^+ oxidisation; and

(iii) intermediates detected during the photocatalytic degradation of organic compounds are typically hydroxylated (such as quinones and catechols found in the oxidation of phenols) and are consistent with those found when aromatics are reacted with known sources of hydroxyl radicals [17] such as Fenton's Reagent.

Identification of reaction intermediates in experiments using competitive reactions and inhibitors have been carried out. Evidence for both mechanisms has been found in the oxidation of acetate which gave reaction products expected from hole reaction (CO_2 and methyl radicals) and those expected from OH• radical oxidation (glycolate and glyoxylate)[18].

Ethanol (an OH• scavenger) was shown to inhibit the photo-oxidation of dichlorobenzene over ZnO [19]. By contrast the oxidation of furfuryl alcohol [20] and monochlorophenols [21] was found to proceed by both pathways.

These studies based on identification of reaction intermediates do not allow an exclusive explanation of the reaction mechanism. For example, intermediates identified in the photo-oxidation of phenol may originate either by OH• radical attack on the phenol ring or by direct hole oxidation to give the cation radical which subsequently undergoes hydration in water [22].

2.1.4 Photocatalysis-Heterogeneous or Homogeneous?

There have been conflicting studies on whether photocatalysis is a heterogeneous process, with reaction taking place at the catalyst surface, or one where OH• radicals leave the catalyst surface and react in solution.

Early studies where data for initial rate-concentration data was fitted to a Langmuir-Hinshelwood type equation was assumed to show that the photocatalytic oxidative process was heterogeneous. It has since been demonstrated that equations of the same type can be derived whether the oxidising species and substrate are both adsorbed, both in solution or one adsorbed and one in solution[13]. Most other evidence indicates that the events are mainly if not totally surface occurring, but fitting data to saturation-type models alone does not define the exact nature of the events.

Using decafluorobiphenyl (DFBP) which was found to be tenaciously adsorbed to metal oxide surfaces (Al_2O_3 and TiO_2) and not to undergo exchange between the two a study was carried out which indicates that the OH• radical is surface bound and unlikely to desorb into solution [23]. When DFBP was adsorbed onto alumina in a solution of H_2O_2 or a TiO_2 sol and irradiated the DFBP was easily photo-oxidised. This indicated that both the OH• radicals from the H_2O_2 and the TiO_2 sols migrate to the alumina surface where the reaction takes place. When TiO_2 beads were used the photo-oxidation was suppressed, suggesting that OH• radicals were not leaving the catalyst surface and diffusing to the alumina. Pentafluorophenol, which easily exchanges between the two surfaces did undergo photo-oxidation under the same conditions.

Further evidence for photocatalysis being a surface effect was found from a study looking at the repeated use of a batch of catalyst to carry out the same oxidation. The distribution of products was found to vary with repeated use, an effect which would not have been seen if the OH• radicals were diffusing and reacting in solution[24].

2.2 The Choice of Semiconductor

There is a wide choice of semiconductors available but only a few are suitable for use as photocatalysts. The semiconductor must be (i) photoactive, (ii) able to utilise visible and/or near-UV light, (iii) stable to corrosion, (iv) biologically and/or chemically inert, and (v) cheap.

Figure 2.4 shows the band positions and redox potentials for a number of common n-type semiconductors.

In order for the semiconductor to be able to participate in reaction (2.2) the redox potential for the photogenerated valence band hole must be sufficiently positive to generate adsorbed OH• radicals, and the redox potential of the photogenerated conduction band electron must be sufficiently negative to reduce adsorbed O_2 to superoxide.

The relationship between the semiconductor band gap energy, E_{bg} (eV) and the threshold wavelength of light , λ_{th} (nm), below which the semiconductor will absorb strongly, is given by:

$$E_{bg} = 1240/\lambda_{th} \qquad (2.12)$$

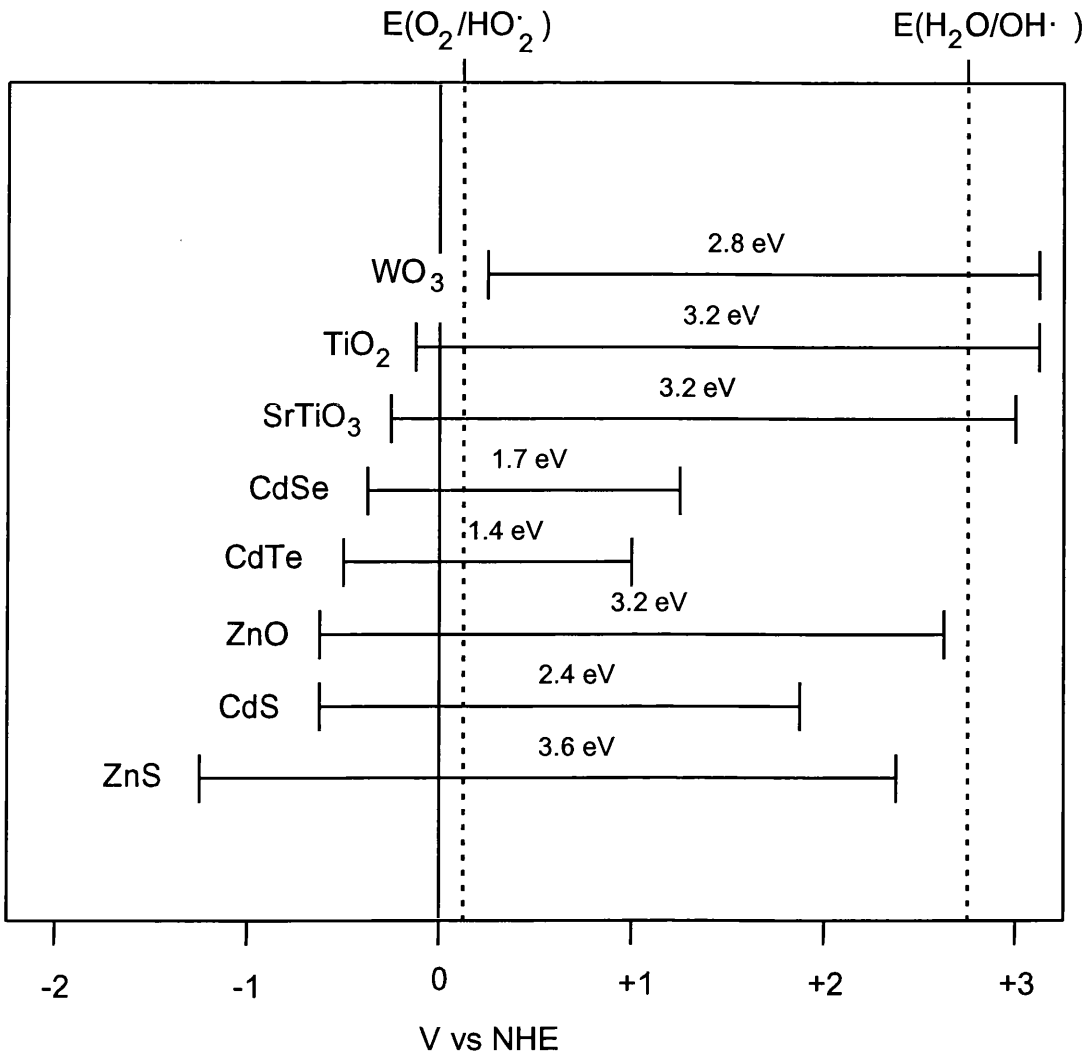

Figure 2.4: *Band Positions for Common n-type Semiconductors and the redox potentials of the $H_20/OH\cdot$ and $O_2/HO\cdot_2$ redox couples.*

Cadmium sulphide (CdS) is an active photocatalyst having the highly desirable feature that it can be activated using visible light, but, as is typical for other visible light absorbing semiconductors, it is liable to photoanodic corrosion:

$$CdS + 2h^{+} \longrightarrow Cd^{2+} + S\downarrow \qquad (2.13)$$

thus rendering it unsuitable for use as an catalyst for water purification.

In most studies [25] TiO_2 appears to be the most effective photocatalyst. Although it is only a UV absorber it is cheap, insoluble, photostable, and non-toxic. It can be seen from the available literature that the most commonly used form of TiO_2 is Degussa P25. This form has become a research standard due to its well defined nature and high activity [26].

Although it has been determined that TiO_2 is the most suitable catalyst for most applications it is still important to choose the correct crystal form. TiO_2 can be found in 2 main crystal forms; anatase and rutile. It has been found in a study using phenol [27] that whereas the anatase form is catalytically active, the rutile form shows no activity. This is surprising given that the redox potentials of the conduction and valence bands in both forms are quite similar. Further investigation, comparing samples of Degussa P25 which had been heated over a range of temperatures (0-1000 °C) showed a loss of activity for samples heated to more than 600 °C [28]. It is known that heating converts anatase to rutile, above 800 °C the crystal structure being completely rutile [29].

In all these studies however, the loss of activity could also be due to a corresponding decrease in specific surface area, typically from 50 down to 5 $m^2 g^{-1}$, suggesting that the method of catalyst preparation could be as important a factor as crystal structure.

It should be noted however that anomalous results have been obtained and various catalyst types should always be evaluated for specific applications. For example it has been found that the rutile form of TiO_2 is substantially better for the oxidation of CN^- [30]. It has also been found that in the presence of hydrogen

peroxide as an electron acceptor rutile forms of TiO_2 can show higher photocatalytic activity [31].

There have been a number of attempts to alter the characteristics of semiconductor catalysts either to increase the rates of charge-transfer reactions and hence rates of photocatalytic degradation or to increase the wavelength range of light which will activate the catalyst into the visible.

The main method used has been doping of the crystal matrix with metal ions.

Fe(III) doping has been reported to inhibit electron-hole recombination reactions [32] although little effect on the efficiency of phenol degradation was reported [33].

Negative effects on doping with Mo and V in TiO_2 have also been reported [34].

A study using mixed Fe/Ti metal colloids have been investigated to broaden the wavelengths suitable for bandgap excitation. At an iron content of 2.5 % the degradation of dichloroacetic acid was 4 times as efficient than with pure TiO_2 colloids [35].

2.3 Photocatalysis of Organic Compounds

The list of organic chemicals found to be photocatalytically degraded and/or mineralised is comprehensive and now covers most classes of organic compounds including alkanes, haloalkanes[36], aliphatic alcohols, aliphatic carboxylic acids[37], alkenes, haloalkenes, aromatics[38,39], haloaromatics[40], phenols[27,41,42], aromatic carboxylic acids[43,44], polymers, surfactants[45,46], herbicides[47,48], pesticides[49], and dyes[50].

In addition to studies on the degradation rates of particular organic compounds there has been experimental work to examine the effect of variables such as catalyst loading, dissolved oxygen concentration, and light intensity [51,3].

2.3.1 Kinetic Considerations

Most studies have found that the data obtained for the initial rate of degradation, r_i, fits a Langmuir-Hinshelwood kinetic scheme given by an equation of the form:

$$r_i = \frac{-d[S]_i}{dt} = \frac{k(S)\,K(S)\,[S]_i}{1 + K(S)\,[S]_i} \qquad (2.14)$$

where, $[S]_i$ = initial concentration of the pollutant S,

K(S) = the Langmuir adsorption constant of species S on the TiO_2 surface, and

k(S) = a constant of proportionality.

The L-H constants represent the equilibrium binding or adsorption constant and the reactivity at the surface.

It is important to note that if the pollutant is a strong UV absorber then at high pollutant concentrations it will begin to screen the catalyst from the ultra-bandgap light and the kinetics of degradation will deviate from equation 2.14.

The effect of light intensity on degradation rate, showing the change from first-order to half-order as the intensity is increased from low to high levels, has been shown [52].

i.e. k(S) is proportional to I_a^{θ}, where I_a is the rate of light adsorption and θ is a power term.

This dependency is also found in other environmental applications of homogeneous and heterogeneous photolytic oxidations, photolytic ozonation for example [53].

This has important consequences for systems using high intensity light sources or concentrated sunlight as efficiencies decrease. This square root dependence has been attributed to electron-hole recombination reactions (second order) becoming more dominant [52] or to bimolecular combination of hydroxyl radicals [54].

It has also been found [51] that k(S) is proportional to the fraction of O_2 adsorbed an the catalyst surface, $f(O_2)$, defined as:

$$f(O_2) = K_{O_2}[O_2] / (1 + K_{O_2}[O_2]) \qquad (2.15)$$

where K_{O2} is the Langmuir adsorption coefficient for O_2.

Oxygen appears to be non-competitively adsorbed on TiO_2 at different surface sites to hydroxyl radicals and organic substrates [51]. Thus a more complex form of equation 2.14 is given by the following expression:

$$r_i = \frac{\gamma K_{O_2}[O_2]\ I_a^{\theta}\ K(S)[S]_i}{(1 + K_{O_2}[O_2])\ \ (1 + K(S)[S])_i} \qquad (2.16)$$

where γ is a proportionality constant.

The overall photocatalytic process is not found to be temperature sensitive, reported activation energies being in the range 5-16 kJ mol^{-1}.

The kinetics of benzene and perchloroethylene degradation in single component and binary component systems have been studied [55]. Using a circulating slurry reactor the single component initial rate data was fitted to a Langmuir-Hinshelwood rate form and the rate constants determined. It was noted that CO_2 production was almost instantaneous with the degradation of PCE but that there was a significant lag between benzene disappearance and evolution of stochiometric quantities of CO_2.

The integrated form of the L-H equation with the constants found from initial rate data was used to model the concentration-time data in individual PCE experiments and good agreement between the calculated and measured values was found. Using the same model for benzene however resulted in considerable overestimation of the observed degradation rates.

This deviation was explained by the production of reaction intermediates from benzene which competed with benzene for hydroxyl radicals. In comparison PCE formed no such long-lived intermediates. To account for these intermediates a term for a competitively adsorbing intermediate was added to the L-H rate equation but this was not found to predict benzene degradation and CO_2 evolution and thus a second intermediate was introduced in a simple 2 intermediate series reaction model scheme. The intermediate kinetic constants were assumed equal and calculated to give the best fit.

For reactions where a significant number of intermediates are formed, the denominator of the L-H equation can be approximated by a term representing the total concentration of total oxidisable organics in solution. Since this remains relatively constant the L-H equation will describe a pseudo-first order degradation. The use of the simplification resulted in a poor description of PCE degradation because few intermediates were present and therefore this can only be used in systems where the reaction is known to proceed via a number of long-lived intermediates.

Further discussion of the kinetic equations used in the analysis of atrazine degradation can be found in section 4.5.

2.3.2 Photocatalysis Studies

The full range of compounds which have been studied in photocatalytic systems can be found in a number of review papers [56], but it is useful to look at a few compounds which are of particular interest in water treatment systems.

2.3.2.1 Pesticides and Herbicides

The photocatalytic degradation of the compound under study here, atrazine, has been investigated [48,57], and a suggested reaction mechanism proposed leading to the conclusion that the breakdown proceeds, not to complete mineralisation ,but to the compound 2,4,6-trihydroxy-1,3,5-triazine (cyanuric acid).

Batch irradiation using P25 TiO_2 powder demonstrated that a 25 ppm atrazine solution was degraded within 15-20 minutes, the TOC falling to a constant in 900

mins for the same experiment. The final TOC value corresponded to a loss of 5 out of the total 8 carbon atoms in the atrazine molecule.

Stoichiometric recovery of nitrogen and chlorine was demonstrated as nitrate and chloride ions and complete removal of atrazine was demonstrated at low levels (ppb). Cyanuric acid has been reported as having a low toxicity [58] and so although the presence of the stable triazine ring meant that complete mineralisation did not occur, photocatalysis was proposed as a possible industrial remediation technique.

Similar results were obtained for the other s-triazine herbicides simizine, trietazine, prometon and prometryn.

2.3.2.2 Halogenated Hydrocarbons

Groundwater contamination by halogenated hydrocarbons used as industrial solvents and degreasing agents has become an increasing problem as their use has become widespread.

It has been shown that many halogenated hydrocarbon compounds, including the major compound formed in the conventional chlorination procedures carried out in water treatment, trichloromethane (a suspected carcinogen) together with other chloromethanes and chloroform, are degraded completely to CO_2 [4,59].

Another unwanted reaction which sometimes occurs in water treatment processes is the reaction of trichloromethane with the bromide ion to chlorobromomethanes and eventually to tribromomethane. Both these compounds have been shown to be mineralised without intermediate production to HBr and CO_2 [4].

The commonly used industrial solvents which can find their way into water sources, trichloroethylene (TCE) and perchloroethylene (PCE), have also been found to be completely degraded, TCE being degraded to form dichloroacetaldehyde as a reaction intermediate [60].

The production of intermediates is an important problem to be tackled in the potential use of photocatalysis and advanced oxidation techniques in general. These techniques are often unspecific in their oxidation reactions and the prediction of side reactions involving free radicals can be complex. This is especially the case in situations where water containing a mixture of contaminants is present. It is important to check that any intermediates produced are not more toxic than any starting material. For example, aromatic chlorobenzenes show long reaction times to complete mineralisation due to the wide range of intermediates which are produced. These intermediates include chlorophenols which are undesirable not least for the fact that their taste is easily detected in drinking water [4].

2.3.2.3 Phenol and Chlorinated Phenols

A study into the oxidation of phenol [42] in a batch system showed that there was an optimum for TiO_2 concentration of 1-3 g/L for the annular slurry reactor under study. This optimum was explained by the shielding effect of high loadings of catalyst leading to less effective use of the incident UV light.

The effect of oxygen purge flow rate on the rate of phenol removal was also found to have an optimum, the degradation rate being decreased at sparge rates above the optimum. This was due to the problem of mixing the larger bubbles of gas formed at the higher sparge rates. The smaller gas / liquid interface per unit volume

and the shortened residence time of the larger bubbles in the reactor may also account for the reduction in phenol degradation rate.

An initial concentration of phenol above a value of 30 mg/L was found to have a negative effect on the pseudo-first-order reaction rate constant and this was explained by increased phenoxide ion adsorption reducing sites for OH• generation.

A study into the degradation of an important class of water pollutants, chlorophenols, has been carried out [39]. The degradations of mono-, di-, and tri-chlorophenols (MCP, DCP, TCP) and the reaction intermediates were studied and an attempt was made to correlate with structure and known physical characteristics. The apparent first-order rate constants k_{app} were compared with Hammett coefficients. These coefficients are commonly used to estimate the effects of substituents on the rate constants of OH• radical attack. The 1-octonol-water partitioning coefficient was also used as a measure of the partitioning of CP's between water and the TiO_2 surface. A correlation containing these two values was obtained which gave a good fit for almost all of the compounds under study. The intermediates which were found corresponded to the substitution of OH groups at the para and/or ortho sites with respect to the original compound's functionality. These substitutions lead to the removal of a chlorine or hydrogen atom depending on which initially occupied the substitution site.

Another compound which is found as an environmental pollutant is pentachlorophenol PCP which has been used as a pesticide and wood preservative. It has been demonstrated [62] that PCP undergoes photocatalytic degradation via a number of intermediates, the principle compounds being *p*-chloranil,

tetrachlorohydroquinone, and *o*-chloranil. Formate and acetate are also formed in the latter stages of the oxidation.

2.3.2.4 Surfactants and Detergents

Photocatalysis has also been shown to be a useful technique for the degradation of surfactants and detergents. These compounds are widely used in industrial and domestic applications but are not easily environmentally biodegraded.

The two common found surfactant compounds, DBS and BDDAC (benzyldodecyldimethylammonium chloride and sodium dodecylbenenesulphonate) have been shown to be effectively degraded by P25 TiO_2 dispersions leading to a reduction in foaming and complete mineralisation to CO_2 [45]. In general, studies show that degradation rates show the following trend:

anionic > nonionic > cationic surfactants

The cationic surfactants CDBACI and CPCI (cetyldimethylbenzylammonium chloride and cetylpyridinium chloride) have also been shown to be degraded resulting in loss of surface activity although mineralisation was not observed [46].

2.3.3 Supported Catalyst Systems

The addition of photocatalyst in the form of semiconductor powders to domestic water supply treatment systems is undesirable for the following reasons:
(i) the addition of any foreign material into water being treated for human consumption is to be avoided, and any such technique would suffer in comparison with non-invasive technologies.

(ii) expensive downstream removal steps, e.g. filtration, may be required to remove and recycle the catalyst,

(iii) potential catalyst losses would be high, and

(iv) due to the unpredictable reactions which could take place it would be an advantage to keep the catalyst in a defined reactor volume where some form of monitoring of intermediate compounds could take place.

Therefore there has been considerable emphasis on research into supported catalysts including immobilisation of TiO_2 on fibreglass, woven mesh, glass reactor walls, silica gel,and beads.

In a study utilising a supported catalyst [63], the inner tube of a photoreactor was coated with a layer of TiO_2, from a sol-gel preparation method using titanium tetraisopropoxide as a precursor. Aqueous and gaseous feed streams could be pumped continuously through the reactor from a feed reservoir. In this particular study the degradation of 3-chlorosalicylic acid was measured and shown to deviate from simple first-order kinetics. Fitting the data to a Langmuir-Hinshelwood/Hougen-Watson model which describes two adsorbing species, 3-chlorosalicylic acid and oxygen, gave good agreement with experimental results.

TiO_2 deposited on glass beads by thermal decomposition of titanium(IV) alkoxides has been used to photodegrade 2,4,5-trichlorophenol and to recover gold from dilute solutions [64].

In order to assess the activity of the coated beads a characteristic reaction of TiO_2 semiconductor dispersions, the photoinduced charge injection of electrons from the conduction band to the 1,1'-dimethyl-4,4'-bipyridium cation, MV^{2+}, to produce the cation radical MV^{+}, was used. This latter species exhibits a

characteristic blue colour and can be confirmed by an absorption band at 605 nm. This quick and useful test showed that the coated glass beads were photocatalytically active

Photoreduction of a solution of gold(III) (40 ppm) led to its deposition on the bead surface as gold(0), which could be recovered by treating with concentrated nitric acid which reoxidises the gold and removes it from the particle surface without affecting the photocatalytic activity of the beads.

Treatment of 2,4,5-trichlorophenol showed complete mineralisation suggesting that an industrial scale treatment process based on a supported photocatalyst may be possible.

Another supported system using Degussa P25 coated and dried onto the inside of a borosilicate wound spiral tube was used to degrade a range of organics (salicylic acid, phenol, 2-chlorophenol, 4-chlorophenol, benzoic acid, 2-naphthol, naphthalene, and fluorescein) [65]. The rates of degradation were found to increase with an increase in the amount of TiO_2 on the reactor surface and fitted Langmuir type adsorption isotherms. An increase in degradation rate was also found with increasing flow rate through the reactor and a correlation was derived linking degradation rate with initial concentration and flow rate. This result highlighted the fact that degradation rates in a reactor of this type would be mass transfer limited.

A study on a system which combined a silica gel adsorbent with *in situ* photocatalytic oxidation regeneration to remove various organic compounds, including phenol and salicylic acid [66], cited the following advantages over a simple photocatalytic or adsorption system alone:

(i) a substrate which is a strong adsorbent for molecules that are weakly adsorbed on TiO_2 may be chosen, increasing the surface contact time for the photocatalytic degradation to take place;

(ii) the adsorbent may be regenerated *in situ* when the UV light source is switched on; and

(iii) the photocatalysis on TiO_2 is a destructive process in contrast to adsorption in which possibly harmful impurities are transferred from the liquid to the solid phase thus becoming a solid waste disposal problem.

The TiO_2 coated silica gel was packed in an annular photoreactor and pollutant solutions pumped at controlled flow rates using a peristaltic pump. After a period of 8 minutes the outlet concentration of salicylic acid was the same as the inlet, the column having reached it's adsorption capacity. When the UV light was turned on there was a rapid decrease in the outlet concentration indicating rapid photocatalytic oxidation. The process could be repeated by turning the lamp off and on again.

For salicylic acid increasing the inlet concentration increased the rate of solute removal but the photocatalytic degradation process was not fast enough to reduce the concentration down to low levels. Doubling the inlet concentration of phenol however did not change the outlet concentration.

The effect of TiO_2 loading on the silica gel showed that increasing the loading at high concentrations (50μM) had no effect on the degradation rates while at lower initial concentrations (10μM) there was a significant increase in rate. This is explained by the competing effects of increasing solute adsorbed on the surface favouring an increase in photocatalytic oxidation, but with a decrease of the

penetration of light into the silica gel as the loading is increased. It appears that at the lower concentrations there is a change in the balance of these opposing effects with a change in the degree of adsorption becoming more significant.

Further work [67] has led the same author to eliminate porous and/or adsorbent supports as suitable for photocatalytic reactions. It was found on further investigation that although the original substrate concentrations were reduced, corresponding CO_2 production was not observed. This was assumed to be due to adsorption of reaction intermediates onto areas of the porous support not coated with catalyst where further photocatalytic degradation could not occur. This has led to the view that porous supports should not be used in photocatalytic systems where the benefits of mineralisation are required.

2.3.4 Effect of Additives on Photocatalysis

There has been great interest in the effect of various additives on photocatalytic degradation rates.

(i) Compounds which will have a positive effect, by acting as oxidising agents on their own or as electron scavengers, could be added to a photocatalytic system;and

(ii) Compounds found in nature, which will be present in any water purification application, which could have possible detrimental effects due to competitive reactions and/or catalyst fouling.

The effect of inorganic anions on photocatalytic degradation rates has been studied [68] and showed that the presence of chlorides, sulphates, and phosphates all have a detrimental effect. Addition of NaCl (0.05M) decreased the rate of ethanol oxidation from 50 μg C/min to 20 μg C/min and increasing the concentration of

NaCl showed decreasing oxidation rates for ethanol, salicylic acid and aniline. One explanation is that the chloride ions act as a scavenger for oxidising radicals species (·ox).

$$\cdot ox + Cl^- \longrightarrow Cl \cdot \qquad (2.17)$$

The addition of nitrate and perchlorate ions, in the form of $NaClO_4$ and $NaNO_3$, were small and any effect was presumed to be due to partial blocking of active sites on the photocatalyst.

Sulphate ions added as Na_2SO_4 showed a significant effect on degradation rates, the effect taking place immediately on contact with the catalyst and not increasing with contact time as was the case with chloride ions. There was also little effect on increasing the concentration of sulphate ions above 0.01 M. It appears that the sulphate ions are immediately and strongly bound to the catalyst causing deactivation. The catalyst could only be regenerated by washing with alkali (0.1 M) or 0.1 M $NaHCO_3$ and 0.1 M $HClO_4$ solution.

The effect of phosphate ions, as Na_3PO_4, showed the greatest reduction of degradation rates from 85 to 30 μg C/min for salicylic acid and 41 to 23 μg C/min for ethanol when the phosphate concentration was as low as 0.001 M. The behaviour of phosphates was the same as that observed for sulphates in that activity was immediately effected and did not change with time. A similar procedure for regeneration after contact with sulphate ions had to be used. The data was fitted to a model which assumed that the adsorbed anions compete with adsorbed organic species for the photooxidising species to give radical anions. Some of the radical

anions may undergo oxidation reactions with organic species but at decreased rates, the overall effect appearing as catalyst deactivation.

Most aquatic environments, in addition to the presence of inorganic ions, will contain a class of organic molecules known as humic substances. Studies to examine the effect of these compounds include one looking at the effect of fulvic acid, a low pH soluble component, on the degradation of an organophosphate [49]. It was found that rates of degradation are substantially reduced in the presence of fulvic acid at concentrations as low as 25 ppm and this is explained as a result of two major factors:

(i) the substrate was kept from the TiO_2 surface by a combination of two possible mechanisms:

(a) adsorption of the substrate by the fulvic acid molecules, and

(b) competitive adsorption onto the catalyst active sites.

(ii) at high concentrations the fulvic acid adsorbs a large fraction of the incident radiation reducing that which can reach the surface of the TiO_2.

Studies have also looked at possible methods of enhancing the photocatalytic reaction rates by the addition of inorganic oxidising species [40]. Three compounds were examined:

(i) 2-chlorophenol which is photocatalytically degraded rapidly to CO_2 and HCl;

(ii) 2,7-dichlorodibenzo-dioxin, harmful and environmentally persistent, requiring long photocatalytic degradation times; and

(iii) atrazine, showing fast degradation of the primary compound but slow appearance of the final compound, cyanuric acid.

The oxidising species studied were peroxidisulphate and periodate which both act by scavenging for electrons thus preventing unwanted electron-hole recombination reactions and through the production of other strong oxidising species, such as hypoiodate and the sulphate radical ion, which contribute to the overall degradation process.

The degradation of 2-chlorophenol ($1.5x10^{-4}$ M) with the addition of peroxidisulphate and periodate ions increased dramatically, halving the time for total mineralisation, as measured by CO_2 evolution.

The effect on the degradation of 2,7-Dichlorodibenzodioxin is even more dramatic. 0.1M of periodate or peroxydisulphate giving >99% degradation in 30 minutes and 60 minutes respectively compared to times of 180 minutes for TiO_2 alone. Other oxidising agents such as H_2O_2 and chlorate ions have been found only to be slightly beneficial.

Addition of periodate and peroxydisulphate ions at concentrations >1 x 10^{-4}M showed decreases in atrazine degradation times from 30 minutes to 4 minutes. The most interesting result is the speeding up of the degradation of the reaction intermediates. The final product, cyanuric acid, is formed in stochiometric quantities after 0.5 - 1 hour for peroxydisulphate and periodate compared to 70 h for TiO_2 alone. It is possible that the addition of these inorganic species could be used for the degradation of organic pollutants in water treatment systems since they exhibit low toxicity in solution. The products of their reactions, sulphate and iodide, are less toxic and are also formed in other water treatment processes.

2.3.5 The use of Solar Radiation

There have been a number of studies looking at the use of solar radiation as a source of photons for the photocatalytic degradation of aquatic pollutants using parabolic-trough and thin film reactors [6,7,8].

There has been general concern that because there is negligible solar radiation of wavelengths between 280-300 nm it may not be possible to initiate photocatalytic reactions with unmodified TiO_2. Attempts have been made therefore to develop catalysts, usually by doping with metal ions, which can utilise a greater fraction of solar energy. It has been shown that compounds can be degraded by solar systems and these include trichloroethylene, surfactants, trichloromethane, salicylic acid, dioxins and biphenyls.

Work on the degradation of pentachlorophenol in both simulated and actual solar systems [8] demonstrates that there is a potential for the use of solar based systems and in particular demonstrates the effectiveness of the addition of chemical based electron scavengers, in this case peroxydisulphate, on degradation rates.

In a study looking at a wide range of catalyst supports for solar degradation [69] higher degradation rates were found with catalysts with increased specific surface area. Supports which had higher near-UV transmission required lower catalyst loading for the same degradation rate. It was also found that impregnating adsorbent supports such as GAC and a synthetic resin led to increased breakthrough times indicating that a combined photocatalysis/adsorption system may reduce adsorbent usage rates.

2.4 Other Uses of Photocatalysis

There have been a number of studies on uses of photocatalysis other than for the photomineralisation of organic pollutants. An instrument for total organic carbon (TOC) analysis has been developed based on a TiO_2 containing reactor [70]; there are applications including use as a photodeodorant by coating a thin film of TiO_2 onto an interior tile [71]; using TiO_2 as a method of destroying cancer cells [72]; and using TiO_2 coated hollow glass microbeads, which float on water, for the clean up of oil spills [73].

There are a number of other important applications to which photocatalysis has been applied and two in particular which are of interest for water treatment applications.

2.4.1 Heavy Metal Removal

There are a number of examples of transformations of inorganic ions on semiconductor surfaces including chromium, copper, iron, manganese,and mercury.

In most of these reactions a metal species is deposited on the catalyst surface and will eventually lead to catalyst deactivation. Obviously there is more potential for using catalyst in this way to recover high-value metal ions rather that as part of a water treatment process. An important consequence of these inorganic reactions is that in treating water with naturally occurring metals in solution some deposition and catalyst deactivation will be inevitable.

Long term trials of photocatalytic reactors treating mains water showed decreasing degradation rates of test compounds due to the deposition of light blocking compounds such as hydrated ferric oxides on the catalyst surface. These

iron compounds are present in water as ferric humic complexes. Other ions such as Cu, Al and Zn were also found to be removed by the photocatalytic reactor by analysing concentrations entering and leaving the reactor [67].

2.4.2 Photocatalytic Disinfection

Another potential use of photocatalytic reactions is in disinfection of potable water. Using traditional methods of disinfection such as chlorination, it has been found that, depending on the levels of TOC, the disinfection treatment can actually increase the levels of microbial growth. This is due to the amount of carbon which is available for microbial growth increasing as organic compounds are converted into forms which are easily assimilated (known as AOC or Assimilable Organic Carbon). This can then lead to problems of microorganism regrowth in supply tanks and water mains.

The compounds which make up the bulk of the AOC have been identified as aldehydes, ketones and carboxylic acids.

Formaldehyde, acetaldehyde, and other higher molecular weight carbonyl compounds have been found after chlorination, the most widely used disinfection technique in the UK. In addition, chlorination also suffers from by-product formation of trihalomethanes which are believed to be carcinogenic. Disinfection with chlorine dioxide (ClO_2) has the advantage over simple chlorination in that trichloromethanes are not produced but the problem of aldehyde and ketone by-products is still present. Aldehydes and Ketones are also found in other techniques such as H_2O_2 and Ozone treatment.

In the case of ozone, which has been examined as a potential technique for primary disinfection coupled with a secondary residual treatment, there are two major problems. Firstly naturally occurring bromine ions are oxidised and form brominated organics of which the effects on humans are unknown. Secondly AOC levels are typically doubled by ozone treatment.

Treatment with TiO_2 systems offers the possibility of complete oxidation of small organic compounds which provide a large proportion of the total AOC. The concentrations of secondary organic by-products which would result in systems which continue to use free chlorine as a residual disinfection would also be reduced. In particular trihalomethanes have been shown to be easily oxidised by photocatalytic techniques [4].

There are a number of problems which are associated with this potential use of photocatalysis for disinfection. Although the main benefit over ozone use appears to be higher concentrations of hydroxyl radicals (the major oxidising species in both systems) this is obviously effected by the catalyst type used. Any system in which production rates are low or in which compounds are not fully mineralised could lead to the same problems of high AOC concentrations. It will be seen in section 4.1.2 that in the case of atrazine the oxidisation process produces a number of relatively long-lived intermediates which are precisely in that group of compounds which form AOC. Namely aldehydes, ketones, and carbonyl compounds in general.

2.5 Catalyst Preparation

There have been many studies into the preparation of metal oxide semiconductors, including some specifically for use as photocatalysts.

Most of these methods are based on the controlled hydrolysis of the metal alkoxides or $TiCl_4$ known as sol-gel methods. The advantages of sol-gel techniques are:

(i) that by using controlled cohydrolysis of mixed alkoxides, doped particles can be prepared [74];

(ii) colloidal solutions or very fine particulate suspensions can be prepared; and

(iii) the colloidal sols can be used to coat very finely divided material onto support surfaces.

An example is the hydrolysis of titanium tetraisopropoxide which proceeds according to the following reaction:

$$Ti(iso\text{-}OC_3H_7)_4 + 4\,H_2O \longrightarrow Ti(OH)_4 + 4\,C_3H_7OH \qquad (2.18)$$

TiO_2 being formed when the product of hydrolysis is heated in air.

TiO_2 membranes can also be prepared via two hydrolysis methods [75]. Either:

(i) via a particulate sol using an acid peptising agent to prevent aggregation; or

(ii) using a polymeric sol which can lead to transparent gels on evaporation of water.

It was found that the preparation of particulate free sols was difficult and needed careful control of the hydrolysis conditions, the mole ratio of water to titanium needing to be <4. After hydrolysis the sol-gel can either be; fired to evaporate water and any remaining solvent, and the resulting TiO_2 powder used as

an unsupported catalyst; or used to coat a support surface e.g. glass beads, reactor walls.

The difficulty in achieving a controlled hydrolysis is demonstrated in attempts to produce stable, gelled, clear solutions for the preparation of TiO_2 fibres [76]. A method to suppress precipitation of the alkoxides by using glycols or ethanolamine and therefore to make sol-gel preparation easier has been described [77]. The solutions prepared were used to coat glass substrates, layers up to a thickness of 1μm were formed by multiple coating.

2.6 Analysis Techniques

The wide range of analysis techniques available for pesticide and herbicide analysis have been reviewed [78]. Included are the standard methods of gas chromatography (GC) and high performance liquid chromatography (HPLC) which are particularly suited for the separation and analysis of reaction intermediates.

There are also a number of sample preparation techniques for analysing low concentrations of pollutants and extracting samples from complex sample matrices.

Analysis of atrazine and separation of it's degradation products by reverse phase HPLC (C8), with UV detection at 220 nm, using a methanol:water mobile phase has been demonstrated[79].

The use of an HPLC microbore column separation, using solid phase extraction (SPE) and diode array detection for the quantitative measurement of 17 triazine and phenylurea pesticides, was a technique which could measure concentrations down to 50 ng/L [80,81].

An automated method of SPE, specifically used in the water industry for the analysis of pesticides, has been demonstrated [82] together with details of the development procedure required to apply SPE to other specific extractions.

Other techniques described include on-column trace enrichment [83], GC-mass spectroscopy analysis [84], GC-NPD [85], and Enzyme-Linked Immunosorbent Assays (ELISA's) for triazine analysis [86].

For further discussion of the applicability of the various analysis and sample preparation techniques available to the current project see chapter 3.

3 Materials and Methods

Photocatalysis experiments were initially carried out in a batch-scale reactor to provide data for the degradation rates of atrazine and information on reaction intermediates formed in the breakdown process. These experiments also provided samples which could be used to develop the analytical techniques used throughout the study. It was important to develop techniques which would:

(i) allow the rapid and reproducible measurement of atrazine concentration; and

(ii) identify reaction intermediates.

In addition it was important to develop the associated sample preparation techniques which were required prior to analysis

A suitable form of TiO_2 had to be developed to allow it's use in a large, continuous, pilot-scale reactor. In practice this meant the use of either large particles of bulk catalyst or a catalyst layer immobilised onto a support. A number of possible solutions to this problem were evaluated and are described in sections 3.8 and 3.9.

Finally, experiments were carried out to look at the pilot-scale degradation of atrazine at low concentrations, close to those found in potable water sources.

3.1 Materials

All chemicals used were of analytical reagent grade unless otherwise stated.

Atrazine (6-chloro-N^2-ethyl-N^4-isopropyl-1,3,5-triazine-2, 4-diamine) used for photocatalysis experiments was obtained from Ciba Geigy, while purified atrazine and reaction intermediate standards were obtained from Promochem. All reagents were used as supplied without further purification.

Samples of P25 TiO_2, and P25 tablets were supplied by Degussa. WDB TiO_2 was obtained from SCM. A summary of physical and chemical data supplied from Degussa is shown in table 3.1.

***Table 3.1**:Physicochemical Data on Degussa Titanium Dioxide Samples.*

Titanium Dioxide P25	
Behaviour in the presence of water	Hydrophilic
BET Surface Area (m_2/g)	50 ± 15
Average Primary Particle Size (nm)	21
Tapped Density (g/L)	approx. 100
Density (g/L)	approx. 3.7
pH (4% aqueous solution)	3 - 4
P25 Tablets	
Chemical Composition	>99.5% anatase
Shape	5 x 5 mm cylinders
BET Surface Area (m_2/g)	40
Pore Volume (ml/g)	0.23
Pore Size Distribution	
No Pores Smaller than (nm)	8
Main Pore Range (nm)	10 - 30
Crushing Strength (N)	85
Abrasion Loss (%)	1.5
Bulk Density (g/L)	1270

Acetonitrile used for preparing HPLC mobile phase was obtained from Fisons and was "HPLC-Far UV" grade. All other solvents and chemicals were "HPLC" grade for HPLC analysis and "Pesticide" grade for GC-MS analysis.

Water used for preparing the HPLC mobile phase and for making all solutions for batch scale experiments was from a Millipore Maxima ultra-pure water unit fed from a Millipore Ultima RO unit.

Water used in the pilot scale experiments was softened Bath mains water (Zephyr Water Treatment).

Ceramic steatite beads, diameter 3.5 mm, were obtained from Morgan Matroc Ltd. These beads are commonly used in the grinding and milling industry and were chosen as a possible catalyst support because of their hardness and resistance to wear.

Glass ballotini, diameter 250μm, were obtained from Jencons.

3.2 Solid Phase Extraction

Solid Phase Extraction (SPE) is a technique which uses the selective adsorption between compounds of interest and a chemically modified silica adsorbent for sample extraction and concentration. SPE is routinely used in the analysis of drinking water quality [82], and the technique used in this study was adapted from one such method [80]. Disposable SPE cartridges were used, both to transfer samples from water into a solvent suitable for injection onto a GC capillary column, and to concentrate low levels of atrazine so that quantitative analysis by HPLC was possible.

The extractions were carried out using C18 reverse phase, silica-based, Bond Elute cartridges (Varian) and a Vac-Elute (Varian) system for extraction of a large number of samples (up to 24) at one time.

The SPE technique used is shown schematically in figure 3.1.

Cartridges were conditioned with 10ml of "pesticide" or "HPLC" grade methanol followed by 10 ml of UHQ water. The samples, which were contained in brown glass 1L bottles, were weighed and positioned around the Vac Elute module. Sample tubing was placed into each bottle and connected to the cartridges fitted into the module. The samples were then drawn through the cartridges under vacuum. It is important that the sample was added before the cartridges have a chance to dry out from the conditioning step to prevent channelling and therefore reduced sample recovery.

For samples which contained a large amount of fine catalyst, care was taken that none of it passed through the SPE cartridge as this led to blocking and reduced extraction times. If necessary, the samples were left to settle out and the sample inlet tubing positioned so as to leave behind any catalyst in the sample bottles. The remaining catalyst was washed with 100 ml of UHQ water, left to settle and then passed through the SPE cartridge to remove any adsorbed organics.

After passing the sample through the cartridges, the compounds of interest having been retained on the packing material, the transfer tubing was removed and the vacuum pump left running for 1 hr, pulling air through the cartridges until the packing had dried out. This allowed the elution solvent to fully wet the packing giving high and reproducible sample recoveries.

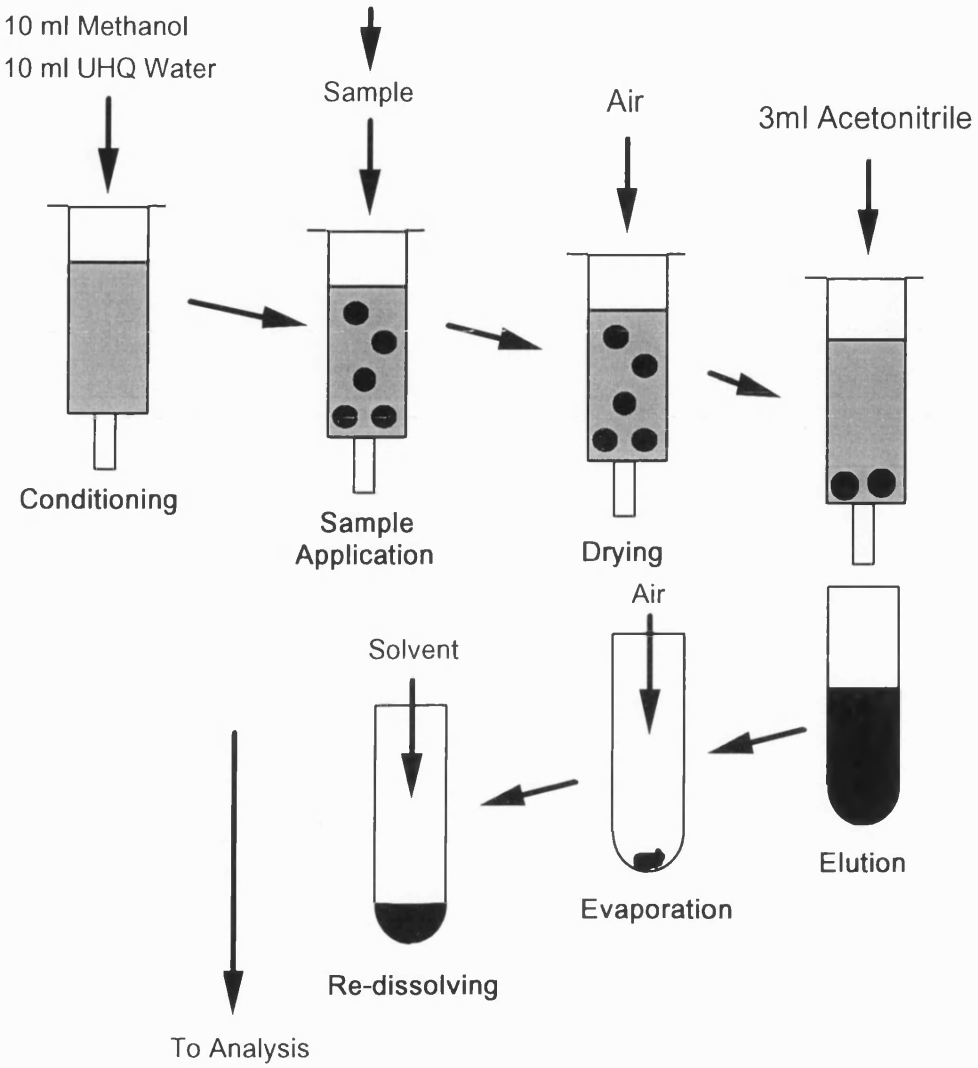

Figure 3.1 : *Schematic of Solid Phase Extraction Procedure.*

After drying, the vacuum pump was switched off and 3 ml of the elution solvent (acetonitrile) added to each cartridge. The eluted sample was allowed to drip into a test tube under gravity, the vacuum pump being turned on to extract any remaining solvent. After elution the solvent was evaporated under vacuum, aided by blowing a stream of air into the sample tube, the process usually taking 1-2 hr. When the sample had been evaporated to dryness it was redissolved in a small volume of the desired analysis solvent.

In the case of the HPLC analysis, after evaporation, 0.5 ml of the starting mobile phase (20% acetonitrile / water) was added.

In the case of GC-MS analysis the sample was redissolved in 1 ml of ethyl acetate.

Control experiments showed that the SPE cartridges extracted atrazine at efficiencies of 95-98% .

3.3 Analysis of Atrazine and Intermediates

Atrazine and the range of breakdown products formed by the photocatalytic degradation process were analysed quantitatively by high performance liquid chromatography (HPLC) and qualitatively by gas chromatography coupled with a mass specific detector (GC-MS).

Analysis by GC-ECD (Electron Capture Detector) was evaluated, but it was found that this method was neither sensitive enough, atrazine possessing only one highly electronegative chlorine atom, or reproducible.

Total organic carbon (TOC) measurement which is used to measure the degree of mineralisation, proved to be unreliable and irreproducible and was therefore not include as a general analytical technique. Data for the concentrations of the principle intermediates, and in particular the desethyl-desisopropyl compound, give a good indication as to the extent of mineralisation. It should also be noted that conversion to the desethyl-desisopropyl intermediate represents the maximum reduction in TOC achievable using basic photocatalytic oxidations. (5 out a total of 8 carbon atoms having been lost, with no further TOC reduction on conversion to cyanuric acid. See figure 4.4 for chemical structures of these intermediate compounds)

3.3.1 HPLC Analysis

HPLC analysis was performed using a Gilson system consisting of two 306 pumps, an 811B mixer, and a 115 UV detector. The system was coupled to a SGE LS-3200 auto-sampler/auto injector so a number of samples could be stored in vials and run with the minimum of operator supervision.

Separations were performed on a Spherisorb C8 (Fisons) reverse phase column (250 mm x 4.7 mm) using a method adapted from a Hewlett Packard application [80].

Using an isocratic elution, measurement of atrazine was possible but peaks corresponding to reaction intermediates were eluted together. In order to elute reaction intermediate peaks and give a good separation between these compounds and atrazine itself (the most important function of this analysis being to provide a measurement of atrazine concentration) a gradient elution was used consisting of acetonitrile and water and was prepared as follows:

"Far-UV HPLC" grade acetonitrile and UHQ water (Millipore Maxima) were mixed to give the following mobile phase compositions:

Pump A: A 20% acetonitrile / water ; 1mM ammonium acetate solution

Pump B: A 100% acetonitrile solution

Both solutions were filtered through a 0.2μm nylon membrane in an all glass apparatus (Millipore) and further degassed, prior to pump priming, by sparging with helium.

Retention time data was obtained by analysing solutions of atrazine and each intermediate in single and multicomponent samples to check for possible interference effects. Calibration data for sample component peak height vs.

concentration was obtained by performing serial dilutions on atrazine and each intermediate in turn.

Samples straight from the reactor, in the case of high concentration experiments, or from the sample preparation stage (section 3.2), were filtered through 0.2 μm Nylon syringe sample filters (Fisons), capped in glass sample vials, and placed in the autosampler carousel.

The SGE autosampler/autoinjector operated by the use of a double sheathed needle. The outer sheath, which had a row of holes above the sample level, allowed for the pressurisation of the vial head-space with nitrogen. This forced the sample up the inner needle, through the silica sample transfer tubing, and into the sample loop of the Valco HPLC injection valve.

It was necessary to carry out an experiment to measure the time required to flush and fill the transfer tubing and sample loop. This was measured and a one second safety margin added giving a total vial pressurisation time (at 50 psi) of 6 seconds.

The analysis method was input into the Gilson software as described in the operators manual . The method details are shown in appendix A1.

When analysing a number of samples consecutively it was important that the time between autoinjections was longer than that for the analysis method (by at least 1 minute) in order to allow the software to wait for the next injection. The details of the parameters which had to be input on the autosampler front panel are shown in appendix A2.

After injection, samples were eluted using a gradient of 20 to 50% acetonitrile in 15 minutes and holding for 10 minutes. The method then returned the column to

the starting mobile phase composition in 15 minutes ready for the next injection and analysis, giving a total analysis time of 40 minutes.

Peaks were analysed by measuring the UV absorbance at 210 nm, the data being stored by the Gilson software. In order to give a qualitative determination of the intermediate peaks a number of standards were run corresponding to the main dealkylated atrazine molecules. Concentrations were calculated by using the calibration data obtained from serial dilutions of the atrazine and intermediate standards.

The calibration data for atrazine is shown in figure 3.2 as a plot of peak height for a range of atrazine concentrations at a sensitivity of 0.02 F.S.D. This data for atrazine and the other intermediate standards is also shown in figure 3.3 as a linear regression expression with the retention time for each compound. It was found that the limit of detection for atrazine, using a 100 μL sample loop, was 0.04 mg/L.

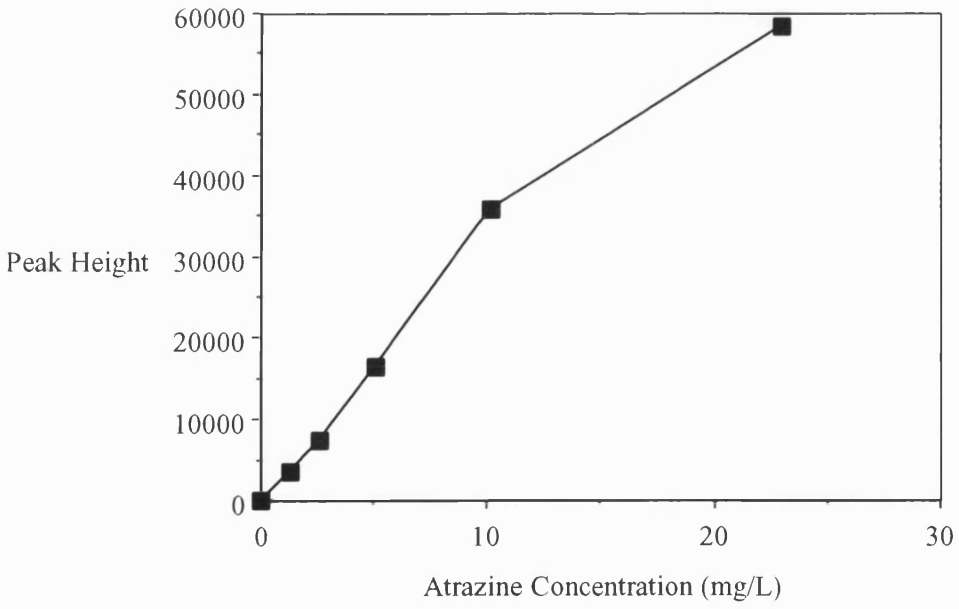

Figure 3.2: *HPLC Calibration Curve for Atrazine*

Compound	Retention Time (min)	Calibration Equation
Atrazine	17.58	y = 2532.2 x
Desethyl Atrazine	9.34	y = 8847.0 x
Desisopropyl Atrazine	6.68	y = 7055.4 x
Desethyl-Desisopropyl Atrazine	3.43	y = 5719.6 x

Figure 3.3: *HPLC Calibration for Atrazine and Reaction Intermediates.*

The one reaction intermediate which was difficult to analyse was cyanuric acid. This was because, with three OH groups attached to the triazine ring, the molecule was highly polar and retention on a reverse phase support was small. This meant that cyanuric acid eluted with the sample solvent front and in many experiments there would be further interference from any other unretained compounds present in the sample, such as inorganic ions. This was a particular problem with experiments where nitrate ions were present, since they absorb UV light at wavelengths used to analyse triazine compounds, and experiments in the pilot reactor using softened water where a broad peak was eluted with the solvent front.

Methods for the analysis of cyanuric acid have been reported but the methods are either complex [57] and/or do not allow for the separation of the whole range of intermediates, cyanuric acid, and atrazine in the one analysis [87]. It was therefore decided that the accurate measurement of cyanuric acid would be a lesser priority especially in light of the small production rates expected for the experimental run times used here compared to previous studies [57]. In some experiments a change in

the peak height at the solvent front has been commented on as a possible change in cyanuric acid concentration, but it should be noted that other effects, such as production of nitrate ions from the loss of the nitrogen atoms in atrazine, may also account for this change.

3.3.2 Gas Chromatography - Mass Spectroscopy

In order to determine the range of reaction intermediates formed by the photocatalytic degradation of atrazine, samples from a series of batch experiments were analysed by GC-MS using a Hewlett Packard 5890 series II GC and a 5991A mass selective detector. Samples from the batch runs were extracted using SPE cartridges by the method described in section 3.2. High initial atrazine concentrations were used to maximise the quantities of intermediates formed.

Samples for GC analysis have to be prepared in an organic solvent having

(i) a low boiling point;

(ii) a low expansion volume when vaporised; and

(iii) a high solubility for the compounds of interest.

It was determined by running standards of atrazine in a variety of solvents that ethyl acetate gave the best results. The standard SPE method was therefore modified to produce suitable samples for the GC-MS by re-dissolving with ethyl acetate rather than acetonitrile. The extracted samples were capped into glass sample vials and auto-injected into the GC. Samples were analysed according to the method shown in table 3.1.

As with HPLC analysis, standards of atrazine and the available reaction intermediates were analysed. The standard mass spectra obtained are shown in Appendix B2.

Table 3.1: GC-MS Method Details.

Column Type	SGE BPX-5 25m x 0.22 mm x 0.25 μm film thickness
Injection Volume	5 stops, 100 μL
Injector Temperature	250 °C
Detector Temperature	285 °C
InitialColumn Temperature	50 °C
Initial Time	2 min
Rate 1	50 °C/min to 150 °C
Rate 2	5 °C/min to 260 °C
MS Solvent Delay	4.25 min

3.4 Light Intensity Measurement - Actinometry

Chemical Actinometers are photochemical systems which can be used to measure Light Intensity (or Optical Radiation Intensity) in terms of the number of photons per second emitted by a radiation source.

For photocatalytic systems this measure is important since it allows the calculation of the apparent quantum efficiency Φ, defined as the initial rate of disappearance of a substrate divided by the theoretical maximum rate of photon adsorption. This assumes that all the photons that enter the photoreactor are adsorbed by the TiO_2 catalyst and that light scattering losses are negligible.

The potassium ferrioxalate actinometer used here is very sensitive within a wide range of wavelengths from 253.7 to 577 nm, and is easy to use [88].

The basis of this actinometer is the reduction of Fe^{3+} ions to Fe^{2+} when a solution of $K_3Fe(C_2O_4)_3$ in sulphuric acid is irradiated with light, the reaction scheme being shown in equations 3.1-3.3.

$$[Fe^{3+}(C_2O_4)_3]^{3-} \longrightarrow [Fe^{2+}(C_2O_4)_2]^{2-} + C_2O_4^- \qquad (3.1)$$

$$[Fe^{3+}(C_2O_4)_3]^{3-} + C_2O_4^- \longrightarrow [Fe^{3+}(C_2O_4)_3]^{2-} + (C_2O_4)^{2-} \qquad (3.2)$$

$$[Fe^{3+}(C_2O_4)_3]^{2-} \longrightarrow [Fe^{2+}(C_2O_4)_2]^{2-} + 2CO_2 \qquad (3.3)$$

The product $Fe(C_2O_4)_2$ does not absorb incident light and the Fe^{2+} ions are determined spectrophotometrically as a red-coloured complex with 1,10-phenanthroline.

The $K_3Fe(C_2O_4)_3.3H_2O$ salt was prepared by mixing 3 volumes of 1.5M $K_2C_2O_4$ solution with 1 volume of 1.5M $FeCl_3$ solution. The precipitated $K_3Fe(C_2O_4)_3.3H_2O$ was recrystallised from warm water and dried in warm air.

For the actinometry experiments a 0.006M solution of $K_3Fe(C_2O_4)_3.3H_2O$ was prepared by dissolving 2.947g of solid in 800ml of water, adding 100ml of 1.0*N* Sulphuric acid and diluting the solution to 1L.

All manipulations of the ferrioxalate solutions were carried out in a darkroom using a red photographic safelight.

A calibration graph for the Fe^{2+} complex with 1,10-phenanthroline was then prepared using the following standard solutions:

(A) 0.4×10^{-6} mol of Fe^{2+} ml^{-1} in sulphuric acid. This is freshly prepared from a standardised $0.1M$ $FeSO_4$ solution which is $0.1M$ in sulphuric acid by dilution with $0.1\ N$ sulphuric acid.

(B) 0.1 per cent by weight solution of 1,10-phenanthroline in water.

(C) A buffer solution prepared from 600ml of $1N$ CH_3COONa and 360ml of $1\ N$ sulphuric acid diluted to 1L.

The standard calibration graph was obtained as follows:

To 0,0.5,1.0,2.0,...,4.0, ml of solution **A** a sufficient amount of $0.1\ N$ sulphuric acid was added to make the total volume 10 ml.

2 ml of solution **B** was added and each diluted to 20 ml with solution **C**.

The standards were mixed and left in the dark for about 1 hr until the red complex had developed. After a certain time the absorbance of each standard was measured at 510 nm in a 1 cm cell, using an iron-free blank as the reference solution.

The calibration data is shown in figure 4.33.

The light intensity in the photocatalytic reactors used was then measured by irradiating ferrioxalate solution of the appropriate concentration contained in the reactor.

The batch reactor was filled with 0.006M ferrioxalate solution, the solution sparged with oxygen-free nitrogen, and the UV light source was turned on for the desired illumination time. The actinometry experiment was carried out in conditions which eliminated as much ambient light as possible, but an actinometer solution left in the laboratory was used as a blank.

After the desired irradiation time (t), the solution was well mixed and an aliquot volume (V_2) of 10 ml was pipetted into a 25 ml volumetric flask. 2ml of the phenanthroline solution was added together with 5 ml of buffer solution. The solution was diluted with water to the 25 ml mark and mixed well. After 1 hr the absorption of the solution was measured at 510 nm using the blank solution as a reference.

The addition of buffer solution and the storage of the phenanthroline in the dark are important in eliminating common irreproducible actinometry results.

The number of Fe^{2+} ions (mol) formed during the irradiation can be calculated from equation 3.4

$$n_{Fe^{2+}} = \frac{V_1 V_3 C_{Fe^{2+}}}{V_2} \qquad (3.4)$$

where,

V_1 = volume of actinometer solution irradiated (ml)

V_2 = volume of aliquot taken for analysis (ml)

V_3 = final volume to which the aliquot (V_2) is diluted (ml)

$C_{Fe^{2+}}$ = concentration of Fe^{2+} ions from calibration (mol/ml)

The number of quanta absorbed by the actinometer (n_a) is given by:

$$n_a = \frac{n_{Fe^{2+}}}{\Phi_\lambda} \qquad (3.5)$$

where Φ_λ is the quantum yield for the Fe^{2+} formation at a particular wavelength found from standard tables [126].

The number of quanta absorbed by the actinometer (n_a) per second is obtained from:

$$n_a = \frac{n_{Fe^{2+}}}{\Phi_\lambda t} \qquad (3.6)$$

where t is the time of irradiation in seconds.

Calibration data and the calculated values of the photon flux found for the batch reactor are shown in section 4.4.

3.5 Dissolved Oxygen Measurement

Measurements of dissolved oxygen concentration (DO) were made with a Jenway 9071 portable DO meter. The meter was calibrated with a sodium sulphite solution (0%) and water saturated air (100%), according to the manufacturers instructions.

3.6 Methyl Viologen Assay

One of the characteristic reactions of TiO_2 semiconductor dispersions is the photoinduced charge induction of electrons from the conduction band to the 1,1'-dimethyl-4,4'-bipyridinium cation, MV^{2+}, to produce the cation radical $MV^{+\cdot}$. Solutions of this species have a characteristic blue colour which can be confirmed

its typical adsorption band at 605 nm [64]. This reaction was used as a simple test of the photocatalytic activity of immobilised catalyst samples.

Experiments were carried out in a Photophysics Cuvette reactor. A solution of methyl viologen was prepared by dissolving 0.18 g in 100 ml of UHQ water. The catalyst samples were added to 2 ml of the stock methyl viologen (MV^{2+}) in a 3 ml quartz cuvette, and the cuvette placed in the sample holder. The cuvette was then illuminated with 350 nm light for 10 minutes. A blue/green fluorescence could be seen as an indication of the formation of the $MV^{+\cdot}$ cation radical. After illumination the sample was filtered through a 0.2 μm syringe filter and the absorbance at 605 nm measured.

A more sensitive measure of the $MV^{+\cdot}$ cation radical was by fluorescence spectroscopy. Samples which had been previously illuminated at 350 nm were excited at 396nm (Perkin Elmer 3000) and the emission at 520nm was measured.

3.7 SEM

All scanning electron microscopy was carried out using a T330 electron microscope (Joel (U.K.) Ltd., Welwyn Garden City, Hertfordshire). Samples of attached catalyst were vacuum dried, mounted on carbon stubs and sputter coated with carbon.

X-ray microanalysis, which was used to identify and map metals on the catalyst surface, was performed using an X-Ray-EDS Link Systems AN10000.

3.8 Catalyst Preparation

Various types of TiO_2 were prepared in the laboratory based on sol-gel techniques with titanium tetraisopropoxide $Ti(OC_3H_7)_4$ as a precursor.

In most experiments it was decided to use methods or adapt methods which produce clear colloidal titania sols. This technique was chosen to produce catalyst films which consisted of layers of quantum sized particles. This gave catalyst having a high efficiency of photoactivation coupled with lower rates of electron-hole recombination than those found in bulk particles.

In order to simplify the description of results obtained, each catalyst type has been assigned an id. with the format SG# (for sol-gel).

Results from these various preparation methods can be found in section 4.3 together with SEM pictures and a discussion as to the suitability of each catalyst for photocatalytic reactions.

3.8.1 General Preparation Methods

The following methods were used to prepare catalyst samples which could be evaluated in the batch-scale reactor.

SG1 In a method adapted from work to produce clear TiO_2 sols [89], 10 ml of titanium tetraisopropoxide ($Ti(OC_3H_7)_4$) was added dropwise to 130 ml ultra pure water acidified with 2 ml of nitric acid (HNO_3) as a peptising agent. The solution was stirred at 50°C for 2-3h until the solution was completely clear. In addition to clearing the solution it was observed that heating caused an increase in solution viscosity making subsequent coating of supports more effective. Thus it was

confirmed that, by careful addition of the alkoxide, the use of a peptising agent, and aging of the solution, a colloidal sol could be produced. It was also found that the resulting solution was clear for 24h after which it became cloudy as TiO_2 precipitates formed.

SG2 Glass ballottini (Jencons), with diameter 1.4 mm, were coated with the sol-gel solution prepared by method SG1. Beads were added to a clear solution and stirred for 10 min before filtering through a Buchner Funnel to allow the recycling of any unused solution. The beads were then transferred to a silica high-temperature crucible and heated at 400°C for 1h.

SG3 After method SG2 the beads were coated with a fine layer of TiO_2 but it was noticed that some of this material was unattached and could be removed easily with gentle rubbing. To avoid this unattached catalyst from interfering in degradation experiments a batch of beads were washed in water and any loose material decanted off.

SG4 It was found that method SG2 left some beads not fully coated with sol-gel prior to firing, partly due to the solution adhesive properties and viscosity and partly due to the filtering process, so a batch was produced by firing beads in a solution filled crucible.

SG5 A batch of glass beads was coated with P25 TiO_2 by mixing with a slurry in water and heating at 120°C until dry.

SG6 It was decided that using colloidal sols did not give sufficient loadings and therefore a batch of beads were coated with TiO_2 from a fast hydrolysis.

20-30g of beads were added to 50 ml $Ti(OC_3H_7)_4$ in a 250ml conical flask. 150ml water was added, first dropwise, then quickly and the mixture stirred. This quick hydrolysis produced large flocculated particles and thick coatings. The mass containing beads and flocculated material was placed in a crucible and fired at 400° C for 1h to give a mixture of coated beads and particulate TiO_2. After cooling the beads were washed and the fine particles decanted off. It was observed that although some areas of the beads were thickly coated, there were areas on most beads which were catalyst free. In addition thick coatings were easily removed by rubbing and/or washing.

SG7 Unsupported particulate TiO_2 was produced using the method SG6 omitting the glass beads.

SG8 Alumina extrudates (BDH) were coated using method SG4. The extrudates were found not to be catalytically active.

SG9 Silica gel particles (BDH) were coated using method SG4. The silica particles were found not to be catalytically active.

SG10 In an attempt to increase the catalyst loading, a batch of glass beads were given 3 coats using method SG4, with a 100 °C drying between each coating, and a final 400 °C sintering for 1h.

SG11 An alternative sol-gel technique [76] using a co-solvent and HCl as a peptising agent was used.

28.4g $Ti(OC_3H_7)_4$ was mixed with 3 ml of isopropyl alcohol. 3.4g of water was mixed with 3 ml isopropyl alcohol and 1.8g HCl. The water/alcohol/acid solution was added dropwise to the alkoxide/alcohol solution and a batch of glass beads stirred into the mixture. Using this method stable clear colloidal solutions were very difficult to produce.

SG12 A method to produce TiO_2 fibres [90] was used in an attempt to produce filaments which could be used in a reactor.

The sol-gel was produced using a ratio of 28.4g $Ti(OC_3H_7)_4$:1.8g H_2O:11.3g isopropyl alcohol:1.8g HCl. The alkoxide was mixed with half of the isopropyl alcohol and the water was mixed with the remaining alcohol and the HCl. The water mixture was added to the alkoxide dropwise and stirred to give a viscous clear solution. Heating the solution at 50°C caused the solution viscosity to increase but it was found that the point at which fibres could be drawn was quickly passed and the solution solidified. It was decided that the method was not stable enough to produce a useful catalyst.

3.8.2 Preparation Methods for Coating of Ceramic Beads

Three methods were used to coat the steatite ceramic beads.

(i) A P25 slurry mixed with the beads was evaporated at 120°C and sintered at 400°C for 1h.

(ii) A standard sol-gel technique SG4 was used along with a modified method using 10ml isopropyl alcohol as a co-solvent; and

(iii) A modified sol-gel method using diethanolamine (DEA) as a stabilising agent

.

The first two methods did not produce a satisfactory coating, only method (iii) gave a clear, hard coating which could not be manually removed.

It has been reported [77] that diethanolamine (DEA) along with other ethanolamines and glycols were able to suppress the precipitation of the oxides from the alcoholic solutions of the metal oxides. This meant that the addition of water was less critical and the hydrolysis and subsequent polymerisation reactions could be controlled. Thus, rapid gel formation, cloudy solutions of oxide precipitates, and solutions of low viscosity leading to poor support coating could all be avoided.

10.5g DEA was added to 28.4g $Ti(OC_3H_7)_4$ and stirred until thoroughly mixed. A mixture of 1.8ml water and 3.6ml ethanol was added dropwise to the alkoxide/DEA solution. The sol-gel solution was then poured over a batch of ceramic beads and fired at 650°C for 1h. The elevated temperature was required to burn off carbon deposited from the DEA solution. This method had the advantage over standard sol-gel methods of producing viscous, clear solutions without the need for heating, aging, or a peptising agent.

3.9 Heat Treatment

All sintering of TiO_2 samples, for heat treatment of TiO_2 tablets and as part of the sol-gel preparation techniques, was carried out in a Carbolite CSF 1100 furnace. Samples were contained in high temperature silica crucibles.

The effectiveness of heat treating TiO_2 tablets was estimated by crushing the samples manually, the changes in strength being pronounced and easily observed.

3.10 Batch Photocatalysis

All batch photocatalysis experiments were carried out in the reactor shown in figure 3.4.

The batch reactor consists of a glass vessel with an inlet and sintered glass plate for gas sparging, and a sampling port with septum seal. A quartz inner sleeve, with a jacket for cooling, is fitted into the glass vessel with a ground glass seal. The UV light source is contained within the quartz sleeve therefore giving a standard annular photoreactor configuration. The total reactor volume was 500ml and the annular gap was 1cm.

Stock solutions of atrazine were prepared in a volumetric flask and stirred until the atrazine had dissolved. Due to the low solubility of atrazine (≈30 mg/L @ 20 °C) the stock solutions were filtered before use to remove undissolved solids and the initial concentrations checked by comparison with HPLC calibrations.

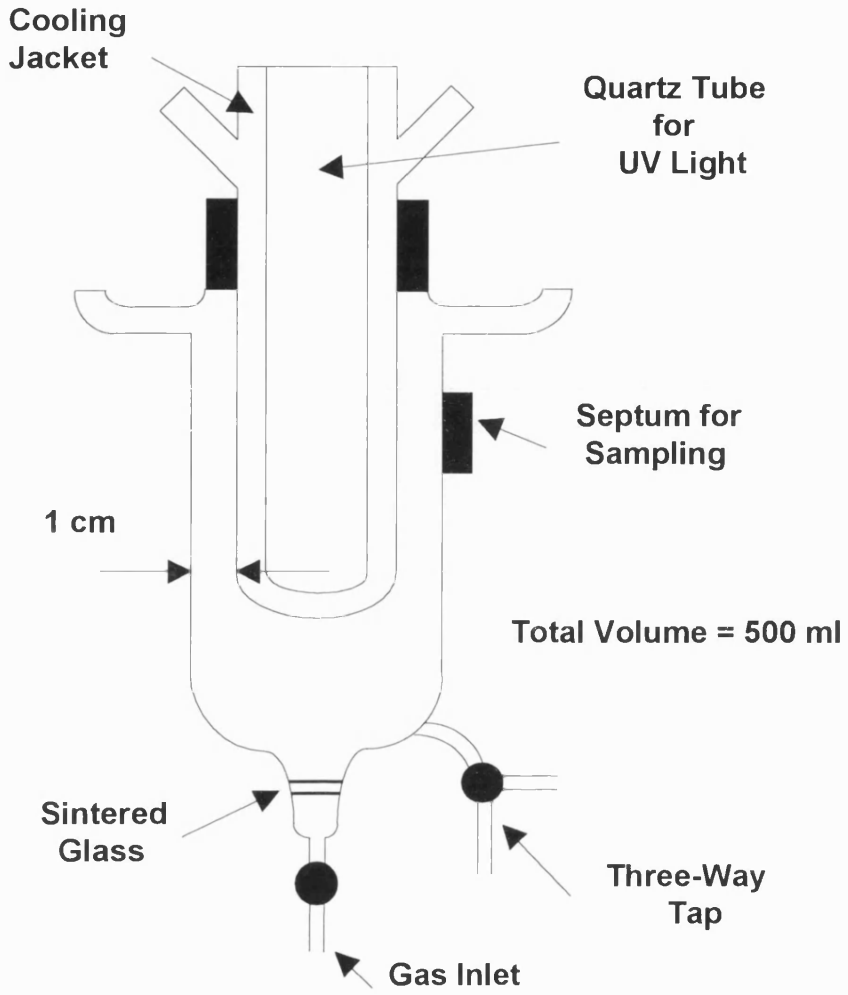

Figure 3.4: *Reactor for Batch Photocatalysis Reactions.*

The amount of catalyst required for a particular experiment was weighed and added to an atrazine solution of the required starting concentration. This mixture was then added to the batch reactor. At time=0 a sample was taken with a syringe through the septum, the UV lamp turned on, and samples taken from then on at regular intervals throughout the experiment as required. Air could be sparged through a rotameter to the reactor gas inlet. Sample size withdrawn for direct HPLC

injection was 0.5 ml (about the minimum vial volume possible). A schematic of the batch reactor set-up is shown in figure 3.5.

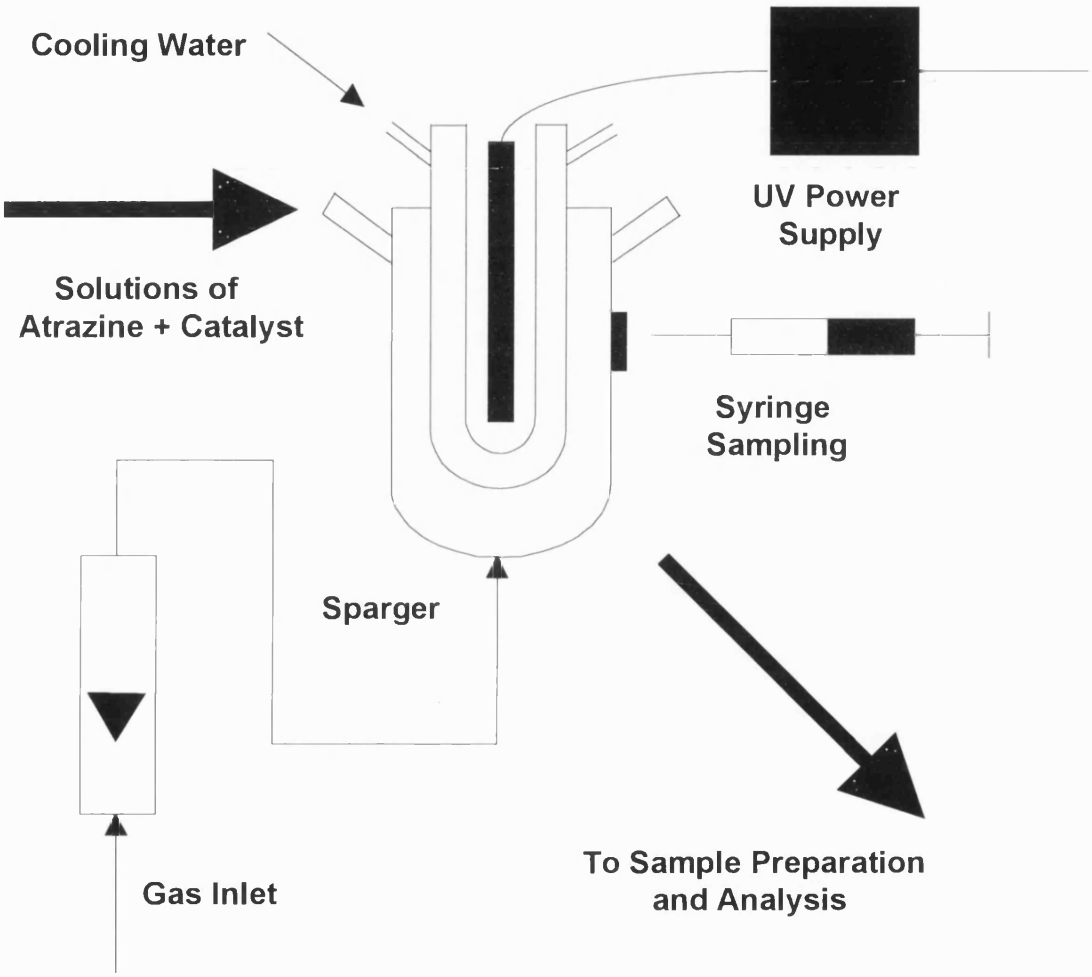

Figure 3.5: *Schematic of the Batch Reactor Experiments*

At the end of experiments where the reaction intermediates were to be analysed by GC-MS analysis, the reactor contents were removed through the drain valve and the SPE procedure carried out as in section 3.2.

3.11 Pilot Scale Reactor

A schematic of the pilot reactor is shown in figure 3.6a. It consists of a holding tank from which pollutant solutions are pumped, through a rotameter, to the reactor inlets. The inlets were situated at the base of the reactor and were positioned so as to impart a swirl motion to the flow in the reactor. The reactor itself was an annular type with a quartz inner sleeve, the dimensions shown in figure 3.6b. This design was intended to provide both good mixing and a longer residence time in the reactor.

The exit from the reactor returns the reactants to the holding tank, passing through a water cooled heat exchanger. Samples were taken from a tap beneath the holding tank and the catalyst was added through an inlet at the top of the reactor.

In order to prepare low concentrations of atrazine (ng/L) a known amount of stock solution was pipetted into the holding tank and diluted with softened water until the desired concentration had been reached. The atrazine solution was then circulated through the system at a low flowrate until thorough mixing had occurred (1 hr). Samples of ≈1L were collected in brown glass Winchester bottles, the exact volume calculated by weighing prior to and after extraction.

A sample at time=0 was taken and the experiment started by switching on the UV lamp. Addition of oxygen, which could start at time=0 or at time<0 as desired, was controlled and measured by a rotameter and entered the system through two sintered glass spargers in each of the reactor inlets. A nitrogen purge through the inner sleeve containing the UV lamp expelled air and prevented potentially hazardous ozone production by direct photolysis.

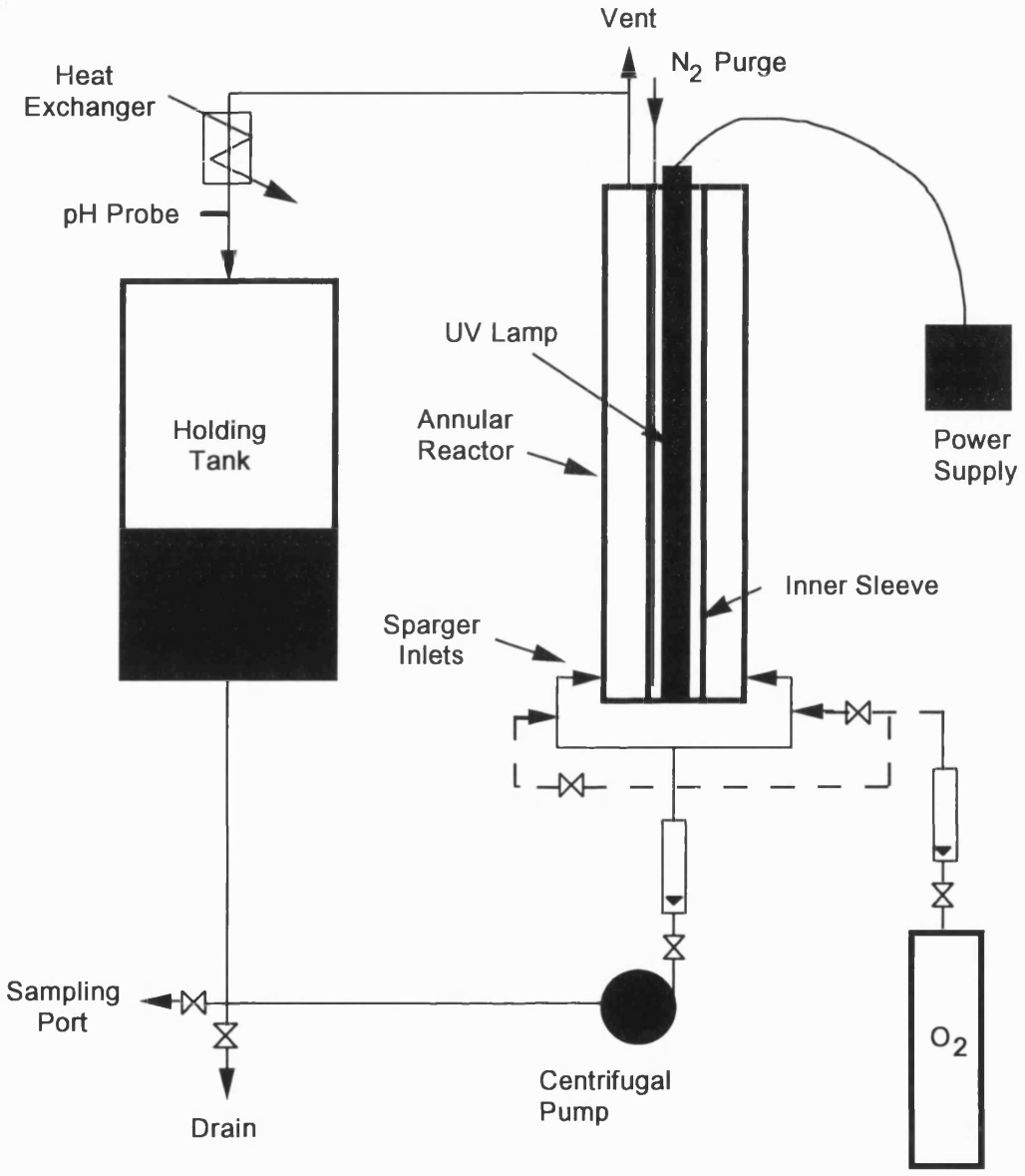

Figure 3.6a: *Schematic of the Pilot Scale Experimental Rig.*

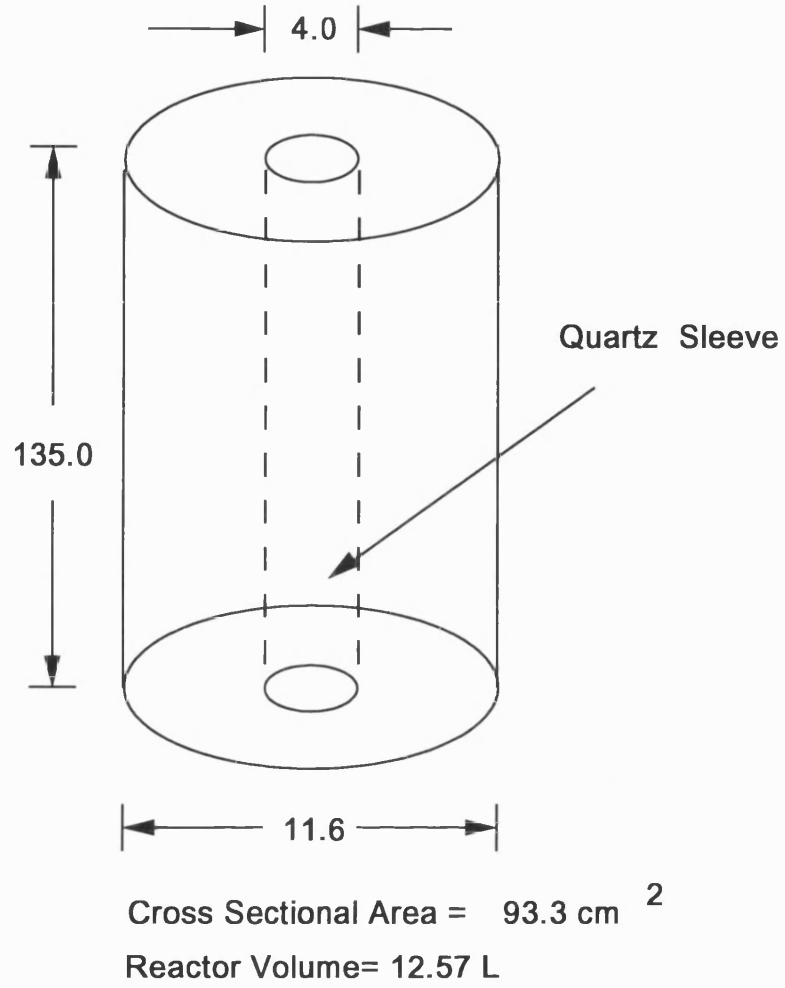

Figure 3.6b: *Pilot Scale Reactor Dimensions.*

Dissolved oxygen concentration, pH, and temperature were monitored throughout the duration of the experiment.

At the end of the experiment the oxygen sparge was stopped, the UV lamp turned off and the valve at the bottom of the reactor closed. This prevented catalyst from being sucked out of the reactor and blocking the inlet lines. Once the valve was closed, the pump was switched off and the reactor drained. The apparatus was then rinsed thoroughly with softened water prior to the next experiment.

3.12 Other Free-Radical Generating Systems

Atrazine degradation experiments were also carried out using two systems where free-radical reactions are known to play a part. This was done to compare the reaction intermediates formed with those detected from photocatalysis experiments.

Fentons reagent is a known hydroxyl free-radical generating system and has been used to study the dealkylation of s-triazine herbicides [91].

3.12.1 Sonication of Atrazine

In the sonication experiment, 50 ml of 30 mg/L atrazine dissolved in UHQ water was sonicated for 2h in a "Soniprep 150" at a power level of $\approx$28 W cm^{-2} . Samples were taken from solution at regular intervals and analysed by HPLC and GC-MS analysis as described previously.

3.12.2 Fentons Reagent Experiment

In the experiment carried out with Fentons reagent, 10 ml of a 30% solution of acidified hydrogen peroxide was added to 100 ml of an atrazine solution containing 8 g of ferrous sulphate-hexahydrate. The solution was stirred for 1 h. At the end of this period a sample was extracted and analysed by GC-MS as described previously.

3.13 Curve Fitting

All fitting of experimental data to model equations was carried out using the UltraFit software package (Biosoft, Cambridge, UK). Ultrafit is a non-linear curve fitting package which allows data to be fitted to either one of a number of preset basic equations (such as exponential decay / first order kinetics) or to user defined

equations. The package uses the Marquardt algorithm which is a standard non-linear least-squares method.

4 Results and Discussion

The presentation of experimental results and discussion will be divided into 2 main sections corresponding to results obtained with either a small-scale batch reactor or the large-scale pilot reactor.

(i) Batch scale experiments were carried out, initially to provide real samples for the validation of the sample preparation and analysis techniques chosen, and also to provide data on the degradation rates of atrazine found in a batch photoreactor. The effect of some important experimental variables were investigated, in particular those which would play an important part in any system treating potable (domestic) water.

Samples from these batch experiments were also used to determine the presence of reaction intermediates by GC-MS analysis, as described in section 3.3.2.

(ii) Pilot scale experiments were carried out to examine the effectiveness of the photocatalytic treatment of low levels of atrazine (ng/L) using a number of catalyst types in the reactor described in section 3.11.

In section 4.3 the supported catalysts which have been prepared for use in the photocatalytic reactors are discussed. Included are SEM pictures of some of the coated glass beads and results from the methyl viologen assay used as a measure of catalytic activity.

Results from the actinometry experiments are given in section 4.4 and the kinetic analysis of atrazine and reaction intermediate data is shown in section 4.5.

4.1 Batch Scale Degradation of Atrazine

A typical set of experimental data obtained from a batch degradation of atrazine is shown in figures 4.1a-d. The HPLC traces show a number of important points:

(i) The peak height corresponding to atrazine reduces with time

(ii) A number of peaks corresponding to reaction intermediates appear at times >0

(iii) With time, the intermediate peaks shift to shorter retention times.

The reduction in the atrazine peak points to the loss of the primary compound although the corresponding appearance of a number of other peaks shows that this is not destruction (mineralisation) but a conversion to intermediate products. The number of these additional peaks also suggests that the destruction process is complex and that at any one time in the degradation process there will be a range of intermediates present.

In general, as the atrazine molecule is broken down, the intermediates become smaller (lower molecular weight), more polar in character as they become hydroxy substituted, and show less retention on the reverse phase C8 HPLC packing. As has been shown in section 3.3.1, the retention times for known reaction intermediates follow the trend:

atrazine> desethyl atrazine> desisopropyl atrazine> desethyl-desisopropyl atrazine

It can be seen from figure 4.1 that as the reaction proceeds the peak corresponding to desethyl-atrazine (at retention time 9.3 min) increases, as it is formed from the parent molecule, and then decreases as it, in turn, is degraded into a smaller or more polar intermediate. Figure 4.1d illustrates a reaction time at which atrazine (retention time 17.2 min), desethyl atrazine, a low concentration of desisopropyl atrazine (retention time 6.4 min), and desethyl-desisopropyl atrazine (retention time 3.6 min) are all present.

A graph showing these changes in atrazine and intermediate concentration with reaction time for typical experimental data is shown in figure 4.2.

For this experiment, after a reaction time of 60 min, concentrations of atrazine, desethyl and desisopropyl intermediates have been reduced to below detection limits and production of desethyl-desisopropyl atrazine has reached a maximum.

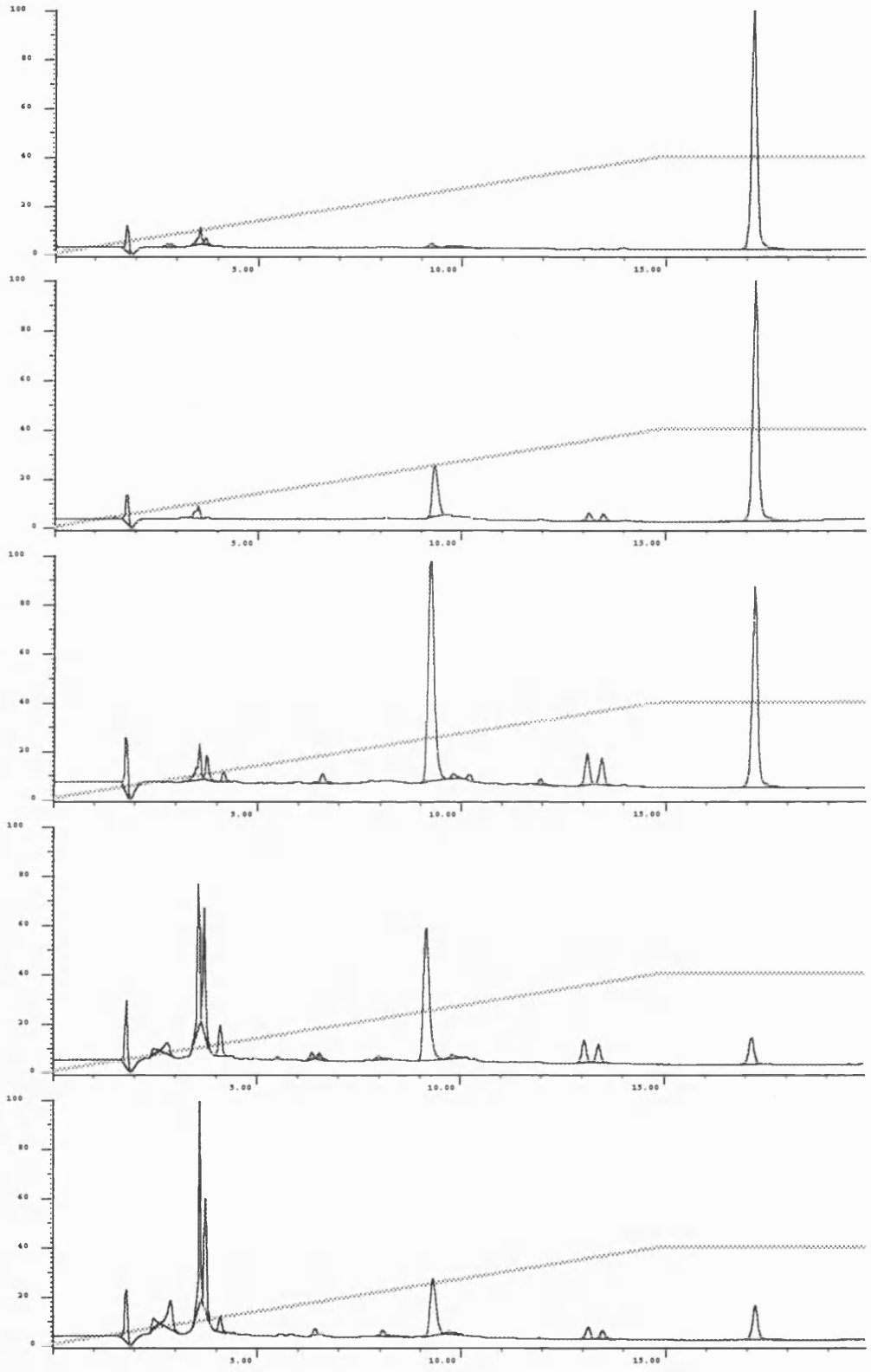

***Figure 4.1**: Typical Set of Experimental HPLC Traces Obtained From the Batch Degradation of Atrazine. Top- 0 min, 5 min, 15 min, 30 min, 60 min - Bottom.*

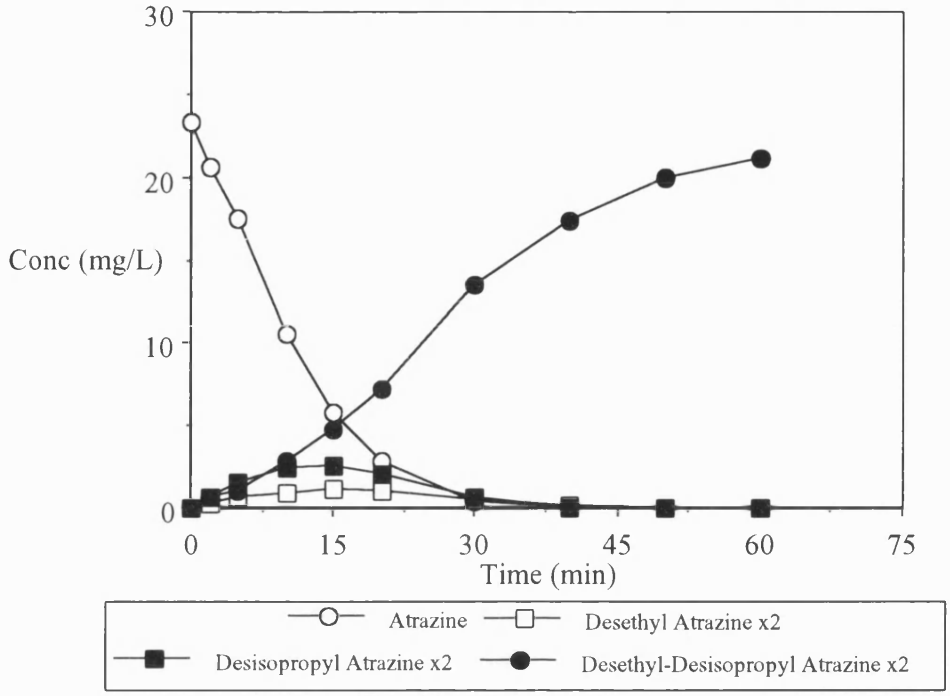

Figure 4.2: *Example of the Degradation of Atrazine and Intermediate Production. (Concentration of Intermediates x2 for Clarity)*

Results obtained from these HPLC analyses offer little insight into reaction schemes, but the possible pathways involved are discussed later in section 4.1.2.

At the reaction times studied and for most catalyst types, little or no reduction in desethyl-desisopropyl atrazine or production of cyanuric acid (the final product formed by the photocatalytic degradation of atrazine found in other studies [40,48,38]) was found.

In the following discussion of experimental results the rates of formation of the major intermediates, and in particular the desethyl-desisopropyl compound, has been used as a further indication of the effectiveness of the degradation process rather than relying solely on the rate of degradation of the parent compound, atrazine.

4.1.2 Identification of Reaction Intermediates

As has already been shown, results from HPLC analysis show that a large number of reaction intermediates are formed in the photocatalytic degradation of atrazine. By comparison with the retention times found for pure standards, the presence of the major dealkylated molecules found by other studies [48,57] has been confirmed. In order to give a more definite confirmation and to attempt to identify some of the other intermediates, samples from batch scale degradation experiments were extracted, concentrated by SPE, and analysed by gas chromatography - mass spectroscopy using the procedure described in section 3.2.

A typical set of results from one such analysis, including GC trace and peak spectra analysis, is shown in figure 4.3.

Using the HP Chemstation software, a library of spectra data can be searched for each peak, the results matched to a table of possible compounds, with a corresponding value for the accuracy of the fit expressed as a percentage.

For compounds not held in the software library or for matches where there is only a poor fit, possible compounds may be identified by knowledge of the possible reaction pathways and a manual interpretation of the mass spectra.

A number of experiments were carried out specifically for GC-MS analysis using high initial atrazine concentrations (to maximise intermediate concentrations), short reaction times (to maximise to range of intermediates). Data from other reaction systems known to involve free radical mechanisms (sonication [92], Fentons reagent [93]) was also obtained.

Data from each separate experiment is presented in tabular form in appendix B1 giving the mass ion, the position of the other major ions, information on whether a Cl atom is present (shown by the chlorine isotope mass appearing 2 units higher than the mass ion at approx. 1/3 of the abundance), and a cross reference with a known compound structure shown in figure 4.4a or a possible compound structure shown in figure 4.4b.

Pages 74-84

Figure 4.3: *Typical GC-MS Trace and Associated Peak Spectra Analysis*

File: H:\RUNR12\0201002.D
Operator: David
Date Acquired: 23 Aug 92 1:07 am
Method File: atreyth7.M
Sample Name: Extraction from R12
Misc Info:
ALS vial: 2

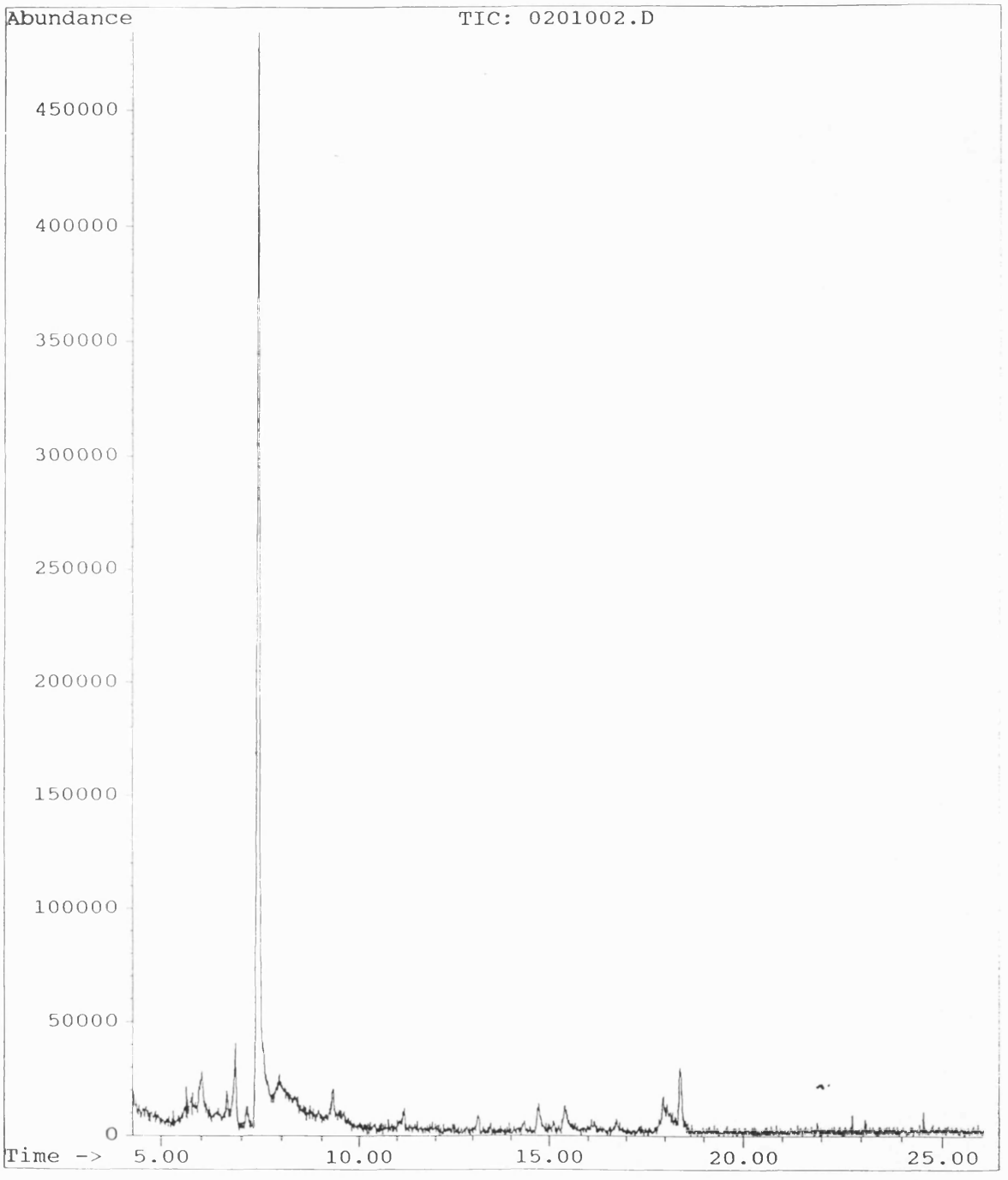

File: H:\RUNR12\0201002.D
Operator: David
Date Acquired: 23 Aug 92 1:07 am
Method File: atreyth7.M
Sample Name: Extraction from R12
Misc Info:
ALS vial: 2

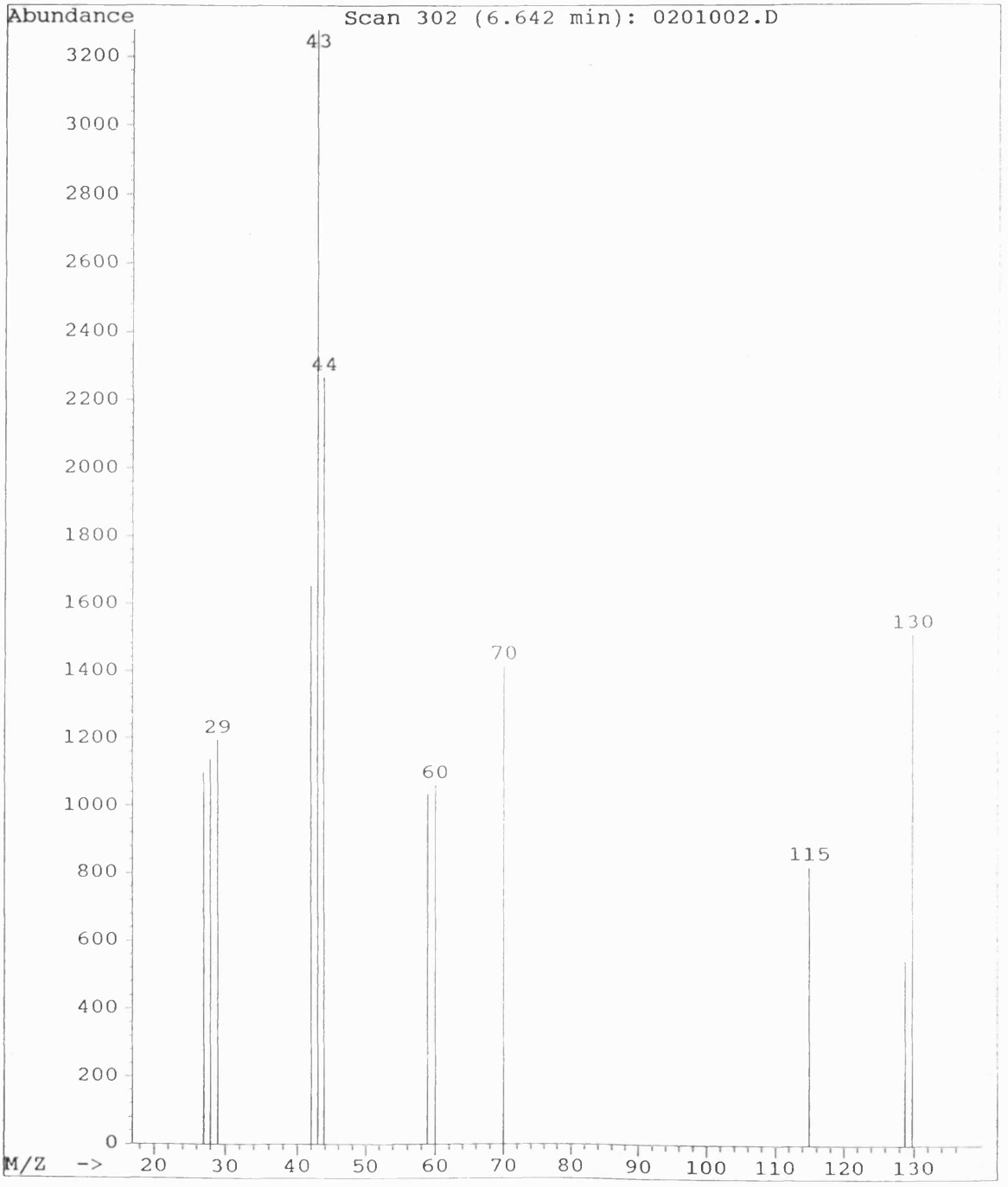

Library Searched : NBS49K.L
Quality : 42
ID : 1,3,5-Triazine-2,4,6(1H,3H,5H)-trione

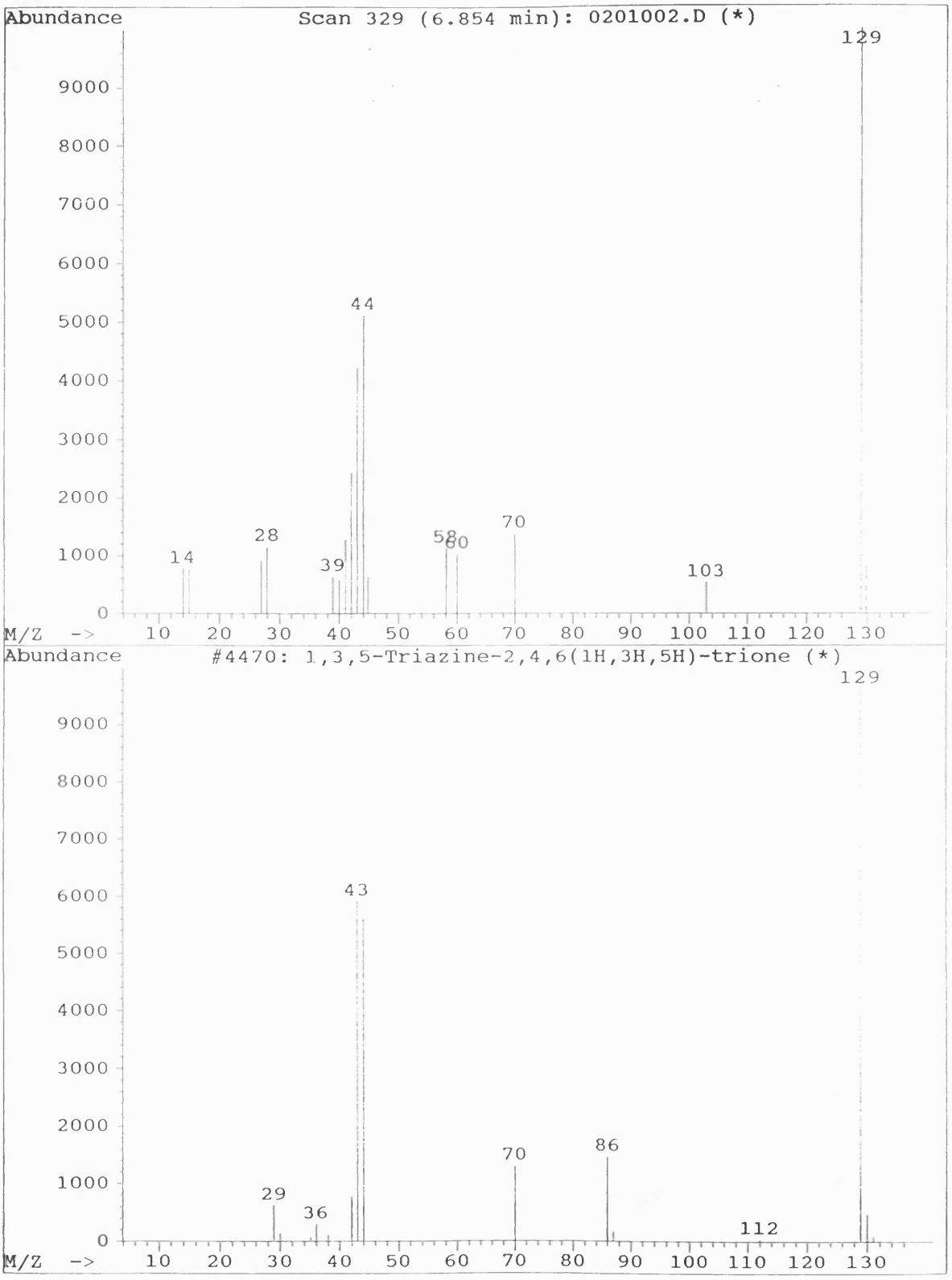

Library Searched : NBS49K.L
Quality : 42
ID : 1,3,5-Triazine-2,4,6(1H,3H,5H)-trione

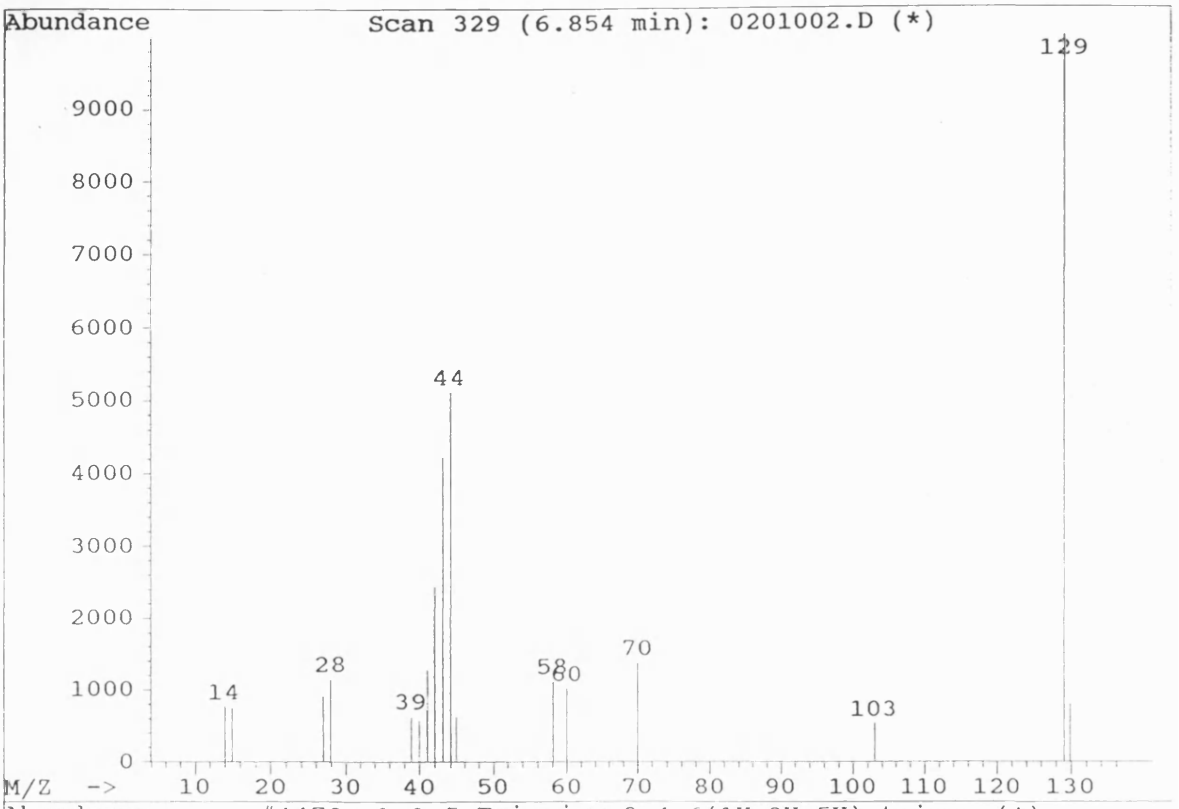

File: H:\RUNR12\0201002.D
Operator: David
Date Acquired: 23 Aug 92 1:07 am
Method File: atreyth7.M
Sample Name: Extraction from R12
Misc Info:
ALS vial: 2

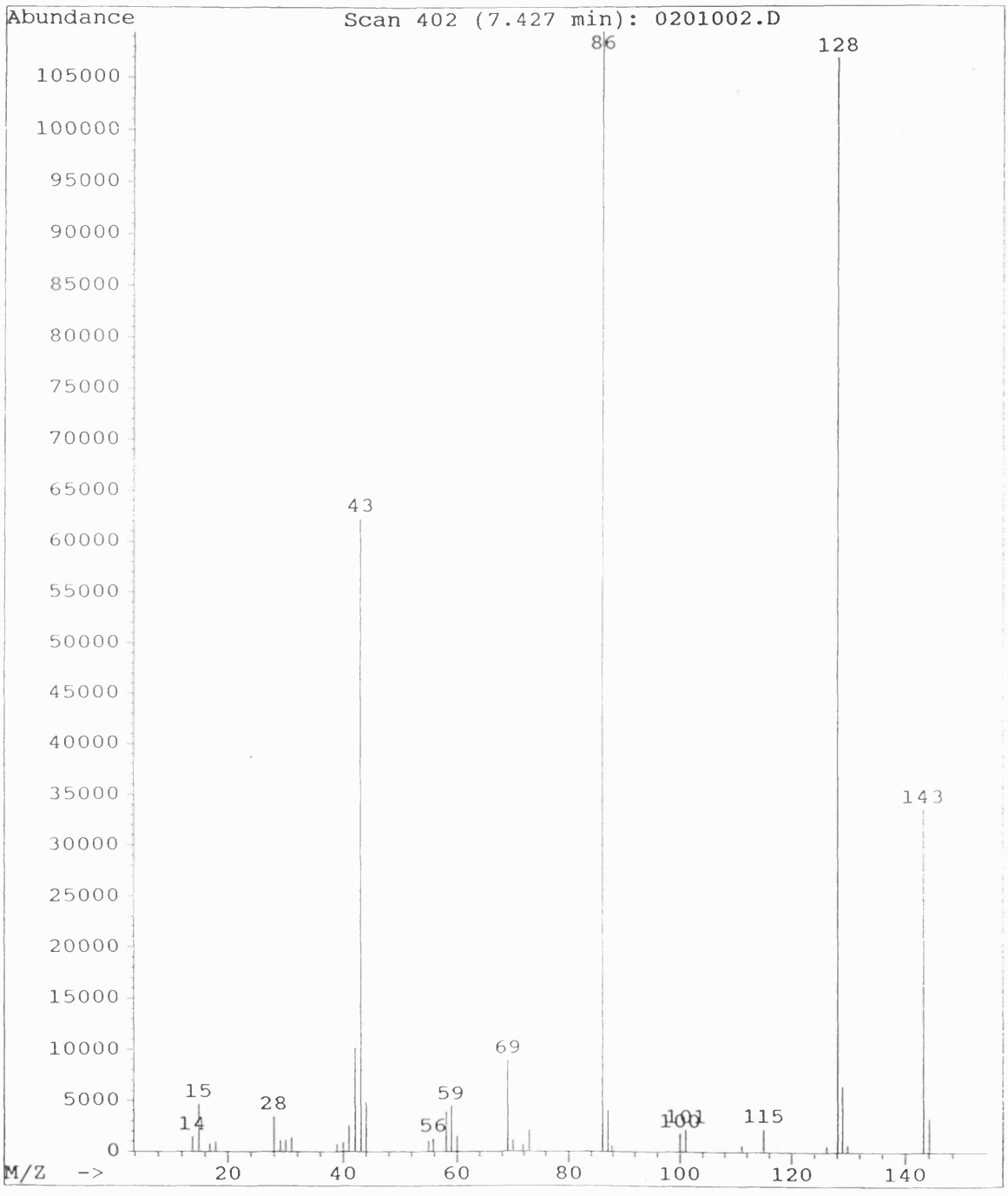

File: H:\RUNR12\0201002.D
Operator: David
Date Acquired: 23 Aug 92 1:07 am
Method File: atreyth7.M
Sample Name: Extraction from R12
Misc Info:
ALS vial: 2

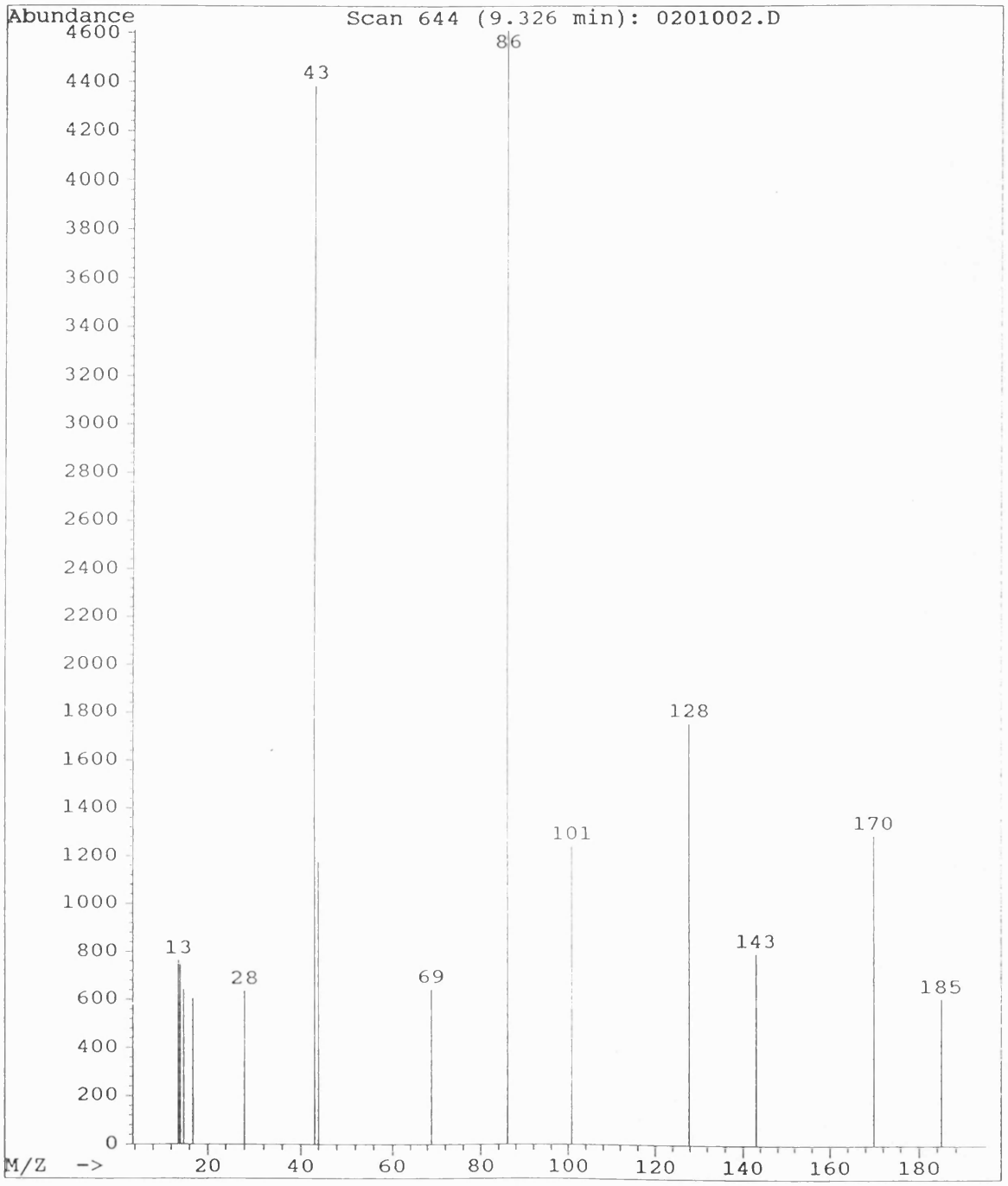

File: H:\RUNR12\0201002.D
Operator: David
Date Acquired: 23 Aug 92 1:07 am
Method File: atreyth7.M
Sample Name: Extraction from R12
Misc Info:
ALS vial: 2

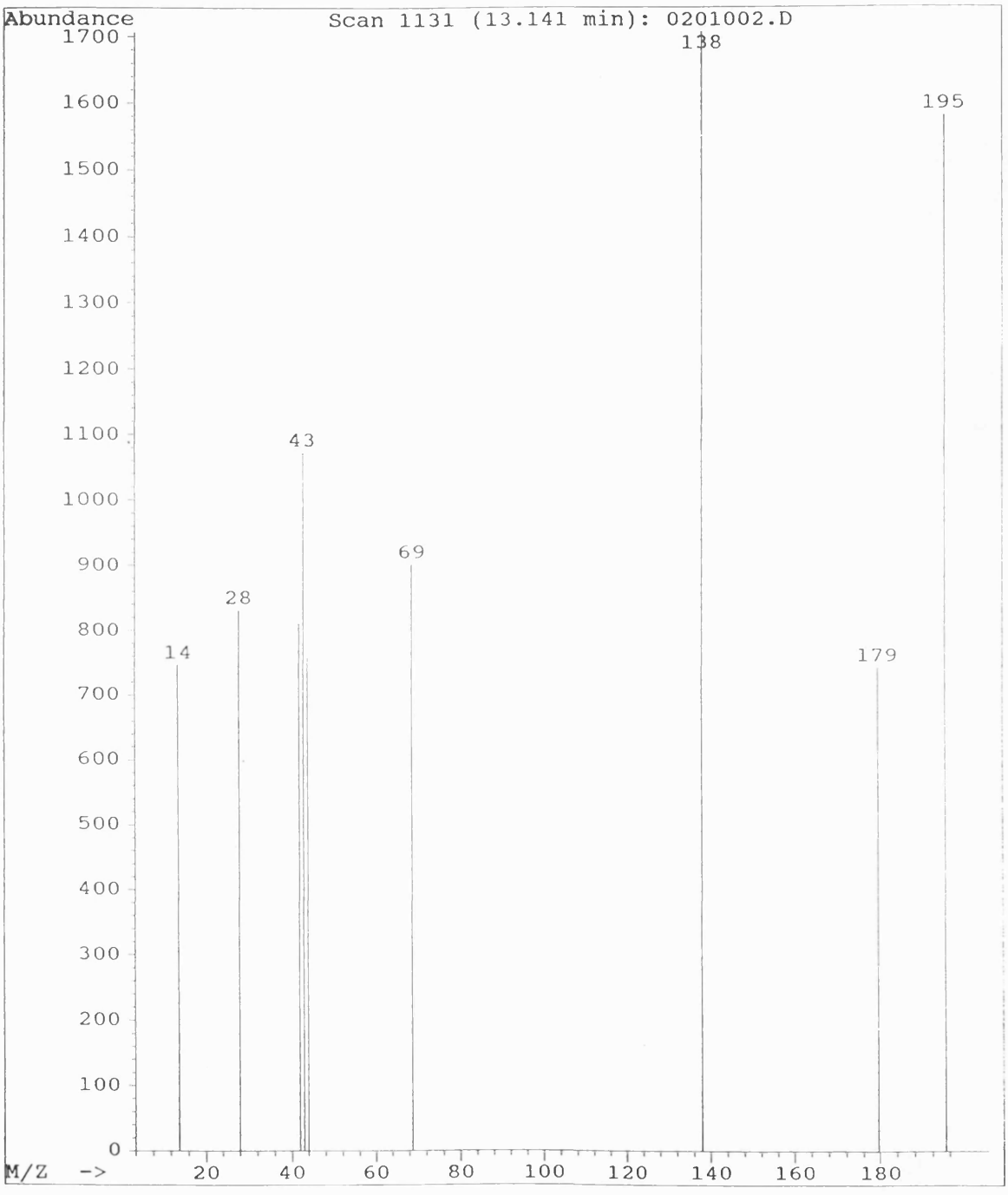

File: H:\RUNR12\0201002.D
Operator: David
Date Acquired: 23 Aug 92 1:07 am
Method File: atreyth7.M
Sample Name: Extraction from R12
Misc Info:
ALS vial: 2

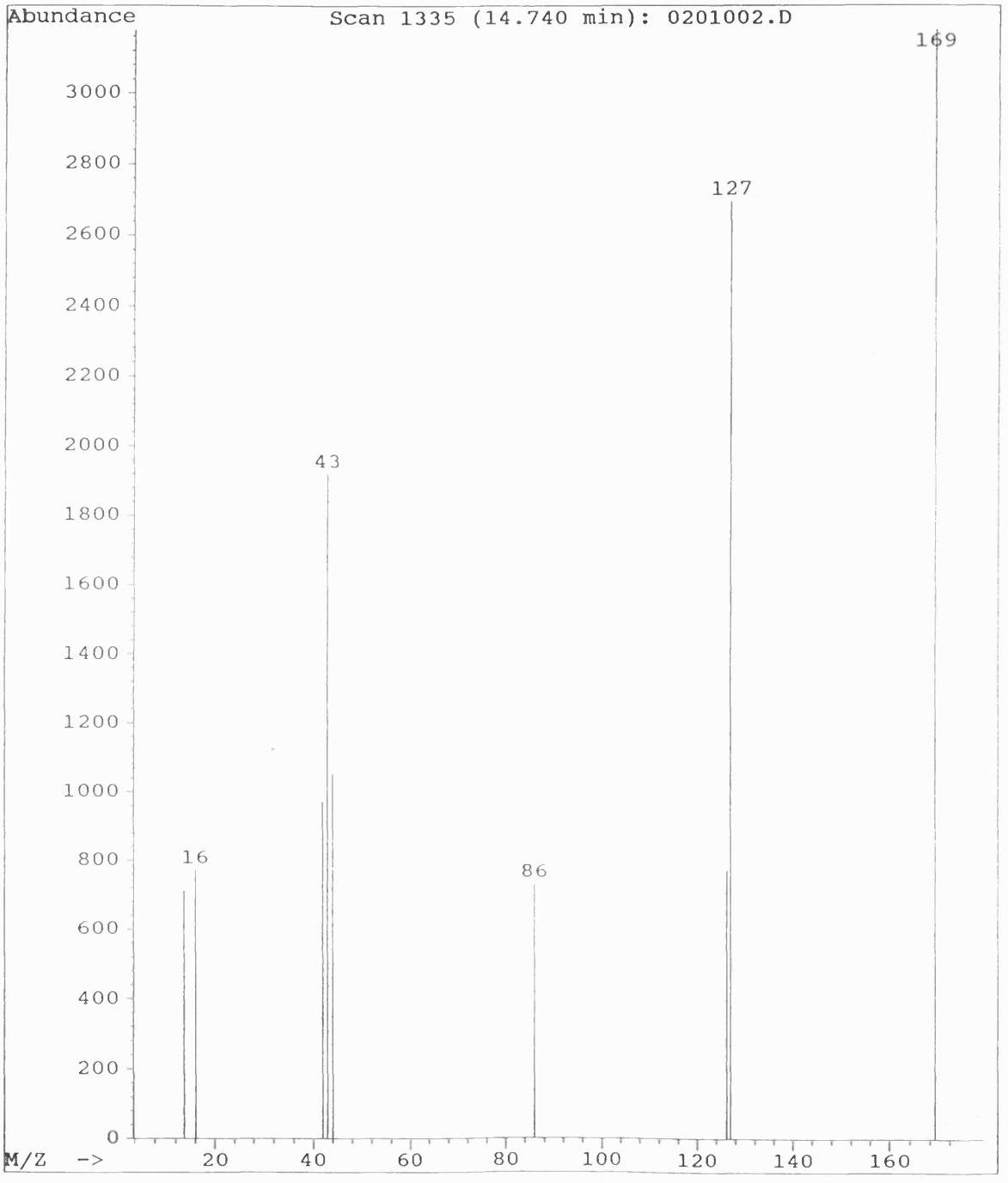

File: H:\RUNR12\0201002.D
Operator: David
Date Acquired: 23 Aug 92 1:07 am
Method File: atreyth7.M
Sample Name: Extraction from R12
Misc Info:
ALS vial: 2

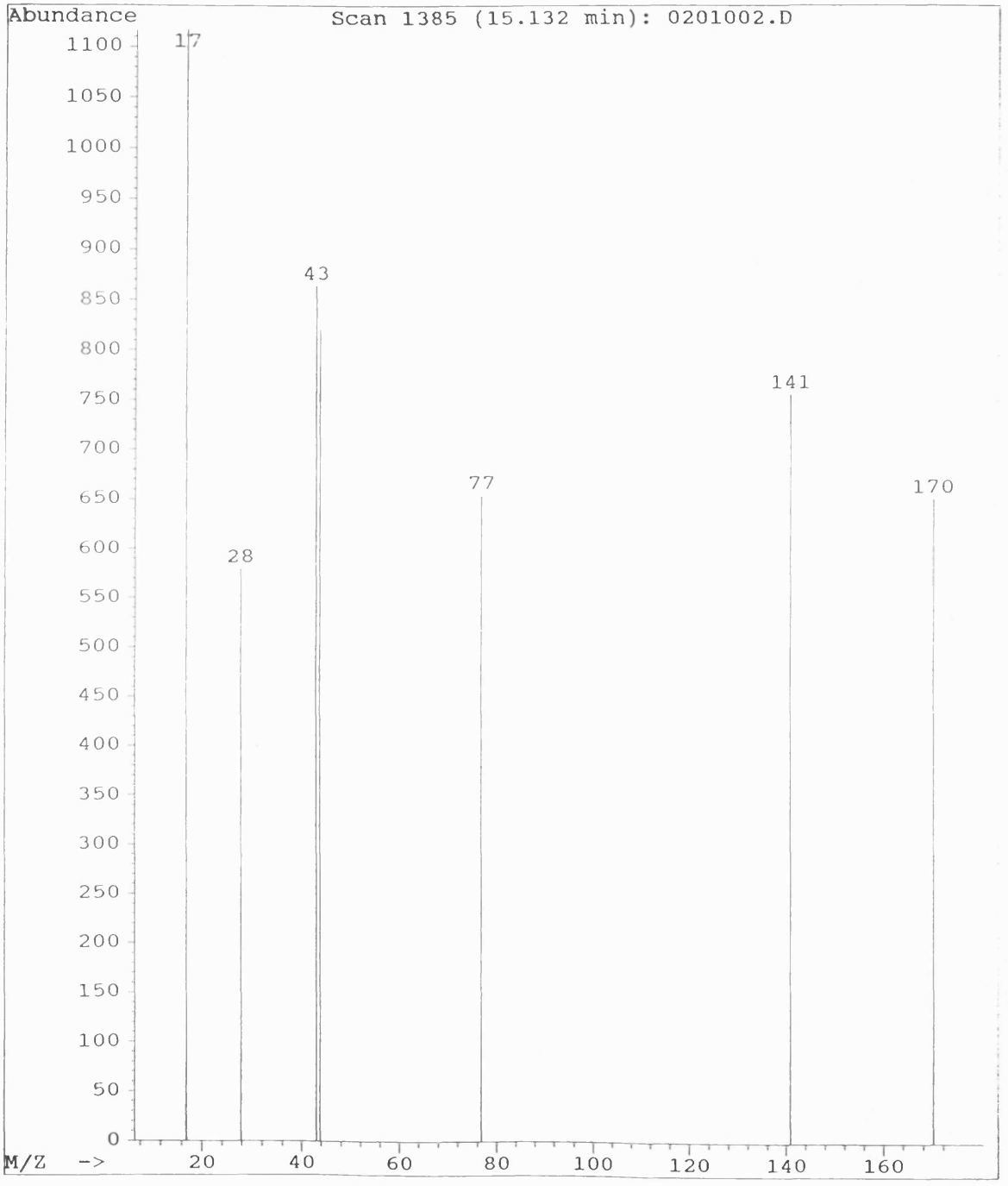

File: H:\RUNR12\0201002.D
Operator: David
Date Acquired: 23 Aug 92 1:07 am
Method File: atreyth7.M
Sample Name: Extraction from R12
Misc Info:
ALS vial: 2

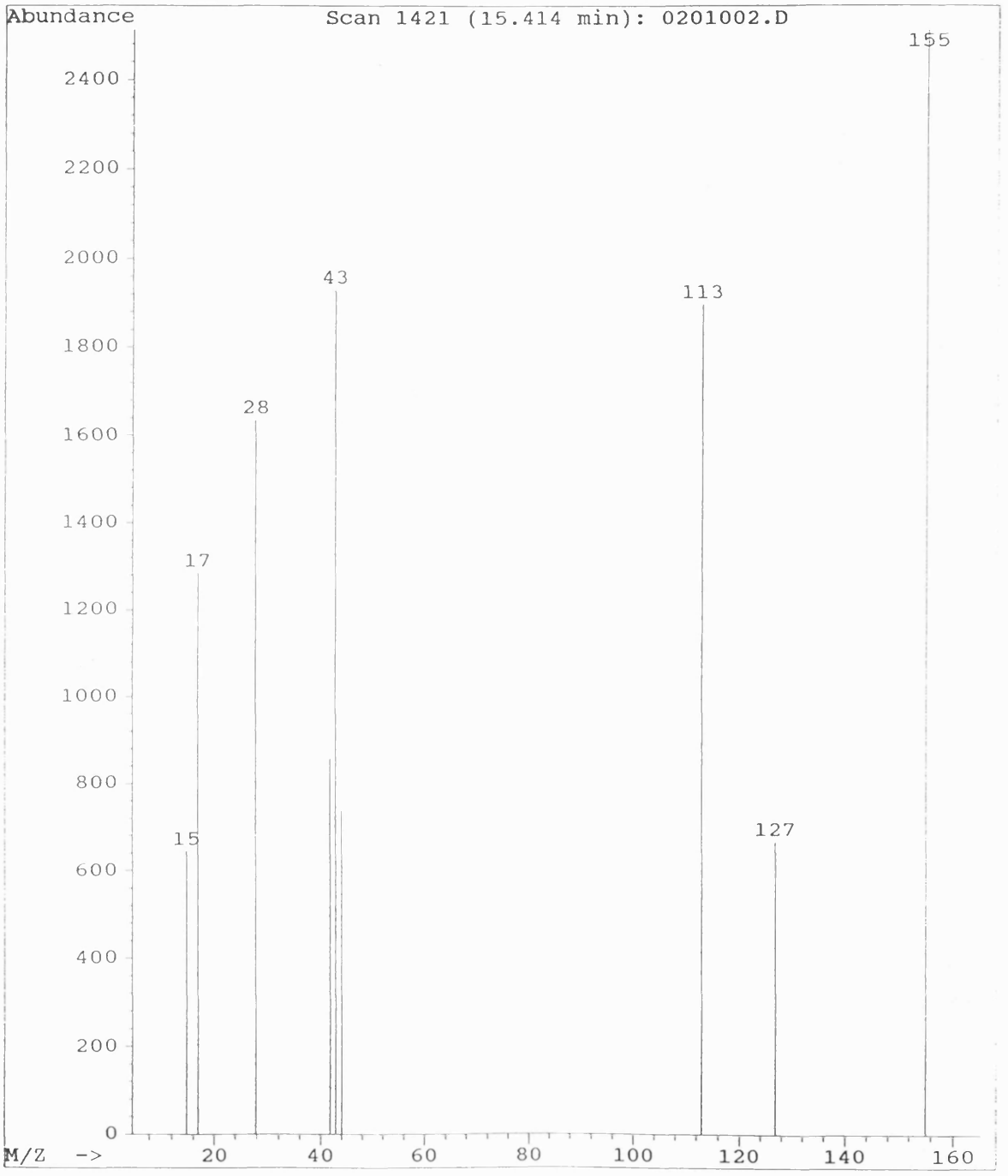

File: H:\RUNR12\0201002.D
Operator: David
Date Acquired: 23 Aug 92 1:07 am
Method File: atreyth7.M
Sample Name: Extraction from R12
Misc Info:
ALS vial: 2

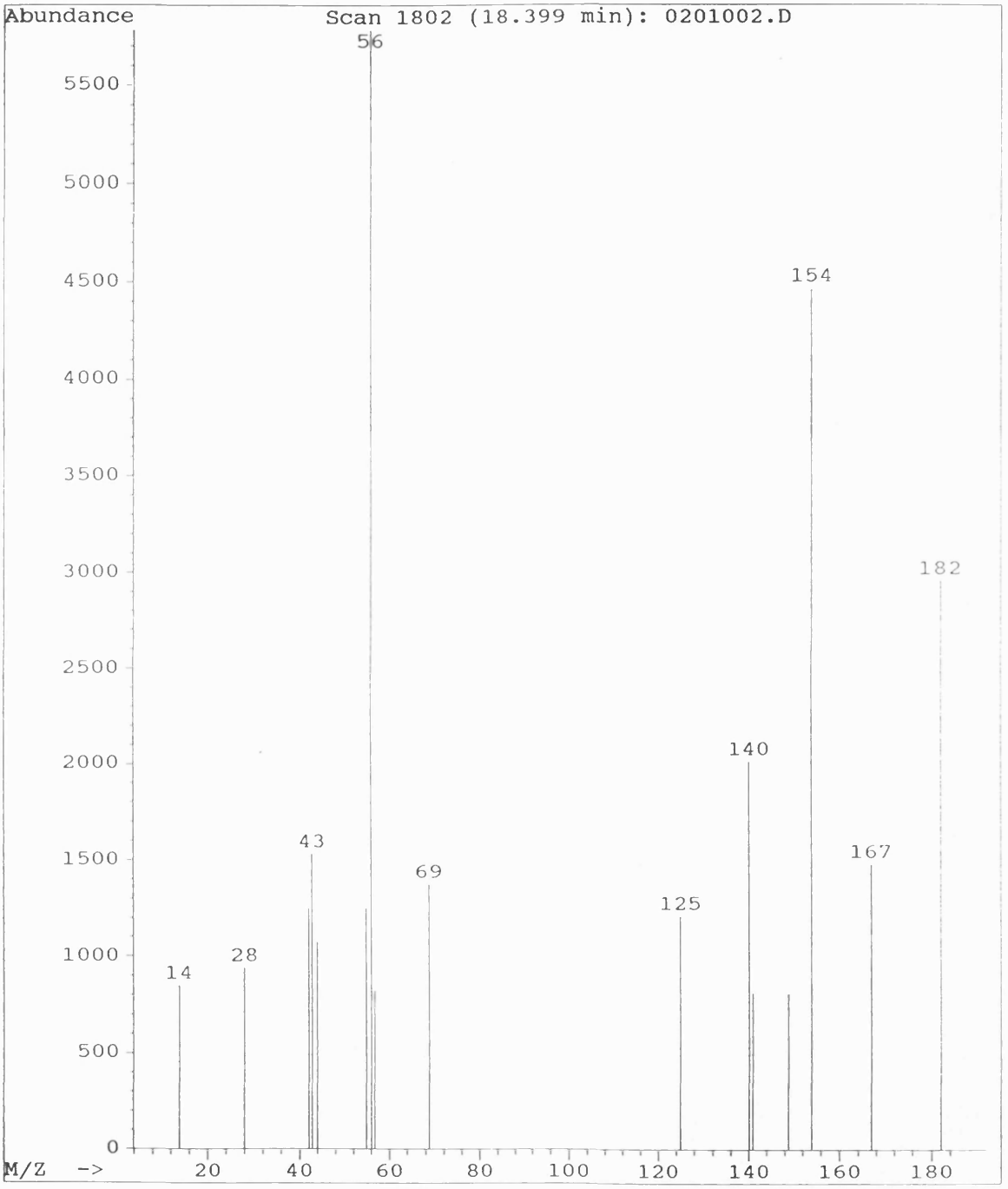

The deduction of compound structure is based on the ionisation of major side groups each giving rise to an ion at a value of (mass ion - molecular weight of fragment) known as a neutral loss. Some of these characteristic neutral losses are given in table 4.1.

Table 4.1: *Some Characteristic Mass Spectroscopy Neutral Losses.*

Mass	**Composition**	**Possible Functionality**
15	CH_3	methyl
16	CH_4	methyl
	NH_2	amide
17	OH	acid, tert. alcohol
18	H_2O	alcohol, aldehyde
26	C_2H_2	aromatic
28	CO	phenol
29	C_2H_5	alkyl
30	CH_2O	methoxy
31	CH_3O	methoxy
35	Cl	chloro compound
36	HCl	chloro compound
42	CH_2CO	acetate
43	C_3H_7	propyl

It has also been found [94] that the mass spectra of the closely related s-triazines, simizine and propazine, give rise to a number of characteristic low mass ions (m/e 42,43,44,55,62,69,87,104,110) and the presence of some of these in the spectra of atrazine intermediates also gave confirmation that these were indeed triazine intermediates.

The spectra of the parent molecule atrazine showed decomposition with loss of CH_3 and $CH_3CH{=}CH_2$ to give the m/e 200 and 173 ions. Spectra obtained for atrazine and known intermediates, where standards are available, are shown in appendix B2 and the spectra data obtained from degradation experiments are shown in appendix B1. Using the analysis techniques described above, comparing possible neutral ion losses with known reaction pathways, possible structures for some of these compounds have been hypothesised and are shown in figure 4.4b.

It should be noted that in order to confirm these compounds, further work, not covered in this study, would be necessary using purified standards. It can be said however that a number of oxidised compounds with substituted CH_3O, C=O and CHO groups have been tentatively identified. These are all oxidised forms of atrazine or dealkylated intermediates, which would be expected in a highly oxidising environment such as that found in a photocatalytic reaction system.

An important practical outcome of this study is the number and range of intermediate compounds formed. This would be undesirable in the validation of any such system used for water purification. The process which makes photocatalytic oxidation an effective destructive purification method, namely the presence of highly oxidising hydroxyl free radicals, is also one of the major drawbacks. The indiscriminate and complex reaction scheme can lead to the potential formation of many complex intermediate forms via free radical reactions. In addition it can be assumed that in a multicomponent system where the number of possible side reactions is increased, the formation of reaction intermediates will be further complicated and the presence of potentially harmful compounds will be difficult to predict.

The major intermediates found in previous studies on atrazine degradation [48,57] namely desethyl, desisopropyl atrazine, desethyl-desisopropyl atrazine and compound C with m/e 187, 173, 145 and 229 respectively have all been found in the present study.

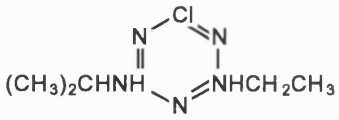

Atrazine

215

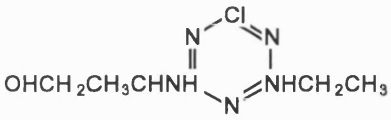

A

231

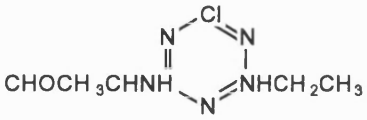

B

229

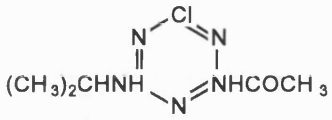

C

229

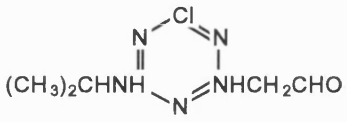

D

229

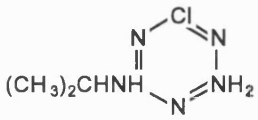

E

187

Desethyl Atrazine

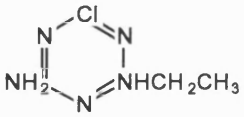

F

173

Desisopropyl Atrazine

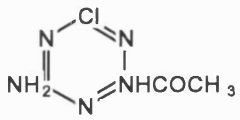

G

187

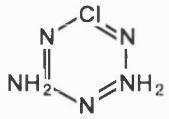

H

145

Desethyl-Desisopropyl Atrazine

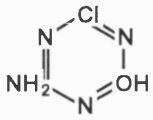

I

146

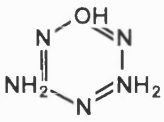

J

127

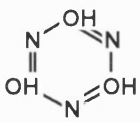

K

129

Figure 4.4a: *Previously Identified Reaction Intermediates from the Photocatalytic Degradation of Atrazine.*

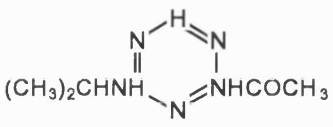

L

195

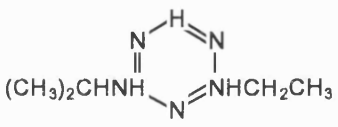

M

181

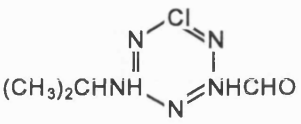

N

215

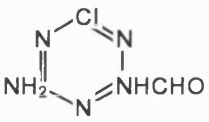

O

173

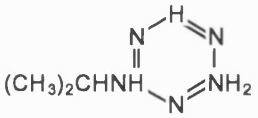

P

153

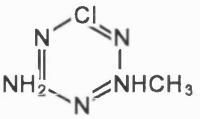

Q

159

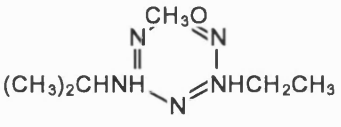

R

211

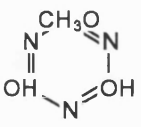

S

143

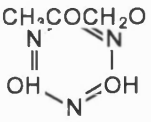

T

185

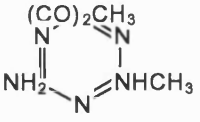

U

181

Figure 4.4b: *Further Reaction Intermediates Identified from the Photocatalytic Degradation of Atrazine by GC-MS Analysis.*

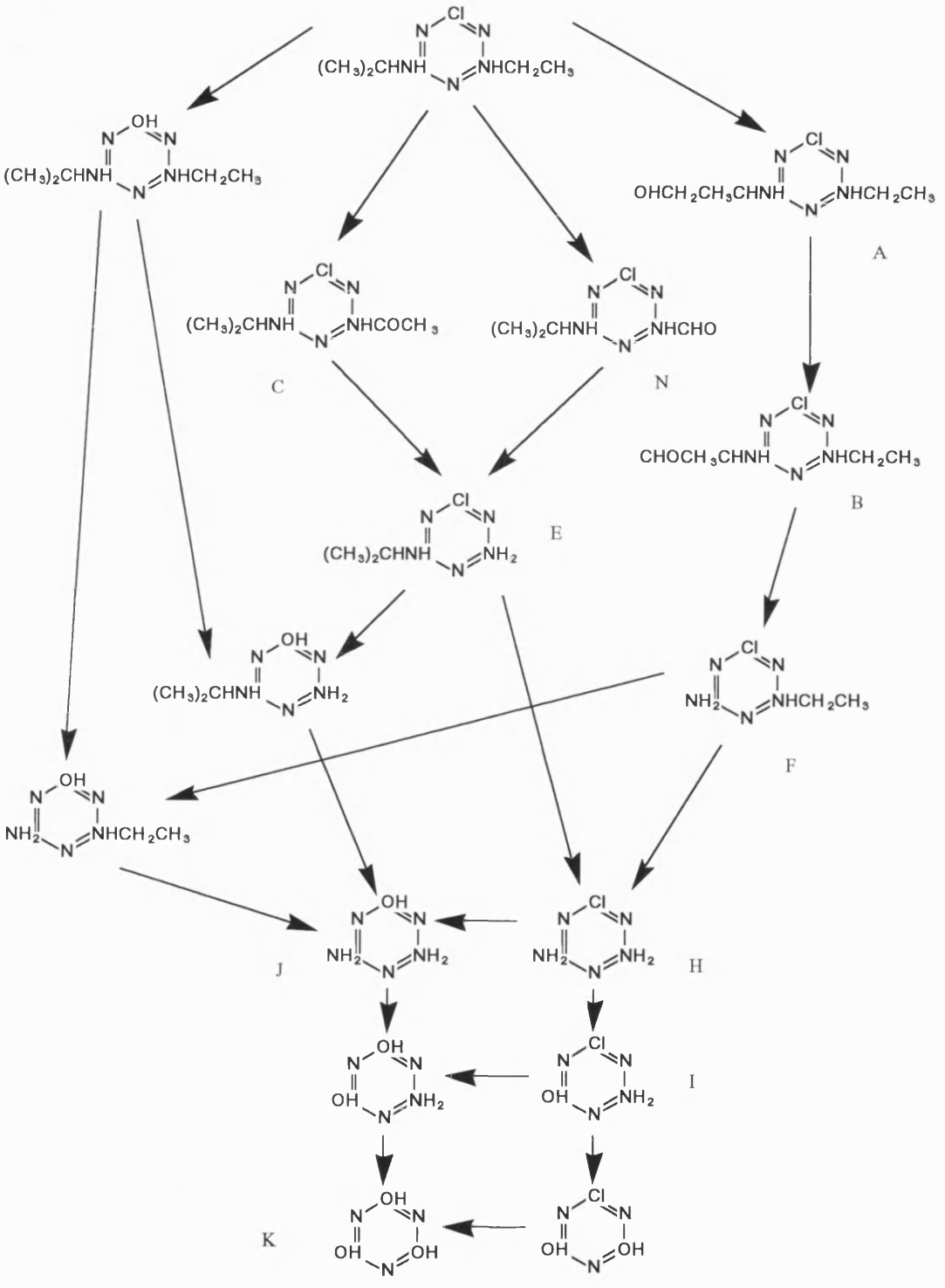

Figure 4.5: *Proposed Atrazine Degradation Reaction Pathway [48].*

A full list of intermediates found in a number of studies on atrazine photocatalytic degradation are shown in figure 4.4a. These compounds A - K have been incorporated into a reaction scheme [48] as shown in figure 4.5.

The major dealkylated intermediates (E,F,H) have all been identified in the present study. An oxidised intermediate m/e 229 has also been found with a similar spectra as reported for compound C. Slight variations in the spectra of compounds having a m/e 229 are shown in the case of two experiments, that using Fentons reagent (a known free-radical generating system - ferrous sulphate/H_2O_2/H_2SO_4) and an experiment using the cuvette micro reactor, show two distinct peaks from the GC trace both with m/e 229 and with slightly differing spectra. In the absence of collaborating evidence it can be assumed that either this represents compound B or compound D (a loss of 28 giving an ion at 201 compared with an ion at 214 for a loss of CH_3, suggesting a CHO group loss.

In addition to these compounds identified previously, a number of additional compounds were identified. These often appeared in experiments with differing conditions suggesting experimental error can be discounted. Possible structures for these compounds are shown in figure 4.4b. Compound P has previously been identified as a reaction intermediate for propazine degradation [94].

Compounds with an OH substitution, i.e. compounds A, S and T, were found only in one experiment (R12) . Cyanuric acid was also detected in this run and R10 and R13.

The other compounds are all variants having the chlorine molecule replaced by either H, CH_3O, and other oxidised groups.

In general it is difficult to come to any firm conclusions about the range and type of intermediates for the different experimental conditions, but a number of interesting points occur:

(i) There are noticeable difference in intermediates between catalyst types with experiments carried out using TiO_2 manufactured in the lab showing more oxidised compounds. (R12, R13, R15)

(ii) WDB TiO_2 which was found to show faster atrazine degradation rates than P25 TiO_2 (see section 4.1.4.2) also shows cyanuric acid as a reaction intermediate (R10) whilst only desethyl-desisopropyl atrazine was found in P25 degradations (R9).

(iii) Desisopropyl atrazine is only detected in the control (no catalyst) experiment. A number of other experiments show the presence of desethyl atrazine and desethyl-desisopropyl atrazine together. This may suggest that with some catalyst types reaction may be via the desethyl intermediate bypassing the parallel reaction via desisopropyl atrazine altogether. In general this shows that reaction mechanism is dependent on catalyst type.

(iv) Reactions using free-radical generating systems (Fentons and Sonication) show similar intermediates as photocatalytic systems, namely desethyl atrazine and oxidised atrazine, but the number and range of intermediates formed is less. This may be a function of the relative effectiveness of the systems and/or the reaction mechanisms being more selective.

(v) The difference in intermediates formed with different types of TiO_2 is further evidence that the major reactions are heterogeneous in nature. Differences in the catalyst surface and crystal structure obviously effect the reactions which occur at the particle surface. If the reactions were homogeneous, with hydroxyl radicals diffusing away from the catalyst and reacting in solution, it would be expected that the distribution of reaction intermediates for each catalyst would be the same.

4.1.3 Effect of Atrazine Concentration on Degradation Rate.

It is known that most photocatalytic reactions show increased reaction rates with an increase in substrate concentration [51] and since, in a system for potable water treatment, pollutant concentrations would be very low it is important to look at how the effectiveness of the degradation process is effected by atrazine concentration.

A series of experiments was therefore carried out, with identical conditions except for the initial atrazine concentration.

A graph of atrazine concentration vs. reaction time for this series is shown in figure 4.6a. It can be seen that the slope of the initial atrazine degradation rate increases with increasing initial atrazine concentration. It can also be seen from figures 4.6b-d that reaction intermediate concentrations also follow a similar trend, higher initial concentrations of atrazine giving higher intermediate production rates.

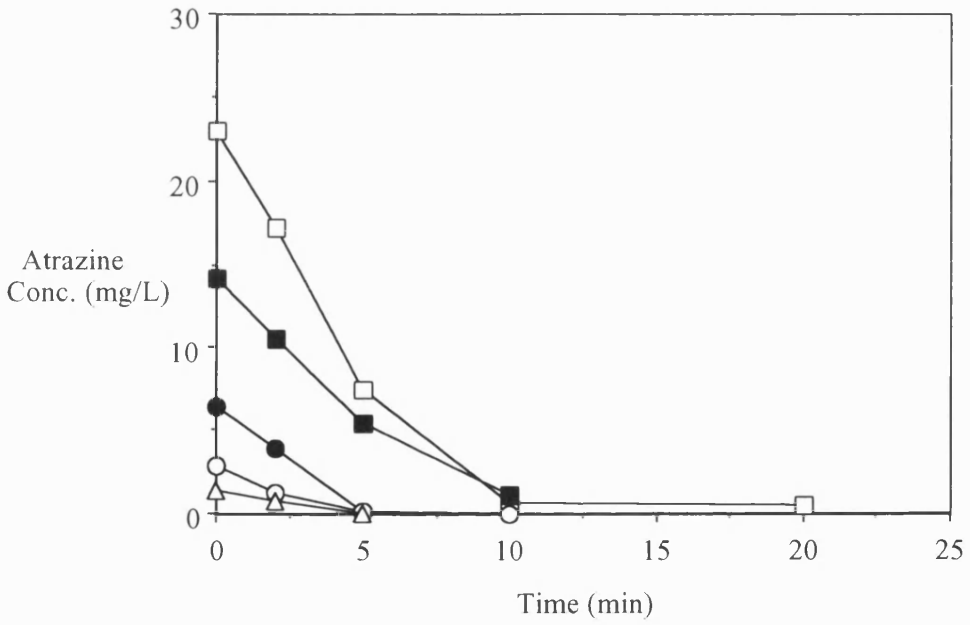

Figure 4.6a: *Effect of Initial Atrazine Concentration on Degradation Rate. Catalyst Loading (P25) 0.05 g/L; 7.5 mg/L* O_2 .

If the initial rate is plotted vs. atrazine concentration, as in figure 4.7, it can be seen that the data can be fitted to a typical Langmuir-Hinshelwood kinetic model. This model describes reaction rates which increase with increasing substrate concentration approaching a constant limiting value. Figure 4.7 shows that in the concentration range studied (limited by the solubility of atrazine in water 30 mg/L @ 20°C) the limiting rate is not reached.

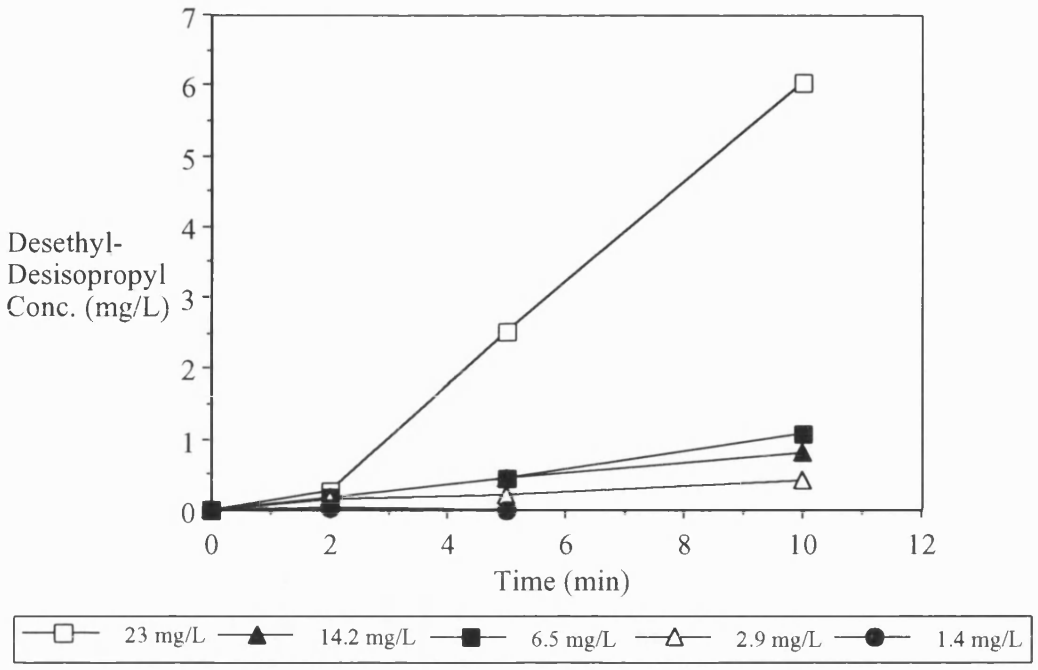

Figure 4.6b: *Effect of Initial Atrazine Concentration on Desethyl-Desisopropyl Atrazine Concentration.*

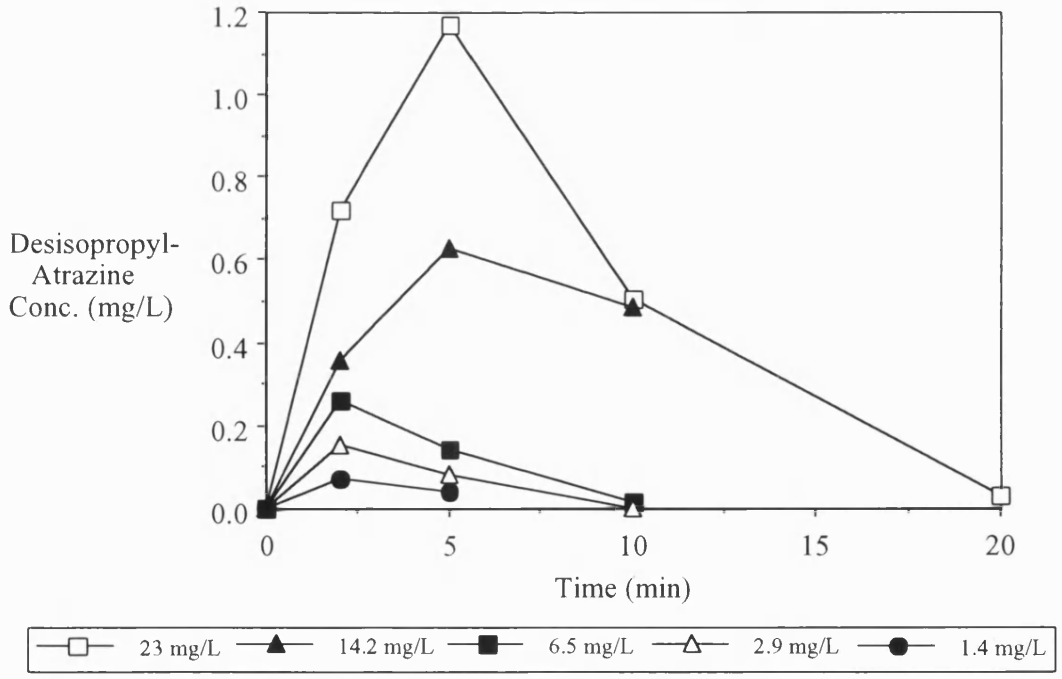

Figure 4.6c: *Effect of Initial Atrazine Concentration on Desisopropyl Atrazine Concentration.*

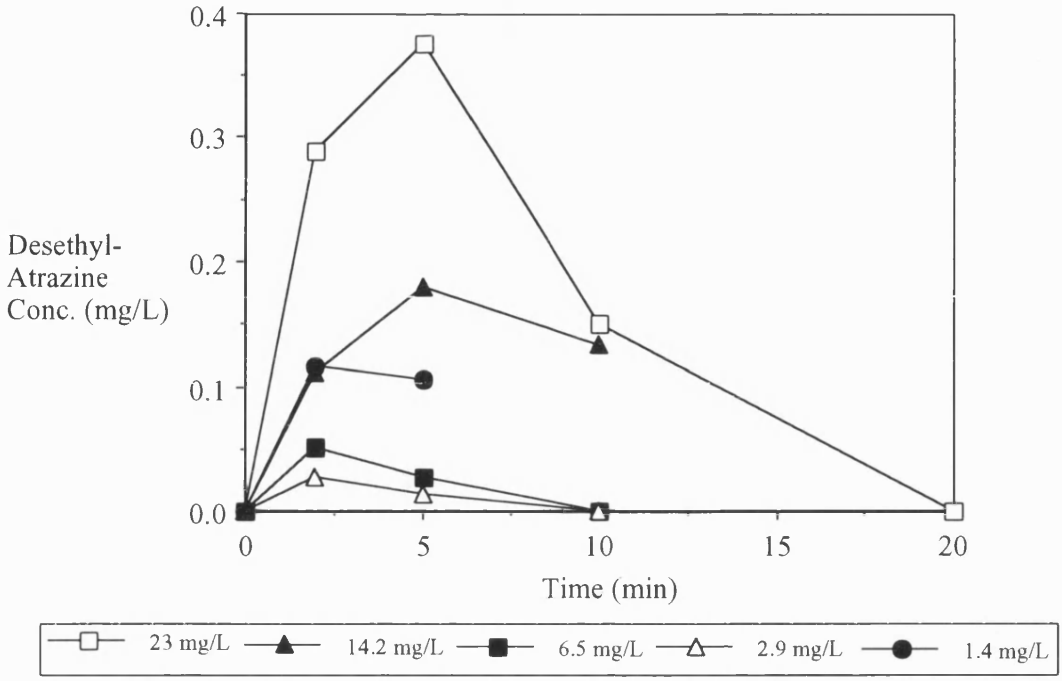

Figure 4.6d: *Effect of Initial Atrazine Concentration on Desethyl Atrazine Concentration.*

Fitting the data to an equation of the form:

$$\text{Initial Rate} = \frac{k_{cat}\, S}{K_m + S} \qquad (4.1)$$

where S=substrate concentration (mg/L)

K_m = the Michaelis constant (mg/L)

k_{cat} = the maximum reaction rate (mg/L.min)

gives values for the constants k_{cat}=5.37 mg/L.min and K_m=21.82 mg/L.

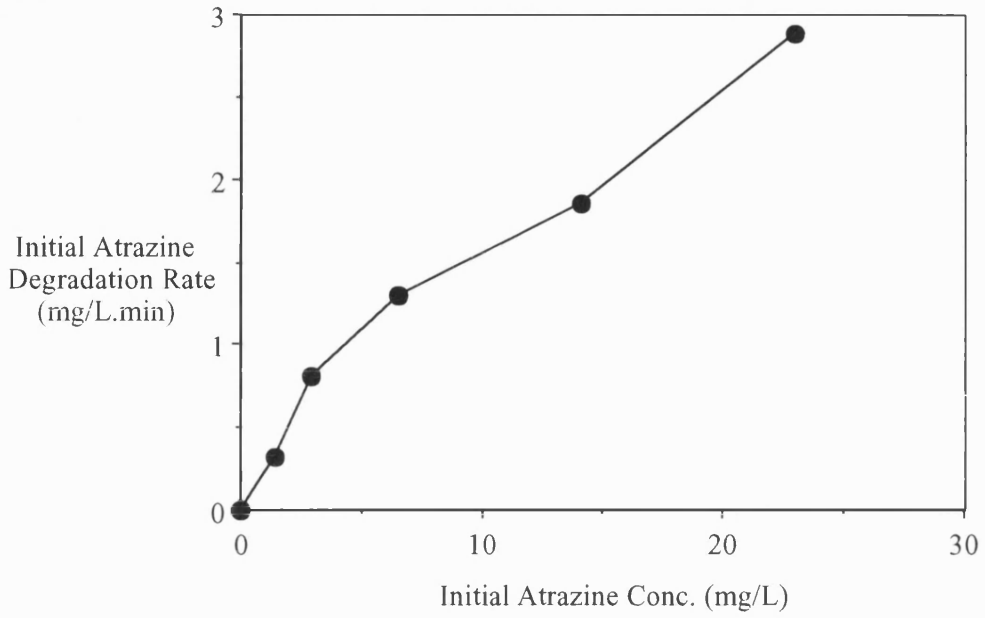

Figure 4.7: *Dependence of Initial Rate of Atrazine Degradation on Initial Concentration.*

Further discussion of Initial Rate-Concentration data can be found in section 4.5.

If the individual degradation rate data shown in figure 4.6a is fitted to a first order kinetic model using the Ultrafit software (section 3.13) using a first order degradation equation:

$$C=C_0 * \exp(-k' * t) \qquad (4.2)$$

where,

C = Atrazine Concentration.

C_0 = Atrazine Concentration at time t.

k' = First order rate constant. (min^{-1})

t = time (min)

the results are shown in table 4.2.

Table 4.2: *First Order Rate Constants (k') and Half-Life ($t_{0.5}$) for Atrazine Degradation.*

Initial Atrazine Concentration (mg/L)	**k' (min^{-1})**	**$t_{0.5}$ (min)**
23.0	0.225	3.26
14.2	0.200	3.59
6.5	0.375	1.93
2.9	0.463	1.52
1.4	0.391	1.83

Many studies of photocatalytic reactions mediated by semi-conductor particles have fitted rate data to a equation from the Langmuir-Hinshelwood (L-H) kinetic model originally postulated for reactions at gas/solid interfaces, where adsorption of the gas substrate was assumed prior to reaction [65,41,95,63,96]. Initial rates of reaction as a function of increased organic substrate concentration, for a given photocatalyst loading give experimental plots of the form found here in figure 4.7, many showing limiting rate behaviour. This has led some workers to argue that this is evidence that the photocatalytic process is essentially heterogeneous in nature, the reaction occurring at the catalyst surface [22]. However, expressions derived from theoretical analysis of a whole range of possible reaction mechanisms [13] show the same kinetic behaviour as described by the L-H model, irrespective of the mode of reaction. That is, an equation of the same form as the L-H model can describe photocatalytic behaviour irrespective of whether (i) the oxidising species and the substrate are both adsorbed, (ii) both species are in solution, (iii) the oxidising species is adsorbed and the substrate is in solution, or (iv) the substrate is adsorbed and the oxidising species is in solution. To attribute a mechanistic description to the photocatalytic process on the basis of observed kinetics alone is therefore not possible. The examples of the L-H relationship, the

Michaelis-Menten model in enzyme kinetics, and examples of homogeneous reduction reactions are all manifestations of the more general group of *saturation-type kinetic* models.

4.1.4 Effect of Catalyst Type

It was important to evaluate different catalyst types and forms in order to assess their catalytic activity in comparison with each other and with the standard research material, Degussa P25.

This comparison was carried out in the batch system, as described in section 3.10, where small quantities of powder, supported catalyst and tableted forms could be easily compared and their catalytic effectiveness measured. There are a number of problems in making a quantitative comparison between different catalyst types since other factors such as particle size, TiO_2 loading, and porosity can all vary, together with any difference in catalytic effectiveness.

The following sections, as well as looking at some different catalyst forms, also look at comparisons of commercially available powdered TiO_2 and the differences between some different metal oxides photocatalysts.

4.1.4.1 Supported Catalyst and Crushed Tablets

Figure 4.8 shows the percent atrazine degradation obtained with some of the different types of catalyst studied; Degussa P25 powder; two forms of coated glass beads; and a sample of crushed P25 tablets. As a comparison, results from a control experiment with no catalyst-UV light only are also shown.

Figure 4.8 is not a quantitative comparison of the effectiveness of these different types although it does indicate general trends. This is because, as has been already stated, a meaningful comparison of powders, crushed tablets, and supported catalyst having different surface areas, porosity and loading is not possible.

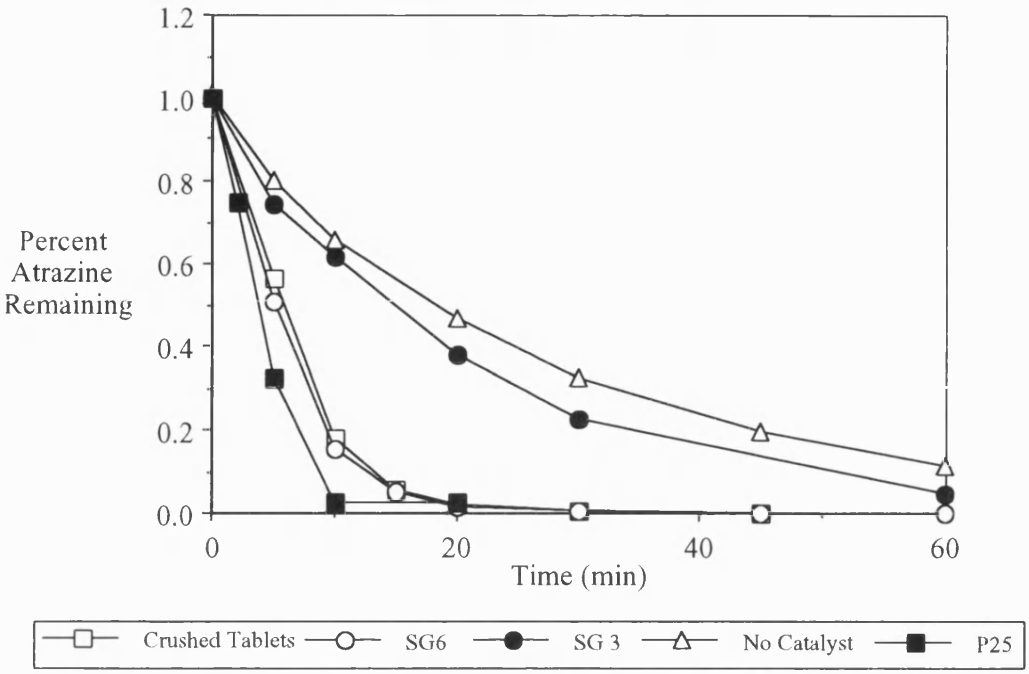

Figure 4.8: *Atrazine Degradation for Different Catalyst Types. Initial Atrazine Conc. 30 mg/L;300 cm/min air sparge.(7.5 mg/L O_2 .) Catalyst Loading 1g P25; 10g Supported Catalyst and Crushed Tablets.*

It can be seen that glass beads coated with a sol-gel derived catalyst layer, from method SG3, show a poor atrazine degradation rate compared with a no catalyst-UV only control experiment. Catalyst obtained from crushed tablets and glass beads coated with TiO_2 precipitates from a fast hydrolysis, SG6, show degradation rates close to that of a powdered catalyst such as P25.

From these preliminary results it appeared that either large particles of bulk catalyst (tablets) or a supported catalyst would possess the required catalytic activity (compared to P25) and would therefore provide a potential catalyst system for the pilot scale reactor.

Further discussion about the supported catalysts which have been prepared can be found in section 4.3.1 which includes SEM pictures of coated glass beads and section 4.3.2 which presents some results from the methyl viologen assay technique for measuring photocatalytic activity.

4.1.4.2 Comparison of Commercial TiO_2 Powders

A better comparison of different types of TiO_2 is between Degussa P25 and SCM WDB which are both commercially available powders. Even here differing surface areas/unit volume, dispersion characteristics, and surface charges etc. can play important effects so again it is not a straight comparison of catalytic activity.

Results of batch degradations using identical loadings of both catalysts are shown in figures 4.9a-c for concentrations of atrazine, desethyl-desisopropyl atrazine, and a polar compound with retention time 1.8 min .

A first-order plot of $\ln(C/C_0)$ against Reaction Time for the two commercial catalysts, P25 and WDB, is shown in figure 4.10 and curve fitting gives first-order rate constants k' and $t_{0.5}$ of 0.155 min^{-1}, 4.58 min and 0.356 min^{-1}, 1.95 min respectively.

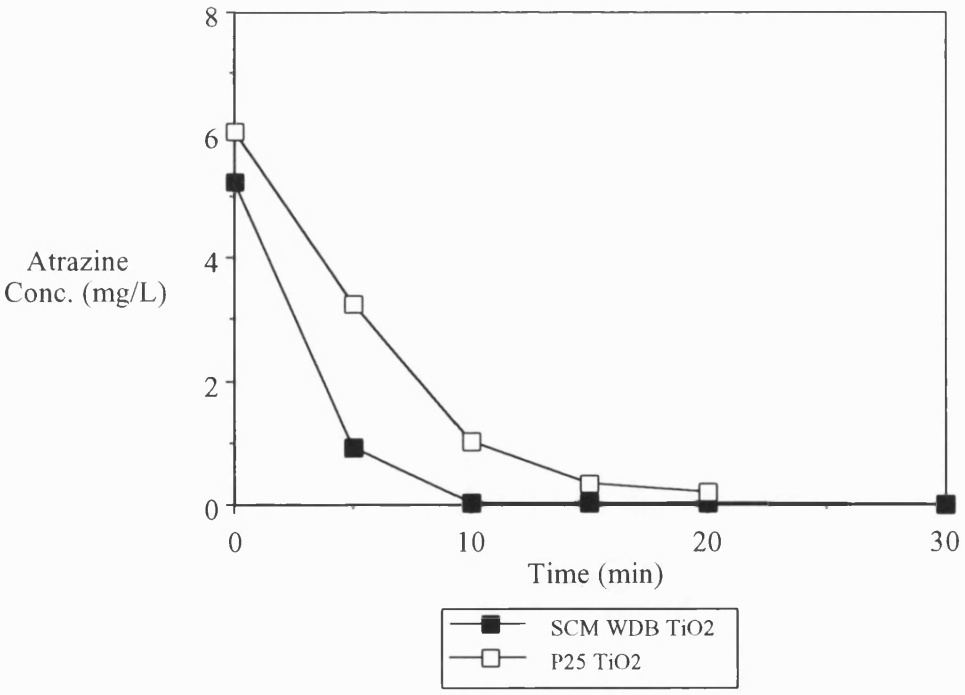

Figure 4.9a: *Comparison of Atrazine Degradation for Commercial TiO_2 samples. Loading (8.4 g/L); 7.5 mg/L O_2 .*

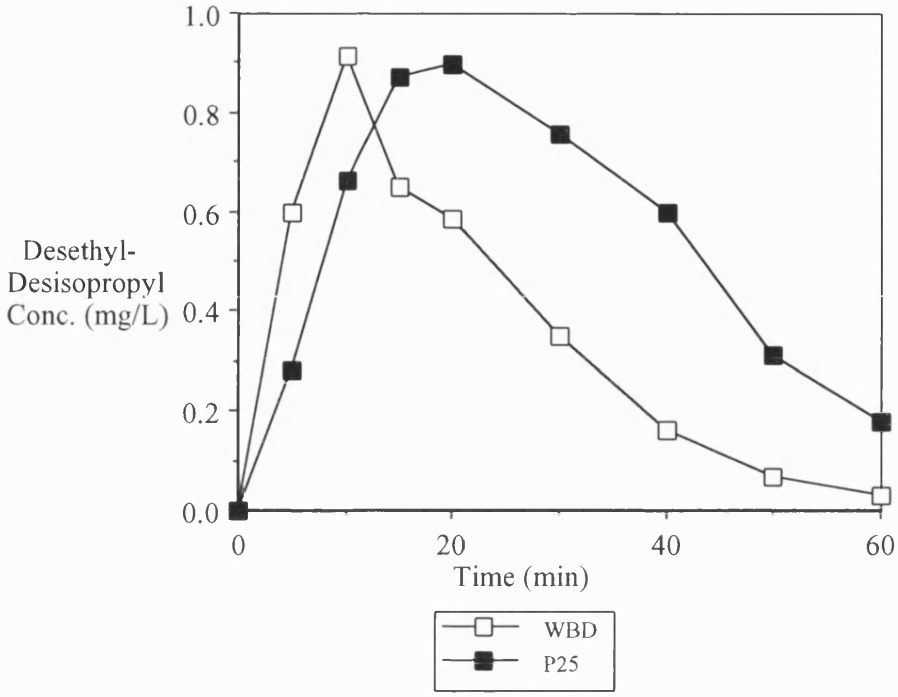

Figure 4.9b: *Comparison of Desethyl-Desisopropyl Atrazine Concentration for Commercial TiO_2 samples.*

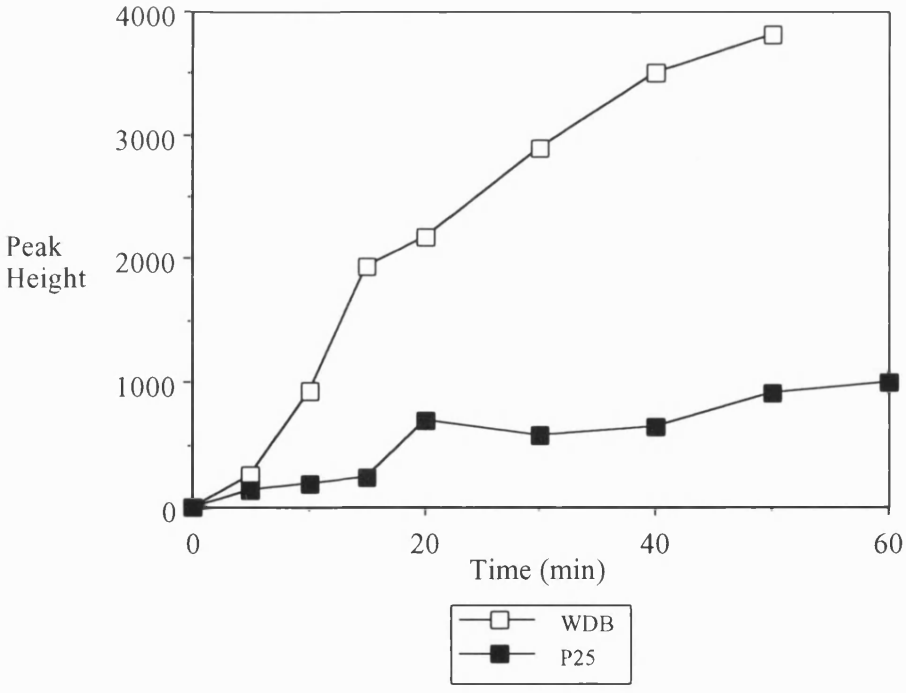

Figure 4.9c: *Comparison of a Polar Intermediate (retention time 1.8 min) for Commercial TiO 2 Samples.*

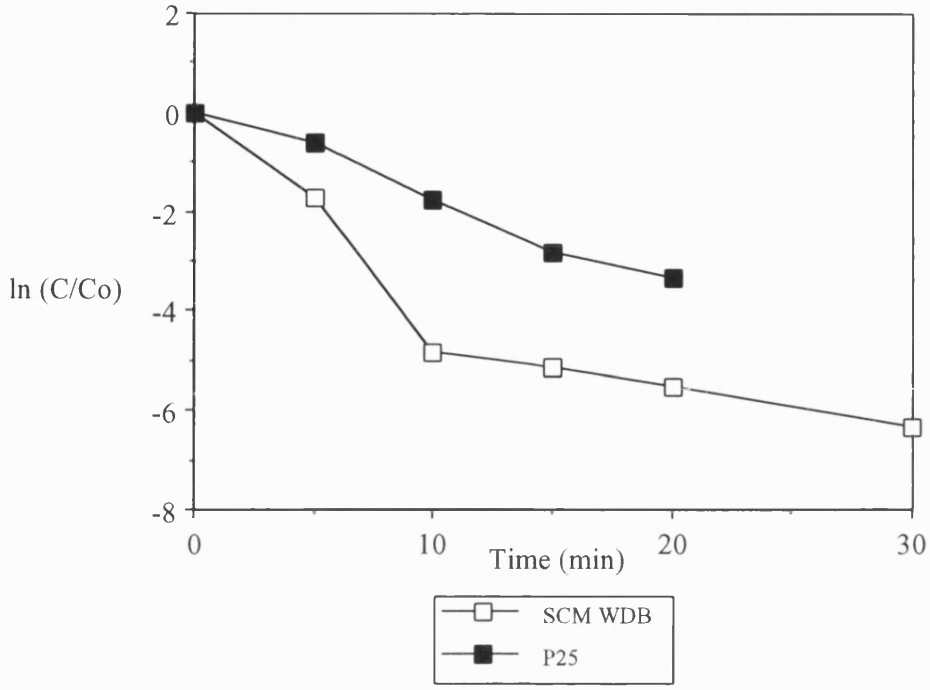

Figure 4.10: *First-Order Plot for Atrazine Degradation using Commercial Catalysts.*

The results shown in figures 4.9 and 4.10 show that the WDB material is the more effective catalyst at removing atrazine in the batch system. Also shown, in figure 4.9b, is that the time taken to reach the maximum concentration of desethyl-desisopropyl atrazine is less for the WDB TiO_2. Figure 4.9c shows the peak height corresponding to a more polar intermediate than desethyl-desisopropyl atrazine, possibly cyanuric acid, and shows that levels of this compound are 4 times higher after 60 minutes illumination for WDB TiO_2.

These results show atrazine degradation rates are higher when using WDB TiO_2 and that the process towards mineralisation is also enhanced compared to P25.

4.1.4.3 Comparison of Metal Oxide Semiconductor Type.

Although it had already been decided to look at the use of titanium dioxide as a catalyst for atrazine degradation because of it's widespread use, availability, known stability to photocorrosion and suitability for photocatalytic reactions, it was

interesting to look at a comparison with some other photocatalytically active metal oxides.

A comparison was therefore made with magnesium oxide (MgO) and zinc oxide (ZnO) and the results shown in figures 4.11a and 4.11b.

Rate constants calculated by fitting the data to a first order kinetic model are shown in table 4.3.

Table 4.3: *First Order Rate Constants for Different Semiconductor Types.*

	TiO_2	ZnO	MgO
k' (min^{-1})	0.088	0.127	0.056
$t_{0.5}$	8.41	5.63	12.14

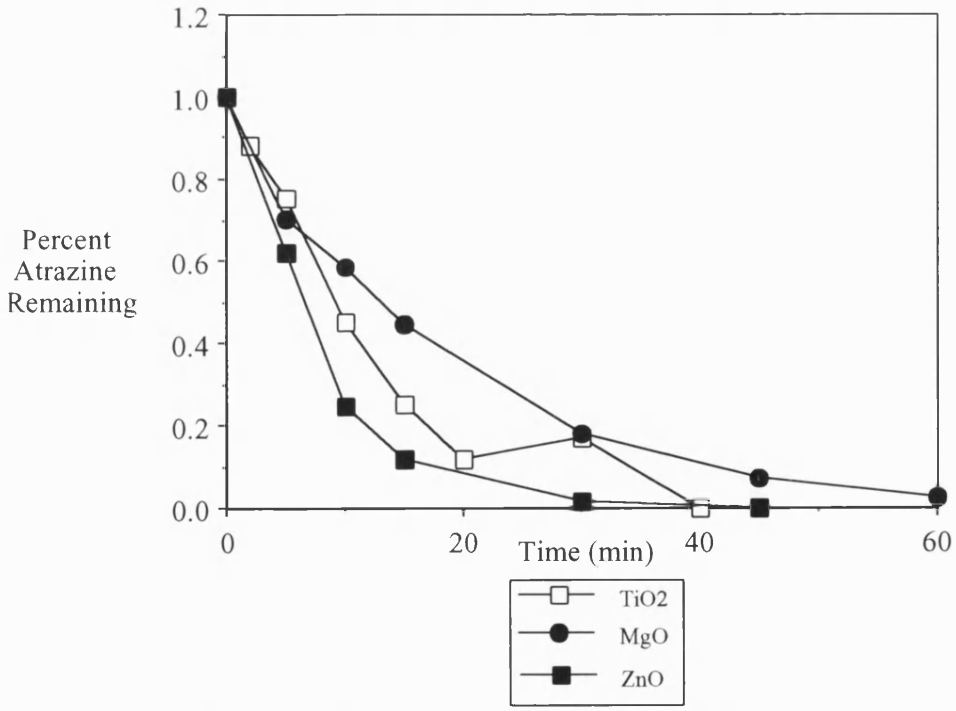

Figure 4.11a: *Effect of Semiconductor Catalyst Metal Oxide Type on Atrazine Degradation in the Batch Reactor. Initial Atrazine Conc. 10 mg/L; Catalyst Loading 1.0 g/L; 7.5 mg/L O_2 .*

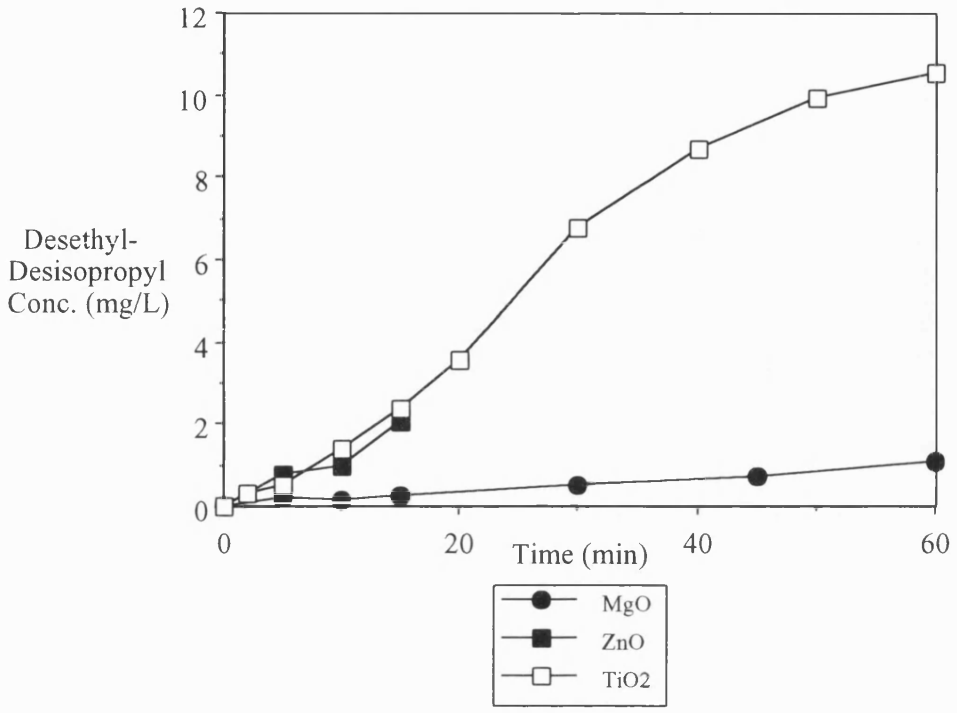

Figure 4.11b: *Effect of Semiconductor Catalyst Metal Oxide Type on Desethyl-Desisopropyl Atrazine Production in the Batch Reactor.*

It can be seen that MgO is far less effective as indicated both by atrazine degradation rate and desethyl-desisopropyl atrazine production rate. ZnO on the other hand shows an increased rate of atrazine degradation and a similar rate of desethyl-desisopropyl atrazine production as found with TiO_2.

It has been reported however that Zn^+ ions have been found in solution after photocatalytic reactions suggesting that it is not as stable as TiO_2 and certainly not suitable for potential water treatment applications [97].

4.1.5 Effect of Catalyst Loading on Degradation Rate.

It has been reported in many studies that for powdered catalyst there is an increase in degradation rate with loading, reaching an optimum. Above this optimum, an increase in TiO_2 concentration prevents UV penetration into the reaction mixture and degradation rates can actually fall [97,42,98].

The UV absorbance of a chosen catalyst, at wavelengths taking part in photocatalysis, is an important factor in determining the overall reaction rates. In any comparison between catalyst types a measure of the amount of UV absorbed will be useful in explaining any differences in observed reaction rates.

In order to investigate the importance of UV absorbance, a comparison of the effect of concentration on UV transmission between the two commercial powdered catalyst forms was carried out. The transmission of different concentrations was measured in a UV spectrophotometer (Cecil 3000 Series), in a 1cm path length cuvette at 350 nm, the results shown in figure 4.12.

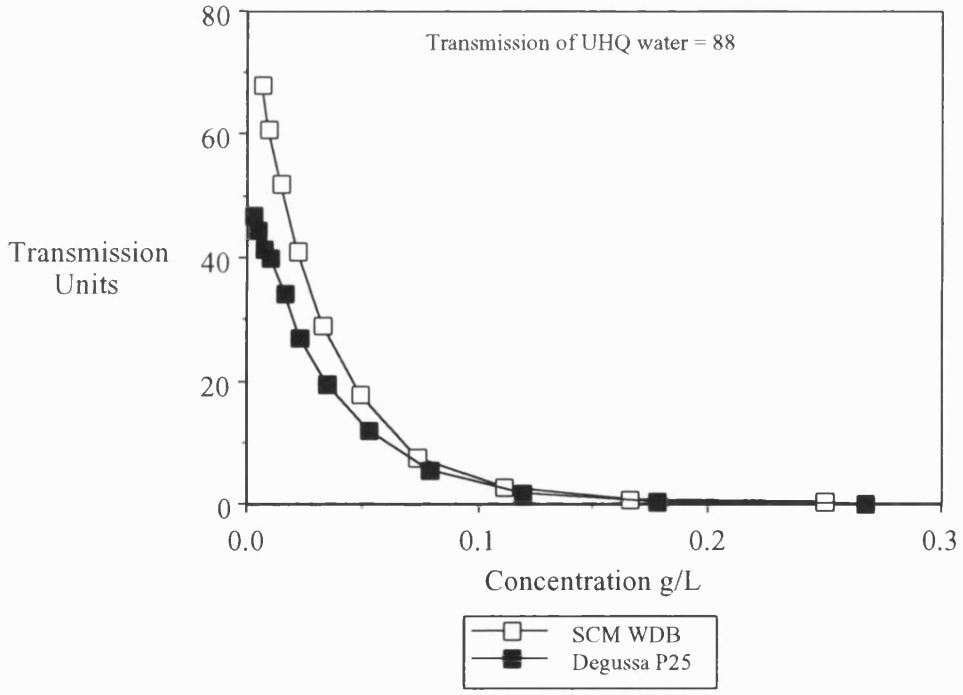

Figure 4.12: *Effect of Concentration on Transmission at 350nm of Commercial TiO_2 samples.*

These results show that, for both TiO_2 types, concentrations above 0.2 g/L show no transmission at path lengths >1cm for UV light of 350nm. Degussa P25 shows more absorbance (and therefore less transmission) at lower concentrations. These differences can be explained either by differences in particle size distribution, the presence of smaller particles in the distribution having an effect at low

concentrations or differences in surface properties leading to light scattering and reflection effects.

As has already been shown in section 4.1.4.2 and figure 4.11 the WDB catalyst is more effective than P25 and although that data was obtained at higher loadings than those where transmission effects play a part it shows that measures of UV absorbance alone are not enough to compare catalysts.

Results from a series of experiments using different loadings of WDB TiO_2 to investigate the effect on atrazine degradation are shown in figure 4.13.

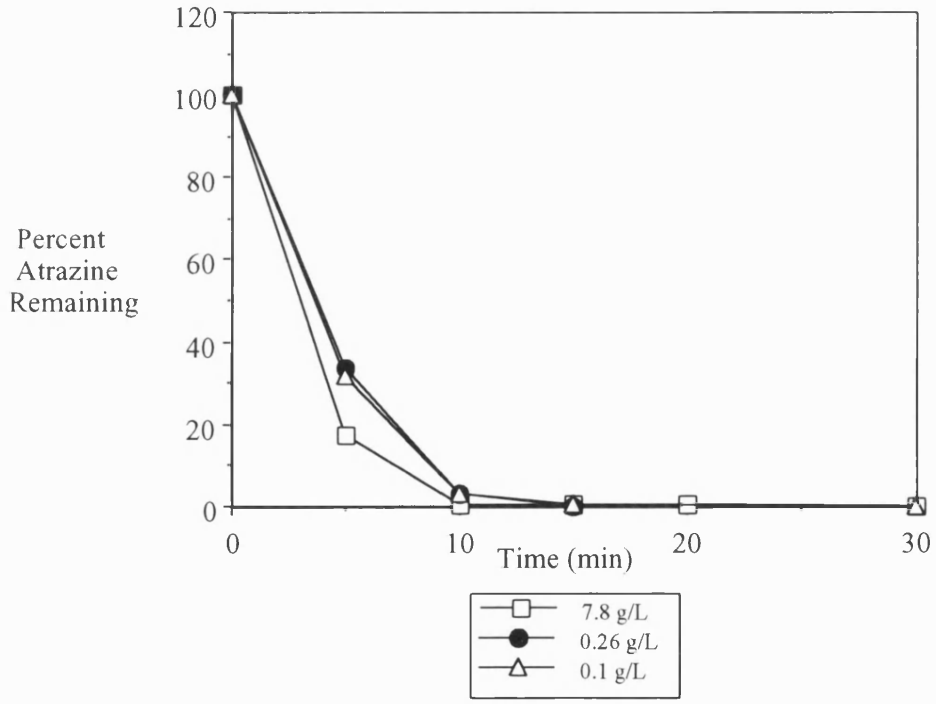

Figure 4.13: *Effect of Catalyst Loading on Atrazine Degradation.Initial Atrazine Conc. 6.0 mg/L; 7.5 mg/L O_2 .*

Figure 4.13 shows that increasing the loading of WDB TiO_2 above the point where an increase in absorbance alone is a factor (≈0.2 g/L) leads to an increase in atrazine degradation rate. First order rate constants are shown in table 4.4.

It can be seen that there is only a small increase in reaction rate on a large increase in the catalyst loading (x 80).

Table 4.4: First Order Rate Constants for Different Loadings of WDB TiO_2.

WDB Loading (g/L)	k' (min^{-1})	$t_{0.5}$ (min)
0.1	0.252	2.77
0.26	0.24	2.9
7.8	0.357	1.94

This shows that the apparent optimum loading from transmission measurements will not necessarily be that found from reaction rate data. This can be explained by the fact that:

(i) mixing occurs in the batch reactor leading to a turnover of catalyst in the region close to the UV light; and

(ii) substrate adsorption will be dependent on the amount of catalyst present in the reactor.

4.1.6 Effect of Inorganic Ions on Degradation of Atrazine

A well defined system is essential in order to measure the degradation rates of a single compound and therefore the batch experiments were carried out using solutions of atrazine made up in ultrapure water, eliminating other effects due to impurities in solution. To apply photocatalysis to a system which could be used to treat "real" water however, the effect of inorganic ions on the degradation rate needed to be ascertained.

In order to look at the effect of inorganic ions a series of experiments was carried out using Degussa P25 and commonly occurring anions and cations at typical concentrations (mg/L).

$CaCO_3$, KCl, Na_2SO_4, and $NaNO_3$ were used at concentrations in the range 13 mg/L to 250 mg/L, at a constant P25 concentration of 0.1 g/L.

Figure 4.14 shows the effect of each inorganic ion (concentrations 15-23 mg/L) on the degradation of atrazine expressed as a percent destruction. It shows that the addition of these inorganic ions improves degradation rates compared to a control using P25 powder in ultrapure water.

The effect of these different ions on the concentrations of the major reaction intermediates is shown in figure 4.15 a-c.

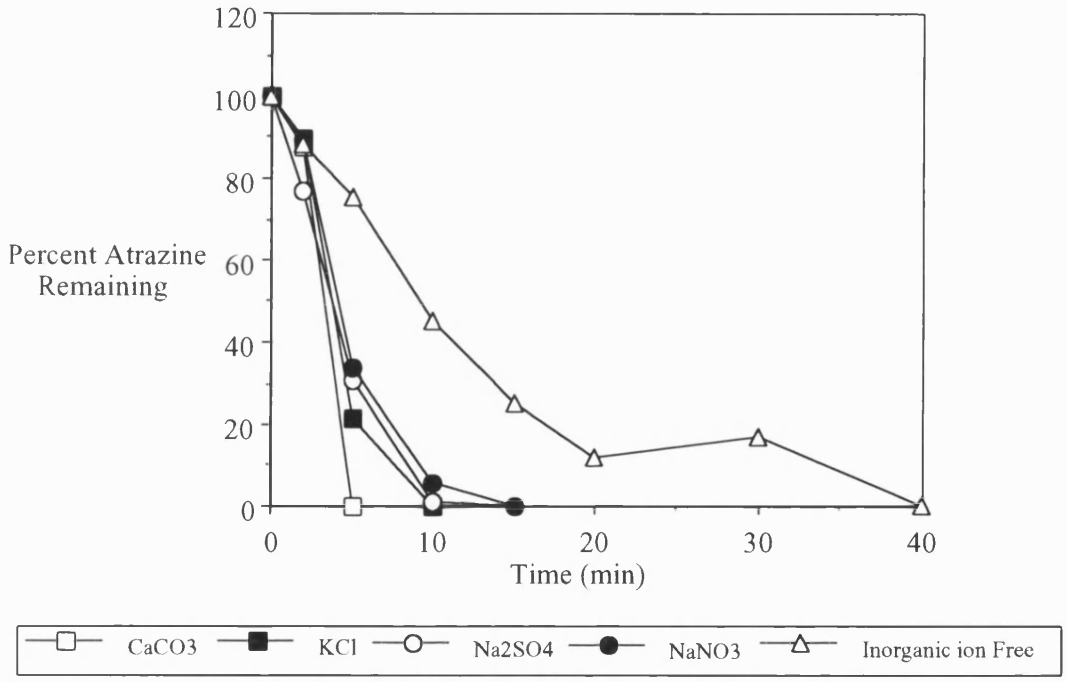

Figure 4.14: *Effect of Inorganic Ions on Degradation of Atrazine in the Batch Reactor. Initial Atrazine Conc. 15 mg/L; 7.5 mg/L* O_2 *.*

It was expected that the addition of inorganic ions would have a negative effect on the oxidation rate, as observed in previous studies [68], but the observed results show that degradation rates are actually enhanced. The only deviation from this observation is in the case of desethyl-desisopropyl atrazine production in the presence of $NaNO_3$ where rates are less than those found in ion-free water. This can be explained by a UV shielding effect of nitrate ions which absorb light at UV wavelengths (see section 3.3.1).

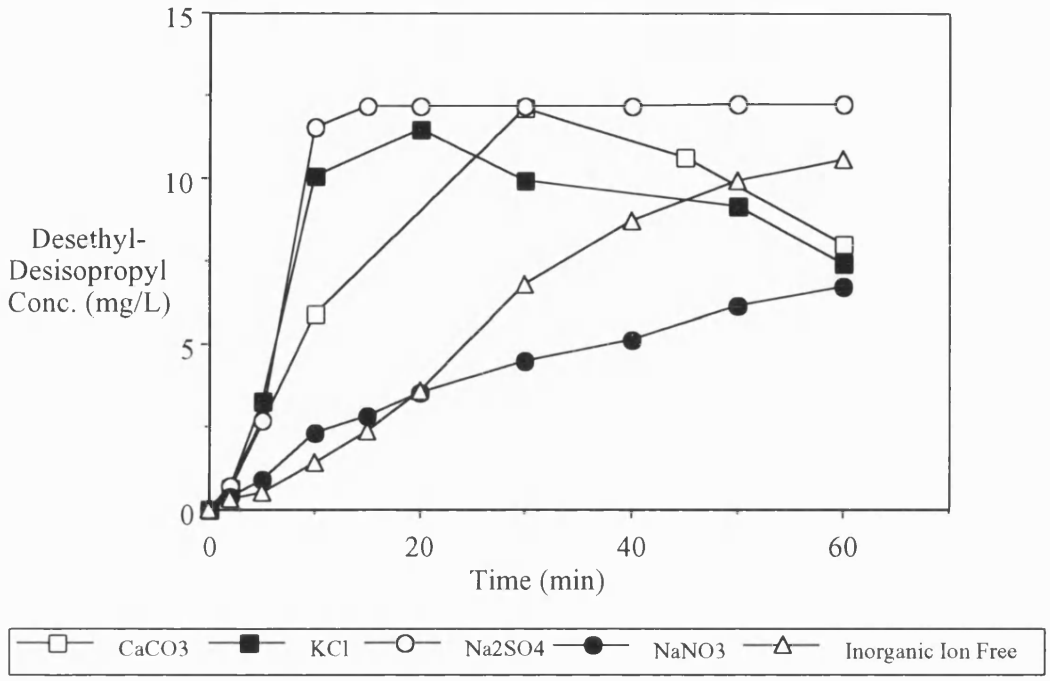

Figure 4.15a: *Effect of Inorganic Ions on Desethyl-Desisopropyl Concentration.*

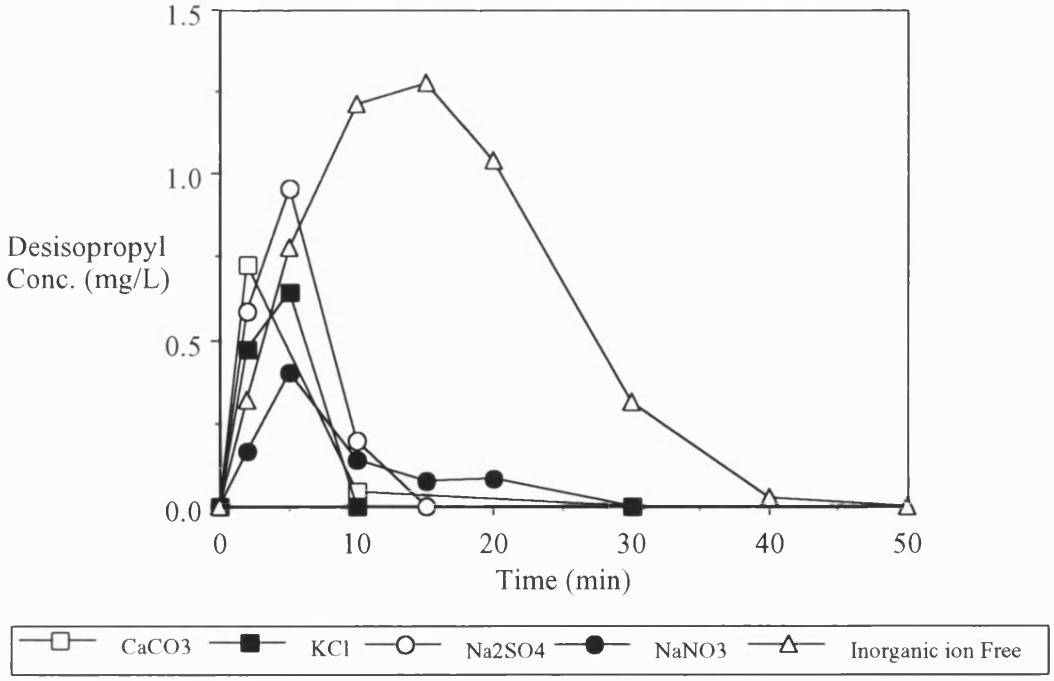

Figure 4.15b: *Effect of Inorganic Ions on Desisopropyl Atrazine Concentration.*

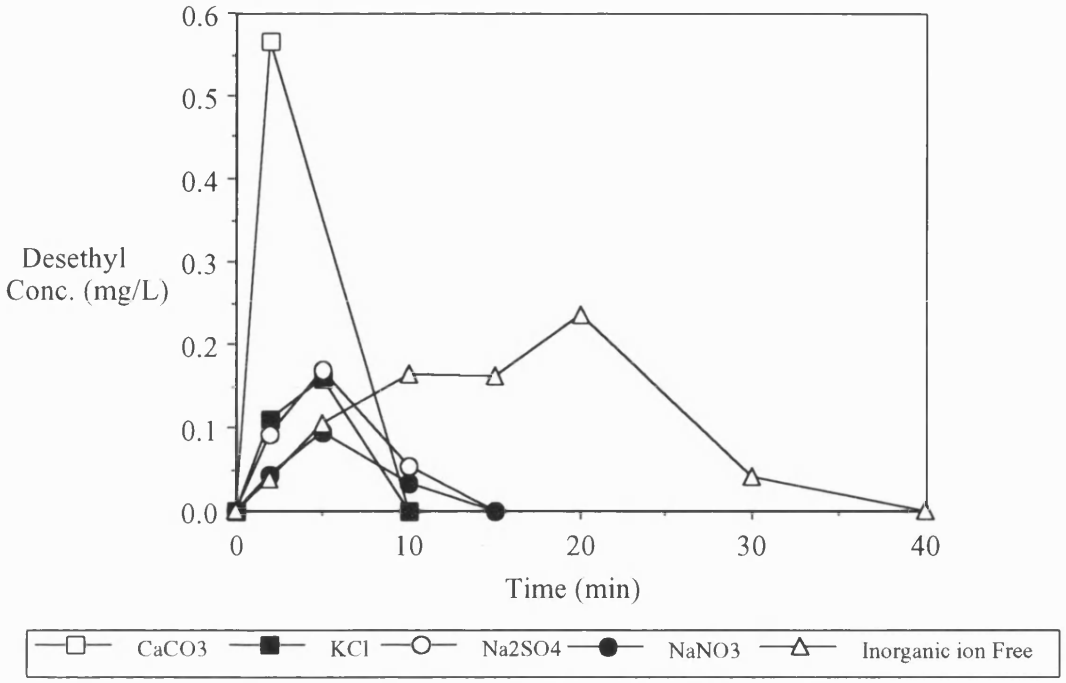

Figure 4.15c: *Effect of Inorganic Ions on Desethyl Atrazine Concentration.*

This overall rate enhancement may possibly be explained by a possible dispersion effect, the addition of inorganic ions preventing particle-particle agglomeration, dispersing fine particles and improving the efficiency of the catalyst by increasing the available surface area for photocatalytic reaction. This effect could outweigh any detrimental effect due to competitive reactions for oxidising radicals taking place between the inorganic ions and atrazine or blocking of catalyst active sites at the low ion concentrations examined here.

It can also be seen that degradation rates in the presence of inorganic ions deviate from a first order model. Initial degradation rates are lower than expected giving an "S-shaped" curve in the cases of 23 mg/L KCl (figure 4.16a), $NaNO_3$ (figure 4.18a), and $CaCO_3$ (figure 4.14). This lag on the observed degradation rates could be explained by two possible mechanisms:

(i) A dispersion effect being linked with charge build-up due to the photocatalytic effect. A short period of illumination is required before any change in surface charge and then in size distribution is observed.

(ii) The diffusion of organic molecules to the catalyst surface sites being affected by the presence of inorganic ions. The adsorption of inorganic ions being favoured in the dark. Thus before illumination the catalyst surface sites are saturated with inorganic ions, the rate of organic degradation being retarded by the need for diffusion to the catalyst surface and replacement of the inorganic ions.

The proposed dispersion effect appears to be reversed in the case of SCM WDB. When a sample of WDB is added to tap water the dispersion is very poor compared to a suspension in UHQ where the dispersion is spontaneous giving a paint-like suspension. (see section 4.1.7)

The effect of inorganic ion concentration on atrazine degradation has been examined for KCl, Na_2SO_4, and $NaNO_3$ and the results obtained are shown in figures 4.16-4.18.

The effect of increasing the concentration of both KCl and $NaSO_4$ was to decrease the rate of atrazine degradation and to reduce the rate of individual intermediate production. In the case of $NaNO_3$ the rates of intermediate production, especially the desethyl-desisopropyl compound, were increased on a change in concentration from 15 to 244 mg/L.

In all cases the atrazine degradation rates are greater than that found in UHQ water.

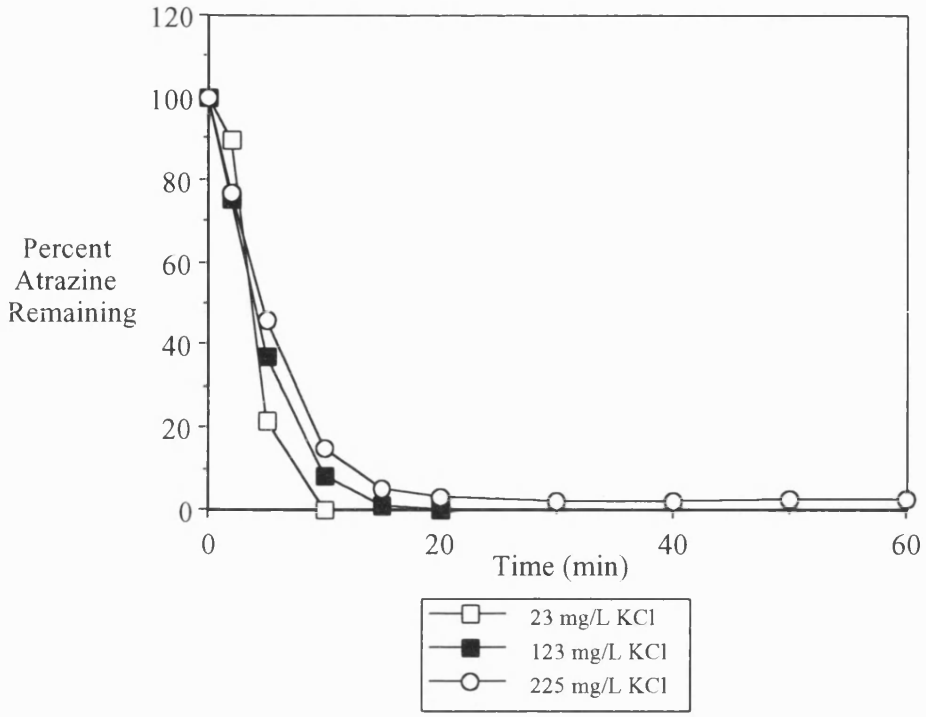

Figure 4.16a: *Effect of KCl Concentration on Atrazine Degradation. Initial Atrazine Concentration 15 mg/L; 7.5 mg/L* O_2 *.*

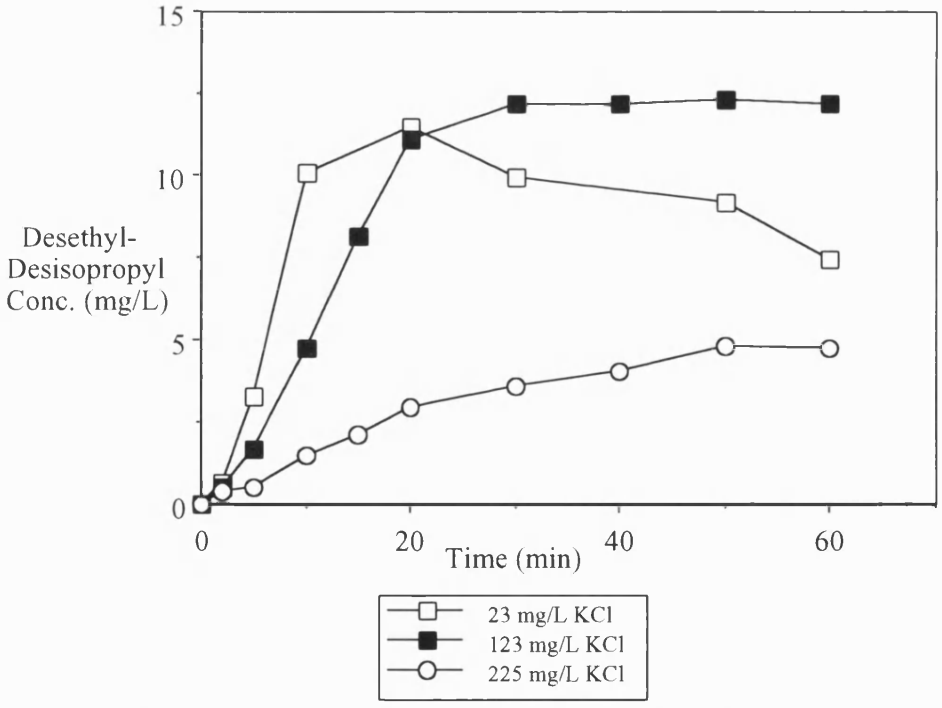

Figure 4.16b: *Effect of KCl Concentration on Desethyl-Desisopropyl Atrazine Concentration.*

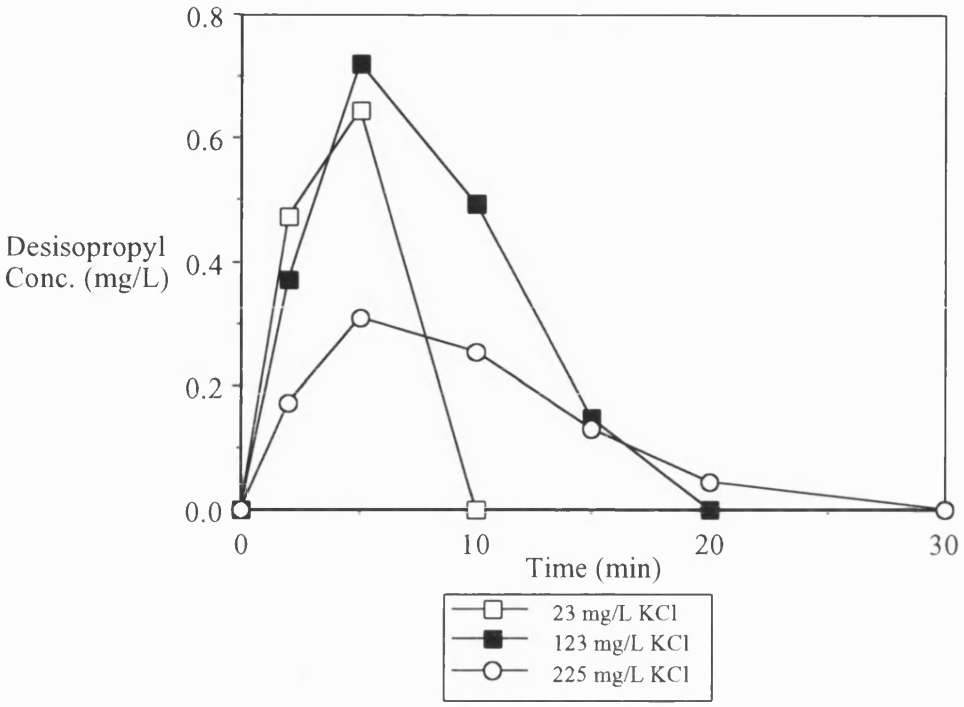

Figure 4.16c: *Effect of KCl Concentration on Desisopropyl Atrazine Concentration.*

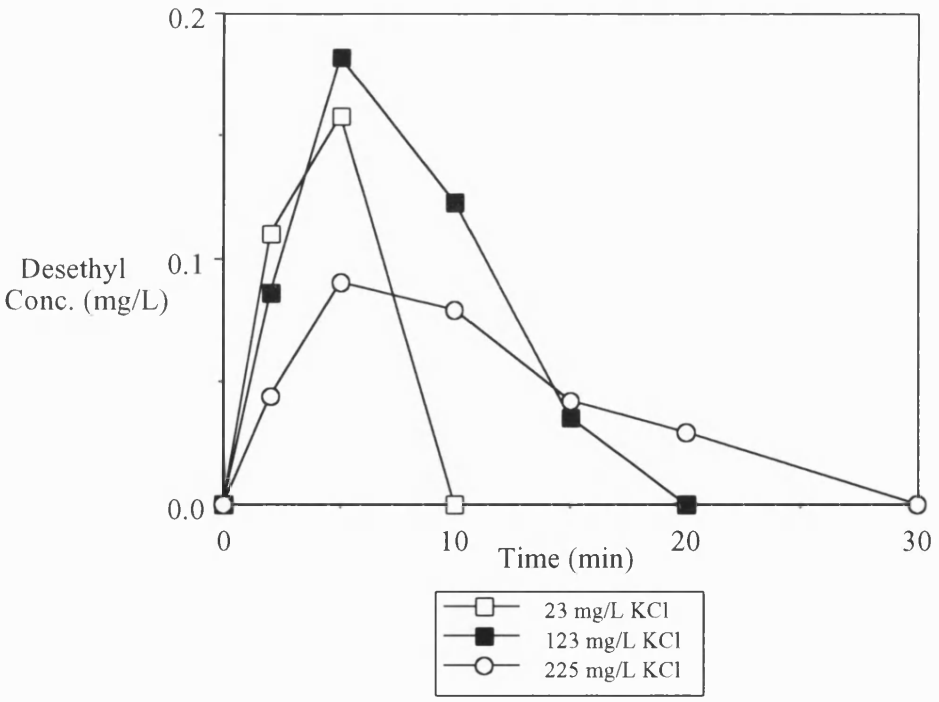

Figure 4.16d: *Effect of KCl Concentration on Desethyl Atrazine Concentration.*

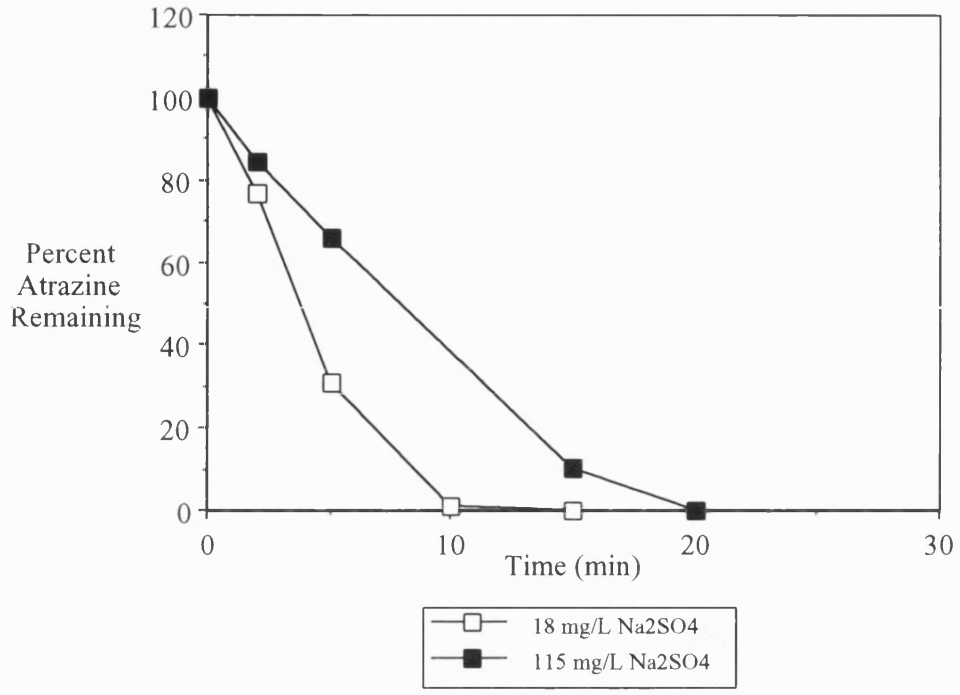

Figure 4.17a: *Effect of $NaSO_4$ Concentration on Atrazine Degradation.Initial Atrazine Concentration 15 mg/L; 7.5 mg/L O_2 .*

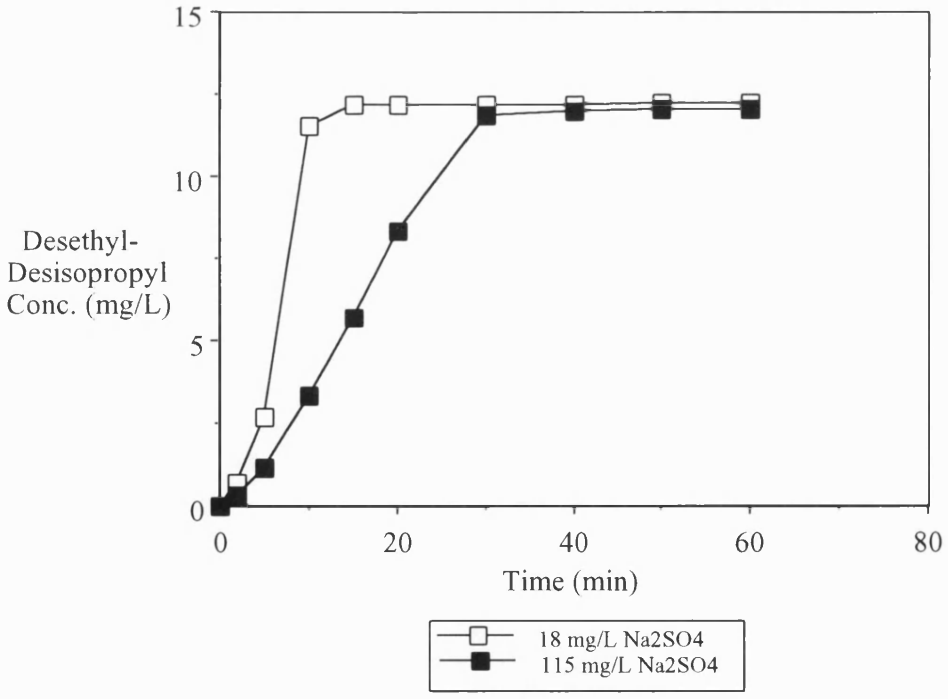

Figure 4.17b: *Effect of $NaSO_4$ Concentration on Desethyl-Desisopropyl Atrazine Concentration.*

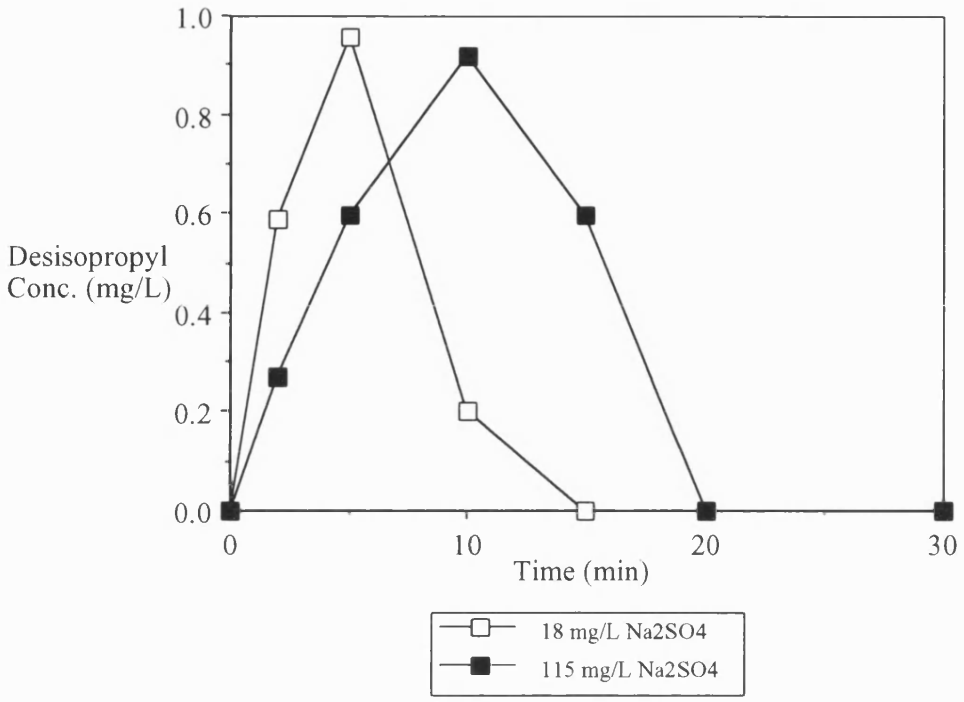

Figure 4.17c: *Effect of $NaSO_4$ Concentration on Desisopropyl Atrazine Concentration.*

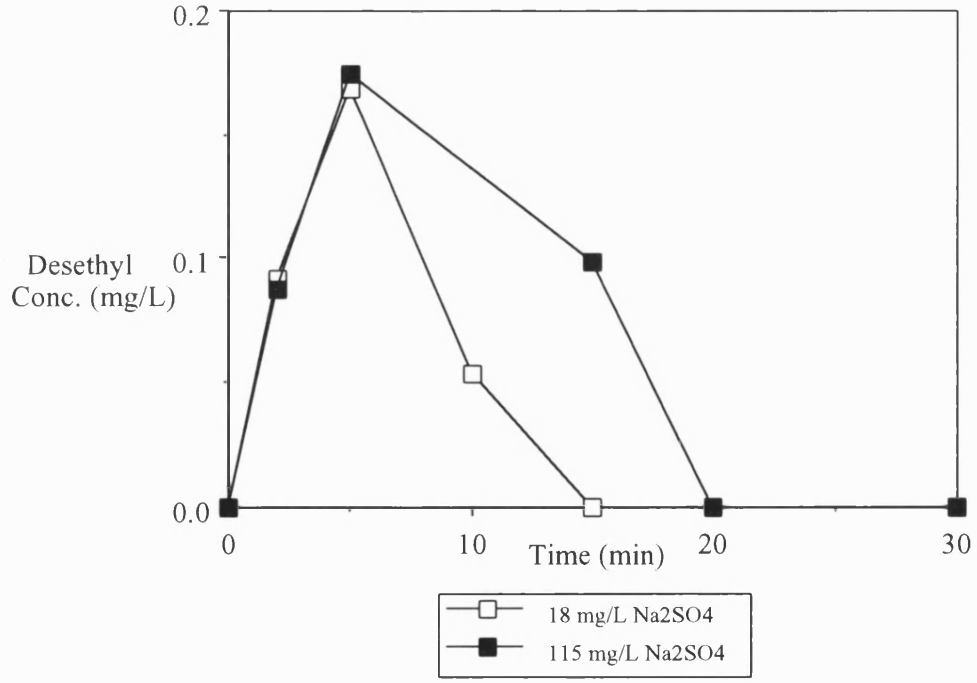

Figure 4.17d: *Effect of $NaSO_4$ Concentration on Desethyl Atrazine Concentration.*

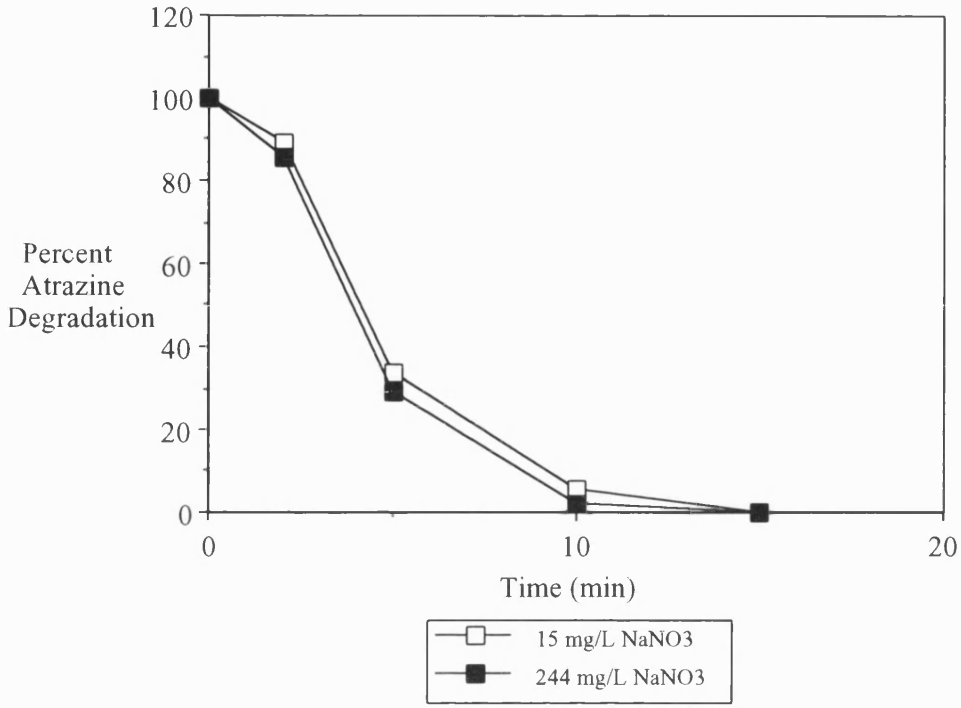

Figure 4.18a: *Effect of $NaNO_3$ Concentration on Atrazine Degradation.Initial Atrazine Concentration 15 mg/L; 7.5 mg/L O_2 .*

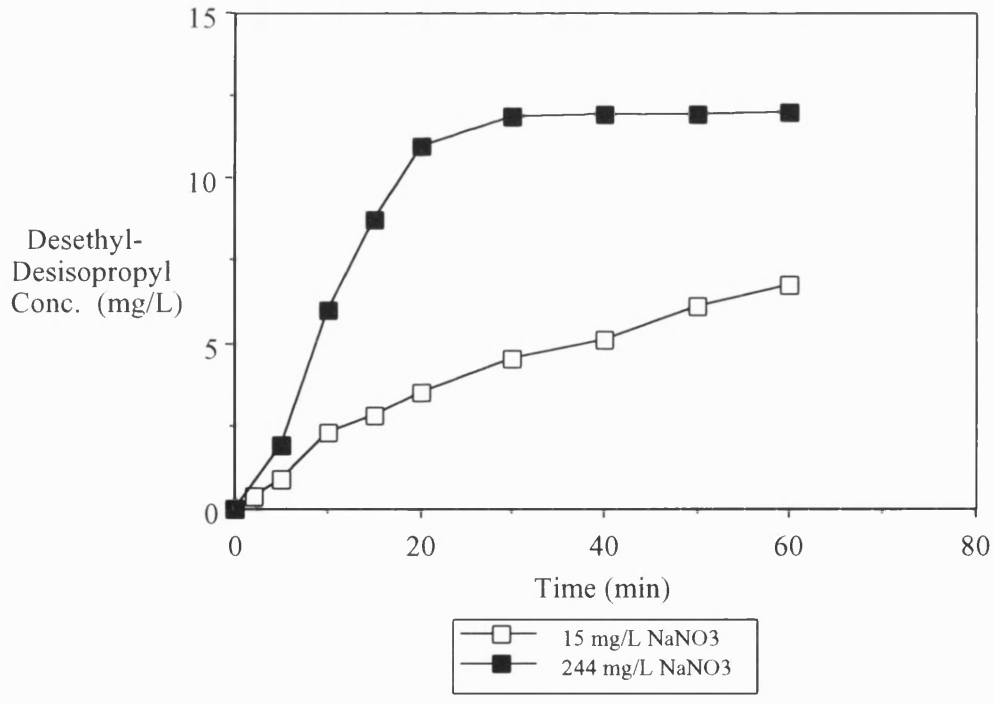

Figure 4.18b: *Effect of $NaNO_3$ Concentration on Desethyl-Desisopropyl Atrazine Concentration.*

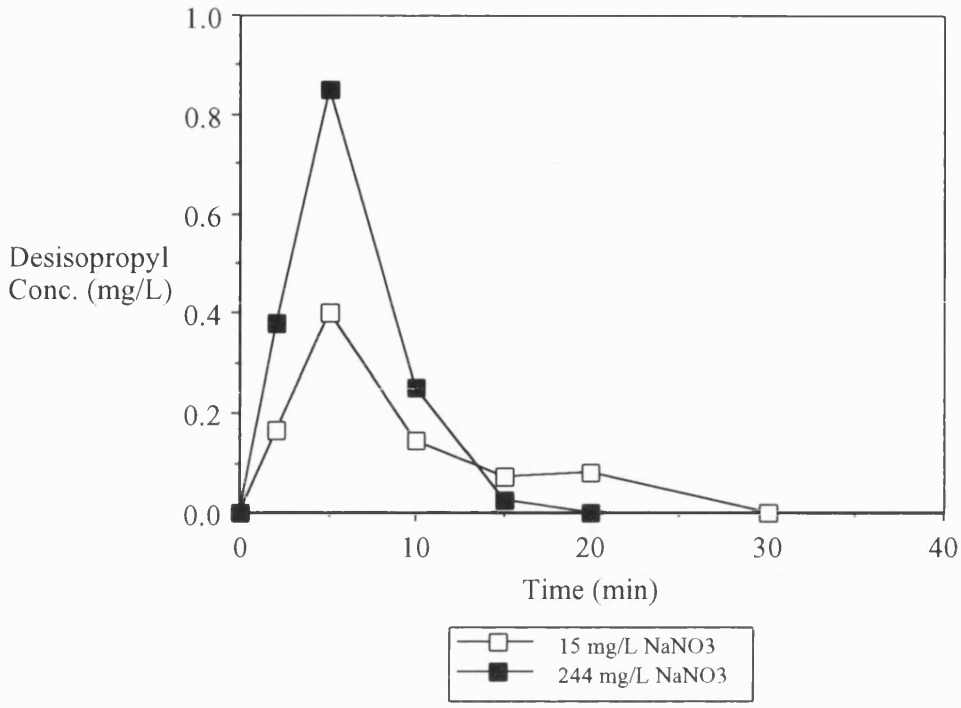

Figure 4.18c: *Effect of $NaNO_3$ Concentration on Desisopropyl Atrazine Concentration.*

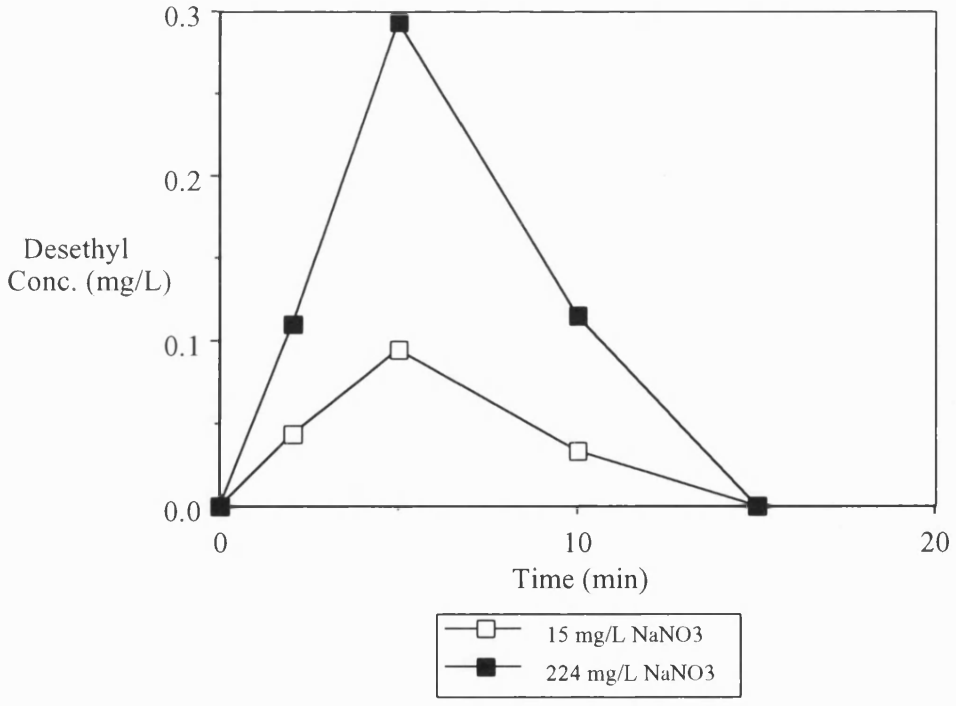

Figure 4.18d: *Effect of $NaNO_3$ Concentration on Desethyl Atrazine Concentration.*

It should be noted that the previous work carried out on inorganic ions[68] used an immobilised coating of TiO_2 on glass and this could have an effect on the observed results. More importantly the data was obtained at a solution pH < the point of zero charge (PZC). For Degussa P25 a value of 6.3 pH units has been reported[99] for the PZC and at pH< this value the surface of the catalyst will be positively charged. This means that anions such as chloride, nitrate, sulphate and carbonate will be attracted from the surface and any detrimental effect on degradation rates will be greatest. Further work[99] has confirmed that at pH 8-13 no effect on degradation rates of 3-chlorophenol was found in the presence of inorganic ions.

Other possibilities which may explain the results in this present study include the possibility of increased atrazine adsorbance in the presence of inorganic ions or a possible scavenging reaction reducing electron-hole recombination and therefore increasing photocatalytic reaction rates.

There is evidence of catalyst dispersion effecting degradation rates in a study on phenol over an anatase form of TiO_2 [41]. It was found that stirring of a catalyst solution reduced the average particle diameter d_p from 1.88 μm to 0.98 μm for 15 min and 60 min respectively. The effect of illumination further reduced d_p due to an accumulation of surface charge on the catalyst surface. When compared to the case of a poorly stirred solution, this effect of stirring and illumination on particle size resulted in increases in UV light absorbance and hence increased reaction rates.

4.1.7 Effect of Tap Water Compared with UHQ Water

In order to examine the effect of a "real" system, likely to be encountered in any industrial application of photocatalytic oxidation in water treatment, a comparison was made of a batch atrazine degradation in UHQ water and Bath mains tap water. SCM WDB TiO_2 was used for this study as it had already proved to be the most effective powdered catalyst for the degradation of atrazine.

When suspensions of the WDB catalyst were prepared it was noted that the dispersion characteristics in UHQ and tap water differed markedly. When WDB TiO_2 was added to UHQ water it formed a spontaneous opaque paint-like dispersion. When the same material was added to tap water the dispersion was very poor, the material appeared to agglomerate and precipitate out of solution. The dispersion could be improved by mixing but the dispersion was not stable and agglomerates appeared to reform in a matter of minutes.

In the batch degradation experiments themselves, the catalyst solution was mixed by gas sparging and thus the problems of the catalyst settling out did not occur. The results presented in figure 4.19 show that the inorganic ions, dissolved organic matter and other factors present in tap water, together with any changes in particle size distribution, have a detrimental effect on rate of atrazine degradation and rates of reaction intermediate production and degradation.

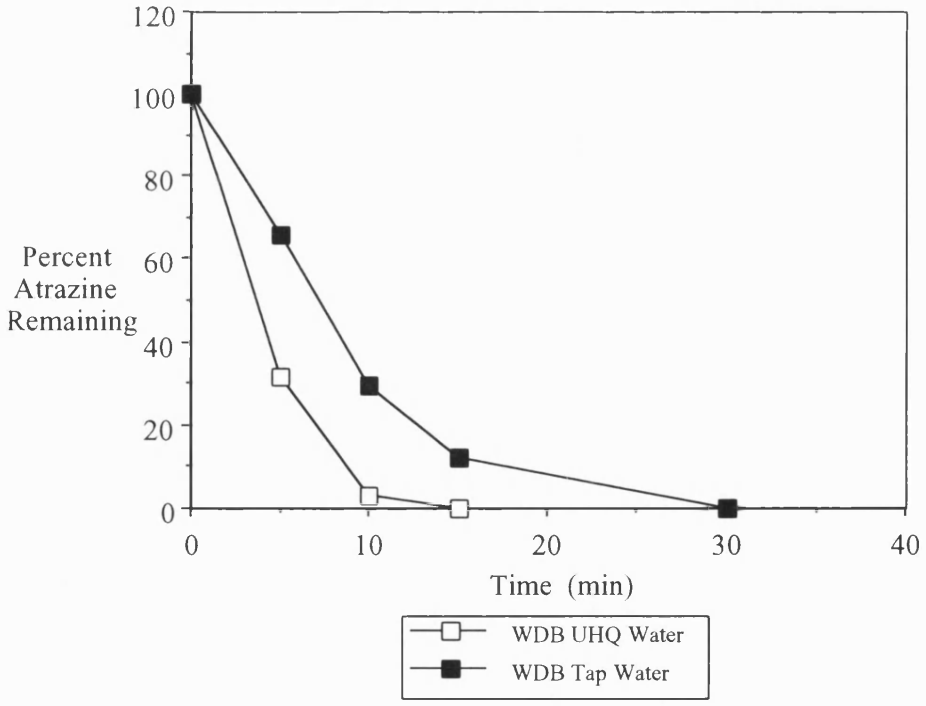

Figure 4.19a: *Comparison of the Effect of Tap Water and UHQ Water on Atrazine Degradation using WDB TiO_2. Initial Atrazine Conc. 5mg/L; 7.5 mg/L O_2 .*

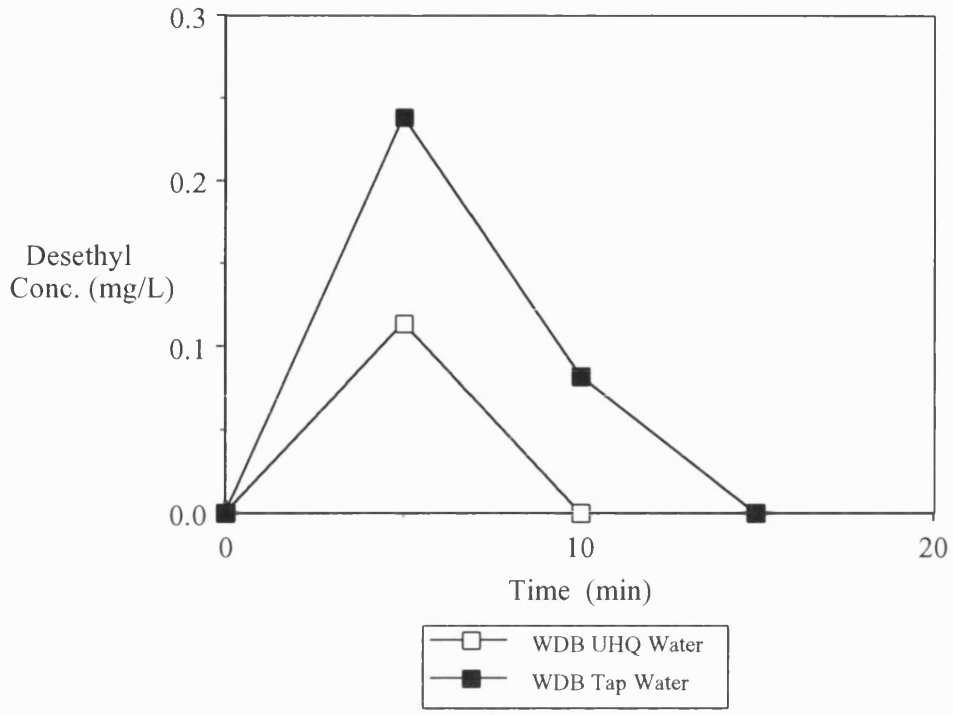

Figure 4.19b: *Comparison of the Effect of Tap Water and UHQ Water on Desethyl Atrazine Concentration using WDB TiO_2.*

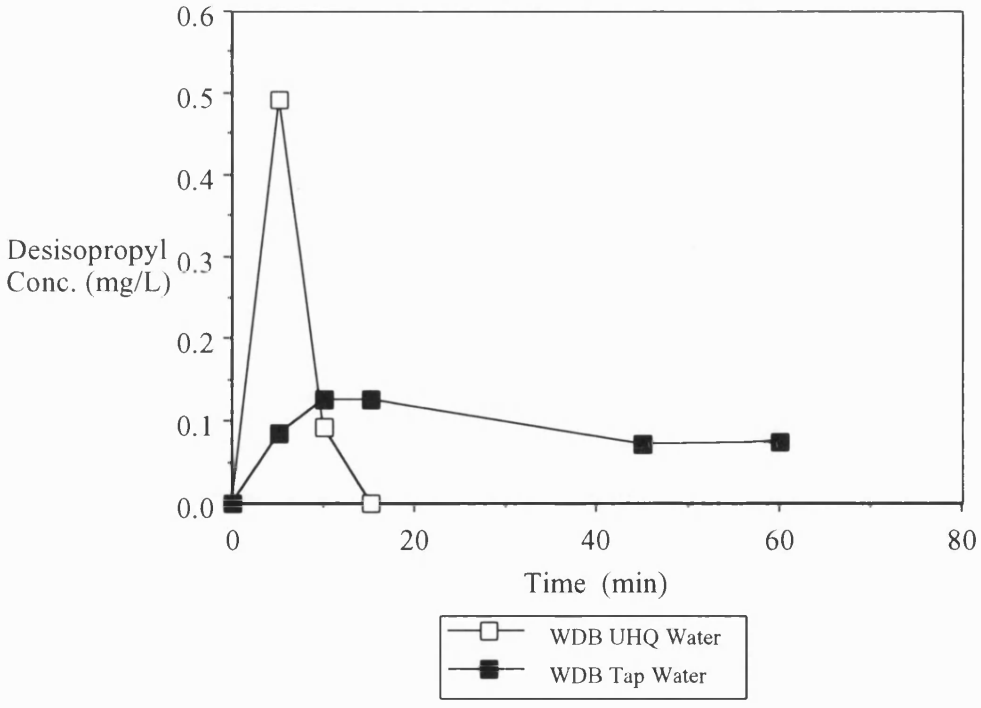

Figure 4.19c: *Comparison of the Effect of Tap Water and UHQ Water on Desisopropyl Atrazine Concentration using WDB TiO_2.*

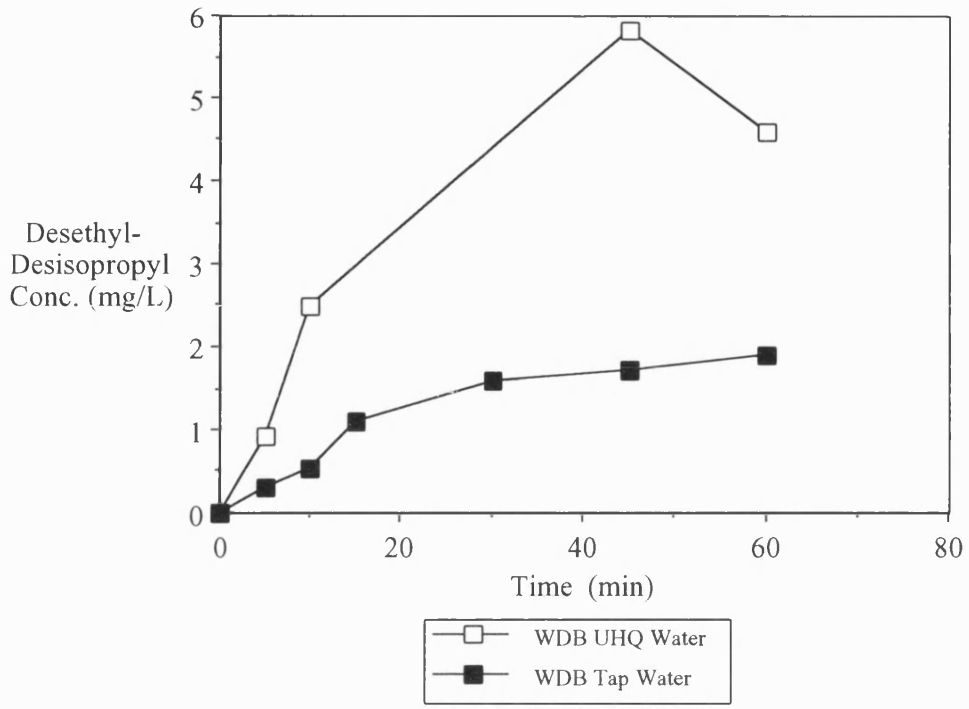

Figure 4.19d: *Comparison of the Effect of Tap Water and UHQ Water on Desethyl-Desisopropyl Atrazine Concentration using WDB TiO_2.*

It can be seen from figures 4.19c and 4.19d that concentrations of desisopropyl and desethyl-desisopropyl atrazine for the experiment carried out in tap water show slow increases and little subsequent degradation. This behaviour can be explained by fouling of the catalyst surface and blocking of active sites by compounds present in tap water (inorganic ions and/or dissolved organic material).

First-order rate constants for atrazine degradation using WDB TiO_2 for both systems are shown in table 4.5:

Table 4.5: *First Rate Constants for Atrazine Degradation Using WDB TiO_2 in Tap and UHQ Water.*

	k' (min^{-1})	**$t_{0.5}$ (min)**
Tap Water	0.177	6.18
UHQ Water	0.253	2.76

In order to compare the degradation rates of atrazine in tap water and ultrapure water without encountering the possible problems of dispersion and differences in size distribution described above, it was decided to compare the rates found when using a form of TiO_2 which is not subject to these dispersion effects and therefore samples of crushed tablets were used.

The results obtained are shown in figure 4.20 and show that again in this case the rates of degradation in UHQ water are significantly greater than those in tap water.

The poor degradation in tap water also shows evidence of reaching a limiting value or "plateau" the percent atrazine remaining at ≈10% at long reaction times >100 min.

First-order kinetic constants for the two systems are shown in table 4.6.

Table 4.6: *First Order Rate Constants for Atrazine Degradation Using Crushed Tablets in Tap and UHQ Water.*

	k' (min^{-1})	**$t_{0.5}$ (min)**
Tap Water	0.0579	11.32
UHQ Water	0.154	4.623

There is also some evidence that the use of tap water has a detrimental effect on the catalyst since a repeat of the UHQ experiment using a batch of catalyst used in the tap water experiments showed a decrease in degradation rate. This cumulative effect on catalyst fouling has been reported [51], the activity having to be restored by washing with 0.1 M $NaHCO_3$ solution.

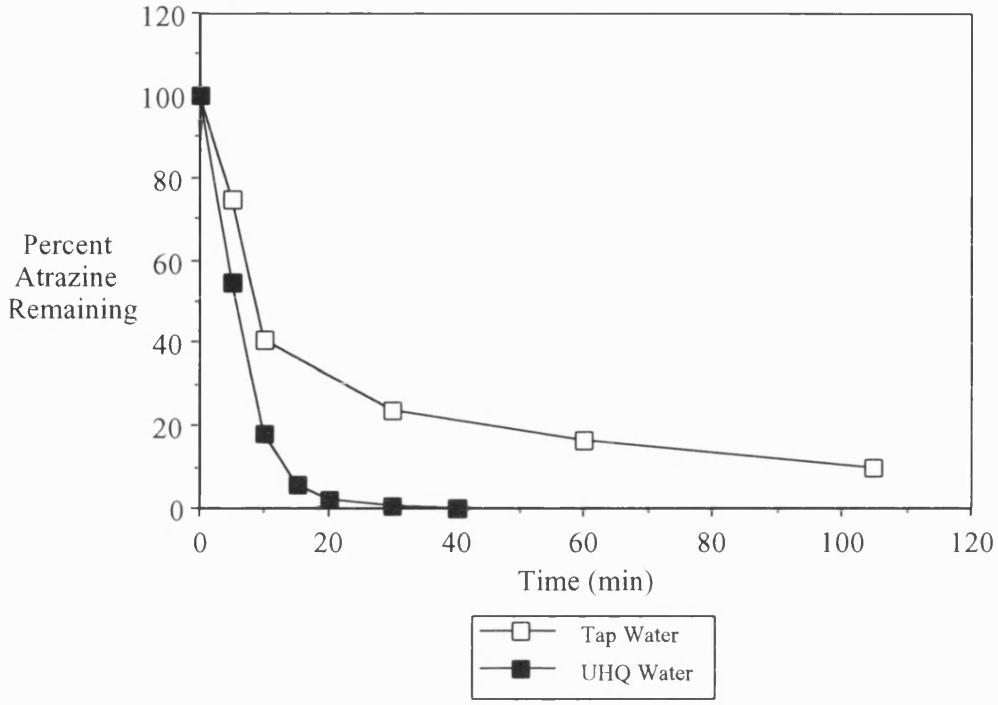

Figure 4.20a: *Comparison of the Effect of UHQ Water and Tap Water on the Degradation of Atrazine using Crushed TiO_2 Tablets.*

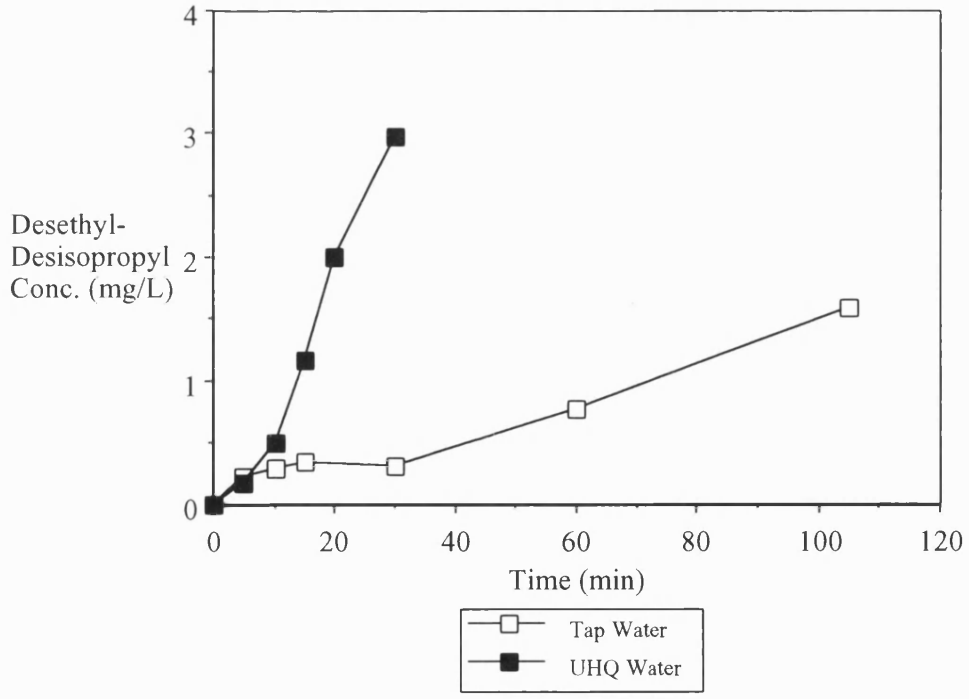

Figure 4.20b: *Comparison of the Effect of UHQ Water and Tap Water on the Concentration of Desethyl-Desisopropyl Atrazine using Crushed TiO_2 Tablets.*

These results obtained with tap water are important since they show that degradation rates and possible catalyst fouling are greatly effected by compounds present in potable water supplies.

4.2 Pilot Scale Photocatalytic Degradation of Atrazine

Experiments in the pilot scale reactor, as described in section 3.11, were carried out at atrazine concentrations at the ng/L level to simulate conditions in "real" potable water sources. Initially, batches of crushed and whole TiO_2 tablets were used as catalyst, followed by tablets which had been heat treated to improve their attrition resistance, coated ceramic beads, and finally P25 powder. All reactions were carried out using softened Bath mains water.

4.2.1 Experimental Problems

4.2.1.1 Analytical Problems

There were a number of analytical problems specific to the pilot-scale experiments. Firstly, reaction intermediates could not be detected due to low concentration and interference on the HPLC trace from compounds in the softened water, concentrated by the solid phase extraction (SPE) process. Secondly, some control experiments showed increases in atrazine concentration with time. This was explained by unwanted carry-over from one experiment to the next from the reused catalyst. Washing between experiments was carried out but in retrospect washing plus illumination would be a better option.

4.2.1.2 Attrition Problems

Initial Experiments using the pilot scale reactor, as described in section 3.11, were carried out using batches of crushed (sieved to be > 1.8 mm) and mixtures of crushed and whole Degussa P25 tablets. A major problem during these experiments was the high rates of attrition of the tablets, as the bed of particles was rotated and

ground on the reactor wall, leading to the circulated atrazine solution becoming cloudy.

The amount of attrition was quantified by measuring the absorbance at 350 nm of the solution in the holding tank. At the start of an experiment an initial sample was taken and used as a blank. As the catalyst was broken up in the reactor due to the swirl motion, the concentration of fine particles carried into solution increased, samples were taken at regular intervals and the absorbance at 350nm measured . The increase in absorbance was converted to a concentration of fines based on a calibration made using P25 and is shown in figure 4.21.

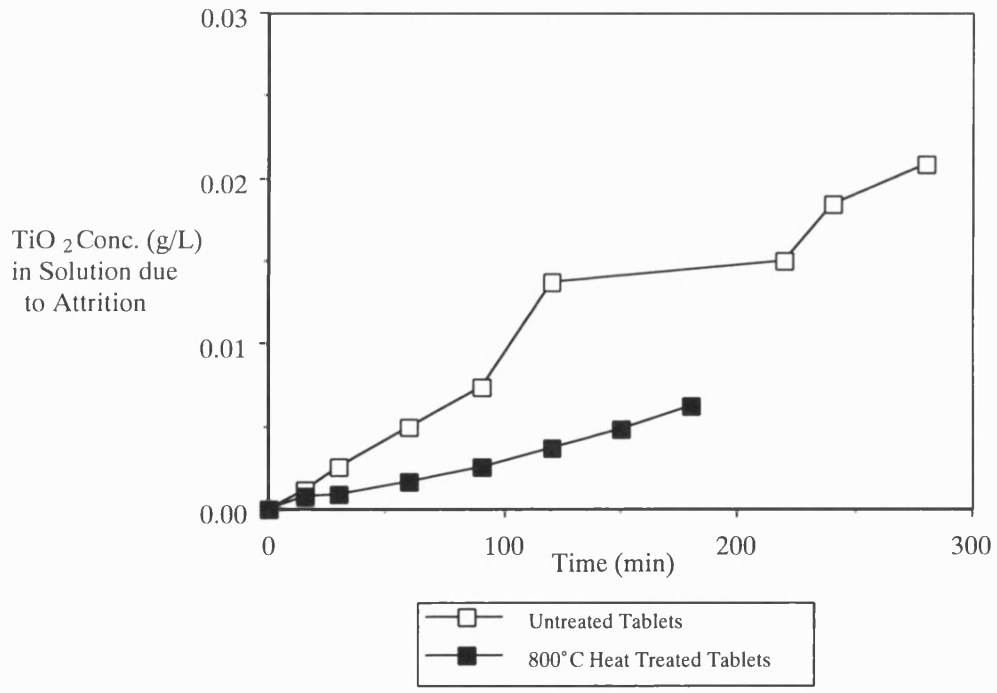

Figure 4.21: *Effect of TiO_2 Tablet Attrition in Pilot Reactor on Fines Concentration in solution.*

This catalyst attrition caused a number problems both for the experimental program and the practical use of this reactor system:

(i) The total catalyst present in the system consisted of the particles introduced into the reactor at the start of the experiment and the fines which were produced over the duration of an experimental run. These fines were carried out from the reactor

and were circulated through the system, being lost at the end of an experiment. Thus the actual loading remaining in the reactor decreased over a series of experiments.

(ii) During an experiment the mean particle size of the catalyst was reduced and the particle dispersion in the reactor was increased, both effects leading to more efficient usage of the UV light.

In practice this meant that the reactor was being run as a mixture of particulate TiO_2 and a fine suspension similar to P25 TiO_2.

Both these effects meant that conditions were not only changing between, but also during experimental runs.

From a practical point of view the production of fines in this reactor system is undesirable. Any catalyst lost from the system would have to be replaced or recovered downstream increasing the running costs. Any system which introduced catalyst fines into the treated water would suffer in comparison with non-invasive methods such as fixed bed GAC filtration.

Using the calibration data for UV absorbance of P25 powder the amount of catalyst lost from the reactor can be estimated at 3g over 5 h for untreated tablets and 1.64g over 5 hr for tablets heat treated to 800°C from starting loadings of 300 g.

Experiments at a lower flowrate were carried out to attempt to reduce the amount of particle/reactor wall grinding and therefore limit the effects of attrition but had only a small effect. In addition reducing the flowrate also had the detrimental effect of reducing mixing and axial dispersion in the reactor.

4.2.2 Experiments with Crushed and Whole Tablets

Initial experiments were carried out using mixtures of whole and crushed tablets to look at the rates of atrazine degradation expected in the pilot reactor.

The results in figure 4.22 show the benefit of increasing catalyst loading up to a total of 2.7 Kg of crushed and whole tablets.

It can be seen that the overall atrazine degradation increases with increasing catalyst loading. It can also be seen that a plateau effect is observed, similar to that

for the results obtained with tap water in the batch reactor, with higher loadings delaying the onset of activity loss. This can be explained by the soft water used in the pilot scale experiments having the same or similar catalyst fouling characteristics since it will contain many of the same components as tap water.

The lower initial degradation rate observed for a loading of 2.7 Kg compared to 300g may be due to a lower proportion of the total loading being particles smaller than the whole tablets. The smaller particles, which will be more efficient catalysts due to their larger surface area to volume ratio, could be shielded from UV illumination by the larger, whole tablets present at the higher loading.

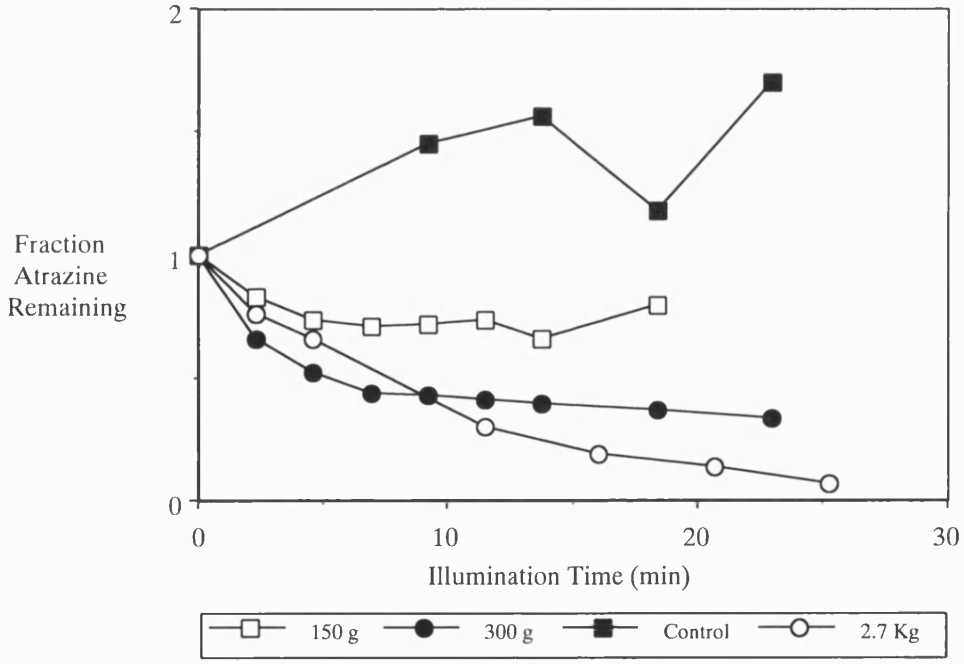

Figure 4.22: *Effect of Tablet Loading on Pilot Scale Atrazine Degradation. Initial Atrazine Concentration 200-300 ng/L ;Total Flowrate 30 L/min; Oxygen Sparge Rate 1.5 L/min.*

4.2.3 Heat Treatment of Tablets

It was decided that one possible route for reducing attrition in the reactor was to attempt to increase the mechanical strength of the tablets by sintering at high temperatures.

Initial tests, heating batches of tablets at 450 °C, 550 °C, 650 °C, 800 °C, and 1000 °C, showed that the mechanical resistance to crushing showed little increase up to 650 °C, a considerable improvement at 800 °C and a large improvement at 1000 °C. This increase in strength was accompanied by a reduction in tablet size and, for those tablets heated to 1000 °C, also a change in colour from white to grey.

In order to ascertain the effectiveness these heat treated tablets would have in the pilot reactor, it was important to compare the photocatalytic activity with unheated tablets. The whole tablets themselves could not be tested in the small-scale batch system since there would be no mixing and turnover of particles. Batches of the heat treated tablets were therefore crushed, sieved to the size range 300-180 μm, added to the batch reactor and the degradation of atrazine measured as described previously in section 3.10.

The results from these batch experiments are shown in figure 4.23a and 4.23b, for atrazine degradation and desethyl-desisopropyl atrazine production respectively.

This shows that the tablets heated to 1000 °C lose their activity and show degradation rates close to that of the control (i.e.UV photolysis only). The tablets heated to 800 °C however ,which showed an appreciable improvement in mechanical strength, showed only a small loss in activity compared to the un heat treated tablets. It was therefore decided that using these tablets, heat treated to 800 °C, in the pilot reactor could give rise to satisfactory degradation rates together with reduced tablet attrition.

Comparison of the production rates of desethyl-desisopropyl atrazine shown in figure 4.23b also confirmed that tablets heated to 800 °C retained much of their catalytic activity compared to those heated to 1000 °C.

This change in activity with heat treatment has been reported before together with a change in TiO_2 crystal form from anatase to rutile [31]. Since in general anatase forms have been found to be more catalytically active than rutile forms (which sometimes show no photocatalytic activity) this result is well explained.

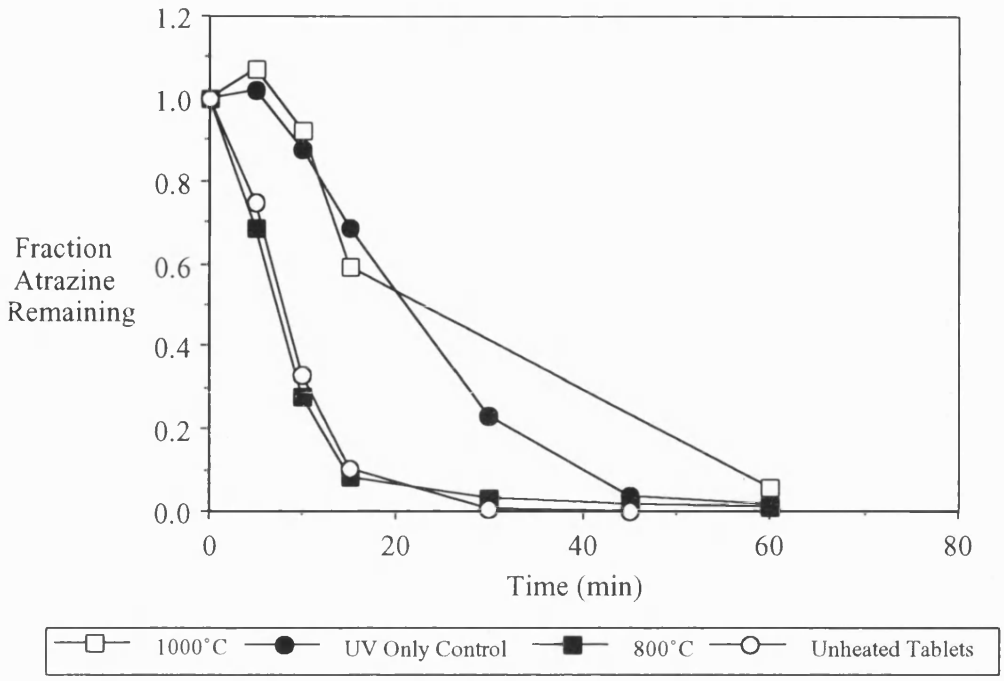

Figure 4.23a: *Effect of Tablet Heat Treatment on Batch Degradation of Atrazine. Initial Atrazine Conc. 9 mg/L; 7.5 mg/L* O_2 *.*

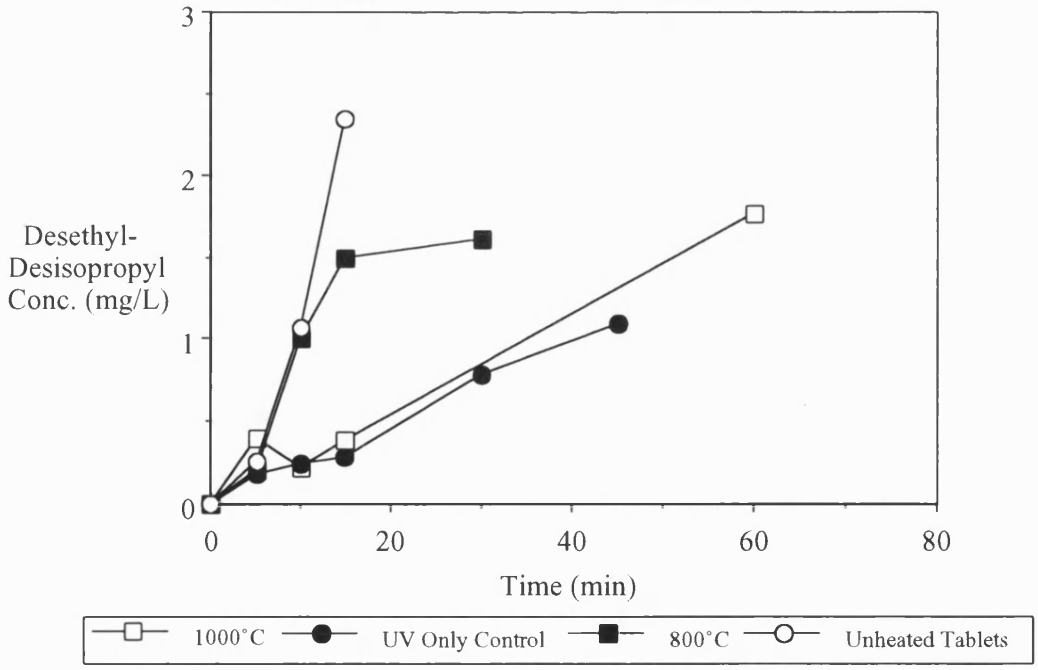

Figure 4.23b: *Effect of Tablet Heat Treatment on Production of Desethyl-Desisopropyl Atrazine.*

4.2.4 Heat Treated Tablets in the Pilot Reactor

The pilot reactor was emptied of the previously used catalyst, 900 g of tablets heated to 800 °C for 1h were added to the reactor and a number of initial observations were made. At a flowrate of 25-40 L/min the bed of tablets was fluidised and at higher flowrates of 80-90 L/min the bed was lifted and was suspended in a band half way up the reactor. It was decided that the best chance for reducing the attrition was to increase the amount of heat treated tablets and run the reactor as a fluidised system at a low flowrate where the inter-particle attrition would be less than that caused by particles being ground on the wall of the reactor.

A series of experiments were therefore carried out using a larger mass of catalyst (10 Kg) and operating as a fluidised system with only a small turnover of particles. Running at the lowest flowrate which gave a sufficient mixing of the catalyst (25 L/min) showed poor rates of degradation, close to that for a no catalyst control, as shown in figure 4.24.

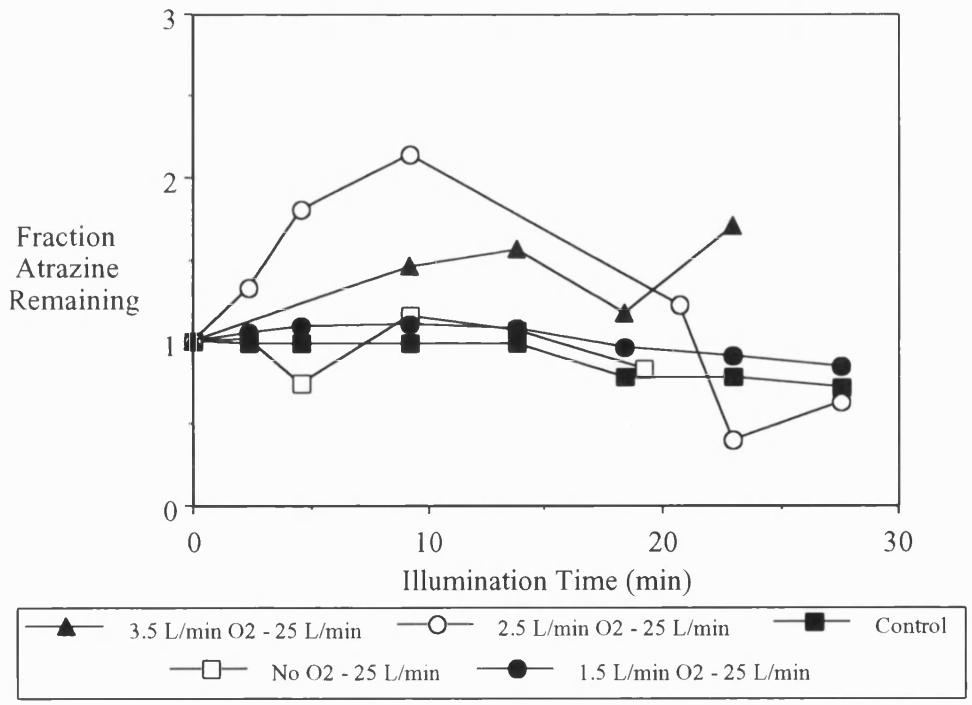

Figure 4.24: *Pilot Scale Atrazine Degradation Using Heat Treated Tablets.Initial Atrazine Conc. 150 ng/L*

Running the reactor at a higher flowrates of 35 L/min to 60 L/min and for longer illumination times show the maximum overall degradation of atrazine obtained to be 85 % for an illumination time of 100 min.

Results from these experiments are shown in figure 4.25a, and in figure 4.25b for longer illumination times.

It was found that although attrition rates were slightly reduced the catalyst still disintergrated with time and the same problems of fines production were experienced.

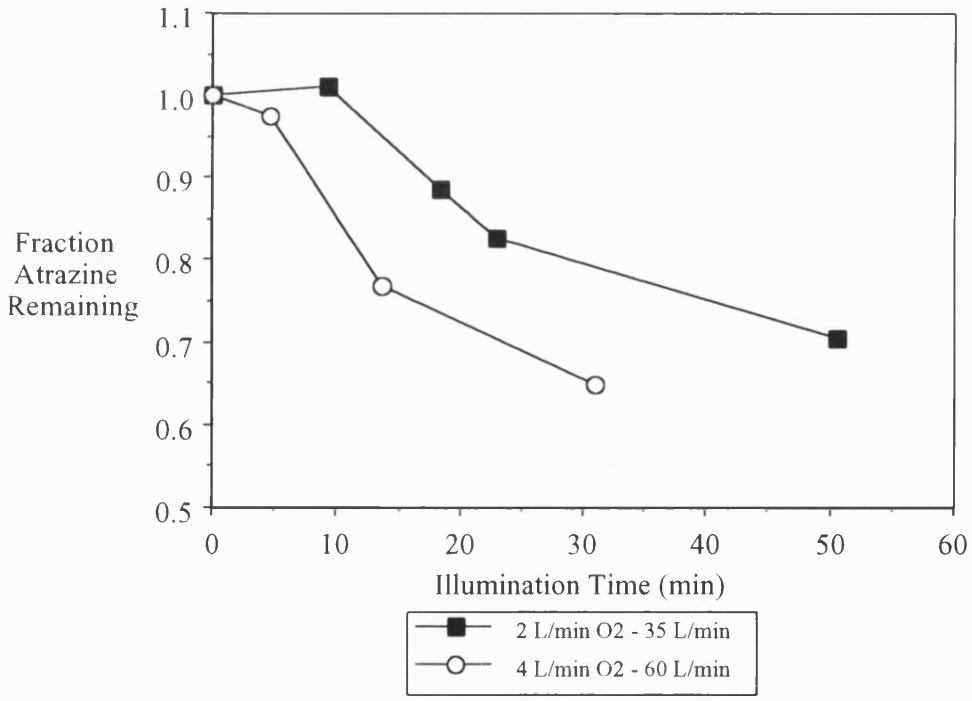

Figure 4.25a: *Pilot Degradation of Atrazine Using Heat Treated Tablets (10 Kg)*

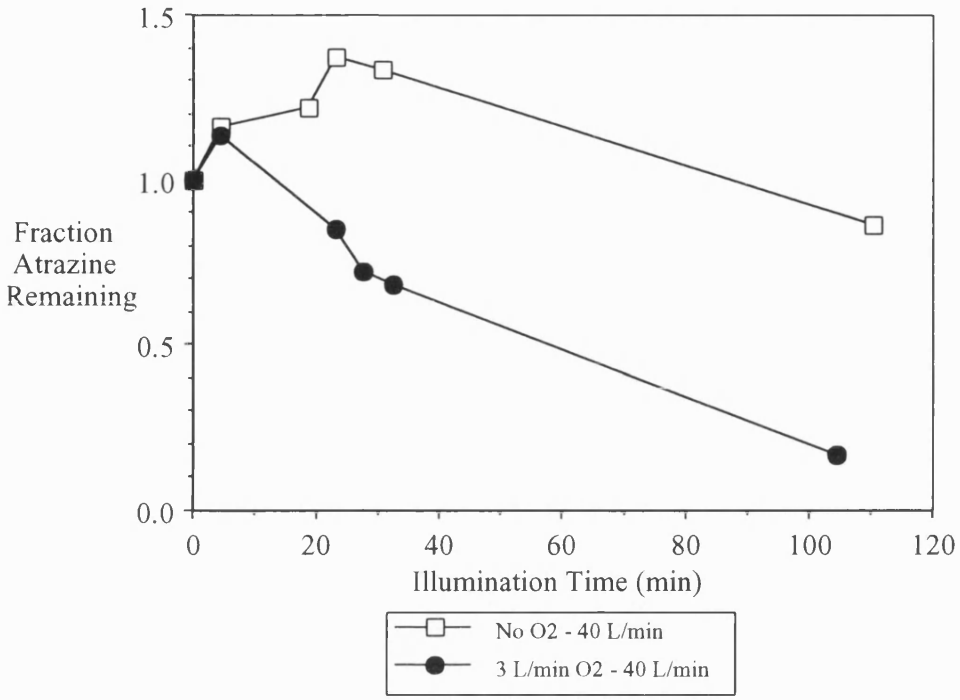

Figure 4.25b: *Pilot Degradation of Atrazine Using Heat Treated Tablets (10 Kg) for Longer Illumination Times.*

4.2.5 Experiments With Coated Ceramic Beads.

In order to be able to operate the pilot scale reactor without the catalyst suffering attrition it was decided to develop a system based on a supported photocatalyst. It was decided to use the sol-gel method modified with diethanolamine (DEA) giving a coating on steatite beads using the method described in section 3.8.2.

It was impossible to determine the amount or activity of the titania coating on the beads due to the unsuitability of using large particles in the batch reactor. The beads, which were checked by visual examination for successfull coating, were introduced into the pilot reactor.

The results from experiments carried out with the supported catalyst are shown in figure 4.26. Very low rates of degradation were found and samples of catalyst removed from the reactor showed that, even though the support was robust

enough to survive intact inside the reactor, the coating was removed due to the particle-particle attrition in the fluidised bed.

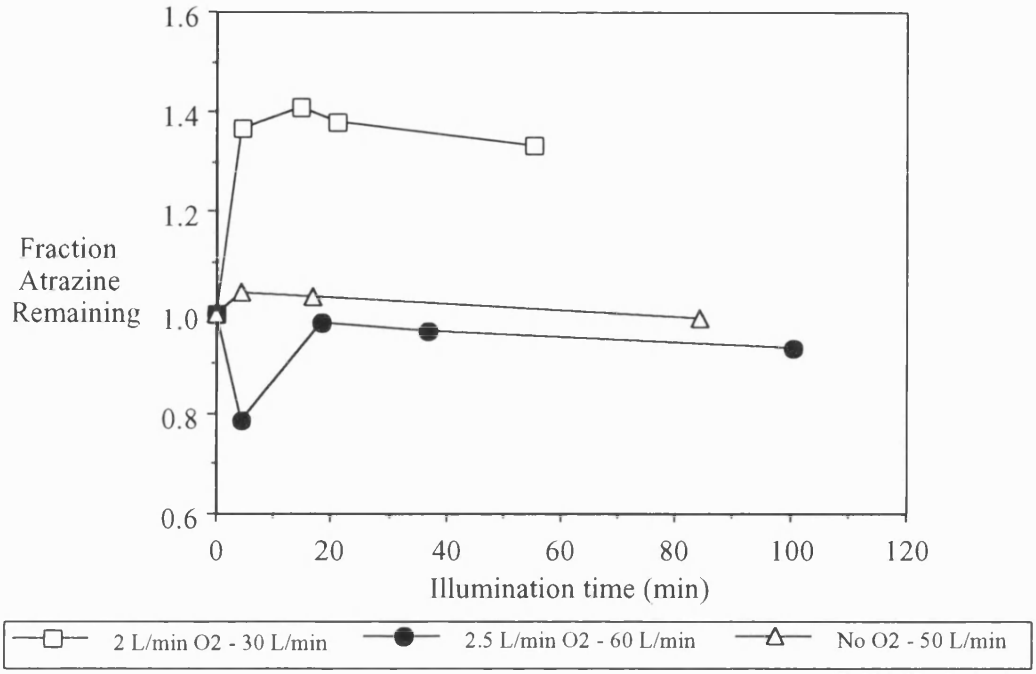

Figure 4.26: *Pilot Scale Atrazine Degradation Using Coated Ceramic Beads.*

4.2.6 Pilot Scale Degradation using Degussa P25 Powder

After careful assessment it was decided that the reactor was not suitable for either particulate or supported catalyst due to the problems of attrition. Therefore a series of experiments was carried out using Degussa P25 powder circulated through the pilot rig. This would provide a comparison with the data obtained with the particulate catalyst and information for a system which could be run without the need for a catalyst free output stream.

The results from this series of experiments are shown in figure 4.27 and 4.28. The results show that an increase in catalyst loading led to an increase in degradation rate as did an increase in oxygen sparge rate. Again there is evidence of loss of activity leading to the plateau effect.

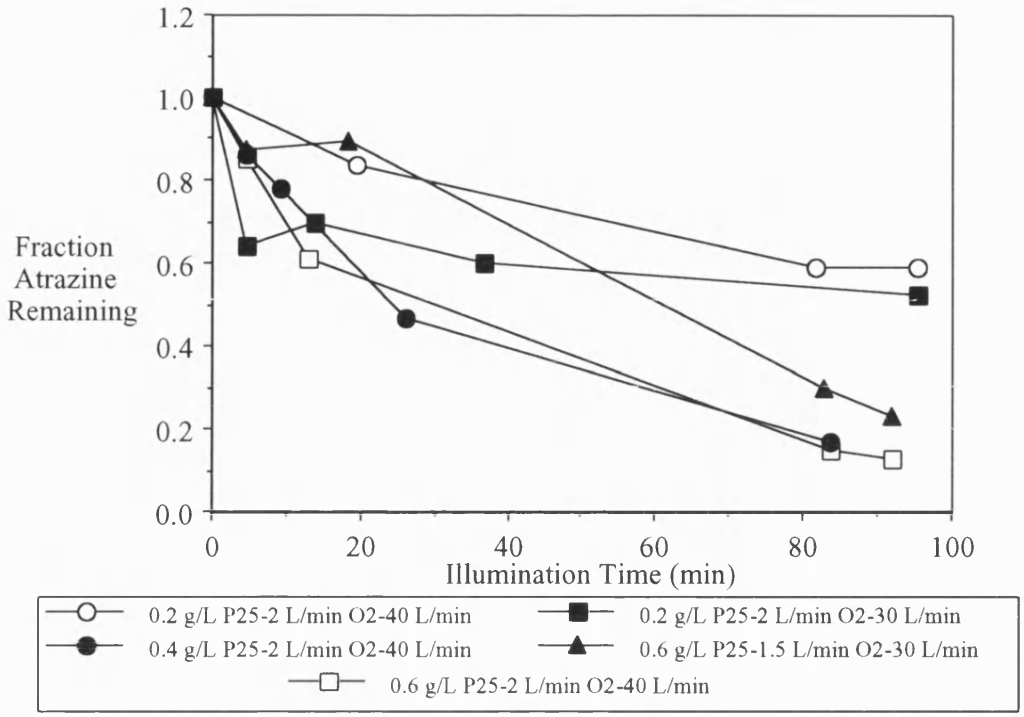

Figure 4.27: *Effect of P25 Loading on Pilot Scale Atrazine Degradation. Initial Atrazine Conc. 150-200 ng/L*

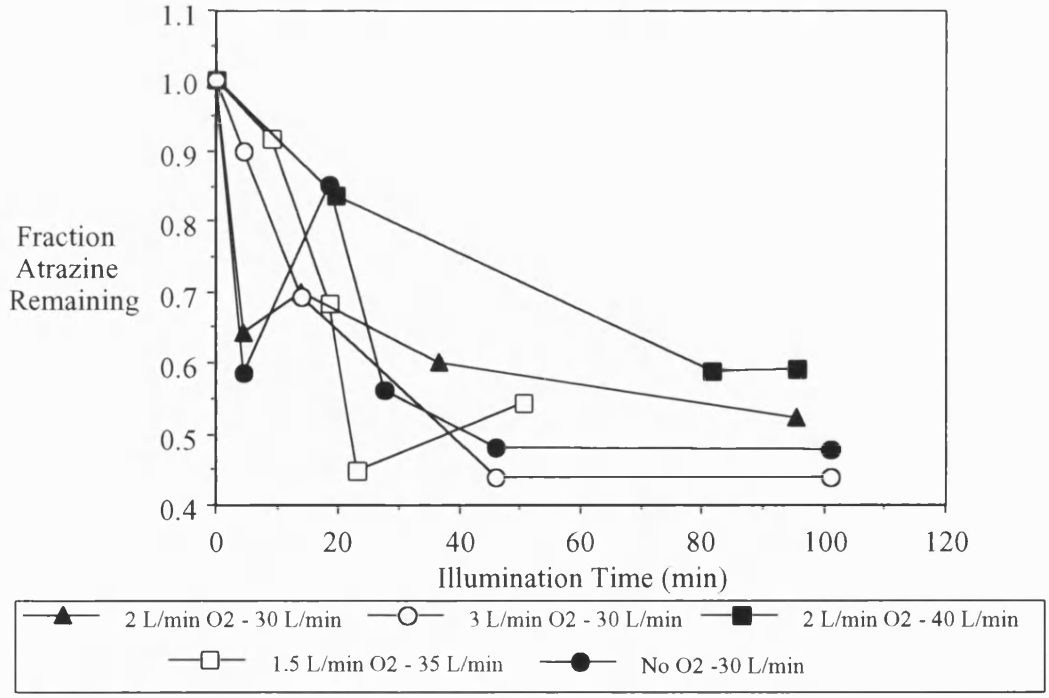

Figure 4.28: *Effect of Oxygen Sparge Rate and Flowrate on Pilot Scale Degradation Using P25 Catalyst. P25 Loading 0.2 g/L; Atrazine Conc. 150-200 ng/L.*

4.3 Prepared Catalyst

4.3.1 Scanning Electron Microscope (S.E.M) Pictures

Samples of coated glass beads were analysed by SEM and X-ray microanalysis to asses the effectiveness of sol-gel attachment techniques.

Figure 4.29 shows the SEM pictures obtained and Figure 4.30 show the accompanying micrographs.

Figure 4.29a shows the surface of a glass bead coated using preparation method SG2. It can be seen that the surface of the bead has been coated with a layer which can be estimated at 1μm. It can also be seen that the surface is cracked and that surface coverage in this particular coating technique would not be perfect. Possible causes of poor coating are chemical (the bead having a surface layer which prevents the sol-gel solution from wetting the bead) and physical (mechanical loss of coating during the coating process and bead-bead contact while in the sol-gel solution).

A SEM showing the whole bead, figure 4.29b shows a number of circular areas where cracking has occurred and this is probably due to areas where adjacent beads were touching during the coating or firing process.

Figure 4.29c shows that areas of coating contain higher concentrations of titanium than the plain bead surface. Figure 4.29d showing the whole bead indicates that the areas where contact has occurred show thicker layers and greater concentrations of titanium.

Testing the activity of beads coated using methods SG3 in the cuvette photoreactor showed no loss of atrazine. A test using the methyl viologen assay showed no difference with a control measured at 605 nm (λmax). An experiment using a batch of SG3 coated beads in the batch reactor shows degradation rates only slightly greater than a control as seen in figure 4.8.

Figures 4.30a and 4.30b show the difference in X-ray diffraction micrographs for coated and uncoated beads and clearly show a titanium peak for coated beads.

Pages 136-137

Figure 4.29 SEM Pictures of Sol-Gel Coated Glass Beads.

a Close-Up of Glass Bead Surface Coated With Titania From Preparation Method SG2.

b Whole Bead Showing Cracked Areas.

c Element Analysis of Close-Up Bead Surface

d Element Analysis of Whole Bead.

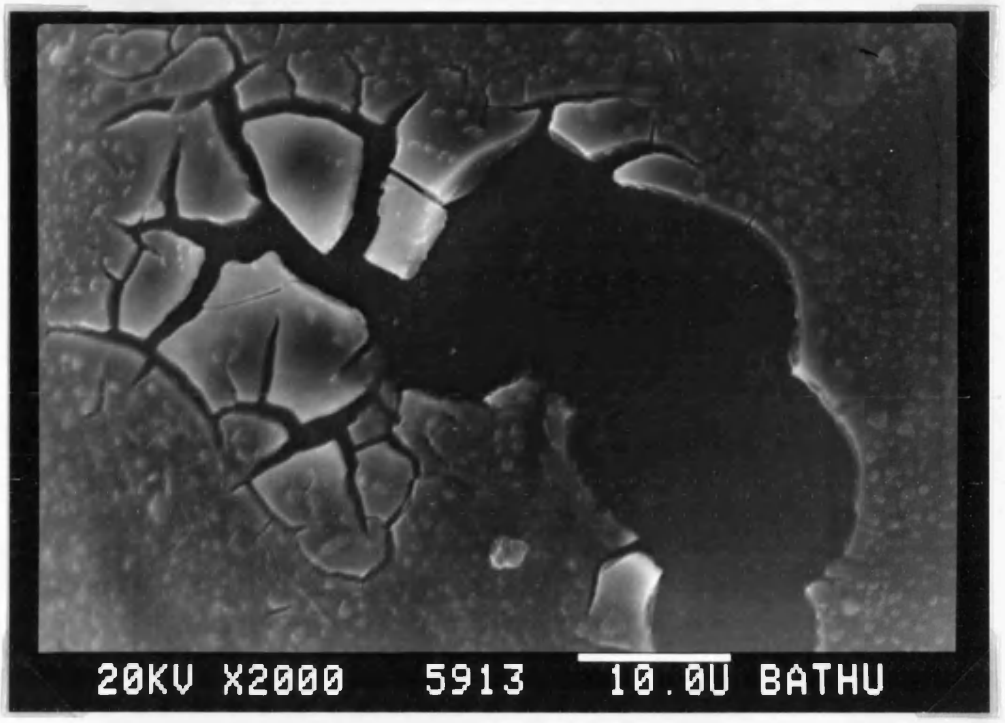

Figure 4.29a: Close-Up of Bead Surface Coated with Titania from Preparation Method SG2

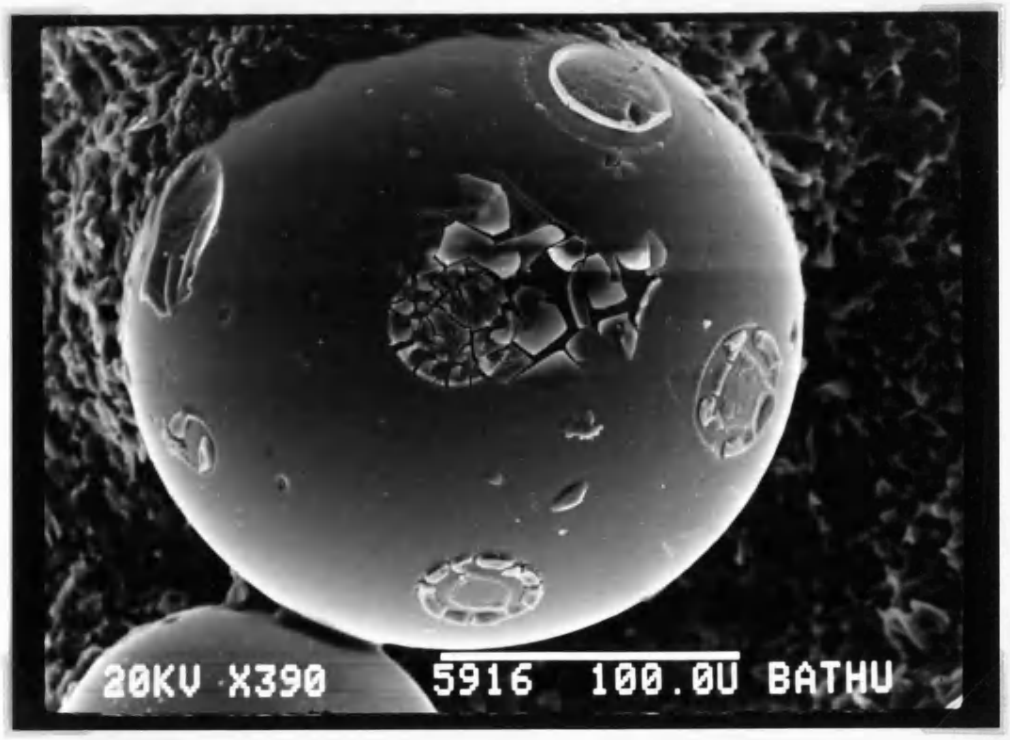

Figure 4.29b: Whole Bead Showing Cracked Areas

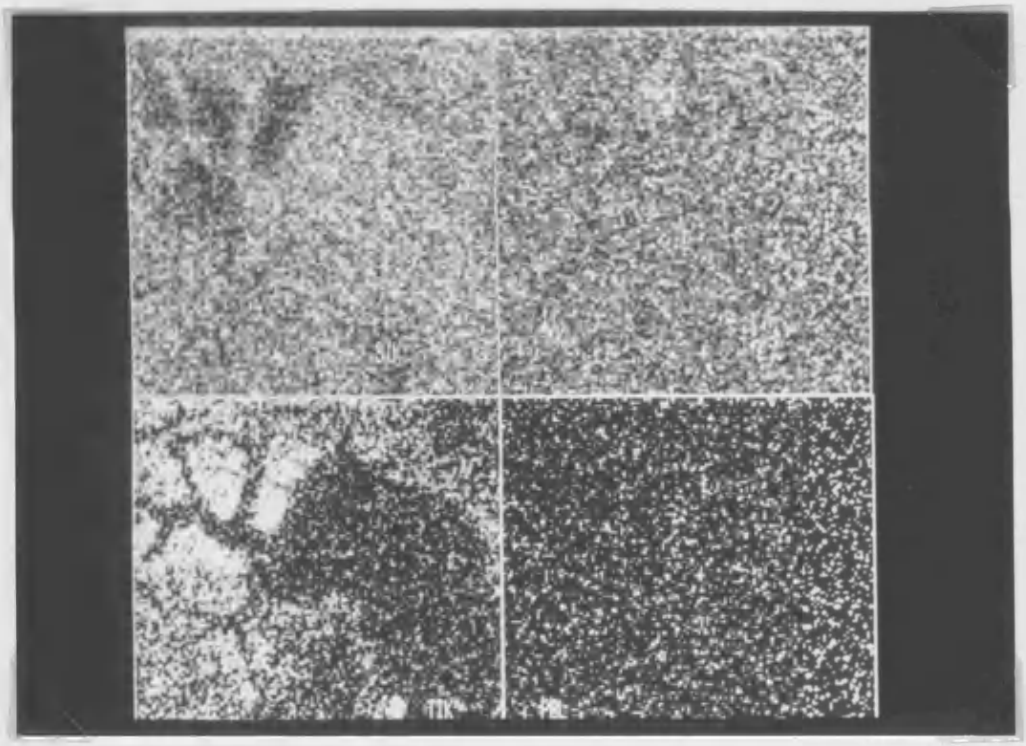

Figure 4.29c: Element Analysis of Close-Up Bead Surface. (Clockwise from Top Left - Silicon, Potassium, Lead, Titanium)

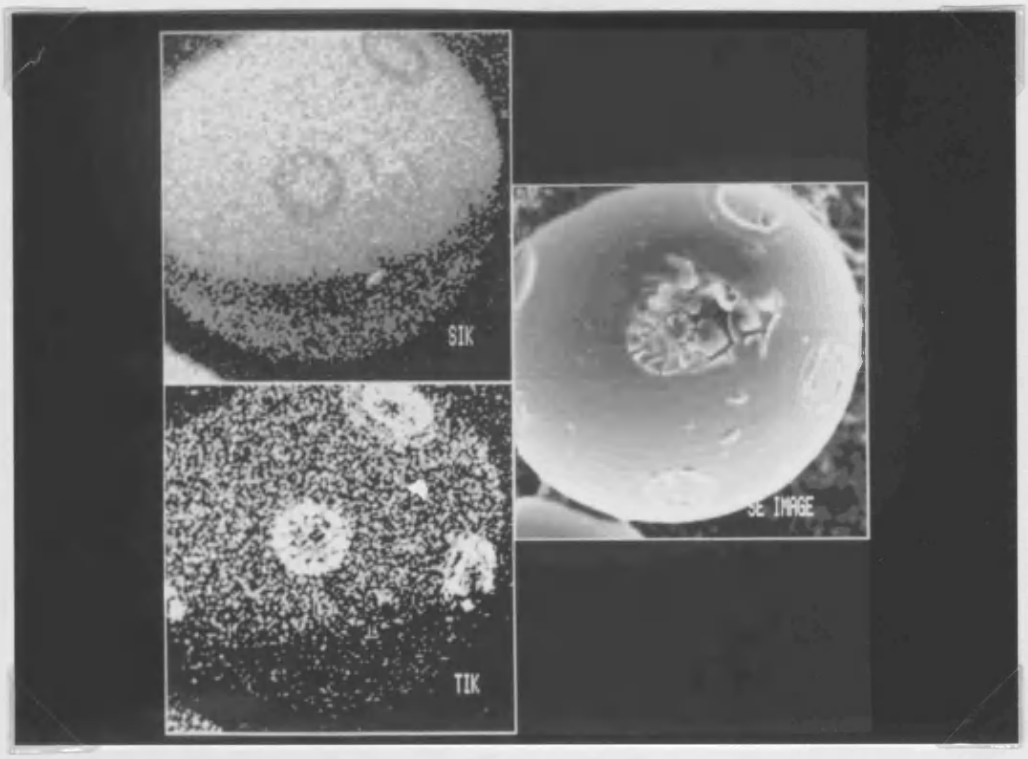

Figure 4.29d: Element Analysis of Whole Bead. (Clockwise from Top Left - Silicon, SEM Image, Titanium)

Pages 139-140

Figure 4.30 X-Ray Micrographs of Sol-Gel Coated and Uncoated Glass Beads

a X-Ray Difraction Micrograph - Uncoated Bead

b X-Ray Difraction Micrograph - Coated Bead

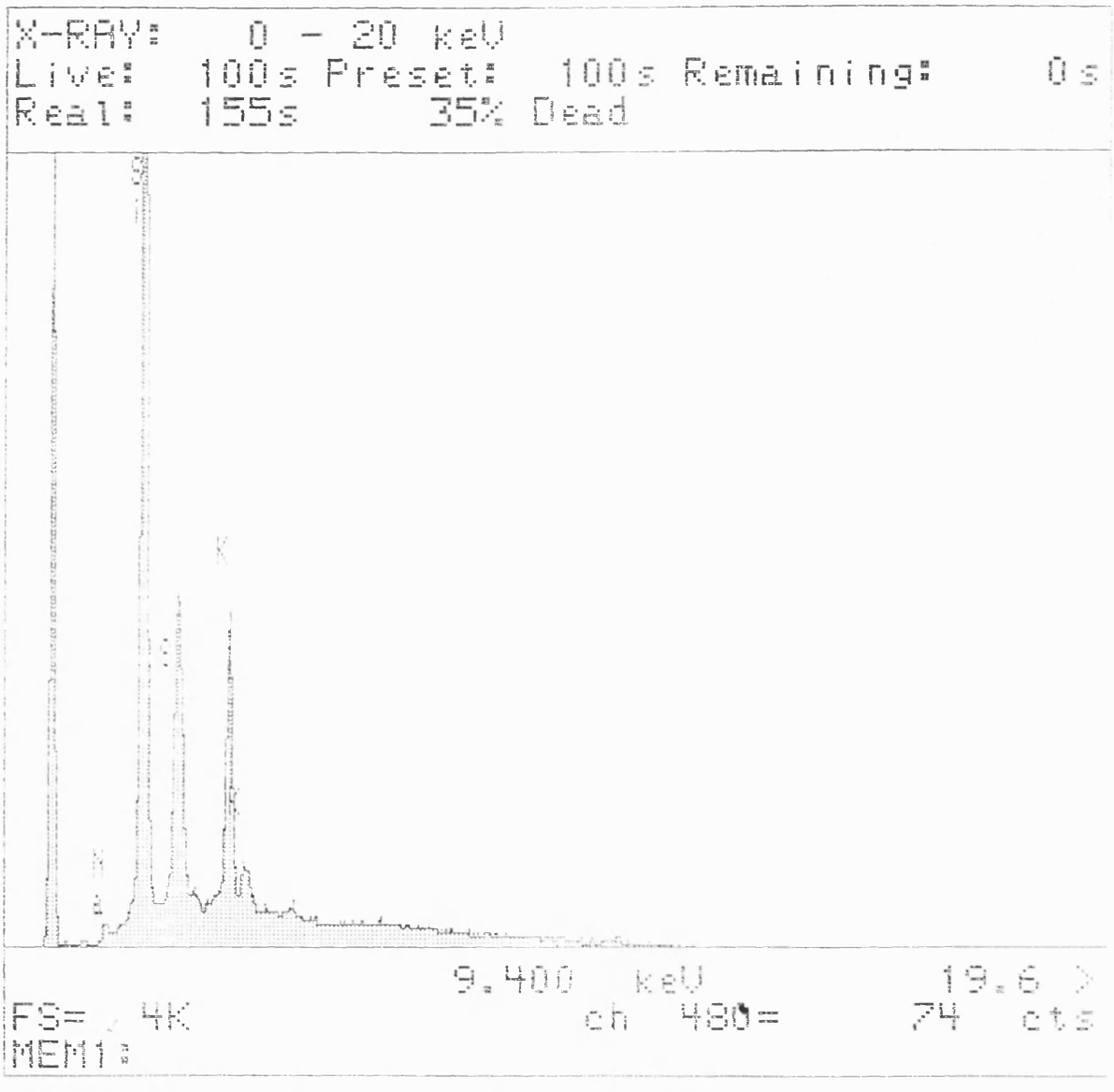
X-RAY: 0 - 20 keV
Live: 100s Preset: 100s Remaining: 0s
Real: 155s 35% Dead
9.400 keV 19.6 >
FS= 4K ch 480= 74 cts
MEM1:

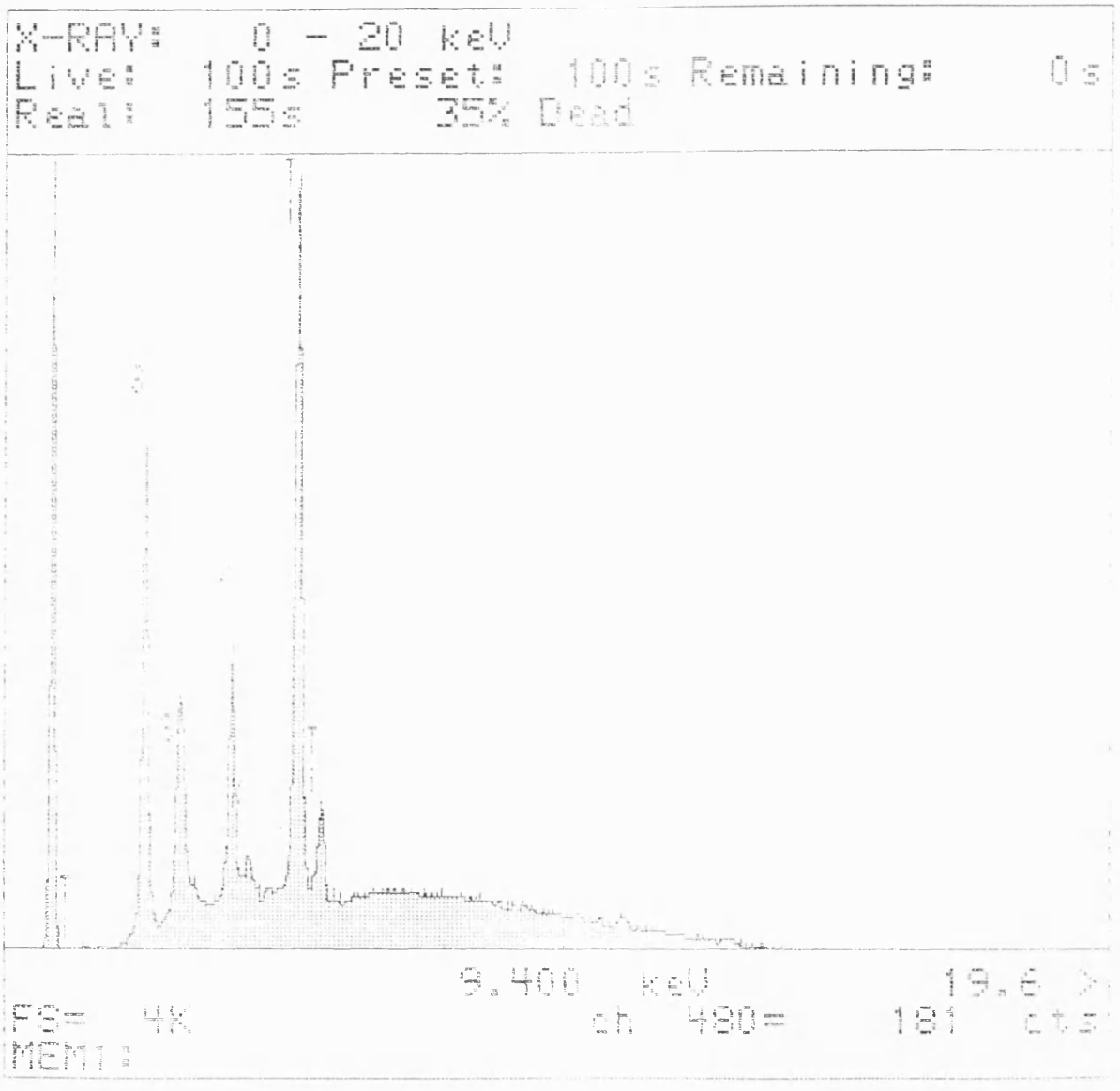
X-RAY: 0 - 20 keV
Live: 100s Preset: 100s Remaining: 0s
Real: 155s 35% Dead
9.400 keV
ch 480= 181 cts

In conclusion for glass beads coated with sol-gel TiO_2 using method SG3 evidence from SEM and X-ray microanalysis suggest that the beads are successfully coated although actual degradation tests show that atrazine degradation rates are little more than those found due to UV only. This could be explained by the catalyst not being photocatalytically active when produced from this method or the amounts of catalyst attached and therefore the total loadings in the batch reactor being too small.

In general it can be seen that although SEM is useful in assessing the physical attachment of a particular coating technique, degradation tests are the only real test of the effectiveness of a particular coating technique.

In order to check that the TiO_2 catalyst being produced from the sol-gel preparation methods was active and to confirm that the low degradation rates obtained with the coated beads was most likely due to poor loadings, a sample of unattached TiO_2 obtained from preparation method SG7 was tested in the batch reactor. The results from HPLC analysis shown in figure 4.31 and GC-MS of reaction intermediates shown in appendix B1 show that the TiO_2 obtained is indeed catalytically active.

Preparation methods SG8 and SG9 using alumina and silica gel respectively as a support both gave catalyst which showed no activity using the methyl viologen assay. Both supports were porous and in addition to showing no activity some disadvantages of using porous supports have become apparent [67], and so no other porous or absorbent supports were investigated.

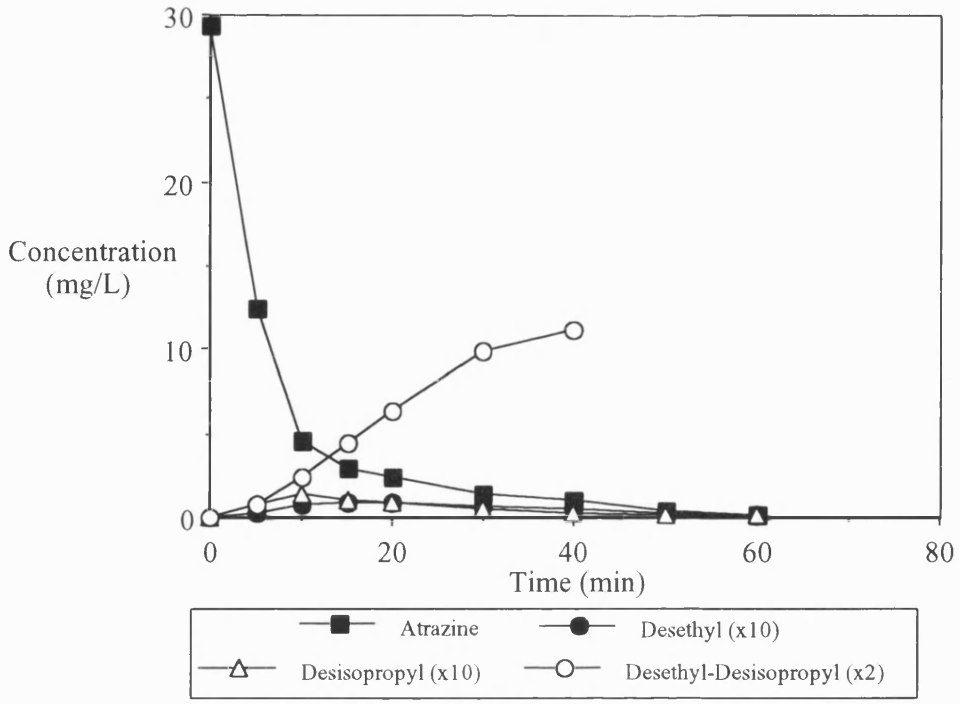

Figure 4.31: *Batch Degradation of Atrazine to Demonstrate the Activity of Sol-Gel Prepared Catalyst SG7.*

4.3.2 Semiconductor Assay

The semiconductor assay which was evaluated to provide a quick and sensitive measure of catalyst activity was based on the reduction of methyl viologen. It has been reported that methyl viologen is a useful compound for the investigation of photocatalytic systems[64]. When UV light illuminates a solution of TiO_2 in a solution of MV^{2+} the cation MV^{+} is formed. This species has a characteristic blue colour with an absorbance at 605 nm. In initial evaluation studies in the cuvette photoreactor a blue colouration was observed at the catalyst surface during illumination, but at the end of an experiment after mixing the concentration was insufficient to allow it's determination in a spectrophotometer. It was also noted however that the solution appeared to fluoresce with a blue/green colour when illuminated with 350 nm UV light in the cuvette reactor and it was this property that was used to develop the assay.

The results from the assay measurements carried out as described in section 3.6 are shown in figure 4.32.

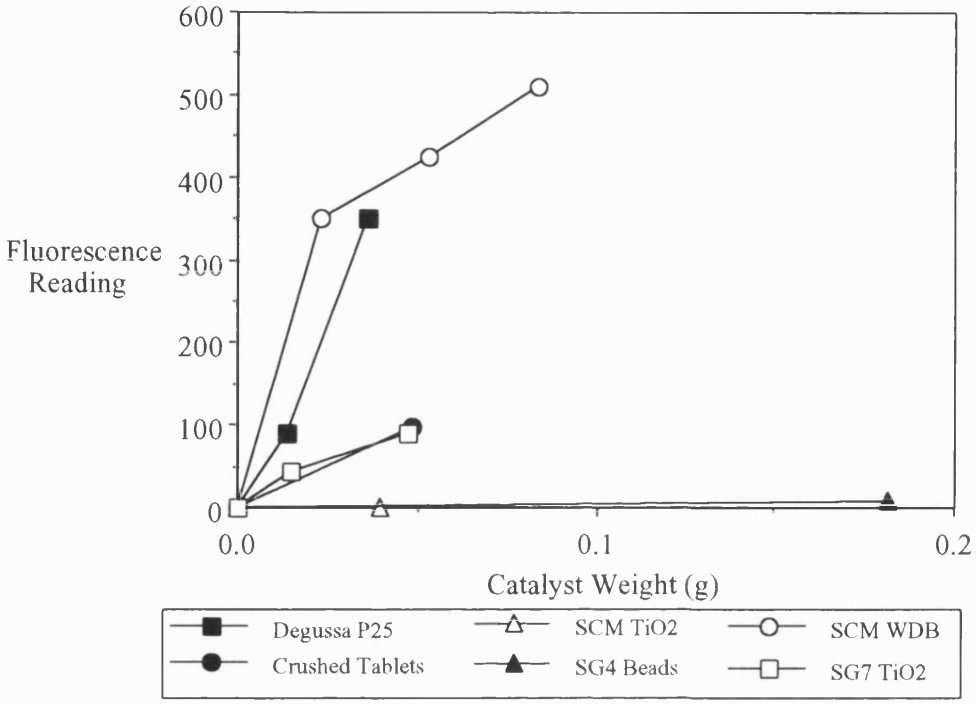

Figure 4.32: *Methyl Viologen Semiconductor Assay for Various Catalyst Types.*

A number of different forms of TiO_2 were tested to see whether there was any correlation between the amount of fluorescent species formed and the photocatalytic activity as expressed as atrazine degradation. A number of different catalyst loadings were also evaluated to check whether the assay gave a linear response and was therefore a practical assay technique.

It can be seen that the amount of fluorescent species produced is greater for catalyst types which are more photocatalytically active and give rise to higher atrazine degradation rates in batch reactor experiments. Thus SCM WDB gives the highest reading for a given concentration, followed by Degussa P25. Crushed tablets and TiO_2 from preparation method SG7 gave similar fluorescence readings. Finally

coated glass beads using method SG4 and a sample of photocatalytically inactive rutile TiO_2 (SCM TiO_2) gave very low readings.

Unfortunately it can be seen from the results in figure 4.32 that the assay response is not linear. At higher loadings of catalyst, and therefore higher concentrations of the fluorescent MV^+ species, the slope of the curve reduces. This can be explained by the commonly observed effect in fluorescence spectroscopy of quenching.

4.4 Actinometry Results.

The calibration data for the measurement of Fe^{2+} ions as outlined in section 3.4 is shown in figure 4.33 as a plot of Abs $_{510nm}$ for various Fe^{2+} concentrations.

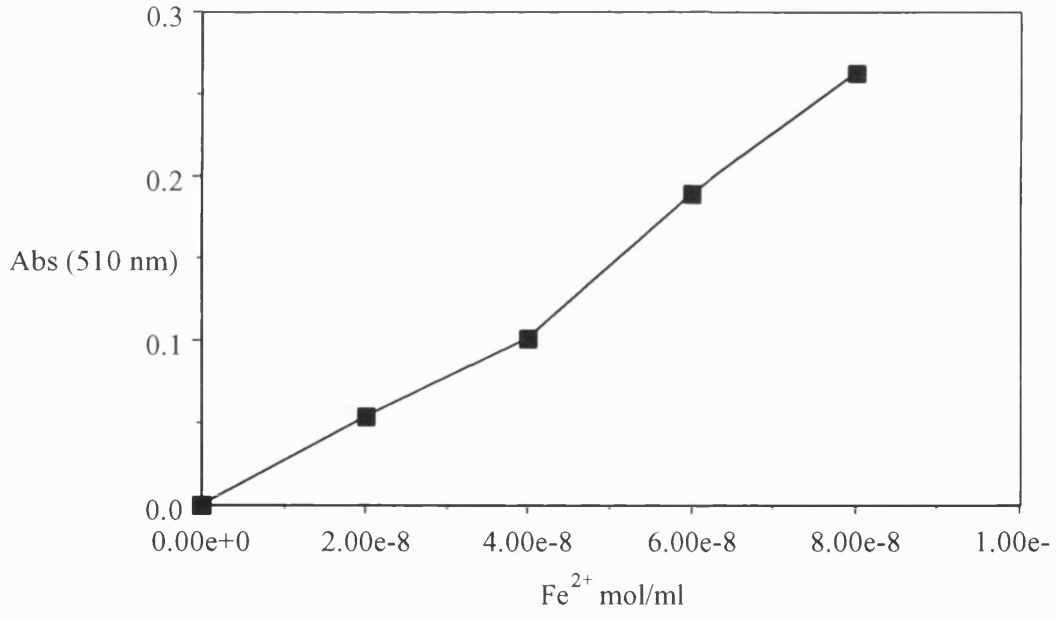

Figure 4.33: *Calibration Data for Actinometry Experiments.*

In the batch reactor, using the 250W medium pressure mercury lamp a value of 7.07 x 10^{-8} mol Fe2+ ml-1 was measured for a 5 second illumination time. Using

equation 3.4 this gives a value of 6.363 x 10^{-5} moles of Fe^{2+} ions formed in the reactor.

The spectral data for the 250W mercury lamp used is given in table 4.7 and figure 4.34

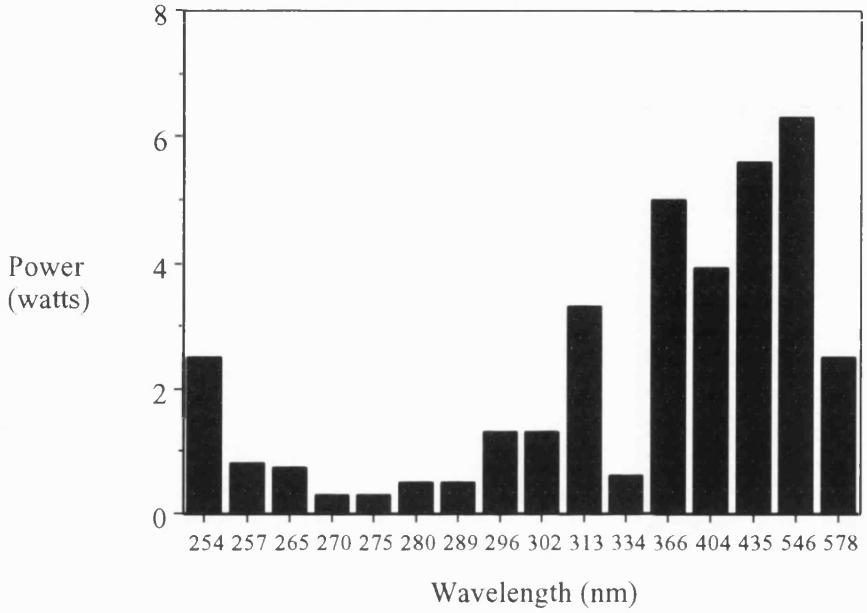

Figure 4.34: *250W Medium Pressure Mercury Lamp Spectral Power Output.*

Table 4.7: *Lamp Power Output and Calculated Values for Energy Output and Photon Flux*

Wavelength (nm)	**Power (Watts)**	**Energy (kcal/ein)**	**Photon Flux (ein/sec) x 10^6**
254	2.5	112.56	5.31
257	0.8	111.25	1.72
265	0.75	107.89	1.66
270	0.3	105.89	0.68
275	0.3	103.97	0.69
280	0.5	102.11	1.17

289	0.5	98.93	1.21
296	1.3	96.59	3.22
302	1.3	94.67	3.28
313	3.3	91.35	8.63
334	0.6	85.6	1.68
366	5.0	78.12	15.3
404	3.9	70.77	13.2
435	5.6	65.73	20.4
546	6.3	52.36	28.8
578	2.5	49.47	12.1

where:

$$\text{Energy (kcal/Ein)} = \frac{2.8591 \times 10^4}{\text{Wavelength (nm)}}$$

and,

$$\text{Photon Flux (Ein/s)} = \frac{\text{Power (watts)}}{4184 \times \text{Energy (kcal/Ein)}}$$

Since the light emitted from the mercury lamp used is polychromatic and the data for the actinometer quantum yields has been measured for monochromatic light, the quantum yield value used in eqn 3.6 must be the sum of the discrete values weighted for each line in the lamp spectral output. This is given in equation 4.3.

$$\Phi_{Fe^{2+}} = \sum_{\lambda=\lambda_{min}}^{\lambda=436nm} \frac{P\lambda}{P_{total}} \Phi_{Fe^{2+},\lambda} \qquad (4.3)$$

Where:

$P\lambda$ = photon flux emitted from the lamp at wavelength λ

P_{total} = total photon flux emitted by the lamp between λ_{min} and $\lambda_{=436nm}$

$\Phi_{Fe^{2+},\lambda}$ = quantum yield at wavelength λ

λ_{min} = wavelength cut-off (184nm for quartz, 310nm for pyrex)

This gives a value of 1.178 and therefore substituting this value, the amount of Fe^{2+} ions formed during the actinometer experiment and the time of illumination gives a value of 1.08 $x10^{-5}$ einstein/sec.

4.5 Degradation Kinetic Analysis

As has already been discussed the standard method of analysing photocatalytic degradation data is to use an equation which describes a saturation-type model such as the Langmuir-Hinshelwood expression. It has been reported that initial rate-initial organic concentration data fits saturation-type models for many different systems [50,100,101,102,55]. It has already been shown, in section 4.1.3 and figure 4.7, that atrazine shows similar behaviour although the data obtained does not reach a constant rate within the range studied, bounded by the limit of solubility.

The results of fitting this data to an equation of the form in eqn 4.1 using the UltraFit software is shown in figure 4.35.

Equation 4.1 is a Michaelis-Menten type rate expression where k_{cat} is the maximum reaction rate and K_m is the Michaelis constant which represents the value

of the initial substrate concentration which gives an initial reaction rate half that of the maximum.

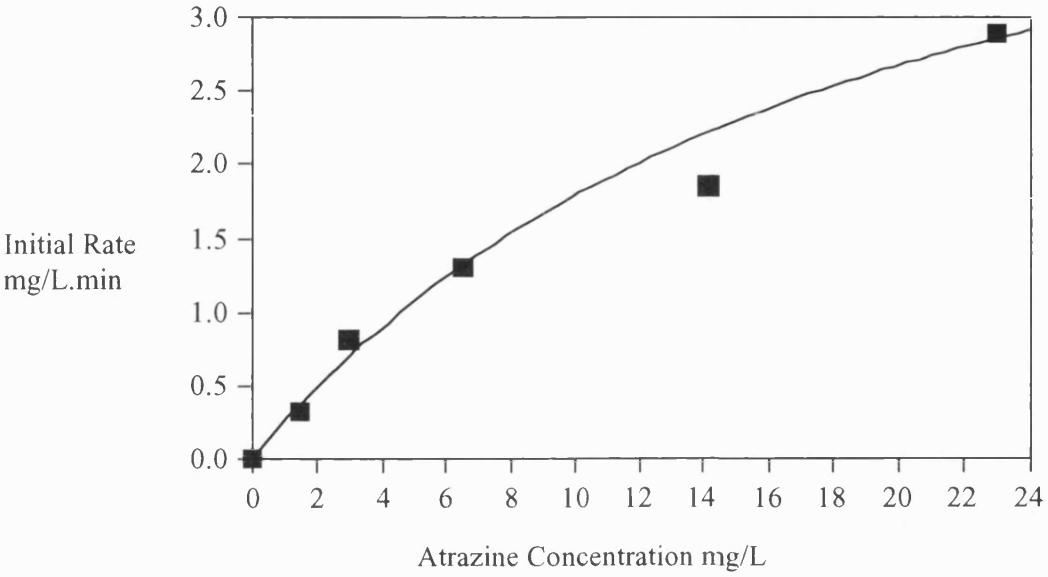

Figure 4.35 : *Initial Degradation Rate v. Atrazine Concentration. Data Fitted to a Model of the Form in Eqn. 4.1 .*

Values for the constants in the equation 4.1 are:

kcat=5.3738 mg/L.min

Km=21.8209 mg/L

This gives constants k1 and k2 in the more commonly expressed Langmuir-Hinshelwood form of this type of equation:

$$\text{Rate} = \frac{k_1 C_A}{1 + k_2 C_A} \qquad (4.4)$$

$\mathbf{k_1}$=0.2462 min^{-1}

$\mathbf{k_2}$=0.0458 $(mg/L)^{-1}$

An equation of this form describes a reaction which is zero order at high concentrations and first order at low concentrations. The transition between these two orders occurs at approximately Ca ≈ 1/k2 which for this data is at ≈21 mg/L. Other information which can be gained from this model is that the first order rate constant is k1=0.2462 min^{-1} and that the maximum rate is k1/k2=5.3 mg/L.min.

Obviously this equation is only applicable for the experimental conditions used for the series of experiments to obtain the rate-concentration data. Changes in dissolved oxygen, catalyst loading and catalyst form would all have an effect in altering the values of the constants k_1 and k_2.

For the individual experiments used to compile the data for the L-H type plot the initial atrazine concentrations were in the range 1.44-23 mg/L. The highest concentration is around the point where reaction order changes from zero to one and so it can be assumed that the individual concentration-time plots for these sets of data will follow first order kinetics.

There is a further explanation as to why concentration-time data follows first order kinetics and this will be described in section 4.17.

If a first order fit is carried out on the concentration-time data, the following values for the rate constant k are found:

Table 4.8: *First Order Rate Constants Calculated from Atrazine Degradation Data.*

Initial Atrazine Concentration (mg/L)	**First Order Rate Constant k' (min^{-1})**	**$t_{0.5}$ (min)**
23.0	0.2251	3.26
14.159	0.2006	3.59
6.504	0.375	1.93
2.925	0.463	1.52
1.44	0.3905	1.83

Taking the data from the experiment with initial atrazine concentration of 23.0 mg/L, a fit was carried out using the model described in figure 4.36.

In this simplified model it was assumed that the degradation of atrazine proceeds via a parallel reaction to either desethyl atrazine or desisopropyl atrazine and then each of these intermediates degrades to desethyl-desisopropyl atrazine. It is further assumed that any subsequent degradation of desethyl-desisopropyl atrazine is negligible and can be ignored. This is a valid assumption as only small amounts of intermediates smaller than the desethyl-desisopropyl intermediate were detected on the HPLC analysis and no drop in desethyl-desisopropyl atrazine concentration was observed.

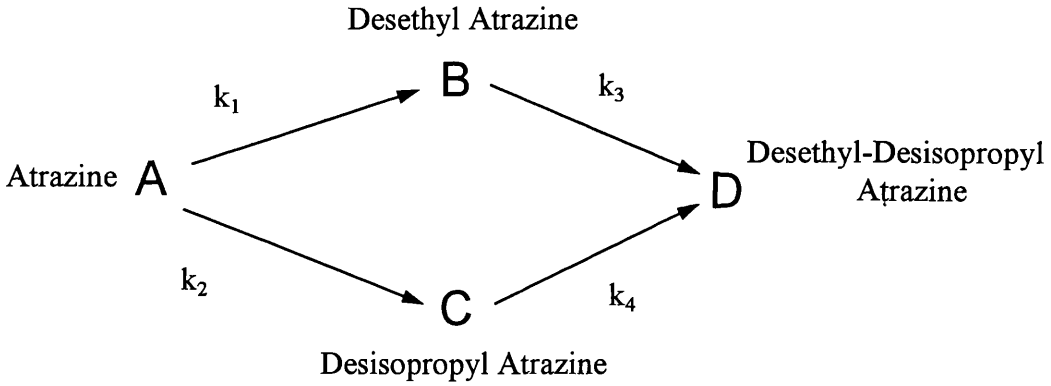

$$-r_A = \frac{dCA}{dt} = k_1C_A + k_2C_A = (k_1+k_2)C_A \xrightarrow{\text{integrate}} C_A = C_{A0}\, e^{-(k1+k2)t} \qquad 4.5$$

$$r_B = \frac{dCB}{dt} = k_1C_A - k_3C_B \qquad 4.6$$

$$r_C = \frac{dCC}{dt} = k_2C_A - k_4C_C \qquad 4.7$$

$$r_D = \frac{dCD}{dt} = k_3C_B + k_4C_C \qquad 4.8$$

Substitute 4.5 into 4.6, multiply through by the integrating factor e^{k3t} and integrate gives:

$$C_B = k_1 C_{A0}\left(\frac{e^{-(k_1+k_2)t}}{k_3-(k_1+k_2)}+\frac{e^{-k_3 t}}{(k_1+k_2)-k_3}\right) \qquad 4.9$$

Similarly,

$$C_C = k_2 C_{A0}\left(\frac{e^{-(k_1+k_2)t}}{k_4-(k_1+k_2)}+\frac{e^{-k_4 t}}{(k_1+k_2)-k_4}\right) \qquad 4.10$$

Assuming $C_{A0}=C_A+C_B+C_C+C_D$

$$C_D = C_{A0}\left\{1-e^{-(k_1+k_2)t}-k_1\left(\frac{e^{-(k_1+k_2)t}}{k_3-(k_1+k_2)}+\frac{e^{-k_3 t}}{(k_1+k_2)-k_3}\right)\cdots\right.$$

$$\left.-k_2\left(\frac{e-(k_1+k_2)t}{k_4-(k_1+k_2)}+\frac{e-k_4 t}{(k_1+k_2)-k_4}\right)\right\} \qquad 4.11$$

Applying these model equations in the UltraFit software gives the following values for the rate constants for each individual fit:

Table 4.9: *Rate Constants Calculated from Model Equations.*

	Atrazine	**Desethyl Atrazine**	**Desisopropyl Atrazine**	**Desethyl-Desisopropyl Atrazine**
k1 + k2	0.2250	-	-	-
k1	-	0.0137	0.2102	5.681e-4
k2	-	0.2640	0.0376	1.4162e-1
k3	-	0.2777	-	-3.369e-1
k4	-	-	0.2478	1.466e-1

The poor comparison between the rate constants and the poor fit in the case of desethyl-desisopropyl atrazine can be explained by the simplified model used to obtain the equations. Firstly the model only takes into account those intermediates which have been quantitatively measured by HPLC analysis, namely the three major dealkylated compounds. The range of other compounds, which amount to a substantial fraction of the total as can be seen by a mass balance, are ignored.

Table 4.10 : *Mass Balance Including Measured Intermediate Concentrations and Calculated Values for Other Intermediates (mM).*

t	Atrazine	Desethyl Atrazine	Desisopropyl Atrazine	Desethyl-Desisopropyl Atrazine	Other Intermediates
0	0.1070	0.0	0.0	0.0	0.0
2	0.0801	1.54e-3	4.16e-3	1.90e-3	0.0193
5	0.0346	2.01e-3	6.75e-3	0.0175	0.0461
10	2.84e-3	8.05e-4	2.93e-3	0.0417	0.0587
20	2.60e-3	3.21e-6	1.69e-4	-	-

The first improvements can be made by forcing the model equations for the intermediates to take into account that the sum of the rate constants for atrazine degradation (found from a first order fit), $k1+k2 = 0.225\ min^{-1}$, the following constants were found:

Table 4.11: Rate Constants From Forced Model.

	Desethyl Atrazine	**Desisopropyl Atrazine**	**Desethyl-Desisopropyl Atrazine**
k1	0..0137	0.0375	0.1182
k2	0.225-0.0137=0.2113	0.225-0.0375=0.1875	0.1355
k3	0.3375	-	0.0204
k4	-	0.2702	0.3138

The model fits were better, but the match between constants obtained from the individual fits are poor.

The main simplification is the omission of any terms representing other intermediates in addition to the desethyl (**B**), desisopropyl (**C**), and desethyl-desisopropyl (**D**) compounds. The model was therefore changed to include an additional lumped term representing all additional intermediates (**I**).

If the model is extended to include this additional term, and this term is represented by a further parallel reaction between atrazine and desethyl-desisopropyl atrazine, then the reaction scheme and associated reactions can be written as follows:

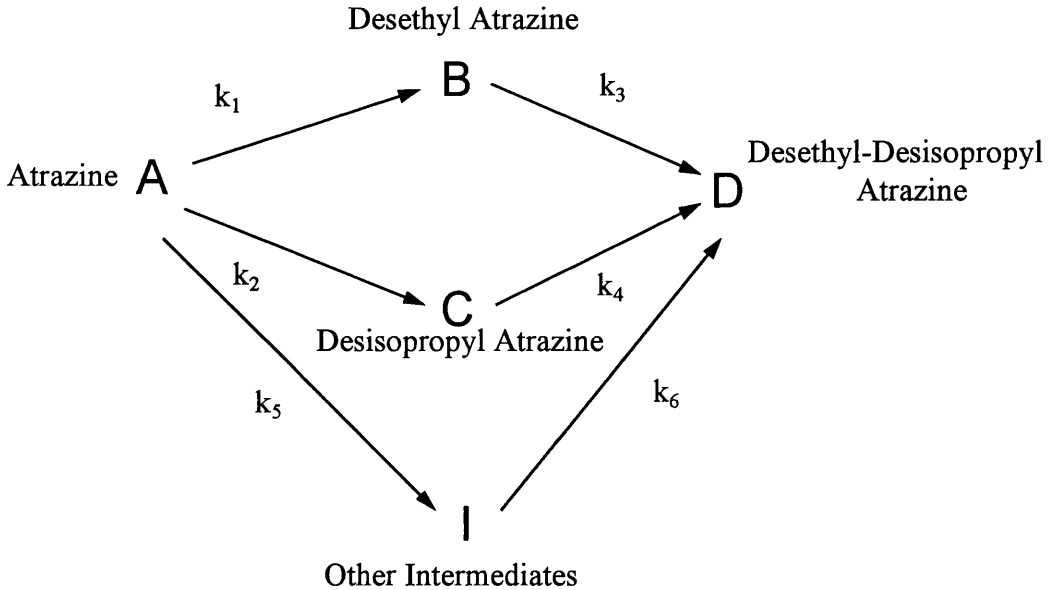

Rewriting the rate equation for compound A (atrazine):

$$-r_A = \frac{dCA}{dt} = k_1C_A + k_2C_A + k_5C_A = (k_1+k_2+k_5)C_A$$

$$\xrightarrow[\text{integrate}]{} \quad C_A = C_{A0}\, e^{-(k1+k2+k5)t} \qquad 4.12$$

including a rate equation for the other intermediates,

$$r_I = \frac{dCI}{dt} = k_5C_A - k_6C_I \qquad 4.13$$

rewriting the rate equation for compound D (desethyl-desisopropyl atrazine),

$$rD = \frac{dCD}{dt} = k_3C_B + k_4C_C + k_6C_I \qquad 4.14$$

integration for compound I gives:

$$C_I = k_5C_{A0}\left(\frac{e^{-(k_1+k_2+k_5)t}}{k_6-(k_1+k_2+k_5)} + \frac{e^{-k_6t}}{(k_1+k_2+k_5)-k_6}\right) \qquad 4.15$$

the rate equations for compounds B and C remain the same except the term

$(k_1+k_2+k_5)$ replaces (k_1+k_2) in equations 4.9 and 4.10.

and therefore the equation for compound D becomes:

$$C_D = C_{A0}\left\{1 - e^{-(k_1+k_2+k_5)t} - k_1\left(\frac{e^{-(k_1+k_2+k_5)t}}{k_3-(k_1+k_2+k_5)} + \frac{e^{-k_3t}}{(k_1+k_2+k_5)-k_3}\right)\cdots\right.$$

$$-k_2\left(\frac{e^{-(k_1+k_2+k_5)t}}{k_4-(k_1+k_2+k_5)} + \frac{e^{-k_4t}}{(k_1+k_2+k_5)-k_4}\right)\cdots$$

$$\left.-k_5\left(\frac{e^{-(k_1+k_2+k_5)t}}{k_6-(k_1+k_2+k_5)} + \frac{e^{-k_6t}}{(k_1+k_2+k_5)-k_6}\right)\right\} \qquad 4.16$$

Using this set of equations in the UltraFit program and using the rate constants from one intermediate fit in the rate equation for the next fit, the following rate contants were found:

Table 4.12: *Rate Constants From Extended Model.*

	Desethyl Atrazine	**Desisopropyl Atrazine**	**Desethyl-Desisopropyl Atrazine**
k1	0.0137	-	-
k2	-	0.0375	-
k3	-	0.1738	-
k4	0.3375	-	-
k5	-	0.2702	-
k6	-	-	0.0600

Figures 4.36 - 4.39 show the equation fits for atrazine and the three major dealkylated intermediates.

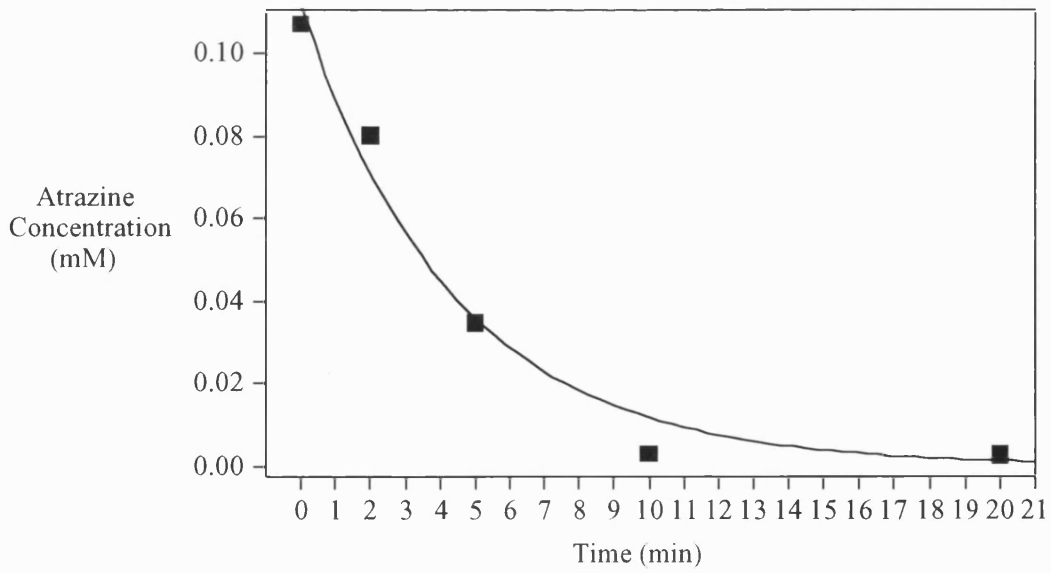

Figure 4.36: *Atrazine Degradation - Model Fit.*

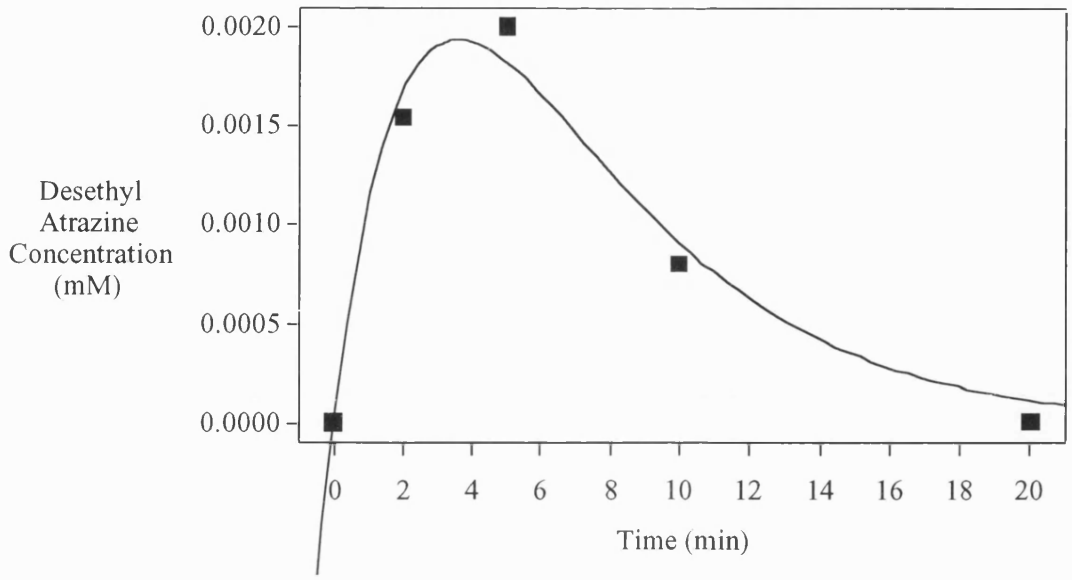

Figure 4.37: *Desethyl Atrazine - Model Fit.*

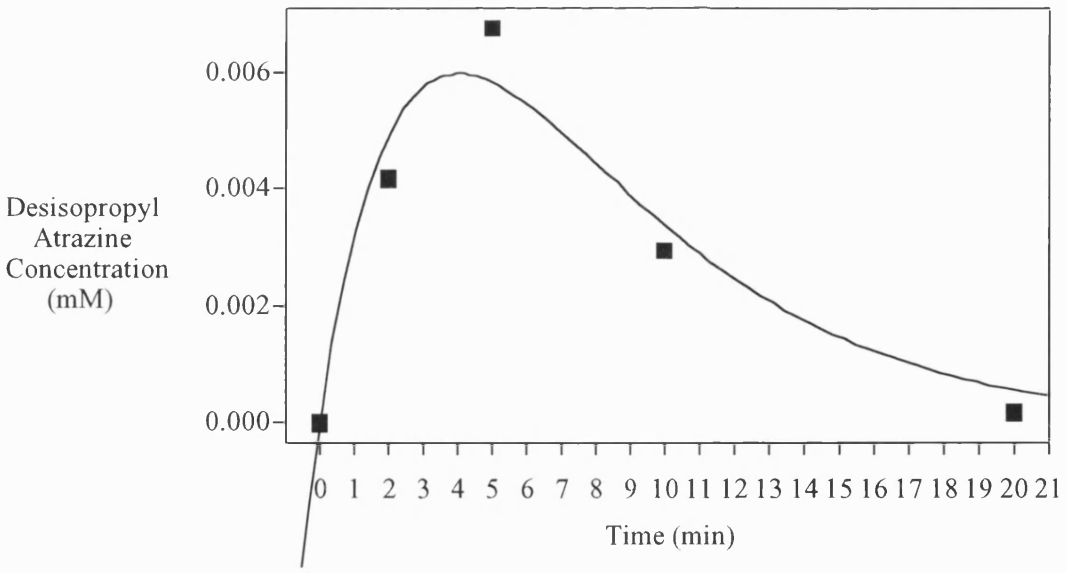

Figure 4.38: *Desisopropyl Atrazine - Model Fit.*

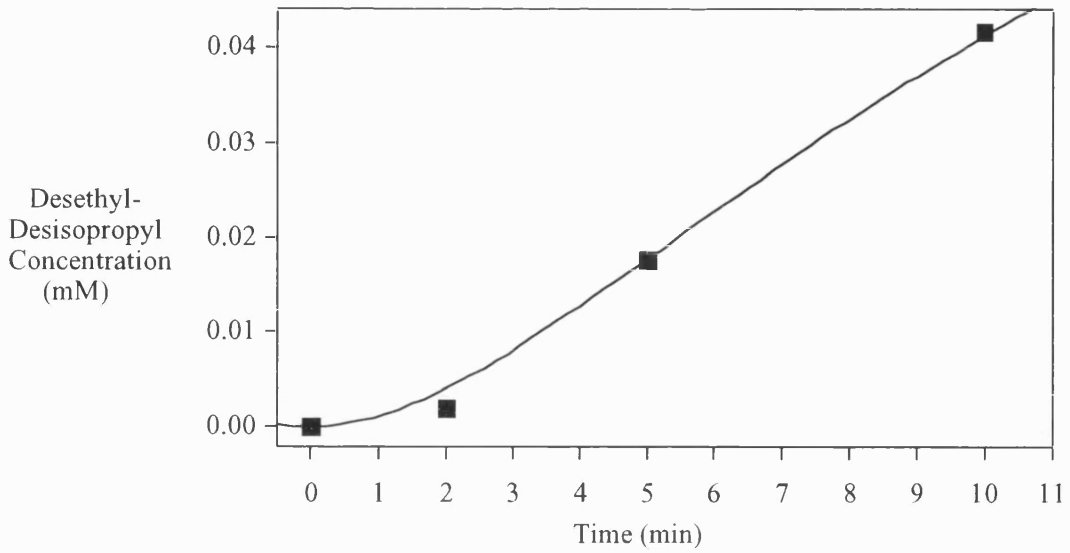

Figure 4.39: *Desethyl-Desisopropyl Atrazine - Model Fit.*

Applying the extended model equations to a further data set the following rate constants were found:

Table 4.13: Rate Constants from Extended Model (Data Set II)

	Desethyl Atrazine	**Desisopropyl Atrazine**	**Desethyl-Desisopropyl Atrazine**
k1	0.0024	-	-
k2	-	0.0206	-
k3	-	0.0647	-
k4	0.0099	-	-
k5	-	0.1030	-
k6	-	-	0.0372

Figures 4.40 - 4.43 show the kinetic model fits for atrazine and each reaction intermediate.

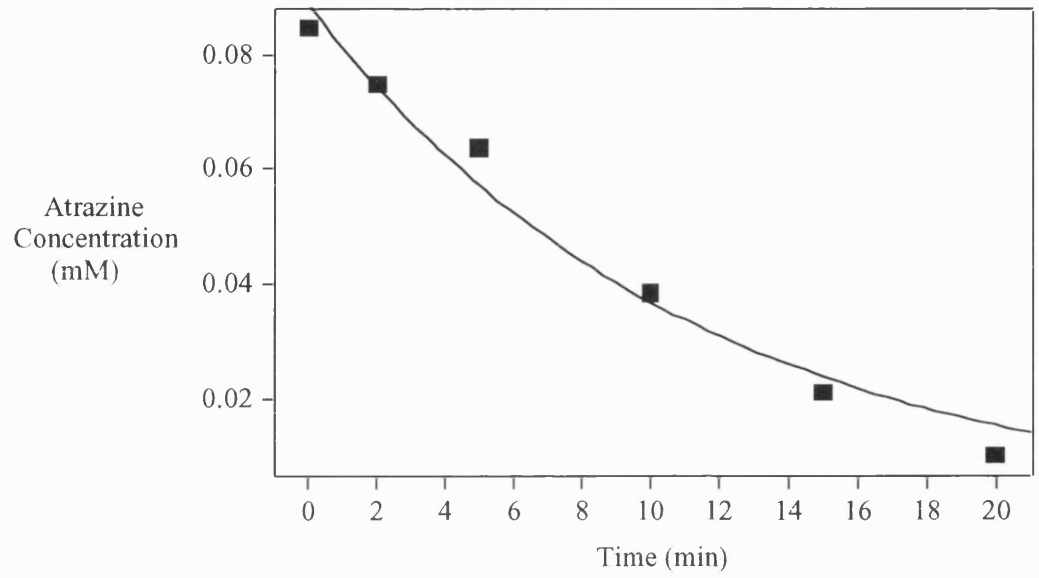

Figure 4.40 : *Atrazine Degradation. Model Fit.*

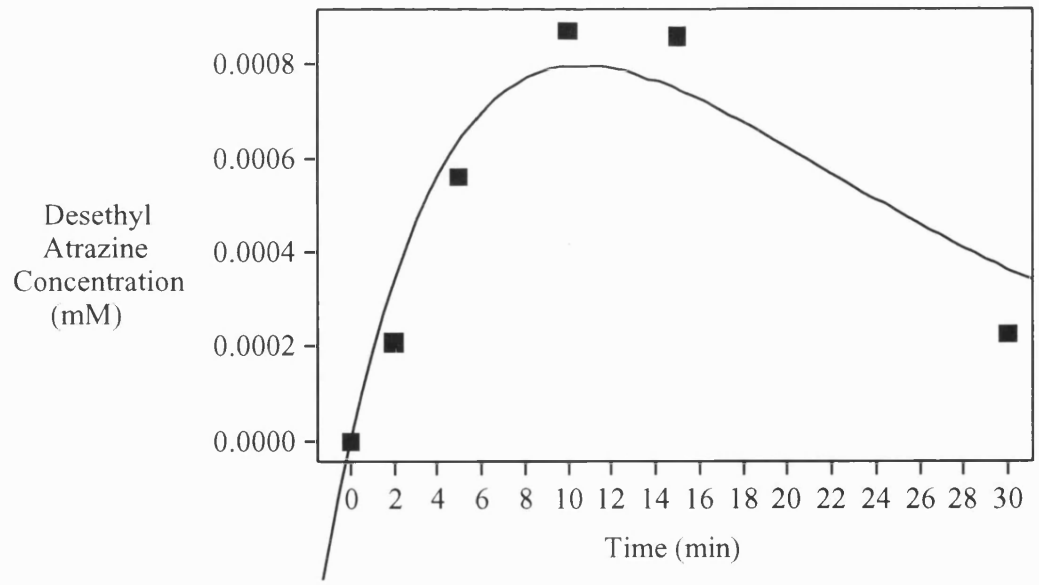

Figure 4.41 : *Desethyl Atrazine. Model Fit.*

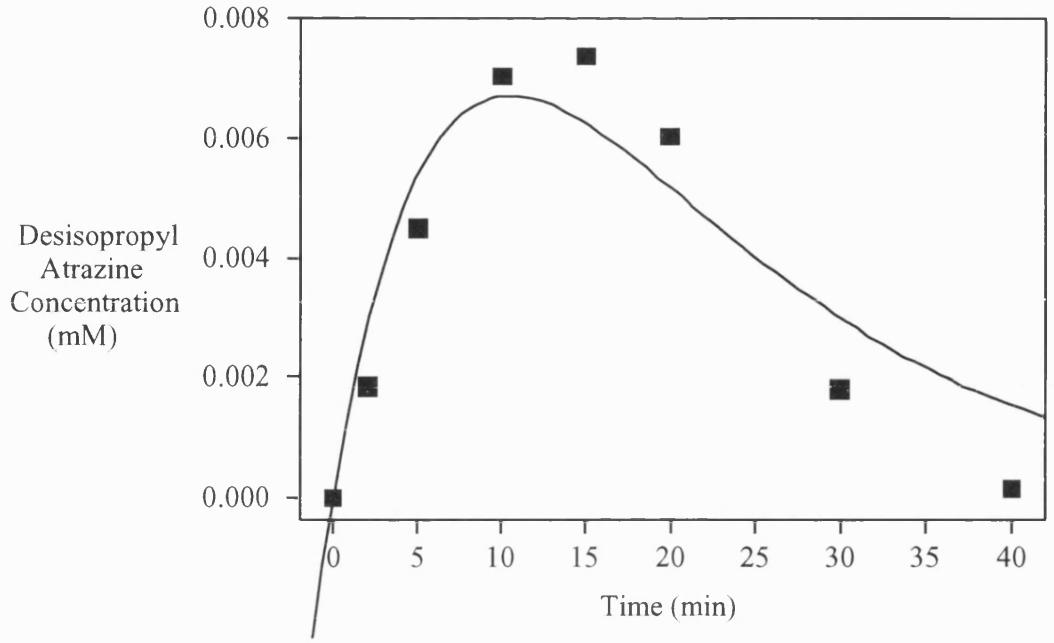

Figure 4.42 : *Desisopropyl Atrazine. Model Fit.*

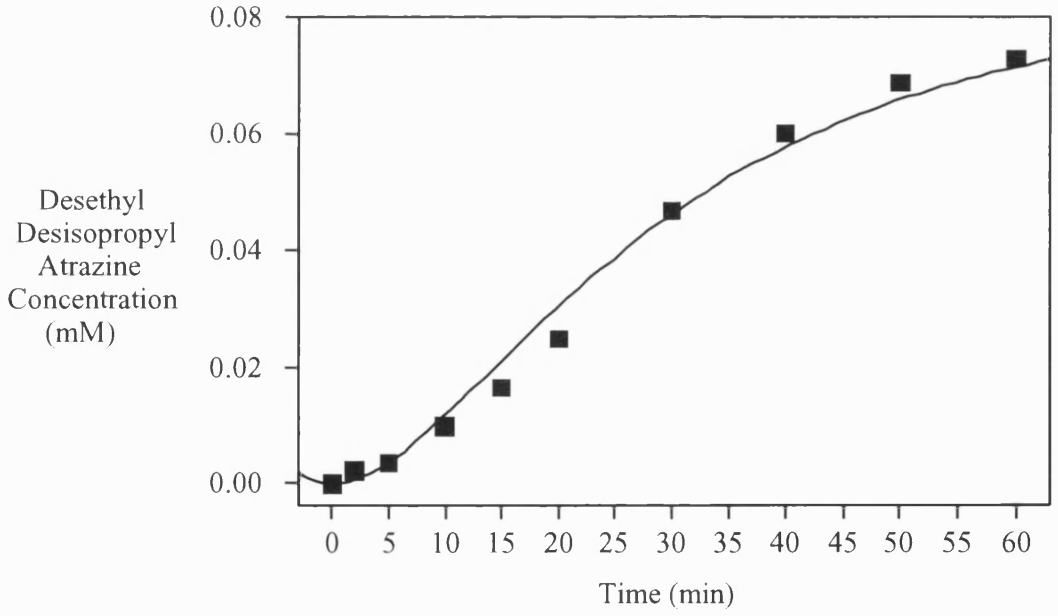

Figure 4.43 : *Desethyl Desisopropyl Atrazine. Model Fit.*

A further kinetic simplification can be made which has been applied in a number of studies[41,97]. If the degradation reaction proceeds via a number of reaction intermediates which compete for reaction sites on the catalyst surface so

that the total oxidisable carbon concentration remains constant while the concentration of the primary pollutant is decreasing, the denominator in the standard Langmuir-Hinshelwood equation can be approximated by:

$$1+K_1C_1+\sum_{i=2}^{n}K_iC_i \approx 1+K_1C_1^{o} \qquad 4.17$$

where:

the subscript 1 refers to the primary organic compound and,

C^o_1 = the initial concentration of the primary compound.

This simplification has been used to explain the observed (apparent) first order degradation of primary organic compared with L-H form of initial rate-concentration data [55]. The two assumptions are that with little or no mineralisation the TOC concentration remains constant and that the adsorption coefficients for the reaction intermediates are the same (a good assumption in the case of atrazine since the intermediates are of the same form).

Taking the value of K=9.937 from a fit of the initial rate data expressed in terms of mM atrazine, the value of k1 can be calculated as follows (using the calculated apparent first order rate constant for atrazine degradation of 0.2251)

k1=0.2551(1+9.937x0.107)

=0.4644

When these values are used to predict atrazine concentration with reaction time and compared with observed measurements the results are shown in figure 4.44.

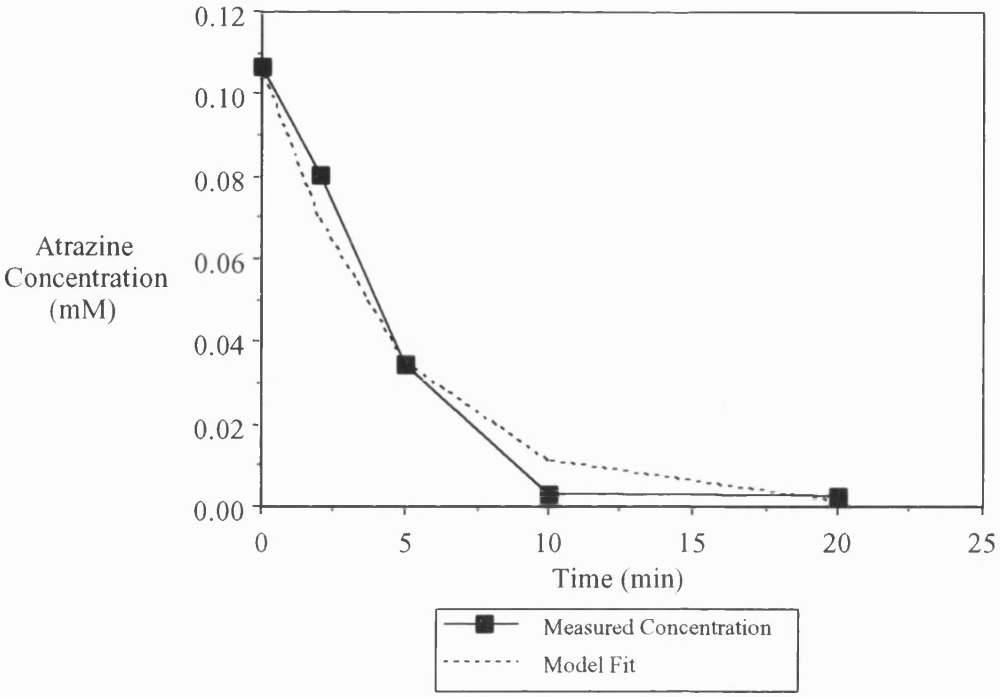

Figure 4.44: *Comparison Between Observed Atrazine Degradation and the Model Prediction Based on a Simplification in equn. 4.17.*

In general the procedure of fitting a kinetic model and obtaining rate constants for a system which is poorly defined leads to values with large errors. In this case since there are a large number of intermediates for which there is no data, the equations which are used to model the system are not constrained and the kinetic constants show poor correlation between each other when calculated from different intermediate data. An attempt has been made to try and put some more constraints on the model but it would appear that deriving a kinetic model for a compound such as atrazine which breaks down via a large number of intermediates is of no benefit.

4.6 Errors and Reproducibility

There are a number of factors which have affected the accuracy and reproducibility of the degradation experiments. Firstly there is the accuracy of the analysis technique used for the quantitative determination, in this case HPLC. In a repeat analysis of an atrazine standard (mean concentration 2.3 mg/L; n=5), the

standard error was found to be ±0.082 mg/L. Obviously this value would be expected to increase at lower concentrations, but as most of the data points in the batch studies are at concentrations higher than 2.3 mg/L, the standard error will be lower. Since the data points on the batch reactor graphs are of the same order as the standard error, error bars are not included.

Other errors applicable to the batch studies include changes in the lamp UV output as the lamp gradually expires over it's lifetime and potential problems of the lamp not striking correctly. The latter can usually be determined visually and is usually due to the lamp being too cold at start-up. The problem of the lamp output gradually changing over time meant that comparison of results obtained, separated by a long period of time, were not relied on. In most cases comparisons were made on consecutive experiments.

In the pilot scale experiments the data is subject to greater errors due to the low levels of atrazine being analysed. Individual SPE recoveries were >95% and a number of repeats of the whole analysis method, SPE and HPLC, gave a standard error of 15 ng/L (mean 200 ng/L; n=4). This has important implications for the batch scale results as some of the differences observed are within this error of 7.5%.

Other errors which are important in the pilot scale reactor are again the lamp not striking and possible TiO_2 build up on the reactor walls over time, the reactor being difficult to clean on a regular basis.

5 Conclusions

The following sections discuss the conclusions drawn from the present work. These include the applicability of using photocatalysis as a water treatment technique, both for treatment of water which is essentially clean but requires removal of trace contaminants to bring it up to a standard suitable for drinking and treatment of water which has gross contamination. There is also a discussion of the applicability of photocatalytic treatment for the removal of atrazine and other s-triazine herbicides specifically. Some of the techniques used in this study are also discussed and some ideas for further work are also presented.

5.1 Applicability of Photocatalysis to Water Treatment

It has been demonstrated in many studies that photocatalysis is a potential technique for the destruction of a wide range of organic compounds. In many cases this process proceeds to complete mineralisation of the pollutant to CO_2 and H_2O. It has also been shown that the photocatalytic process can be used for the removal of heavy metals and the destruction of microbial contamination. In general these processes are brought about by the highly oxidising environment which is mostly due to the production of highly reactive hydroxyl radicals.

As the list of compounds which have been photocatalytically degraded grows, the more photocatalysis has been talked about as a possible water treatment technique for removal of organic contaminants on a large scale.

However a number of initial problems quickly became apparent:

Firstly, studies where some measure of the extent of mineralisation was made (either monitoring CO_2 evolution or TOC reduction), in addition to the primary compound

degradation, showed that for many compounds complete disappearance of the primary compound was not accompanied by stochiometric production of CO_2. This was particularly noted for aromatic or high molecular weight aliphatic compounds where the degradation took place via one or more intermediates. Thus promising results based on primary organic degradation had to be reassessed in the light of the need for complete mineralisation/TOC removal.

It has also been noted that any production of reaction intermediates would have to be well defined in any potable water treatment because of the possibility of producing intermediates which were as/or more undesirable than the primary pollutant.

A second problem which became quickly apparent was the problems of reactor scale up.

Most of the studies into degradation of individual organics have been carried out in batch reactors or circulated batch reactors with typical volumes <1L. Indeed some of the early studies were in volumes as small as 5ml and although valuable data has been obtained as to whether compounds degrade or not and what intermediates are formed the information is unsuitable for scale-up.

The most common reactor type used in these studies has been an annular configuration, with a UV lamp contained in a quartz or Pyrex sleeve suspended in a cylindrical reactor. This reactor type is very well suited to small scale batch reactors (such as that used in this study) where the total reacting volume is small and the annular gap is only a few cm across. Obviously any scale-up of this type of reactor will suffer a loss of efficiency, since the intensity of light decreases linearly with distance from a line lamp source (Beer's Law). In addition, for a slurry reactor, the

TiO_2 attenuates the UV light further and penetration is only a few cm for loadings of a few g/L. Therefore if this type of reactor is used the number of UV lamps has to be increased to compensate for the increase in reactor diameter.

A further problem was the form of TiO_2 used in these reactions. Most data has been obtained using Degussa P25 powdered TiO_2 because this form is easily available and has been shown to be catalytically active. Although useful for batch scale laboratory studies this form is obviously unsuitable for any potential scale-up. The powdered catalyst would have to be separated from the treated water and recycled to keep the benefit of the process being a catalytic one. Thus methods of either increasing the catalyst size for use in a fluidised bed reactor, or immobilising the catalyst on a support have been investigated.

A further problem encountered is one of low illumination times in flow-through reactors. This means that, in practice, to achieve the high total illumination times needed, long residence times in large reactors or a recycle configuration will be required.

There is also the problem of low reaction rates which has to be overcome if photocatalysis is to form the basis for an economic process.

(i) Reaction rates decrease with decreasing concentration and since most pollutants are at ng or μg levels in UK water supplies reaction rates will be low.

(ii) Multicomponent systems (i.e. the "real systems" encountered in practice) mean that rates of degradation for individual compounds will be reduced.

(iii) Inorganic ions and other compounds present in water will lead to UV screening and/or catalyst fouling.

Another problem, in addition to low reaction rates, are the low quantum efficiencies found for most photocatalytic reactions. The quantum efficiency of a reaction is defined by equation 5.1 as the initial rate of degradation of a substrate divided by the theoretical rate of photon absorption. This assumes that all the photons entering the reactor are absorbed by the TiO_2 although in practice the amount of light scattered or reflected out of the reactor can be substantial.

$$\Phi_i = \frac{\left(\frac{dX_i}{dt}\right)}{\frac{d(h\nu)}{dt}} \qquad (5.1)$$

Where:

Φ_i = the quantum efficiency for species i (mol/einstein)

$\left(\frac{dX_i}{dt}\right)$ = the initial rate of degradation of species X (M/sec)

$\frac{d(h\nu)}{dt}$ = the incident photon flux per unit volume (ein/sec. L)

Most quantum efficiencies obtained with commercially available titania are of the order of 1% and less. This means that a large amount of the energy being used to illuminate the catalyst is wasted and this has important economic consequences.

In the present study a typical value for the quantum efficiency obtained based on atrazine degradation in the batch reactor is 0.93%.

(A typical degradation rate of 1.12×10^{-7} M/sec and the value of photon flux obtained from the actinometry calculation in section 4.4 of 1.08×10^{-5} ein/sec)

A further discussion of the economic aspects of photocatalysis can be found in section 5.4.

There is also the question of where such a technique would be incorporated into existing treatment systems. Any compounds in the water which absorb UV light will reduce the efficiency of the photocatalytic reactor and thus the water should be as clear of humic, particulate and other compounds which absorb UV light as possible. Thus the photocatalytic step should be placed where essentially clean water is present. It is possible that the photocatalytic step can also provide disinfection as well as organic removal although it appears that some method which provides residual disinfection to prevent microbial growth in supply pipes/tanks etc. is preferable to water supply companies. If ozone disinfection has already been looked at as an disinfection option it may be more useful to look at UV-ozone destruction of organic contaminants. If chlorine disinfection is used, further work is needed to look into the combined effects of radical intermediates formed by the photocatalytic process with chlorine to make sure that potentially harmful by-products are not formed.

If a reactor which uses a moving bed of either bulk TiO_2 or immobilised TiO_2 is used then problems of attrition would have to be overcome.

It has been found in this study that this can be a major problem with both bulk catalyst particles and coatings immobilised onto very hard supports. It should also

be noted that there are problems with the amounts of catalyst that can be coated onto supports giving low loadings and poor degradation rates.

5.2 Specific Applicability of Photocatalysis for Atrazine Degradation

As has been shown in this and previous studies, the herbicide atrazine, and indeed other s-triazine herbicides such as simizine and propazine, are degraded by photocatalytic reactions. The major problem in using photocatalysis as a potential water treatment technique is the number and range of intermediates produced. This means that the overall rates of TOC reduction are low and although atrazine disappears quickly, compounds with structures similar to atrazine persist even after long reaction times. It is possible that these compounds, such as the dealkylated intermediates, would be classed as s-triazine compounds by a regulatory body. The problem of intermediates is further complicated by the apparent indiscriminate and unpredictable nature of their formation, being dependent of catalyst form, environmental considerations and the presence of other oxidisable components in solution. It has also been found that changes in the catalyst surface with time can lead to changes in the distribution of reaction intermediates and this would obviously require that the treated water was constantly monitored.

The case for using photocatalysis for atrazine degradation looks poor especially since it is one of few compounds which is not completely mineralised. As has already been discussed it forms a stable compound, cyanuric acid, the triazine ring being unbroken. It is possible that this compound would be regarded as non-toxic however it is likely that a process which removed the possibility of harmful

intermediates entering the treated water (even if this process was non-destructive) would be favoured over a process which was difficult to fully define.

5.3 Possible Uses

In my view there are three cases in which photocatalysis could be developed to provide particular solutions to pollution problems.

The first is the case where an existing water supply becomes contaminated or falls below pollution limits set by a regulatory body.

In this case a portable unit or units based on a supported catalyst could be inserted into the existing treatment system with flexible couplings either in series or parallel. The process is particularly suited if the compound(s) being removed is(are) quickly degraded via few intermediates.

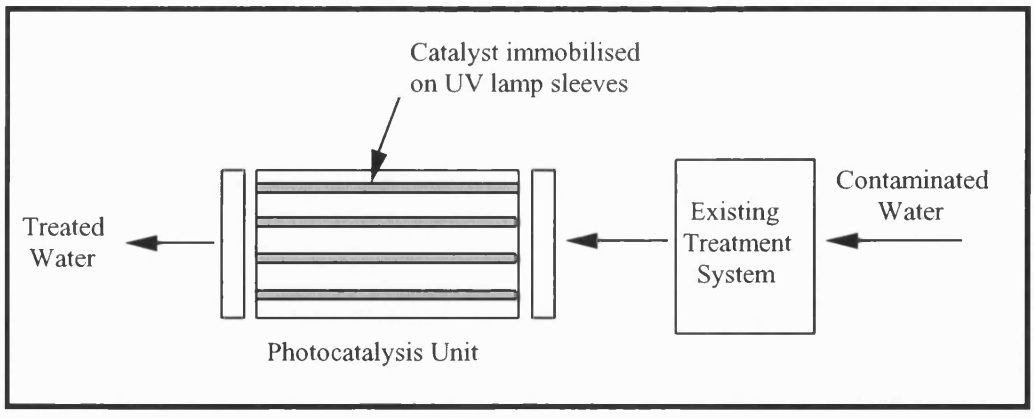

Figure 5.1: *Possible Uses of Photocatalysis. Case 1: Treatment of an Existing Supply which Temporarily Breaks Contaminant Limits.*

The second case is that of gross contamination of a water source or industrial effluent stream.

Here the overall TOC or COD may have to be reduced before further treatment and/or disposal into the environment can take place. In this case the process may not need to be continuous and a batch reactor can be employed using a multi-lamp configuration. In addition, if the decontamination process is not required on a regular basis it may be still economic to use powdered TiO_2 for the catalyst with the possibility of disposing of the reaction mixture as a whole without need for separation. In this type of batch system there is the additional advantage in that the reactor contents may be sampled at intervals and the levels of pollutants and reaction intermediates measured until the desired levels are reached before disposal.

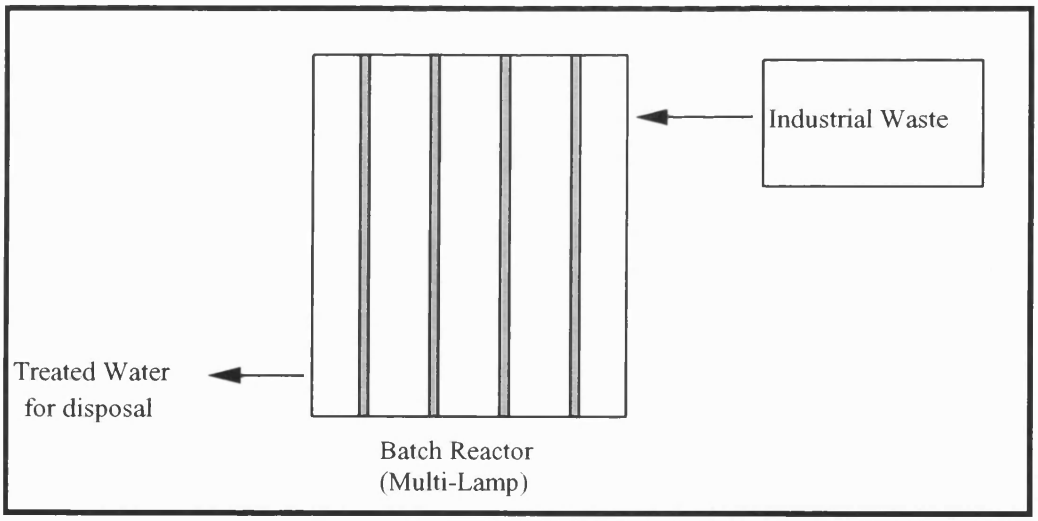

Figure 5.2: *Possible Uses of Photocatalysis. Case 2: Gross Industrial Contamination Prior to Disposal.*

The third potential use is as a field treatment system for polluted streams, rivers and lakes.

Photocatalyst could either be introduced directly into the polluted water and allowed to be activated by sunlight or a portable unit again based on supported catalyst could be used, the contaminated water being pumped through the unit and back into the water source. In both cases the technique is used as a method of remedial clean-up and would obviously need the accompanying identification and removal of the contamination source.

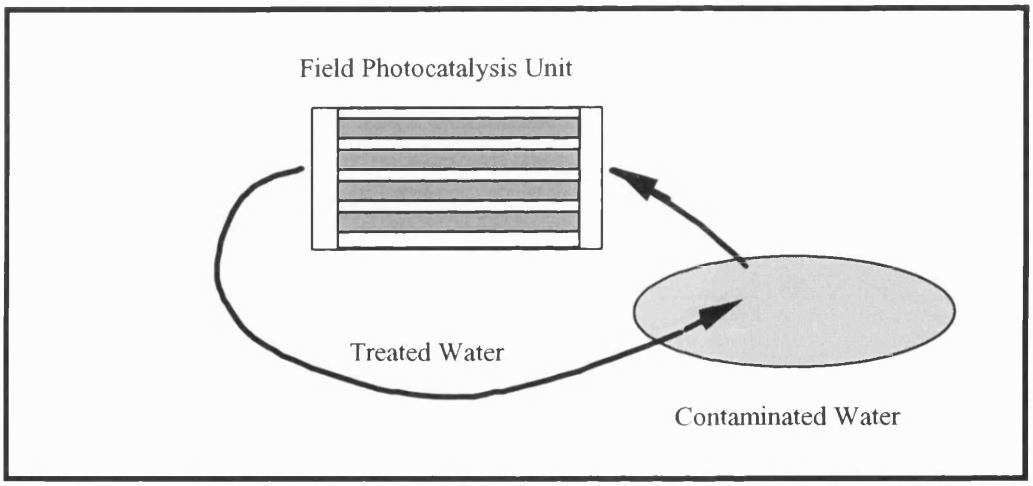

Figure 5.3: *Possible Uses for Photocatalysis. Case 3: Contamination of Surface Water.*

5.4 Economics of Photocatalysis

There have been two recent studies looking at the estimated costs of photocatalytic purification systems. The main comparisons to be made between a photocatalytic based system and one based on activated carbon removal are:

(i) Consumables. The costs of lamp replacement and energy usage, which would depend on local electricity costs, have to be weighed against the major running cost for using GAC which is carbon disposal/replacement or regeneration. In addition the

problems of catalyst losses and catalyst fouling would require that there would also be costs associated with photocatalyst replacement.

(ii) Capital Costs. In general the capital costs associated with a photocatalytic reactor which will include costly glass and quartz components will be greater that the costs for beds of activated carbon. Since most water treatment works include other types of filtration, such as sand filters, it would be possible to easily adapt these to accommodate GAC reducing capital costs even further.

(iii) Labour Costs. The labour costs for photocatalytic reactors would be similar for GAC filtration although additional costs associated with safety issues arising from UV radiation have to be taken into account.

In the first study which compared operating costs for carbon filtration, UV-photocatalysis and UV-ozone to treat various throughputs [51] indicate that photocatalysis could be an alternative to GAC filtration in intermediate to large scale treatment plants. The results from this cost analysis are reproduced in table 5.1.

Table 5.1: *Estimated Running Costs for Various Water Treatment Systems [51].*[a]

System Size / MGD [b]	**0.029**	**0.115**	**0.23**	**0.92**	**2.44**
Carbon [c]	$7.79	4.25	3.19	2.21	1.95
UV-Ozone	$13.00	6.32	4.92	3.83	3.10
UV-Photocatalysis	$9.85	4.36	3.21	2.32	2.00

a Costs updated from original 1987 costs

b Millions of gallons per day

c Incinerative regeneration included in larger size units. No carbon disposal

d UV-Ozone process minus ozone generation/dissolution

The second study looked at the removal of phenol in two situations:

(i) Small volume-high concentration.

The costs of removing 90% of a 100ppm phenol solution by photocatalytic mineralisation and GAC removal were compared. The estimates for the running costs for photocatalytic treatment of 1000 L are shown in table 5.2.

Table 5.2: *Photocatalytic Running Costs for Treatment of 1000L of Phenol.*

Item	**Cost ($)**
Power @ 10c/unit	7.90
Lamp Replacement	1.16
Cost of Catalyst	1.37
Lamp Maintenance	-
Plant Amortisation	-
Total	10.43

The major cost has been identified as the cost of electricity, amounting to 80% of the total if labour charges and plant amortisation is ignored.

It was found that 1 kg of Calgon 400 GAC would be required to reduce the phenol concentration from 100 to 10 ppm a cost of $5. The cost of disposal added an extra $1 to this making a total of $6 per 1000 L.

In this case it can be seen that GAC removal is favoured unless energy costs could be reduced or a 2-fold improvement in catalytic efficiency could be made.

(ii) Large volume-low concentration.

The second system used sunlight to treat water contaminated with 10 ppm phenol. It was calculated that to mineralise 1 million litres of 10 ppm phenol in 8 h would require a lagoon 90 x 90 m^2. Overnight the treated water would be pumped to a settlement tank, the settled catalyst being recycled together with untreated makeup water back to the lagoon. Using a 0.1% TiO_2 suspension would require 1 tonne estimated at $27,500. Assuming 20 reuses of the catalyst amounts to a treatment cost of $1375 per million litres.

It was found that 200 Kg of GAC would be required to carry out the same treatment costing approx. $1000 plus disposal costs which is comparable to solar powered photocatalysis. Thus the lifetime of the catalyst together with the cost of the land area are the critical factors in this scenario.

In any comparison the adsorption characteristics of the pollutants will need to be assessed. It is known that there are some organic pollutants which are not adsorbed by GAC including butylamine, cyclohexamine, ethanol, hydroquinone, adipic acid, choline chloride, diethylene glycol, hexamethylene diamine, morpholine and triethanolamine. Mineralisation of some of these compounds by photocatalysis has been demonstrated and thus the economics of removal will also depend on the adsorption and mineralisation rates of individual pollutants found in each wastewater.

5.5 Further Work

The problems associated with catalyst formulation have already been discussed. Large particles of bulk TiO_2 are commercially available and tabletting

powdered catalyst along with a binder could be a possible route to providing large particles of different types of TiO_2. It would appear that the biggest problem with reactors where the particles are moving relative to the reactor surfaces and to each other is attrition. Unless methods of increasing the strength of tabletted TiO_2 can be found it would appear that these type of reactors, although desirable in terms of UV light use efficiency, are not practicable. Catalyst is lost from the system which has to be replaced, fines get into solution and the size distribution of the catalyst changes with time. A method of coating TiO_2 onto a very robust ceramic support was not effective as low loadings and attrition of the surface coating were found to be problems.

Reactors based on catalyst immobilised onto a stationary support are probably a better solution. It has already been noted that TiO_2 attaches itself well onto glass surface and reactors have been tested where TiO_2 either from suspensions of P25 or from sol-gel methods has been coated onto the walls of annular reactors and onto the UV lamp sleeve. The problems associated with this form of reactor are again problems of low loading and the gap between UV source and catalyst (in the case of catalyst coated on the reactor wall) being large. The most important problem though, is that mass transfer effects play a larger part in the reaction kinetics in this type of reactor than in those which are particulate based. It has already been shown that the primary photocatalytic reactions occur at the catalyst surface and thus in a reactor where the distances between the bulk solution and catalyst surface is large there will have to be better mixing and possible longer reactor residence times to achieve similar conversions to those found in either suspension or particulate reactors.

One possible option for a reactor design which combines the benefits of an immobilised reactor without the drawbacks of a static surface is one in which the catalyst is coated onto a support which can itself move in the reactor [104]

The schematic diagram shown in figure 5.4 shows a reactor based on glass fibres which are anchored at one end of the reactor but are unattached at the other and are therefore free to move in the reactor. Any turbulence introduced into the bulk flow through the reactor will mean that the fibres will move throughout the reactor and in relation to each other but there will be little or no contact between individual fibres thus eliminating problems of attrition.

The UV source in this reactor could either be the traditional lamp placed axially in the reactor, the fibres sitting around the lamp, constantly moving and allowing illumination of fibres at all radial distances from the lamp. Alternatively the catalyst could be coated on optical fibres designed to allow leakage of light from the sides thus combining the catalyst support and light source in one.

The addition of oxygen into the reactor would be brought about using membrane fibres distributed through the optical fibres allowing the oxygenation of the reactor contents without forming bubbles which bypass the catalyst surface wasting oxygen.

The reactor described in [104] has experienced a few problems namely the loss of TiO_2 from the fibres due to a poor coating technique. Work is continuing to improve this method.

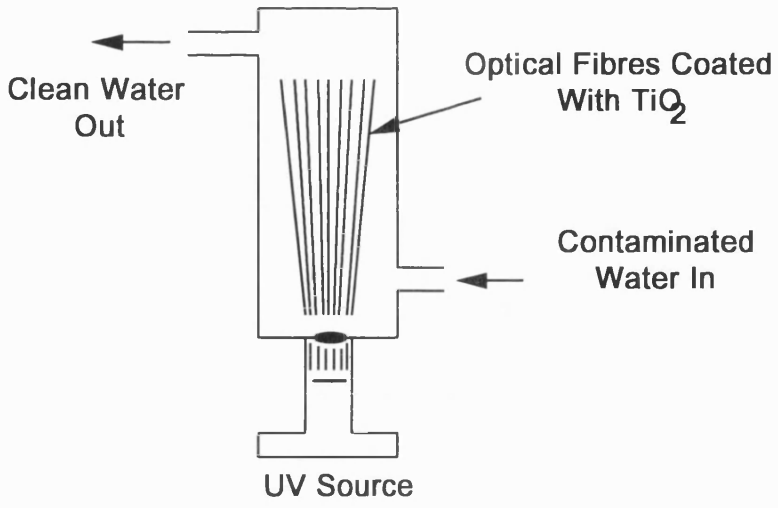

***Figure 5.4** : Fibre Optic Reactor [104].*

Any catalyst developments could use the useful methyl viologen assay to give some indication as to the coating activity as has been demonstrated this has proved a useful technique for a fast measure.

Further work on possible size distribution changes found when catalyst is dispersed in solutions of different ions is needed although as has been mentioned any effect on surface charges may be initiated by the photocatalytic effect itself and therefore may only be seen under illumination.

In order to improve the kinetic model individual initial rate-concentration data could be measured for each available reaction intermediate. The individual rate constants fitted to Langmuir-Hinshelwood equations could then be used in the reaction schemes described in section 4.5 to see whether the individual data can be applied the the multicomponent case (primary compound and intermediates present). However the problem of other intermediates is still present leading to an ill-defined overall kinetic scheme.

Appendix A1

The software for running the Gilson HPLC can be divided into 4 basic areas. Below are the values input and used for the analysis method stored as **Atrazine**.

Run Details

Run Time	40 min
Loop Begin	0 min
Loop End	39.90 min
No. of Loops	(input as ≥ total no. of samples in autosampler)
Integration Start	0.10 min
Integration Time	24.90 min
Peak Width	0.5
Peak Sensitivity	2.0 %

Mobile Phase

Time	Flowrate	% Pump B
0	0.8	0
15	0.8	40
25	0.8	40
40	0.8	0

Note: Pump B contains 100% acetonitrile in this analysis.

Contact Events

These are inputs which tell the software to perform some function on receiving an external signal (in this case from the autosampler / autoinjector)

Time	Contact	Action	Label
0.10	A	Wait	Injection

Analysis Events

Time	Event
0.1	All Valleys

Appendix A2

The SGE autosampler / autoinjector is controlled by means of a front panel and LCD display. For the HPLC method **Atrazine** the following control parameters were used.

No of Injections I	01	
Flush Time F	6	; @ 50 psi
Run Time	42	; longer than HPLC method run time
No. of Samples	up to 32	

In addition, samples were usually run with a wash sequence to minimise sample carry-over from one injection to the next. Alternate vials containing the same solvent as the samples (either water or the starting mobile phase - 20% acetonitrile / water) were placed in the carousel and the wash button depressed prior to starting a run. In the wash mode, after each injection the needle, transfer tubing and injection loop is washed through prior to the next injection.

Pages 183-187

Appendix B1: *Mass Spectra Data From Batch Experiments Using Various Forms of TiO_2 Catalyst.*

UV Only Control
SG 3 Coated Beads
Degussa P25
SCM WDB
SG 6 Coated Beads
SG7 TiO_2
TiO_2 from Ti Tetraethoxide
Crushed Tablets
SG 7 TiO_2
Sonication
Freeze Dried Sample
Fentons Reagent
Cuvette Reactor

Experiment : Control

Mass Ion	Cl	Other Ions	Compound
153		138 111	P
181		166 139 111	M
173	*	145 110	Desisopropyl
187	*	172 145 110	Desethyl
215	*	200 187 172 145 110	N
229	*	215 186 172 145 110	Oxidised

Experiment : SG3 Coated Beads

Mass Ion	Cl	Other Ions	Compound
153		138 111	P
181		166 111	M
154		139 126 111	
187	*	172 145 110	Desethyl
195		168 138 111	L
215	*	200 187 172 145	N
196		153 139 111	
229	*	215 186 172 145 110	Oxidised
210		195 153 126 111	
221		206 179 164 151 111	
235		220 206 178 164 151 111	
215	*	200 173 158 132	Atrazine

Experiment : Degussa P25

Mass Ion	Cl	Other Ions	Compound
211	*	141 112 100	R
201		187 159 149 110	
145	*	110	Desethyl-Desisop

Experiment : SCM WDB

Mass Ion	Cl	Other Ions	Compound
159	*	145 71	Q
129		111 85 71 43	Cyanuric Acid

Experiment : SG6 Coated Beads

Mass Ion	Cl	Other Ions	Compound
187	*	172 145 129 111	Desethyl
181		138 111	M
195		180 152 138 111	L
215	*	200 167 153 111	Atrazine

Experiment : SG7 TiO_2

Mass Ion	Cl	Other Ions	Compound
130		115 70 43	
129		43	Cyanuric Acid
143		128 86 43	S
185		170 143 128	T
195		179 138	L
169		127	
170		141	
155		127 113	
182		167 154 140 125	

Experiment : TiO_2 from Ti Tetraethoxide

Mass Ion	Cl	Other Ions	Compound
68		41 27	1 H- Pyrazole
138		123 69 43	
153		138 111	P
145		110	Deseth-Desisop
173	*	158 145 130 110	Desisopropyl
195		180 152 138 111	L
170		141 77	
129		111	Cyanuric Acid

Experiment : Crushed Tablets

Mass Ion	Cl	Other Ions	Compound
143		128	S
166		143 128	
215	*	200 173	Atrazine
187	*	145 110	Desethyl
195		167 145 111	L
229		201 187 145 110	Oxidised

Experiment : SG7 TiO_2

Mass Ion	Cl	Other Ions	Compound
144		129 70 44	
143		128 86 43	S
153		138 111 69 43	P
206		191 164 143 128	
181		166 138 111	M
145	*	110 68 43	Deseth-Desisop
187	*	172 145 110	Desethyl
229	*	214 200 187 172 145 110	Oxidised
252		238 223 195 181 153 139 111	
238		195 168 153 139 111	

Experiment : Sonication

Mass Ion	Cl	Other Ions	Compound
187	*	172 158 145 110	Desethyl
215	*	200 173	Atrazine
229	*	214 172 145 110	Oxidised

Experiment : Freeze Dried Sample

Mass Ion	Cl	Other Ions	Compound
145	*	110	Deseth-Desisop
187		172 111	Desethyl
215		200 173 110	Atrazine
187		159 145 110	

Experiment : Fentons

Mass Ion	Cl	Other Ions	Compound
187	*	172 158 145 110	Desethyl
229	*	214 172 145 110	Oxidised
229	*	201 187 159 145 110	Oxidised

Experiment : Cuvette Reactor (No Filter)

Mass Ion	Cl	Other Ions	Compound
153		138 111	P
181		166 138 111	M
187	*	172 145 110	Desethyl
229	*	214 200 173	Oxidised
215	*	200 187 172 145	N
229		214 200 186 158 110	Oxidised

Pages 189-191

Appendix B2: *Mass Spectra of Standards*

Desethyl Atrazine
Desisopropyl Atrazine
Desethyl-Desisopropyl Atrazine

File: G:\ATINTER1\0301002.D
Operator: David
Date Acquired: 17 Jun 92 5:45 am
Method File: atreyth6.M
Sample Name: atrazine-desethyl in et ac
Misc Info:
ALS vial: 3

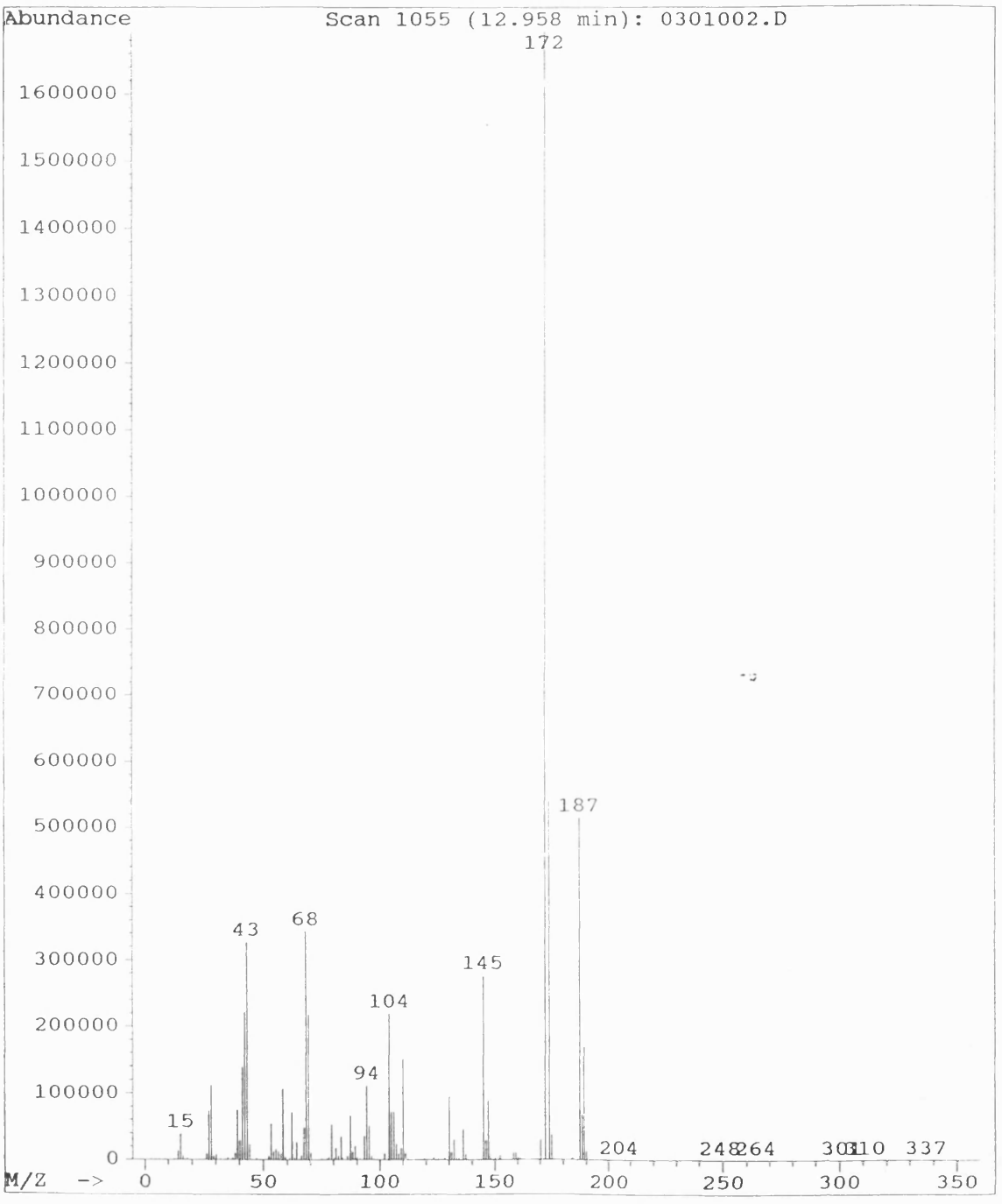

File: H:\INTER2\0201002.D
Operator: David
Date Acquired: 22 Jun 92 4:03 am
Method File: atreyth6.M
Sample Name: Atrazine-desisopropyl in Et Ac
Misc Info:
ALS vial: 2

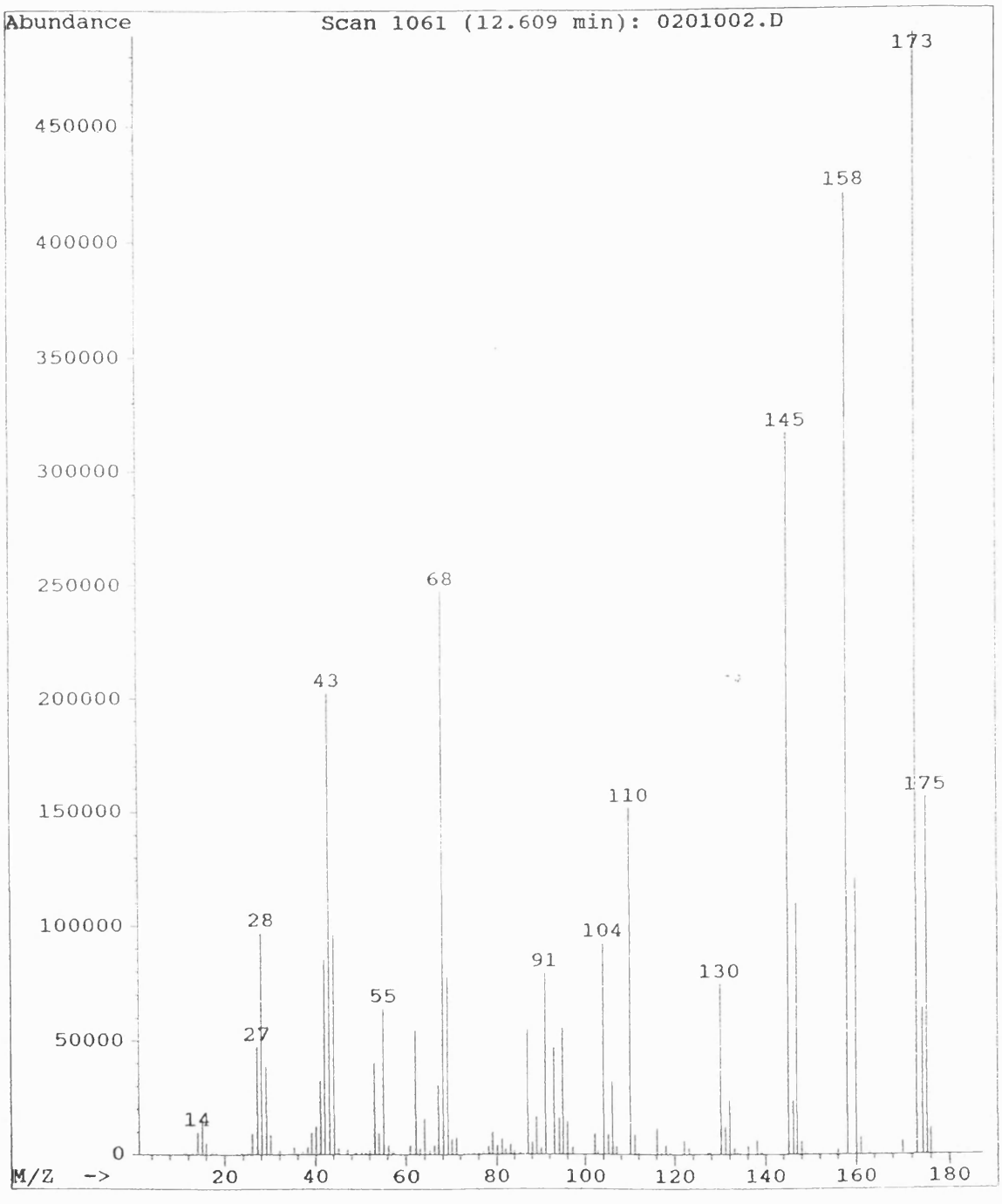

File: G:\ATINTER1\0401003.D
Operator: David
Date Acquired: 17 Jun 92 6:18 am
Method File: atreyth6.M
Sample Name: atrazine-desethyl-desisopropyl in et ac
Misc Info:
ALS vial: 4

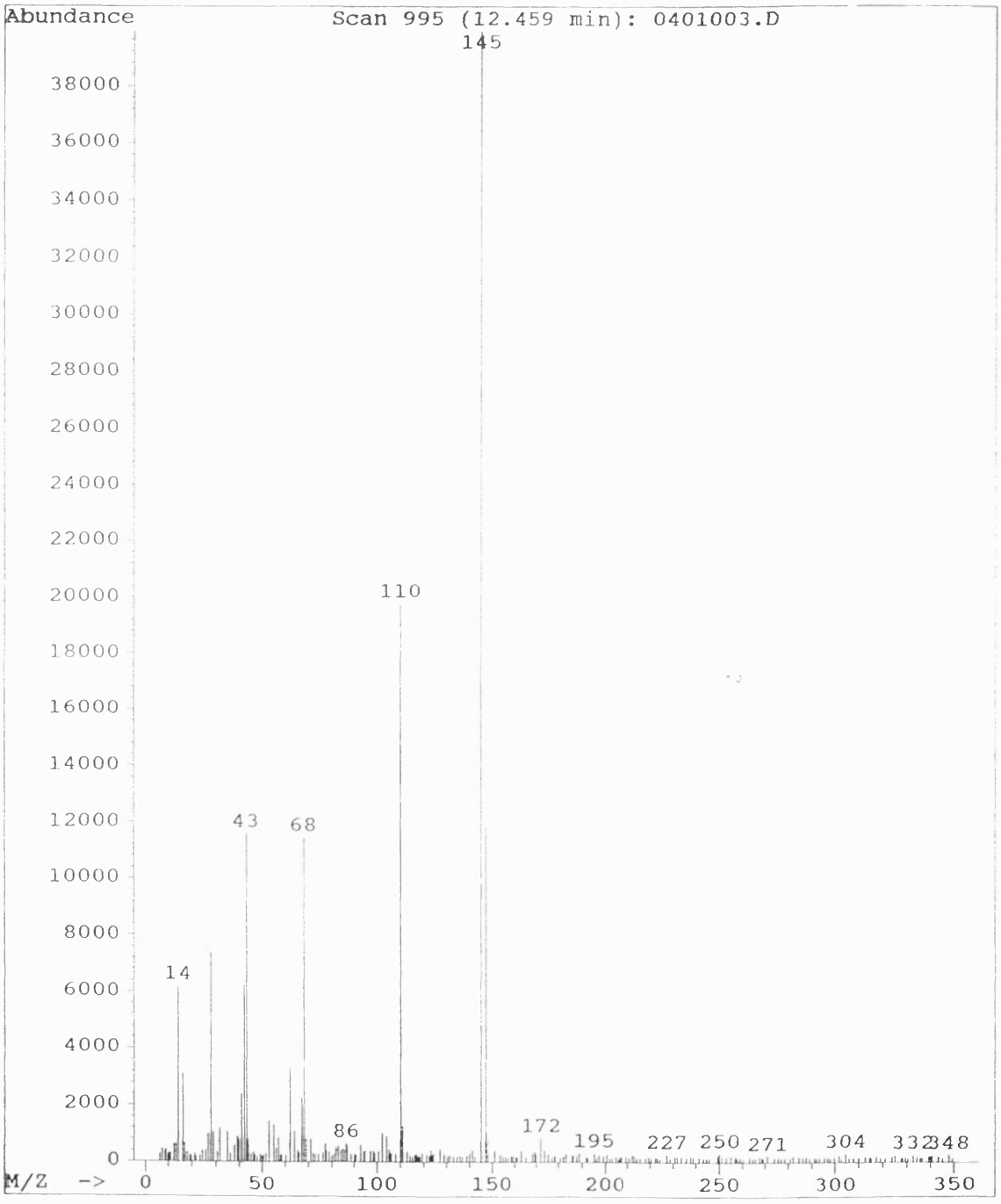

Appendix C: Sonication of Atrazine

In the sonication experiment, which is known to be another free radical generating system[92,103], 50 ml of 30 mg/L atrazine in UHQ water was sonicated for 2h in a "Soniprep 150" at a power level of ≈28 W cm^{-2}

Figure C1 shows the concentrations of atrazine and the major dealkylated intermediates during the experiment.

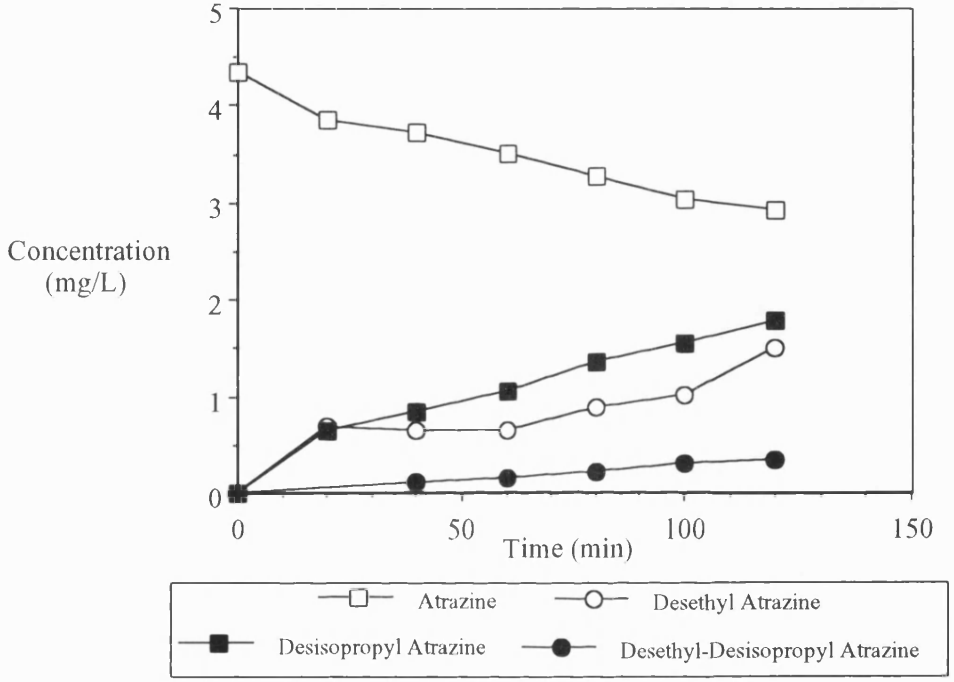

Figure C1: *Sonication of Atrazine. Concentration of intermediates (x10).*

The results from the GC-MS analysis of the solution after 120 min were discussed in section 4.1.2 and are shown in appendix B1.

References

[1] P.C. Kearney, M.T. Muldoon, C.J. Somich. "UV-Ozonation of Eleven Major Pesticides as a Waste Disposal Pretreatment" *Chemosphere* 1987, 16, 2321-2330.

[2] F.J. Beltran, G. Ovejero, B. Acedo. "Oxidation of Atrazine in Water by Ultraviolet Radiation Combined with Hydrogen Peroxide" *Wat. Res.* 1993, 27, 1013-1021.

[3] D. Ollis, E. Pelizzetti, N. Serpone. "Photocatalysed Destruction of Water Contaminants" *Environ. Sci. Technol.* 1991, 25, 1522-1529.

[4] D.Ollis. "Contaminant Degradation in Water" *Environ. Sci. Technol.* 1985, 19, 480-484.

[5] Photocatalytic Purification and Treatment of Water and Air. Ed D.F. Ollis, H. Al-Ekabi. Proceedings of the 1st International Conference on TiO_2 Photocatalytic Purification and Treatment of Water and Air, London, Ontario, Canada, 8-13 Nov 1992.

[6] R. Matthews. "Solar-Electric Water Purification using Photocatalytic Oxidation with TiO_2 as a Stationary Phase" *Solar. Energy* 1987, 38, 405-413.

[7] R. Matthews. "Titanium Dioxide and Solar Purification of Water" *Sunworld* 1985, 9, 3-5.

[8] C. Minero, E. Pelzzetti, S. Malato, J. Blancob. "Large Solar Plant Photocatalytic Water Decontamination: Degradation of Pentachlorophenol" *Chemosphere* 1993, 26, 2103-2119.

[9] The Pesticide Manual. 9th Edn. Ed. Charles R. Worthing (British Crop Protection Council)

[10] EEC Directive no. 80/778, 15 July 1980.

[11] M. Gratzel (Ed.) "Energy Resources Through Photochemistry and Catalysis" Academic Press 1983.

[12] J.F. Le Page (Ed.) "Applied Heterogeneous Catalysis" Editions Technip, Paris, 1987.

[13] C.T. Turchi, D.F. Ollis. "Photocatalytic Degradation of Organic Water Contaminants: Mechanisms Involving Hydroxyl Radical Attack" *J. Catal.* 1990, 122, 178-192.

[14] R.B. Draper and M.A. Fox. "Titanium Dioxide Photoxidation of Thiocyanate - (SCN)2 - Studied by Diffuse Reflectance Flash-Photolysis" *J. Phys. Chem.* 94 (1990) 4628-4634.

[15] C.D. Jaeger, A. Bard. "Spin Trapping and ESR Detection of Radical Intermediates in the Photodecomposition of Water at TiO_2 Particulate Systems" *J. Phys. Chem.* 1979, 83, 3146-3152 .

[16]. M.-A. Fox, C. Chen. "Mechanistic Features of the Semiconductor Photocatalysed Olefin to Carbonyl Oxidative Cleavage" *J. Am. Chem. Soc.* 1981, 103, 6757- 6759 .

[17] M. Barbeni, C. Minero, E. Pelizzetti, E. Borgarello, N. Serpone. "Chemical Degradation of Chlorophenols With Fenton's Reagent" *Chemosphere* 1987, 16, 2225-2237 .

[18]. D.W. Bahnemann, in *"Proc. Symp. Semiconductor Photoelectrochemistry"*. Ed. C. Koval, The Electrochemistry Soc. Inc., Pennington N.J. (1991)

[19] T. Sehili, P. Boule and J. Lemaire. "Photocatalysed Transformation of Chloroaromatic Derivatives on Zinc Oxide. 2. Dichlorobenzenes" *J. Photochem. Photobiol. A:Chem* 50 (1989) 103-116.

[20] C. Richard and J. Lemaire. "Analytical and Kinetic Study of the Phototransformation of Furfuryl Alcohol in Aqueous ZnO Suspensions" *J. Photochem. Photobiol. A:Chem* 55 (1990) 127-134.

[21] T. Sehili, P. Boule and J. Lemaire. "Photocatalysed Transformation of Chloroaromatic Derivatives on Zinc Oxide. 3. Chlorophenols" *J. Photochem. Photobiol. A:Chem* 50 (1989) 117-127.

[22] N. Serpone, E. Pelizzetti, H. Hidaka. "Identifying Primary Events and the Nature of Intermediates Formed During the Photocatalysed Oxidation of Organics Mediated by Irradiated Semiconductors" in [5].

[23] C. Minero, F. Catozzo, E. Pelizzetti. "Role of Adsorption in Photocatalysed Reactions of Organic Molecules in Aqueous TiO_2 Suspensions" *Langmuir* 1992, 8, 481-486.

[24] E. Pelizzetti, C. Minero, E. Borgarello, L. Tinucci, and N. Serpone "Photocatalytic Activity and Selectivity of Titania Colloids and Particles Prepared by the Sol-Gel Technique: Photooxidation of Phenol and Atrazine" *Langmuir* (1993), 9, 2995-3001.

[25] M. Barbini, E. Pramauro, E. Pelizzetti. "Photodegradation of Pentachlorophenol Catalysed by Semiconductor Particles" *Chemosphere* 1985, 14, 195-208.

[26] M. Nargiello, T. Herz. "Physical-Chemical Characteristics of P-25 Making it Extreamely Suited as the Catalyst in Photodegradation of Organic Compounds" in [5].

[27] K. Okamoto, Y. Yammoto, H. Tanaka, M. Tanaka, A. Itaya. "Heterogeneous Photocatalytic Decomposition of Phenol over TiO_2 Powder" *Bull. Chem. Soc. Jpn.* 1985, 58, 2015-2022.

[28] A. Mills, S. Morris, R.H. Davies. "Photomineralization of 4-Chlorophenol Sensitized by Titanium Dioxide: A Study of the Effects of Annealing the Photocatalyst at Different Temperatures" *J. Photochem. Photobiol. A Chem.* 1993, 71, 285-289.

[29] S.A. Selim, Ch. A. Philip, S. Hanafi, H.P.Boehm. "Effect of Thermal Treatment on the Structure and Texture of Titania" *J. Mat. Sci.* 1990, 25, 4678-4687.

[30] X. Domenech "Photocatalysis for Aqueous Phase Decontamination: Is TiO_2 the Better Choice?" in [5].

[31] K. Tenaka, T. Hisanaga and A.O. Rivera "Effect of Crystal Form of TiO_2 on the Photocatalytic Degradation of Pollutants" in [5].

[32] W. Choi, A. Termin, M.R. Hoffmann "The Role of Metal Ion Dopants in Quantum-Sized TiO_2 : Correlation Between Photoreactivity and Charge Carrier Recombination Dynamics" *J. Phys. Chem.* (1994) 98, 13669-13679.

[33] L. Palmisano, V. Augugliaro, A. Sclafani, M. Schiavello "Activity of Chromium Ion Doped Titania for the Dinitrogen Reduction to Ammonia and for Phenol Photodegradation" *J. Phys. Chem.* (1988), 92, 6710-6713.

[34] Z. Luo, Q.H. Gao "Decrease in the Photoactivity of Titanium Pigment on Doping with Transition Metals" *J. Photochem. Photobiol. A:Chem* (1992), 63, 367-375.

[35] D. Bocklemann, R. Goslich, D. Bahnemann. In *Solar Thermal Energy Utilization*; M. Becker, K-H. Funken, G. Schneider Eds.Springer Verlag GmbH;Heidelberg 1992 Vol 6 p 397-429.

[36] Y. Mao, C. Schoneich, K-D. Asmus. "Identification of Organic Acids and Other Intermediates in Oxidative Degradation of Chlorinated Ethanes on TiO_2 Surfaces en Route to Mineralisation. A Combined Photocatalytic and Radiation Chemical Study." *J. Phys. Chem.* 1991, 95, 10080-10089.

[37] B. Kraeutler, A.J. Bard. "Heterogeneous Photocatalytic Decomposition of Saturated Carboxylic Acids on TiO_2 Powder. Decarboxylative Route to Alkanes" *J. Amer. Chem. Soc.* 1987, 100, 5985-5992.

[38] E. Pelizzetti, C. Minero, P. Piccinini, M. Vincent. "Phototransformations of Nitrogen Containing Organic Compounds over Irradiated Semiconductor Metal Oxides. Nitrobenzene and Atrazine over TiO_2 and ZnO." *Coord. Chem. Rev.* 1993, 125, 183-194.

[39] J-C. D'Oliveira, C. Guillard, C. Maillard, P. Pichat. "Photocatalytic Destruction of Hazardous Chlorine- or Nitrogen-Containing Aromatics in Water" *J. Environ. Sci. Health.* 1993, A28, 941-962.

[40] E. Pelizzetti, V. Carlin, C. Minero, M. Gratzel. "Enhancement of the Rate of Photocatalytic Degradation of 2-Chlorophenol, 2,7-Dichlorodibenzodioxin and Atrazine by Inorganic Oxidizing Species" *New. J. Chem.* 1991, 15, 351-359.

[41] K. Okamoto, Y. Yammoto, H. Tanaka, M. Tanaka, A. Itaya. "Kinetics of Heterogeneous Photocatalytic Decomposition of Phenol over Anatase TiO_2 Powder" *Bull. Chem. Soc. Jpn.* 1985, 58, 2023-2028.

[42] T.Y. Wei, C.C. Wan. "Heterogeneous Photocatalytic Oxidation of Phenol with Titanium Dioxide Powders" *Ind. Eng. Chem. Res.* 1991, 30, 1293-1300.

[43] J.-C. D'Oliveira, W.D.W. Jayatilake, K. Tennakone, J.-M. Herrmann, P. Pichat. "Heterogeneous Photocatalysis as a Method of Water Decontamination: Degradation of 2-, 3- and 4-Chlorobenzoic Acids over Illuminated TiO_2 at Room Temperature" *New Frontiers in Catalysis Ed. L. Guczi et al. Proc. 10th Intl. Cong. on Catal.*

[44] J. Cunningham, G. Al-Sayyed. "Factors Influencing Efficiencies of TiO_2-Sensitised Photodegradation. Part 1:- Substituted Benzoic Acids: Discrepancies with Dark-Adsorption Parameters" *J. Chem. Soc. Faraday Trans.* 1990, 86, 3935-3941.

[45] J. Zhao, H. Hidaka, A. Takamura, E. Pelizzetti, N. Serpone. "Photodegradation of Surfactants. II. ζ-Potential Measurements in the Photocatalytic Oxidation of Surfactants in Aqueous TiO_2 Dispersions" *Langmuir* 1993, 9, 1646-1650.

[46] I. Poulios, A. Avranas. "Heterogeneous Photocatalytic Degradation of the Cationic Surfactants Cetyldimethylbenzylammonium Chloride and Cetylpyridinium chloride" *Chemical Reactor Technology for Environmentally Safe Reactors. Ed. H.L. de Lasa et al.* 609-615.

[47] G. Chester, M. Anderson, H. Read, S. Esplugas. "A Jacketed Annular Membrane Photocatalytic Reactor for Wastewater Treatment: Degradation of

Formic Acid and Atrazine" *J. Photochem. Photobiol. A: Chem.* 1993, 71, 291-297.

[48] E. Pelizzetti, C. Minero, V. Carlin, M. Vincenti, E. Pramauro. "Identification of Photocatalytic Degradation Pathways of 2-Cl-s-Triazine Herbicides and Detection of Their Decomposition Intermediates" *Chemosphere* 1992, 24, 891-910.

[49] S.T. Hung, M.K.S. Mak. "Titanium Dioxide Photocatalysed Degradation of Organophosphate in a System Simulating the Natural Aquatic Environment" *Environ. Technol.* 1993, 14, 265-269.

[50] L-C. Chen, T-C. Chou. "Kinetics of Photodecolorization of Methyl Orange using Titanium Dioxide as Catalyst" *Ind. Eng. Chem. Res.* 1993, 32, 1520-1527.

[51] A. Mills , R.H. Davies, D. Worsley. "Water Purification by Semiconductor Photocatalysis" *Chemical Society Reviews.* 1993, ,417-425.

[52]. Egerton, King. "The Influence of Light Intensity on Photoactivity in TiO_2 Pigmented Systems" *J. Oil. Col. Chem. Assoc.* 1979, 62, 386- .

[53] G.R. Payton, F.Y. Huang, J.L. Burlson, W.H. Glaze. "Destruction of Pollutants in Water with Ozone in Combination with UV Radiation. 1. General Principles and Oxidation of Trichloroethylene" *Environ. Sci. Technol.* 1982, 16, 448-453.

[54] C. Kormann, D.W. Bahnemann, M.R. Hoffmann. "Photolysis of Chloroform and Other Organic Molecules in Aqueous TiO_2 Suspensions" *Environ. Sci. Technol.* (1991), 25, 494-500.

[55] C.S. Turchi, D.F. Ollis. "Mixed Reactant Photocatalysis: Intermediates and Mutual Rate Inhibition" *J. Catal.* 1989, 119, 483-496.

[56] M.R. Hoffmann, S.T. Martin, W. Choi, D.W. Bahnemann "Environmental Applications of Photocatalysis" *Chem. Rev.* (1995),95, 69-96.

[57] E. Pelizzetti, V. Maurino, V. Carlin, E. Pramauro, O. Zerbinati, M.L. Tosato. "Photocatalytic Degradation of Atrazine and Other s-Triazine Herbicides" *Environ. Sci. Technol.* 1990, 24, 1559-1565.

[58] E. Canelli. "Chemical, Bacteriological, and Toxicological Properties of Cyanuric Acid and Chlorinated Isocyanurates as Applied to Swimming Pool Disinfection" *Amer. J. Pub. Health.* 1974, 64, 155- .

[59] A.L. Pruden, D.F. Ollis. "Degradation of Chloroform by Photoassisted Heterogeneous Catalysis in Dilute Aqueous Suspensions of Titanium Dioxide" *Environ. Sci. Tech.* 1983, 17, 628-631.

[60] S. Yamazaki-Nishida, K.J. Nagano, L.A. Phillips, S. Cervera-March, M.A. Anderson. "Photocatalytic Degradation of Trichloroethylene in the Gas Phase using Titanium Dioxide Pellets" *J. Photochem. Photobiol. A: Chem.* 1993, 70, 95-99.

[61] The First International Conference on TiO_2 Photocatalytic Purification and Treatment of Water and Air. (Abstracts)

[62] G. Mills, M.R. Hoffmann. "Photocatalytic Degradation of Pentachlorophenol on TiO_2 Particles: Identification of Intermediates and Mechanism of Reaction" *Environ. Sci. Technol.* 1993, 27, 1681-1689.

[63] J. Sabate, M.A. Anderson, H. Kikkawa, Q. Xu, S. Cervera-March, C.G. Hill, Jr. "Nature and Properties of Pure and Nb-Doped TiO_2 Ceramic Membranes

Affecting the Photocatalytic Degradation of 3-Chlorosalicylic Acid as a Model of Halogenated Organic Compounds" *J. Catal.* 1992, 134, 36-46.

[64] N. Serpone, E. Borgarello, R. Harris, P. Cahill, M. Borgarello. "Photocatalysis over TiO_2 Supported on a Glass Substrate" *Solar Energy Mat.* 1986, 14, 121-127.

[65] R. Matthews. "Photooxidation of Organic Impurities in Water using Thin Films of Titanium Dioxide" *J. Phys. Chem.* 1987, 91, 3328-3333.

[66] R. Matthews. "An Adsorption Water Purifier with *in Situ* Photocatalytic Regeneration" *J. Catal.* 1988, 113, 549-555.

[67] R.W. Matthews "Photocatalysis in Water Purification: Possibilities, Problems and Prospects", in [5].

[68] M. Abdullah, G.K-C. Low, R. Matthews. "Effects of Common Inorganic Anions on Rates of Photocatalytic Oxidation of Organic Carbon over Illuminated Titanium Dioxide" *J. Phys. Chem.* 1990, 94, 6820-6825.

[69] D.W. Hand, Y. Zhang, E.G. Klun, J.C. Crittenden. "Photocatalytic Decontamination of Water using Sunlight and TiO_2 Impregnated Adsorbent and Non-Adsorbant Supports" in [61]

[70] R. Matthews, M. Abdullah, G.K.C. Low. "Photocatalytic Oxidation for Total Organic Carbon Analysis" *Anal. Chim. Acta.* 1990, 233, 171-179.

[71] T. Watanabe, A. Kitamura, E. Kojima, C. Nakayama, K. Hashimoto, A. Fujishima. "Photocatalytic Activity of TiO_2 Thin Film under Room Light" in [61].

[72] A. Fujishima, K. Hashimoto, R. Cai, H. Sakai, Y. Kubota. "Biochemical Application of TiO_2 Photocatalysts" in [61].

[73] I. Rosenberg, J.R. Brock, A. Heller. "Collection Optics of TiO_2 Photocatalysis on Hollow Glass Microbeads Floating on Oil Slicks" *J. Phys. Chem.* 1992, 96, 3423-3428.

[74] B. Fegley, Jr., E.A. Barringer, H.K. Bowen. "Synthesis and Characterisation of Monosized Doped TiO_2 Particles" *J. Am. Ceram. Soc.* 1984, 67, C113-C116.

[75] M.A. Anderson, M.J. Gieselmann, Q. Xu. "Titania and Alumina Ceramic Membranes" *J. Mem. Sci.* 1988, 39, 243-258.

[76] K. Kamiya, K. Tanimoto, T. Yoko. "Preparation of TiO_2 Fibres by Hydrolysis and Polycondensation of $Ti(O\text{-}i\text{-}C_3H_7)_4$" *J. Mat. Sci. Lett.* 1986, 5, 402-404.

[77] Y. Takahashi, Y. Matsuoka. "Dip-Coating of TiO_2 Films Using a Sol Derived from $Ti(O\text{-}i\text{-}Pr)_4$-diethenolamine-$H_2O$-i-PrOH System" *J. Mat. Sci.* 1988, 23, 2259-2266.

[78] J. Sherma. "Pesticides" *Anal Chem.* 1991, 63, 118R-130R

[79] N.M.J. Vermeulen, Z. Apostolides, D.J.J. Potgieter. "Separation of Atrazine and Some of it's Degradation by High Performance Liquid Chromatography" *J. Chrom.* 1982, 240, 247-253.

[80] R. Reupert, E. Ploger, G.Brausen. "HPLC Determination of 29 Controlled Herbicides in Water Supplies" Hewlett Packard Application Note.

[81] R. Schuster, A. Gratzfeld-Husgen. "HPLC Analysis of Pesticide Traces in the ppt-Range" Hewlett Packard Application Note.

[82] P.J. Naish-Chamberlain, A.R. Cooke. "Automation of Sample Preparation for Pesticide Analysis in Water" *LC-GC Intl.*

[83] V. Coquart, M.-C. Hennion. "Determination of Chlorotriazines in Aqueous Environmental Samples at the ng/L Level Using Preconcentration with a Cation Exchanger and On-Line High-Performance Liquid Chromatography" *J. Chrom.* 1991, 585, 67-73.

[84] P.G. Stoks, A.W. Schwartz. "Determination of s-Triazine Derivatives at the Nanogram Level by Gas-Liquid Chromatography" *J. Chrom.* 1979, 168, 455-460.

[85] J. Hajslova, L. Ryparova, I. Viden, J. Davidek, V. Kocourek, I. Zemanova. "A Comparison of Chromatographic Methods for Determination of s-Triazines in Milk" *Int. J. Environ. Anal. Chem.* 1990, 38, 105-114.

[86] E.M. Thurman, M. Meyer, M. Pomes, C.A. Perry, A.P. Schwab. "Enzyme-Linked Immunosorbent Assay Compared with Gas Chromatography/Mass Spectrometry for the Determination of Triazine Herbicides in Water" *Anal. Chem.* 1990, 62, 2043-2048.

[87] T.V. Briggle, L.M. Allen, R.C. Duncan, C.D. Pfaffenberger. "High Performance Liquid Chromatographic Determination of Cyanuric Acid in Human Urine and Pool Water" *J. Assoc. Off. Anal. Chem.* 1981, 64, 1222-1226.

[88] J.F. Rabek Experimental Methods in Photochemistry and Photophysics Part 1&2 (John Wiley 1982).

[89] B. O'Regan, J. Moser, M. Anderson, M. Gratzel. "Vectorial Electron Injection into Transparent Semiconductor Membranes and Electron Field Effects on the Dynamics of Light-Induced Charge Separation" *J. Phys. Chem.* 1990, 94, 8720-8726.

[90] M. Aizawa, Y. Nakagawa, Y. Nosaka, N. Fujii, H. Miyama. "Preparation of Hollow TiO_2 Fibres" *J. Non. Cryst. Solids.* 1990, 124, 112-115.

[91] J.R. Plimmer, P.C. Kearney, U.I. Klingebiel. "s-Triazine Herbicide Dealkylation by Free-Radical Generating Systems" *J. Agri. Food. Chem.* 1971, 19, 572-573

[92] J.M. Wu, H.S. Huang, C.D. Livengood. "Ultrasonic Destruction of Chlorinated Compounds in Aqueous Solution" *Environ. Progr.* 1992,11,195-201.

[93] R.A. Larson, M.B. Schlauch, K.A. Marley. "Ferric Ion Photodecomposition of Triazines" *J. Agric. Food. Chem.* 1991, 39, 2057-2062.

[94] S. Safe, O. Hutzinger. Mass Spectrometry of Pesticides and Pollutants (CRC Press 1973)

[95] J.-C. D'Oliveira, C. Minero, E. Pelizzetti, P. Pichat. "Photodegradation of Dichlorophenols and Trichlorophenols in TiO_2 Aqueous Suspensions: Kinetic Effects of the Positions of the Cl Atoms and Identification of the Intermediates" *J. Photochem. Photobiol. A: Chem.* 1993, 72, 261-267.

[96] H. Al-Ekabi, N. Serpone. "Kinetic Studies in Heterogeneous Photocatalysis. 1. Photocatalytic Degradation of Chlorinated Phenols in Aerated Aqueous Solutions over TiO_2 Supported on a Glass Matrix" *J. Phys. Chem.* 1988, 92, 5726-5731.

[97] V. Augugliaro, L. Palmisano, A. Sclafani, C. Minero, E. Pelizzetti. "Photocatalytic Degradation of Phenol in Aqueous Titanium Dioxide Dispersions" *Toxicol. Environ. Chem.* 1988, 16, 89-109.

[98] Y. Ku, C-B. Hsieh. "Photodecomposition of 2,4-Dichlorophenol in Aqueous Solution Catalyzed by Cadmium Sulfide Particles" *Ind. Eng. Chem. Res.* 1992, 31, 1823-1826.

[99] P. Pichat, C. Guillard, C. Maillard, L. Amalric, J.-C. D'Oliveira. "TiO_2 Photocatalytic Destruction of Water Aromatic Pollutants: Intermediates; Properties-Degradability Correlation; Effects of Inorganic Ions and TiO_2 Surface Area; Comparisons with H_2O_2 Processes" in [5].

[100] R. Matthews. "Carbon Dioxide Formation from Organic Solutes in Suspensions of Ultraviolet-Irradiated TiO_2. Effect of Solute Concentration" *Aust. J. Chem.* 1987, 40, 667-675.

[101] C. Minero, C. Aliberti, E. Pelizzetti, R. Terzian, N. Serpone. "Kinetic Studies in Heterogeneous Photocatalysis. 6. AM1 Simulated Sunlight Photodegradation over Titania in Aqueous Media: A First Case of Fluorinated Aromatics and Identification of Intermediates" *Langmuir* 1991, 7, 928-936.

[102] J. Sabate, M.A. Anderson, H. Kikkawa, M. Edwards, C.G. Hill, Jr. "A Kinetic Study of the Photocatalytic Degradation of 3-Chlorosalicylic Acid over TiO_2 Membranes Supported on Glass" *J. Catal.* 1991, 127, 167-177.

[103] N. Serpone, R. Terzian, H. Hidaka, E. Pelizzetti. "Ultrasonic Induced Dehalogenation and Oxidation of 2-, 3-, and 4-Chlorophenol in Air-Equilibrated Aqueous Media. Similarities with Irradiated Semiconductor Particlates" *J. Phys. Chem.* 1994, 98, 2634-2640.

[104] W.A. Zeltner, C.G.Hill. Jr, M.A. Anderson "Supported Titania for Photodegradation" *Chemtech* 1993, 23, 21-28.